BioMed Research International

Translational Neuroimaging of the Mood and Anxiety Disorders

Guest Editors: Su Lui, Qiyong Gong, Yong He, Georg Northoff, and John A. Sweeney

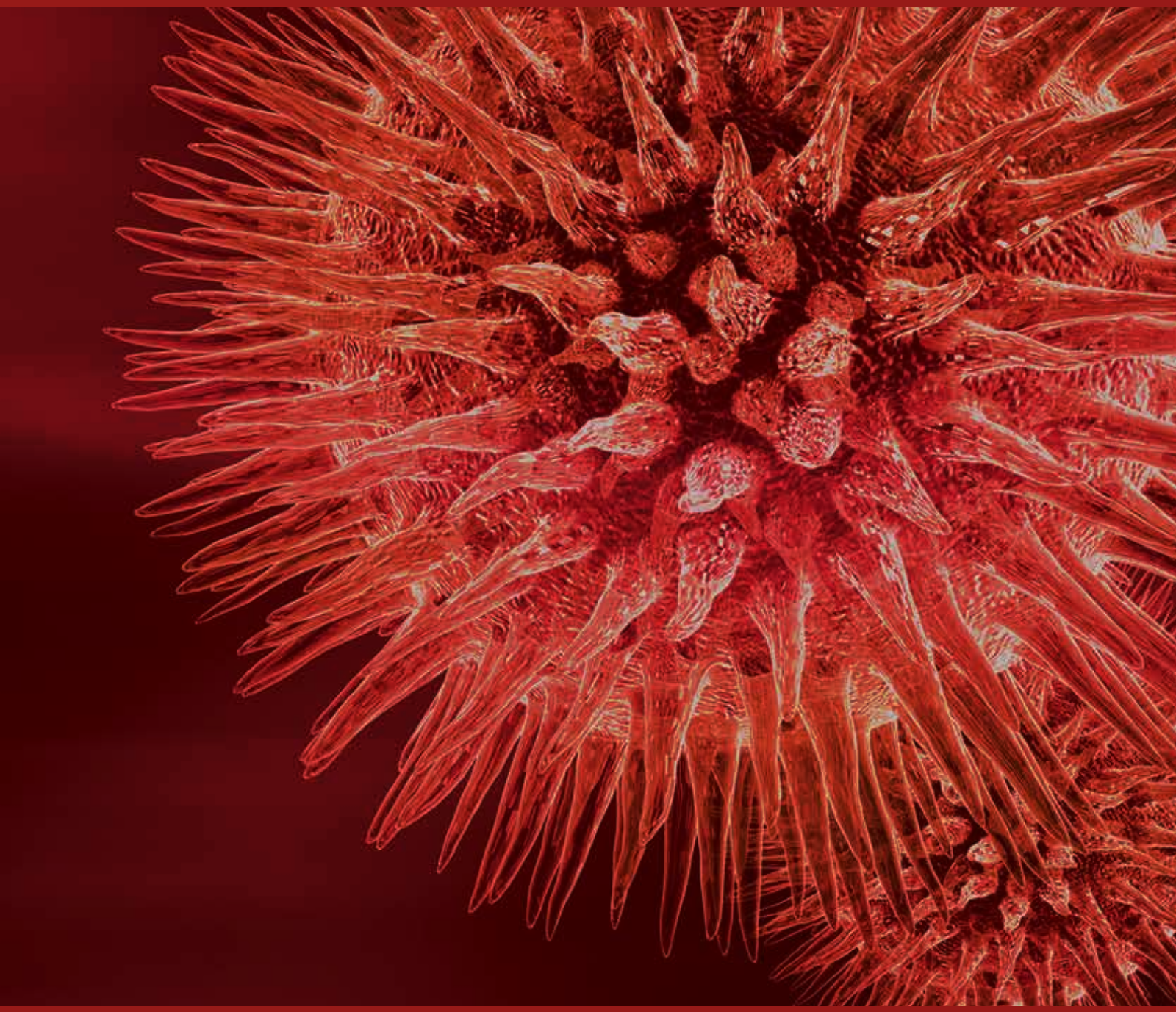

Translational Neuroimaging of the Mood and Anxiety Disorders

BioMed Research International

Translational Neuroimaging of the Mood and Anxiety Disorders

Guest Editors: Su Lui, Qiyong Gong, Yong He, Georg Northoff, and John A. Sweeney

Contents

Hindawi Publishing Corporation
BioMed Research International
Volume 2014, Article ID 240769, 2 pages
http://dx.doi.org/10.1155/2014/240769

Editorial

Translational Neuroimaging of the Mood and Anxiety Disorders

Su Lui,[1] Qiyong Gong,[1] Yong He,[2] Georg Northoff,[3] and John A. Sweeney[4]

[1] *Huaxi MR Research Center (HMRRC), Department of Radiology, Psychiatry and Neurology, West China Hospital of Sichuan University, Chengdu, Sichuan 610041, China*
[2] *State Key Laboratory of Cognitive Neuroscience and Learning, Beijing Normal University, Beijing 100875, China*
[3] *Unit of Mind, Brain Imaging and Neuroethics, University of Ottawa Institute of Mental Health Research, Ottawa, ON, Canada K1Z 7K4*
[4] *Departments of Psychiatry and Pediatrics, University of Texas Southwestern Medical Center, Dallas, TX 75390-9086, USA*

Correspondence should be addressed to Qiyong Gong; qiyonggong@hmrrc.org.cn

Received 5 May 2014; Accepted 5 May 2014; Published 12 May 2014

Mood and anxiety disorders include all types of depression, bipolar disorders, and anxiety disorders and are among the top 10 causes of disability worldwide. There is no effective diagnosis or treatment mainly due to our poor understanding of the underlying pathophysiology and particularly the lack of objective biomarkers for diagnosis and prognosis. In recent years, researchers have made remarkable advances in understanding the cerebral deficits in patients with mood andanxiety disorders using various brain imaging methods such as computed tomography (CT), magnetic resonance imaging (MRI), and positron emission tomography (PET). Particularly over the past two decades, with the development of novel neuroimaging methods (e.g., structural MRI, functional MRI, diffusion MRI, and EEG/MEG), researchers have made great strides forward in the understanding of both anatomical and functional cerebral deficits in patients with mood andanxiety disorders.

To accelerate the process of translating these new techniques to clinical applications, a number of important issues must be addressed such as their ability to consistently detect characteristic cerebral deficits in individuals with mood andanxiety disorders, the relationships of cerebral deficits to clinical symptoms and genetic characteristics, and the degree to which the deficits respond to different therapies. In this special issue, several research groups report findings that address some of these issues.

The paper by X. Wang et al. addresses the role of self-perspective in reappraisal process of depressed patients. With functional MRI, the authors found that impaired modulatory effects of amygdala in depressed patients are compensated for by increased utilization of cognitive control resources, with dissociable effects for different self-perspectives in reappraisal. The study by S. Deppermann et al. used functional near-infrared spectroscopy (fNIRS) to monitor the treatment effect of repetitive transcranial magnetic stimulation (rTMS) on panic disorder (PD). Their findings support that PD is characterized by prefrontal hypoactivation during cognitive performance. The study by T.-Y. Liu et al. investigated the cortical abnormalities of early emotion perception in patients with major depressive disorder (MDD) and bipolar disorder (BD) using magnetoencephalography (MEG), which showed the potential of MEG measurements in separating MDD from BD.

The study by K. Hilbert et al. used fMRI to investigate the influence of stimulus modality on neural fear processing in dental phobia, which enlarges our knowledge about neural correlates of phobias. The paper by N. Jaworska et al. assessed cortical thickness using high resolution MRI in patients with varying ages of MDD onset and trauma history. Their findings demonstrate that anatomical brain deficits can be expressed differently in relation to age of onset of depression and the presence of childhood trauma. The paper by B. E. Depue et al. used MRI to determine whether comorbid post-traumatic stress disorder (PTSD) and mild traumatic brain injury (mTBI) are characterized by altered brain structure in the same regions as has been observed when PTSD or

TBI is present without the other condition using both voxel-based morphometry and surface-based morphometry. These are highly comorbid conditions, and thus this study addresses an important clinical question. Their findings suggest that alterations in brain anatomy in veterans with comorbid PTSD/mTBI are associated with both cognitive deficits and trauma symptoms related to PTSD. The study by C. Qiu et al. used diffusion tensor imaging (DTI) to characterize white-matter microstructural changes in patients with social anxiety disorder (SAD) and to describe their relationship to the severity of psychological symptoms. The study by H.-J. Li et al. employed a new index-surface-based regional homogeneity (ReHo) to analyze resting fMRI data in MDD patients, which may provide a new useful index to explore the pathophysiological mechanism of MDD. The paper by M. H. Serpa et al. evaluated the diagnostic performance of a neuroanatomical pattern classification method for discriminating psychotic MDD, bipolar I disorder (BD-I), and healthy controls using patients early in the course of illness. Though the findings are negative, perhaps related to the smaller sample size, this paper illustrates a very promising method for combining structural MRI data with other indices to characterize and differentiate individuals with mood disorders. The study by A. Sekiguchi et al. examined the white-matter integrity in 25 subjects 1 year after a Japanese earthquake to clarify the long-term effects of the severe psychological trauma on brain white matter. The study showed the potential ability of DTI in predicting the prognosis of physically healthy survivors after severe psychological trauma. Finally, the study by C. N. Kuswanto et al. examined the relationship between the *GRIN2B gene* and cerebral white-matter changes in BD, which is an example of an important line of work investigating relations between neuroimaging findings and genetic factors. Their findings enhance our understanding of the link between dysregulated glutamatergic neurotransmission and neuroimaging endophenotypes in BD.

In summary, the papers in this series highlight several important research strategies that are making it increasingly evident that the neuroimaging findings are of translational value for psychiatry. The results from these psychiatric neuroimaging studies not only help us to understand the pathogenesis of the mood and anxiety disorders but also show great potential to provide urgently needed objective biomarkers for clinical diagnosis and evaluation. Ultimately, psychiatric imaging may play an important role not only in differential diagnosis but also in monitoring the effects of therapeutic intervention on brain to advance drug discovery and clinical practice in the long run.

Su Lui
Qiyong Gong
Yong He
Georg Northoff
John A. Sweeney

Hindawi Publishing Corporation
BioMed Research International
Volume 2014, Article ID 390865, 11 pages
http://dx.doi.org/10.1155/2014/390865

Research Article

Dissociable Self Effects for Emotion Regulation: A Study of Chinese Major Depressive Outpatients

Xiaoxia Wang,[1] Zhengzhi Feng,[1] Daiquan Zhou,[2] Xu Lei,[3] Tongquan Liao,[4] Li Zhang,[1] Bing Ji,[2] and Jing Li[2]

[1] *Department of General Psychology, College of Psychology, Third Military Medical University, Street 30, Gaotanyan of Shapingba District, Chongqing 400038, China*
[2] *Radiology Department, Southwest Hospital, Third Military Medical University, Chongqing 400037, China*
[3] *School of Psychology, Southwest University, Chongqing 400715, China*
[4] *Xin Qiao Hospital, Third Military Medical University, Chongqing 400038, China*

Correspondence should be addressed to Zhengzhi Feng; fengzhengzhi@gmail.com

Received 9 September 2013; Revised 19 February 2014; Accepted 6 March 2014; Published 3 April 2014

Academic Editor: Yong He

Reappraisal is an adaptive emotion regulation strategy while the role of self-perspective in reappraisal process of depressed patients is largely unknown in terms of goals (valence/arousal) and tactics (detachment/immersion). In this study, 12 depressed individuals and 15 controls were scanned with MRI during which they either attend naturally to emotional stimuli, or adopt detachment/immersion strategy. Behaviorally, no group differences in self-reported emotion regulation effectiveness were found. In addition, we observed that (1) patients were less able to downregulate amygdala activation with recruitment of more dorsal lateral prefrontal cortex (dlPFC) when adopting detachment strategy regardless of valence, and this preserved ability to regulate emotion was inversely associated with severity of symptoms; (2) patients had deficits in upregulating amygdala activation when adopting immersion strategy, with less inferior frontal gyrus (IFG) activation and strengthening coupling of dlPFC and ventral medial prefrontal cortex (vmPFC) with amygdala; (3) comparison between groups yielded that patients showed stronger vmPFC activation under either self-detached or self-immersed condition. In conclusion, impaired modulatory effects of amygdala in depressed patients are compensated with strengthening cognitive control resources, with dissociable effects for different self-perspectives in reappraisal. These results may help clarify the role of self-perspective underlying reappraisal in major depression.

1. Introduction

According to the fourth edition of Diagnostic and Statistical Manual of Mental Disorders (DSM-IV), anhedonia and/or a lingering low mood are the defining characteristics of major depressive disorder (MDD). A body of evidence implies a trait-like role of maladaptive emotion regulation strategies in MDD vulnerability [1], among which the strategy of reappraisal has received the most extensive attention. In clinical settings, reappraisal plays a pivotal role in cognitive behavioral therapy (CBT) interventions [2] that predicts resilience in depressed patients [3]. Converging neuroimaging evidence indicates that reappraisal engages the lateral and medial sectors of the dorsal/ventral prefrontal cortex and subcortical structures such as amygdala. Notably, these structures are also foci of brain network dysfunction in the neurological models of depression [4, 5] which propose that attenuated top-down cognitive control networks are companied with unrestrained activation in emotional regions (i.e., amygdala) [6–9]. Reappraisal may involve the utilization of cognitive control to regulate semantic representations of affective stimuli which in turn attenuate amygdala reactivity [10]. Moreover, reappraisal is generally viewed as an adaptive emotion regulation strategy which is dysfunctional in depression with less frequency of daily use [11] as well as abnormal neural activation patterns [9, 12, 13]. Therefore, reappraisal may be a promising target for disclosing the vulnerable characteristics of depression.

Operationally, reappraisal refers to a combination of approaches that require generation, maintenance, coordination of top-down cognitive reinterpretation, and bottom-up

appraisal of affective events and monitoring them in working memory over time [14]. Reappraisal strategies can vary in their goals (what is regulated) and tactics (how is emotion regulated), leading to multiple variants of experiment paradigm [15].

The circumplex model of affect suggests that all emotions can be distinguished in terms of varying levels of valence and arousal, with two distinct neural systems mediating the representation of affective states. It is addressed that common as well as distinct neural substrates underlie the regulation of different valences of emotion [16]. Primarily, there could be two reappraisal goals (what people want to achieve) that effectively regulate negative emotion: to upregulate positive emotion and downregulate negative emotion [15]. Positive emotion can be used to counter negative emotion in psychologically resilient individuals [17], spiral upward toward positive reappraisals, and transform negative affect into positive affect, leading to optimal functioning [18]. However, most studies of reappraisal in major depression focus on decreasing negative emotion, possibly due to excessive negative affect prevalent in MDD. To date only two studies to our knowledge explore positive emotion regulation in MDD, and they adopt different reappraisal working definitions. One study reports that depressed individuals fail to sustain activation in neural circuits underlying positive affect [19]. The other study finds no significant differences in downregulating positive affect by reappraisal between normal controls and MDD [12]. Neither study simultaneously investigates both processes, making it open to question whether only one or both processes are impaired. Positive and negative affect may facilitate the use of different sources of information, in terms of relation between self and situation [20]. Nonetheless, restriction to one valence makes it difficult to generalize the conclusion about reappraisal in common emotional state.

Another critical question remains to be answered is what is regulated. Reappraisal can be self- or situation-oriented [21]. The former focuses on reinterpreting the personal meaning of the emotional object to make it more or less self-relevant, while the latter focuses on reinterpreting the consequence or the reality of emotional stimuli without changing one's relationship to the stimuli [22]. In some studies, self-oriented reappraisal with decreasing affect as the regulating goal is also called detached reappraisal [23–25] or distancing reappraisal [15], which is efficient for emotion regulation [26]. In these studies, reappraisal is conceptualized as taking an objective or third-person perspective upon the emotional stimuli/situation. Reappraisal had been the target of clinical research on stress coping and CBT long before the conduction of laboratory experimental research on reappraisal as a form of emotion regulation. In line with this tradition, other researchers with social and clinical background deem self-distancing as a form of self-reflection and introduce psychological distance to distinguish adaptive versus maladaptive self-reflection [26–29]. Recent evidence has linked effectiveness of self-distancing to adaptive behavioral outcomes [27]. It is reported that depressed individuals can benefit from analyzing negative emotion events from a self-distancing perspective [28]. Moreover, evaluative rather than experiential self-referential processing is inherent in depression [30]. However, the modulatory effect of self-focused processing on reappraisal has been deemphasized. One feasible approach is to validate the role of self-focused processing in reappraisal and to manipulate reappraisal strategies along this dimension.

The purpose of this study was to examine the neural mechanisms of self-related reappraisal in Chinese MDD outpatients. Block designs were employed to avoid naturally declining emotion processes when watching emotionally arousing pictures. Emotion control areas such as dorsal lateral prefrontal cortex (dlPFC) and ventral medial prefrontal cortex (vmPFC) were selected as regions of interest since these two areas seemed to be involved in pathogenesis of depression and influence the expression of depressive symptoms [4, 31]. Amygdala was examined because it could act as a neural proxy for changes in emotion induction [22]. We hypothesized that (1) self-related neural networks underlying reappraisal would be differentially activated in depressed patients versus controls; (2) major depression would show abnormal neural activations underlying self-related reappraisal of affect.

2. Methods

2.1. Participants. Twelve unmedicated major depressed outpatients and 15 normal controls were recruited. The patients were diagnosed through a structured clinical interview according to DSM-IV. For depressed patients, an inclusion criterion with current depressed episode was adopted, according to the DSM-IV. All patients were assessed with SDS, BDI, and HAMD before participating into experiment, with mild to moderate depression symptoms (HAMD $\geq$ 18; BDI $\geq$ 14; SDS $\geq$ 35). For healthy controls, semi-standard interviews were conducted and assessed with SDS and BDI, with no current depressed mood (BDI $<$ 4 or SDS $<$ 50). For both groups, exclusion criteria were history of neurological disease or presence of axis I psychiatric disorders, psychiatric medication use within the last two weeks, or implanted cardiac or ferrous metal devices. The patients and normal controls were also assessed with BDI/SDS and the patients with HAMD (24-item version) additionally. Statistically significant differences were found in BDI and SDS scores (Table 1). A written informed consent was obtained from all subjects before experiment. This study was approved by the Ethics Committee of the Third Military Medical University.

2.2. Experimental Procedure. The participants were trained on a computer during a previous session to get familiar with the reappraisal strategies they were to use during the scan. They were instructed to either attend to the visual stimuli or reappraise (self-detached versus self-immersed) their emotion reactions to each picture. Tasks were performed in three consecutive sessions after acquisition of structural images. Emotional stimuli were selected from the International Affective Pictures System (IAPS) [32] and matched for content of scenes and people as well as valence and arousal for each condition (mean valence (V) and arousal (A): neutral/attend, $V = 5.06$, $A = 2.74$; positive/attend,

Table 1: Demographic and clinical data of MDD and normal control groups.

Measure	MDD Mean/SD (n = 12)	Control Mean/SD (n = 15)	Sig.
Gender ratio (male/female)	5/7	7/8	0.55
Age	29.50 (8.46)	25.80 (5.89)	0.07
Years of education	14.00 (3.77)	14.80 (2.83)	0.53
Handedness	right (12)	right (15)	—
BDI	26.17 (12.65)	4.27 (4.23)	0.00
SDS	64.08 (12.60)	36.54 (5.74)	0.00
HAMD	25.23 (4.97)		—

Note: BDI: beck depression inventory; SDS: self-rating depression scale. Both groups were matched for age, sex ratio, and years of education.

V = 7.17, A = 5.45; negative/attend, V = 2.34, A = 5.60; positive/detached, V = 7.26, A = 5.69; negative/detached, V = 2.69, A = 5.82; positive/immersed, V = 6.94, A = 5.30; negative/immersed, V = 2.42, A = 5.09). One-way ANOVA for stimuli in each session resulted in insignificant differences in arousal when taking valence as a factor (all Ps > 0.05). Twelve pictures were used for each valence under each condition and one more neutral picture for the start of each condition. The neutral picture was eliminated from MRI data analysis afterwards to prevent from signal drift.

For the attend condition (session 1), subjects should simply view the picture without taking efforts to alter their emotion; for the self-immersed conditions (session 2), subjects should perceive each picture as real and engage themselves in the situation depicted, by imagining themselves or a loved one in the scene; for the self-detached conditions (session 3), subjects should view the situation as fake or unreal and detach themselves from the situation. The attend condition was set as the control condition. Participants were told not to close their eyes or direct eyes away from the pictures during each trial and be able to relax during the break after each trial (Figure 1).

During the scanning, stimuli were projected onto a screen, reflected by a mirror in front of the subjects. The task was performed in three consecutive sessions ("maintain," "detach," and "immerse"), in the order of the last two sequentially counterbalanced across all subjects. The instruction for each condition was given at the beginning of each block. Each trial consisted of four components: fixation, induction or regulation, rating, and rest. A fixation cross was displayed for 2 s, and then an IAPS picture appeared for 8 s during which subjects either simply viewed or reappraised the picture, followed by an affect rating screen (1 = no intensity to 4 = very intense), and a black blank screen was shown for 8 s for relaxation. A four-point scale was chosen because it forces the subjects to make emotional judgments and was proved to be reliable for emotion discrimination in a previous study [33]. Affect ratings were collected using a two-button response box held in each hand. After experiment, all the subjects were inquired to confirm the effectiveness of emotion regulation.

Figure 1: Sequence of a trials in attend/reappraisal task. Instructions were given prior to each block.

2.3. MRI Data Acquisition. MRI data were collected on a Siemens 3T Allegra MRI scanner. A high-resolution T1-weighted 3D image (T1WI) was acquired, with slice thickness = 4 mm, field of view (FOV) = 240 × 240 × 240 mm^3, and matrix =256 × 256 × 256. Functional images were obtained from 30 gradient-echo T2*-weighted slices (slice thickness = 4 mm) per volume. A single shot gradient-recalled echo-echo planar imaging (SS-GRE-EPI) sequence was used with a time repetition of 2000 ms, a flip angle of 90°, time echo of 30 ms, FOV of 240 × 240 mm^2, matrix of 64 × 64, slice thickness of 4 mm, and slice interval of 0.8 mm. For coregistration, 176 sagittal whole-brain scans were collected by 3-D magnetization-prepared rapid gradient-echo imaging (MPRAGE), with TR = 1970 ms, TE = 3.93 ms, a flip angle = 15°, slice thickness = 1.70 mm, slice interval = 0.85 mm, FOV = 250 × 250 mm^2, and a matrix = 448 × 512.

2.4. Data Analysis

2.4.1. Self-Report Data. The emotional state ratings during the experiment were analyzed with PASW (Version 19, SPSS Inc., Chicago, IL, USA). A two-way ANOVA was conducted to analyze the effect of the emotional picture presentation (negative, neutral, positive) on emotional state in the viewing condition. A 2 × 3 × 2 repeated-measures ANOVA including the factors group (MDD, HC), valence (negative, positive), and condition (attend, self-detachment, self-immersion) was calculated to illuminate the effects of regulation on emotional state. The neutral condition was neglected for the second analysis as there was no neutral picture in the reappraisal condition.

2.4.2. Functional MRI Data. Data were preprocessed and statistically analyzed with SPM 8 (http://www.fil.ion.ucl.ac.uk/spm/software/spm8/) and Matlab 7.8.0 (Math Works, Natick,

MA). The preprocessing included realignment, spatial normalization, and spatial smoothing (8 mm).

GLM Analysis. The first level analysis consisted of seven regressors (attend neutral, attend positive, attend negative, decrease positive, decrease negative, increase positive, and increase negative) modeled with a duration of 8 seconds convolved with the hemodynamic response function. A high-pass filter was applied and six head motion parameters were included as residuals. In a second level analysis, we conducted a repeated measures general linear model (GLM) with emotion and reappraisal as within-subjects factors and group as a between-subjects factor. Post hoc t tests were then performed to examine contrasts between factors with significant main effects and interactions. Significant difference of statistical maps for whole brain analysis was set at $P < 0.05$, corrected for multiple comparisons using cluster-size thresholding (54 voxels^2) based on Monte Carlo simulation.

We then performed region of interest (ROI) analyses upon a priori region of interest implicated in emotion reactivity and regulation (bilateral dlPFC, vmPFC, and amygdala). If vmPFC and dlPFC are critical neural substrates for pathogenesis of depression, then damage to either area should affect the expression of depressive symptoms. We used anatomical masks based on the Talairach daemon database, defined by WFU Pick atlas software (version 3.0; ANSIR Laboratory, WFU School of Medicine, Winston-Salem, NorthCarolina), and set the threshold at $P < 0.05$ with an extent threshold of 5 voxels [34]. As to thresholding, the incorporation of extent threshold into P value effectively achieved equivalent correction for multiple comparisons [35]. ROI time courses were extracted within anatomically defined ROIs by generating the first eigenvariate of 8 mm around the peak voxels using a Matlab package REX (Response Exploration) [36]. Eigenvariates were extracted and global-scaled to produce a time series of functional data in units of percent signal change referenced to the SPM default intracerebral mean of 100.

Psychophysiological Interaction Analysis. This analysis was performed to identify the brain regions that produce a down-regulating effect on the amygdala during emotion regulation. A 10 mm seed region around the peak activation in bilateral amygdala was identified when we contrasted reappraisal and attends condition for each valence between two groups. Time series were extracted for each subject as the first regressor (physiological variable). The second regressor represented psychological variable (condition parameter). The regressor of interest was the interaction between the physiological variable and psychological variable, created from product time series of VOI and the condition parameter. We then created subtraction contrast between conditions of interests, and all individual contrast images were included into a second-level group random-effects analysis, in which task-dependent effects were investigated using a two-sample t test for two groups. Significant activations exhibiting PPI-related amygdala coupling were identified with a threshold $P < 0.001$ (uncorrected).

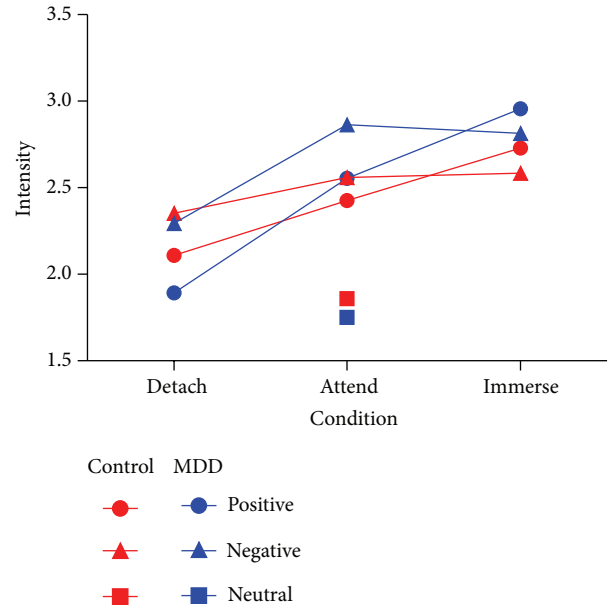

Figure 2: Means and standard deviations of intensity ratings after affect processing during the scan.

3. Results

3.1. Behavioral Results. A one-way ANOVA was computed to analyze the effect of picture type (positive, neutral, negative) on induced emotional reactivity during the attending task. A $2 \times 3 \times 2$ repeated-measures ANOVA was also conducted on factors including group (MDD, normal), condition (attend, self-detachment, self-immersion), and emotion (positive, negative) to examine the effects of cognitive reappraisal on emotional induction (Figure 2).

Emotion Reactivity. We observed a significant main effect of emotion (F (2, 22) = 44.9, $P < 0.001$) during the attending task. Pairwise comparisons showed that negative and positive trials differed from neutral trials ($P < 0.001$). There was no difference between MDD patients and normal controls ($P > 0.455$).

Emotion Regulation. The emotional state ratings yielded a significant main effect of condition (F (2, 21) = 15.620 P = 0.000, partial η^2 = 0.415) and emotion (F (1, 22) = 11.355, P = 0.003, partial η^2 = 0.340) and a significant interaction between condition and emotion (F (2, 21) = 14.215, P = 0.000, partial η^2 = 0.575). Either group main effect or group-related interactions were insignificant ($P > 0.05$). Post hoc contrasts indicated that emotional intensity was significantly regulated via self-detachment (P = 0.001) and self-immersion (P = 0.007), compared to the viewing condition and to each other (P = 0.001). These results suggested that both groups successfully regulated emotions without significant group differences.

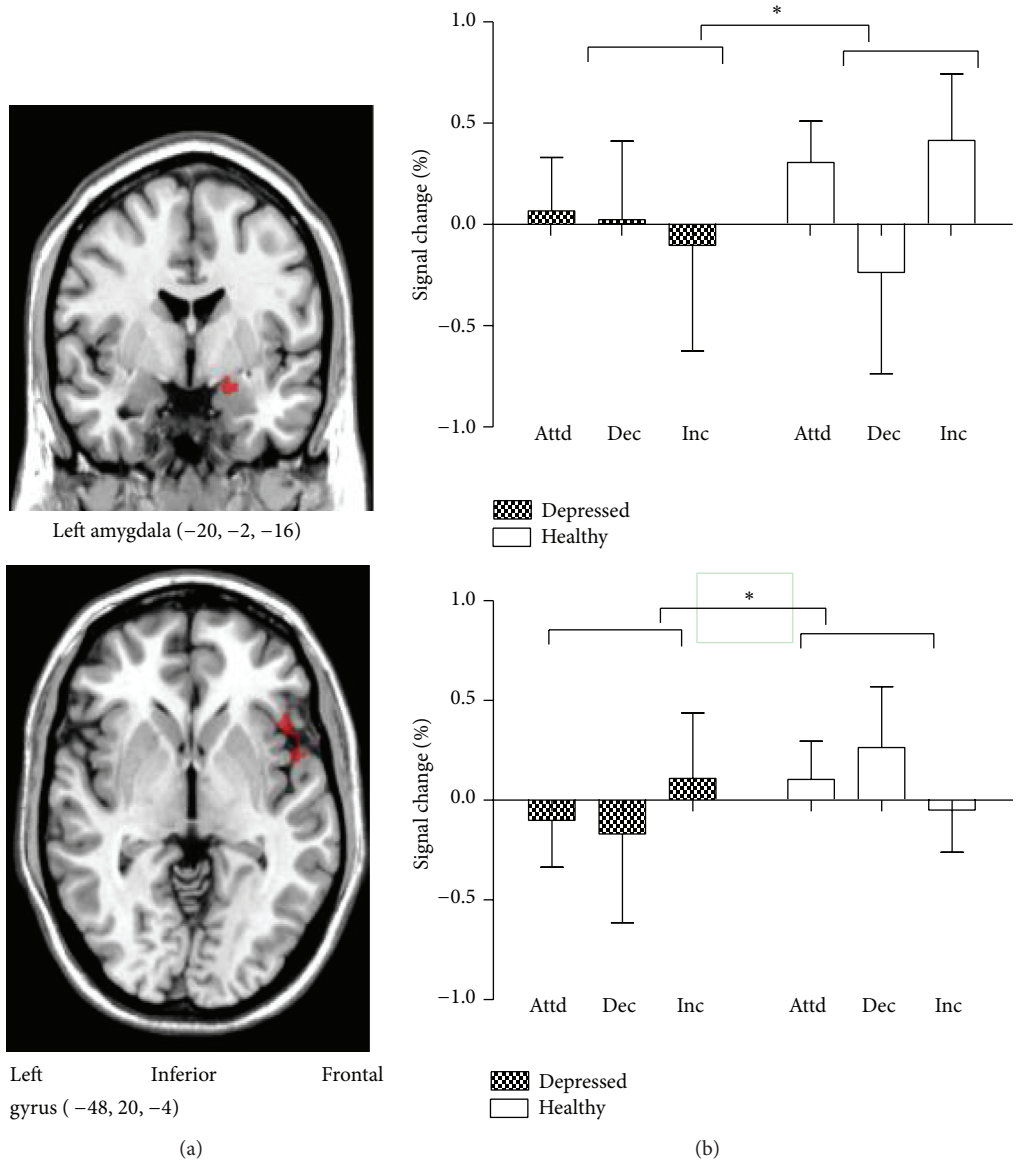

Figure 3: (a) Group × reappraisal interaction: regions activated in "attend," "detach," and "immerse" conditions in both groups. (b) Percent signal change for the following contrasts: "attend/emotional," "detach/emotional," and "immerse/emotional". Note: attd = attend; dec = detach; inc = immerse.

3.2. Functional MRI Results

3.2.1. Activation Analysis

Factor Analysis. We used a full factorial design ANOVA in the second-level group random-effects analysis. There was no significant group × reappraisal × emotion interaction. Group × reappraisal interactions were found in right medial temporal gyrus (MTG), left inferior frontal gyrus (IFG), left superior temporal gyrus (STG), right lingual gyrus, left thalamus, left amygdala, and left insula.

Regarding priori regions, we found activations in left inferior frontal gyrus (IFG) (109 voxels in left IFG, peak at (−48, 20, −4) $t = 3.07$, $P < 0.01$) and left amygdala (40 voxels in left amygdala, peak at (−20, −2, −16) $t = 2.42$, $P < 0.01$). A post hoc t-contrast revealed that the group × reappraisal interaction was explained by hypoactivation of left amygdala in "immerse minus attend" contrast, hypoactivation of left IFG in "detach minus attend" contrast, and hyperactivation of left IFG in "immerse minus attend" contrast. Percent signal changes in each ROI were extracted and entered into SPSS for group × reappraisal two-way ANOVA, resulting in similar activation-deactivation pattern (Figure 3). Because we did not observe significant three-way interaction between group, reappraisal, and emotion, we did not take emotional valence into account. We also observed main effects for group, emotion, and reappraisal.

Region of Interest Analysis. To identify the neural correlates of regulatory effects on amygdala activity due to reappraisal,

Table 2: PPI analysis of left amygdala seed for immersion/emotional condition in both groups.

Region of coactivation	Side	BA	Talairach coordinates			Z score
			x	y	z	
Control > MDD						
Middle temporal gyrus	L	39	−52	−70	30	2.18
Middle temporal gyrus	R	21	60	−18	−24	3.26
Superior temporal gyrus	R	38	44	18	−34	3.05
Medial frontal gyrus	L		−12	56	8	2.89
Control < MDD						
Insula	L		−40	−10	6	5.01
Middle frontal gyrus	R	9	42	42	32	2.75
Superior frontal gyrus	R		26	54	32	2.46
Inferior parietal lobule	R	40	42	−32	62	2.34
Precuneus	R	7	18	−36	58	2.19
Anterior cingulate	R	32	10	36	−10	2.16
Precuneus	L		−6	−44	50	1.97

we performed ROI analysis on bilateral amygdala using one-sample t test in the control group. For detach effects, we observed decreased amygdala activity during "attend/positive > detach/positive" contrast (9 voxels in left amygdala, peak at (−18, −4, −18) $t = 2.17$, $P < 0.05$) and decreased amygdala activity during "attend/negative > detach/negative" contrast (6 voxels in left amygdala, peak at (−20, −10, −10) $t = 2.57$, $P < 0.05$). For immerse effects, we observed increased amygdala activity during "immerse/positive > attend/positive" contrast (30 voxels in right amygdala, peak at (22, −6, −18) $t = 3.56$, $P < 0.005$) and during "immerse/negative > attend/negative" contrast (11 voxels in left amygdala, peak at (−18, −4, −26) $t = 2.77$, $P < 0.01$; 44 voxels in right amygdala, peak at (20, −4, −26) $t = 4.57$, $P < 0.001$). We performed similar test on the patient group and found no regulatory effects of amygdala in any individual contrast.

We then performed a two-sample t test for anatomical ROIs between MDD and the control group. The investigation of all contrasts of interest did not include bilateral amygdala, as no regulation effects of amygdala were found in patients and thus incomparable between groups. For "detach/positive > attend/positive" condition, left vmPFC showed greater activation for patients than for controls (15 voxels in left vmPFC, peak at (−4, 54, −10) $t = 2.61$, $P < 0.01$). For "detach/negative > attend/negative" condition, right dlPFC and vmPFC were more active in patients than in controls (8 voxels in right dlPFC, peak at (14, 40, 20) $t = 1.99$, $P < 0.05$; 37 voxels in right vmPFC, peak at (38, 34, −14) $t = 3.71$, $P < 0.001$; 18 voxels in right vmPFC, peak at (6, 52, −10) $t = 3.13$, $P < 0.005$; 53 voxels in right vmPFC, peak at (10, 34, 20) $t = 2.22$, $P < 0.05$). For "immerse/positive > attend/positive" condition, left vmPFC was more active in patients than in controls, and right vmPFC was more active in controls than in patients (20 voxels in left vmPFC, peak at (−4, 56, −6) $t = 2.23$, $P < 0.05$; 7 voxels in right vmPFC, peak at (24, 34, −12) $t = 0.02$, $P < 0.05$). For "immerse/negative > attend/negative" condition, right dlPFC and bilateral vmPFC showed greater activation for patients than for controls (12 voxels in right dlPFC, peak at (12, 40, 18) $t = 2.26$, $P < 0.05$; 12 voxels in left vmPFC, peak at (−4, 46, 12) $t = 1.84$, $P < 0.05$; 66 voxels in right vmPFC, peak at (10, 38, 18) $t = 2.52$, $P < 0.01$).

In patients, a regression analysis revealed that during detachment of positive emotion, downregulation of left amygdala negatively correlated with HAMD scores ($r = -0.608$, $P = 0.036$, two-tailed), suggesting that the more severe the depression symptom is, the less effective the downregulation of amygdala will be (Figure 4).

3.2.2. Psychophysiological Interaction Analysis. We are specifically interested in amygdala-cortical interactions during reappraisal. The PPI analysis revealed that compared to healthy controls, patients showed significantly enhanced coactivation of left amygdala with right dlPFC (MFG), right vmPFC (anterior cingulate), and right inferior parietal lobule (IPL) (Table 2).

4. Discussions

The current study extends previous findings about neural correlates of reappraisal in MDD along a self-relatedness dimension and confirms the hypotheses that self-relatedness may differentially modulate neural circuits underlying reappraisal for MDD versus normal group, demonstrating inflexible amygdala reactivity and strengthening frontolimbic connection in MDD. Since these neural circuits are involved in the pathology of depression [37], the current study may provide further evidence on how this abnormal functional connectivity pattern translates into emotion dysregulation in depression.

Behaviorally, IAPS stimuli significantly induced emotion in both groups ($P < 0.05$). In addition, both groups were equally effective in using reappraisal strategies to up- and downregulate emotions. Neurally, within-group region-of-interest analysis indicates the regulation effects of reappraisal on amygdala in controls, consistent with previous studies [38–40], suggesting neural correlates as more sensitive

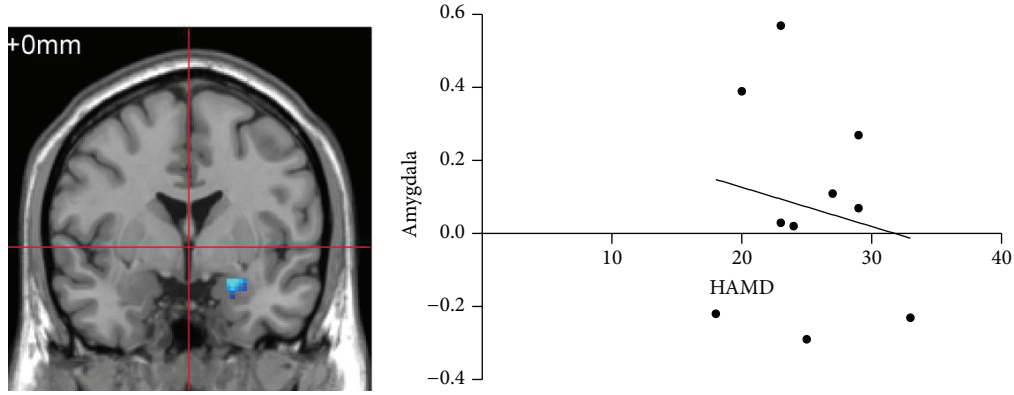

Figure 4: (a) Decreased activation in the left amygdala for patients during detachment of positive emotion. (b) The signal change of amygdala between the detachment and view conditions correlated negatively with HAMD scores ($r = -0.608$, $P = 0.036$).

indices of regulation outcome. It is noteworthy that this pattern of amygdala reactivity was not observed in the MDD group. Previous studies are inconclusive regarding whether the ability to regulate amygdala activation is deteriorated in MDD. One possible explanation for the discrepancy between studies is the heterogeneity of regulation goals, which use self-ratings of valence and/or arousal as behavioral measures. Some studies report that controls and depressed individuals show comparable amygdala responses to emotional stimuli in "detach > attend" contrast [6, 12, 41]. However, Johnstone's study does not observe "decrease-attend" reappraisal effect on amygdala activation in either controls or depressed patients [13]. Empirical evidence indicates that amygdala belongs to both valence and arousal networks [42]. In particular, amygdala is sensitive to arousal when valence remains unchanged and is dormant to valence changes when arousal remains constant [43]. Thus, regulation goals putatively cause distinct amygdala response patterns which may be ignored in previous studies.

Interestingly, Dillon's study using valence ratings as emotion responses revealed comparable regulation outcome between groups in increasing emotion, which differs from current study. Moreover, post hoc contrasts of repeated-measures ANOVA demonstrate that the left amygdala of depressed patients is less activated when immersion strategy is adopted regardless of valence (see in Figure 3). This blunted amygdala activity is aligned with an emotion context insensitivity (ECI) view which depicted flattened emotional responses typical of MDD [44]. Accordingly, event-related potential (ERP) study also addressed diminished brain responses during sustained processing of positive information [45]. Our study was comparable to previous study showing that depression fails to maintain positive emotions, with a different brain foci of positive emotion processing (ventral striatum) [19]. The disparity between studies is comprehensible in that our study adopted emotional arousal as an indicator of regulation outcome, while in Heller's study, emotional valence was adopted. Furthermore, less amygdala activity during immersion is also consistent with its role in representation with arousal [46].

In contrast to healthy controls, depressed individuals exhibit diminished activation in left IFG when detachment strategy is adopted and enhanced activation in left IFG when immersion technique is adopted (see in Figure 3). IFG (BA47) is implicated in inhibitory control in emotional as well as cognitive domains [47]. This abnormal control-related activation can be viewed as a functionally compensatory process in response to behavioral deficits, in spite of preserved emotion regulation behavioral measures for MDD. Altogether, the present results indicate compromised functioning of MDD in resistance to affective interference and inhibiting spontaneous emotional responses and supported the assumption that MDD emotion dysregulation is spanning negative as well as positive affect.

Our study observes that in depressed patients, left vmPFC is more strongly recruited for self-detachment from positive affect, while right vmPFC is more strongly activated for negative affect. Observations are similar concerning self-immersion strategy. Medial prefrontal cortex (MPFC) is central to neural models of depression [48]. In resting state, MDD patients exhibit overall increase in ventromedial PFC activation from pre- to posttreatment [49]. Task-related vmPFC activation is observed in self-oriented reappraisal [21] or when negative emotion is decreased [50]. VmPFC may be responsible for preattentively tagging both explicit and implicit incoming information as self-relevant [51, 52], representing the "Me" mode of self-reflection [53]. Our observations suggest that under both self-detached and self-immersed conditions, depressed patients show an excessive mode of self-relevance detection. This may in turn orient ongoing dorsal-ventral PFC connectivity, in line with positive correlation of elevations of negative affect with brain activations in medial PFC [54]. This self-focused cognitive tendency may constitute a basis for rumination style preferentially prevalent in depression [55].

We further assume that comparisons within each valence might suggest a possibility for hemispheric asymmetry of prefrontal cortex in MDD: left vmPFC is more involved in positive affect reappraisal and right vmPFC more in negative affect reappraisal. However, more conclusive results

may rely on ANOVA including "hemisphere" as one of the factors, which is not considered in this paper because SPM 8 does not allow four-way ANOVA. It is in line with the consensus that positive/negative emotion is parallel to approach/avoidance motivation system [56], which shows evidence of hemispheric specialization in MFG [57].

The PPI analysis exhibited a strengthened coupling between left amygdala and right prefrontal cortex (including dlPFC and vmPFC) and right IPL in MDD when increasing emotion. In comparison, two-sample t test of whole brain analysis showed enhanced activations of dlPFC and vmPFC in MDD, together with over-reactivity of limbic-paralimbic (insula, parahippocampal gyrus) and subcortical (thalamus) structures. DlPFC (BA9, 46) is seen as the neural substrate for emotion regulation [58] and is more preferentially engaged in negative than positive stimuli in depressed patients [59]. Furthermore, dlPFC is responsible for recruiting attention control resources in reappraisal [60] and is more engaged with increasing cognitive load [61]. This result further supports our proposal that MDD may have deficits in upregulating emotion accompanied with heightened inhibitory control. Right IPL is involved in downregulation of emotion through detachment in healthy and depressed group [12], while the absence of detachment-related coactivation with amygdala for MDD is not discussed. Our findings further address a strengthened coupling of right IPL and amygdala for MDD during enhancing emotion. IPL is associated with cognitive inhibition [62], taking the perspectives of others in processing visual information [63] or orienting away from salient stimuli [64]. Collectively, from detachment to immersion, impaired functional connectivity between IPL and amygdala emphasize that depressed patients may have deficits in reappraisal which is essential for regulating emotion in both directions.

A wealth of data suggests that amygdala, insula, and anterior temporal pole are responsible for separately mediating the cognitive, physiological, and experiential aspects of emotional responses, respectively [41]. The insula serves as a strategic neural node in the appraisal of emotional responses [65]. We observed strengthened task-related coupling of amygdala with insula; amygdala response under self-immersion condition was less active in patients than in controls, implying the attenuated ability of MDD to flexibly intensify emotion reactivity. This also confirms MDD's positive emotion dysregulation assumption.

In conclusion, depressed individuals tend to rely more on cognitive control brain networks and enhanced functional coupling between left amygdala and right prefrontal cortex when using reappraisal strategy accompanied by unrestrained self-related affective processing, which applies for both valence of emotion.

4.1. Implications and Limitations. There may be several clinical implications of our findings. First, group differences in the ability to regulate emotion may represent a sign of vulnerability to depressed mood and depressive disorders under stress [66]. Thus, focusing on affect regulation provides a ready bridge to intervention research [67]. Second, the abnormal prefrontal activation in response to an emotion-eliciting context may be second, since the amount of downregulation of positive emotion changes with depression severity, which does not necessarily disappear with symptom recovery or medication. The underlying neurobiological changes could be used to monitor the responsiveness of patients and the effectiveness of psychotherapy.

Until now, the effect of cross-culture variability on reappraisal strategies remains largely unknown. Our study may provide preliminary insights into relevant research. The linguistic nature of emotion regulation strategies may vary among different cultures. As previous findings suggest, emotion-regulation strategies may contribute to differences in emotional experience across western and east Asian cultures [68]. Hence, replication and comparative study between ethnic groups should be targeted.

The present research has several limitations. First, stimuli of personal relevance may need to be adopted (such as autobiographical experiences) in further study. Reappraisal involves momentary relevance and meaning of current stimuli which may vary among individuals, and subject-specific stimuli according to personal relevance may maintain stimulus consistency within individuals [69]. Second, this study does not allow making causal conclusions of reciprocal connection between brain regions. This issue could be further investigated with methods such as dynamic causal modeling (DCM) or granger causal modeling (GCM) for more confirmative conclusions about causal relations or in combination with ERP technique to keep track of ongoing mental processes on finer time scale. Third, the sample size of this study is small, but the findings are well aligned with previous studies of emotion regulation. The findings in this study can serve as a basis for further investigation with a larger sample size and stronger statistical power [70].

Abbreviations

dlPFC: Dorsal lateral prefrontal cortex
IFG: Inferior frontal gyrus
vmPFC: Ventral medial prefrontal cortex
DSM-IV: Fourth edition of Diagnostic and Statistical Manual of Mental Disorders
MDD: Major depressive disorder
CBT: Cognitive behavioral therapy
BDI: Beck depression inventory
SDS: Self-rating depression scale
HAMD: Hamilton rating scale for depression
IAPS: International affective pictures system
FOV: Field of view
TE: Time echo
TR: Time repetition
ROI: Region of interests
VOI: Volume of interests
PPI: Psychophysiological interaction.

Conflict of Interests

The authors declare that there is no conflict of interests regarding the publication of this paper.

Acknowledgments

This research was financially supported by National Natural Science Foundation of China (NSFC30970898). The authors gratefully acknowledge the valuable assistance of Professor Huaqing Meng (the First Affiliated Hospital of Chongqing Medical University, China) and Dr. Chenggang Jiang (Institute of Surgery Research of Daping Hospital, China) for patient recruitment, Dr. Jiuquan Zhang for professional advice of imaging data processing, and Chengju Liao, Jiawen Li, Yun Liu, and Liying Gan for helpful comments.

References

[1] A. Aldao, S. Nolen-Hoeksema, and S. Schweizer, "Emotion-regulation strategies across psychopathology: a meta-analytic review," *Clinical Psychology Review*, vol. 30, no. 2, pp. 217–237, 2010.

[2] H. Lee, A. S. Heller, C. M. van Reekum, B. Nelson, and R. J. Davidson, "Amygdala-prefrontal coupling underlies individual differences in emotion regulation," *Neuroimage*, vol. 62, no. 3, pp. 1575–1581, 2012.

[3] J.-A. Min, J. J. Yu, C. U. Lee, and J.-H. Chae, "Cognitive emotion regulation strategies contributing to resilience in patients with depression and/or anxiety disorders," *Comprehensive Psychiatry*, vol. 54, no. 8, pp. 1190–1197, 2013.

[4] S. G. Disner, C. G. Beevers, E. A. P. Haigh, and A. T. Beck, "Neural mechanisms of the cognitive model of depression," *Nature Reviews: Neuroscience*, vol. 12, no. 8, pp. 467–477, 2011.

[5] K. J. Ressler and H. S. Mayberg, "Targeting abnormal neural circuits in mood and anxiety disorders: from the laboratory to the clinic," *Nature Neuroscience*, vol. 10, no. 9, pp. 1116–1124, 2007.

[6] D. G. Dillon and D. A. Pizzagalli, "Evidence of successful modulation of brain activation and subjective experience during reappraisal of negative emotion in unmedicated depression," *Psychiatry Research: Neuroimaging*, vol. 212, no. 2, pp. 99–107, 2013.

[7] P. Kanske, J. Heissler, S. Schönfelder, and M. Wessa, "Neural correlates of emotion regulation deficits in remitted depression: the influence of regulation strategy, habitual regulation use, and emotional valence," *NeuroImage*, vol. 61, no. 3, pp. 686–693, 2012.

[8] G. Perlman, A. N. Simmons, J. Wu et al., "Amygdala response and functional connectivity during emotion regulation: a study of 14 depressed adolescents," *Journal of Affective Disorders*, vol. 139, no. 1, pp. 75–84, 2012.

[9] M. J. Smoski, S. L. Keng, C. E. Schiller, J. Minkel, and G. S. Dichter, "Neural mechanisms of cognitive reappraisal in remitted major depressive disorder," *Journal of Affective Disorders*, vol. 151, no. 1, pp. 171–177, 2013.

[10] J. T. Buhle, J. A. Silvers, T. D. Wager et al., "Cognitive reappraisal of emotion: a meta-analysis of human neuroimaging studies," *Cereb Cortex*, 2013.

[11] N. Garnefski and V. Kraaij, "The cognitive emotion regulation questionnaire: psychometric features and prospective relationships with depression and anxiety in adults," *European Journal of Psychological Assessment*, vol. 23, no. 3, pp. 141–149, 2007.

[12] S. Erk, A. Mikschl, S. Stier et al., "Acute and sustained effects of cognitive emotion regulation in major depression," *Journal of Neuroscience*, vol. 30, no. 47, pp. 15726–15734, 2010.

[13] T. Johnstone, C. M. van Reekum, H. L. Urry, N. H. Kalin, and R. J. Davidson, "Failure to regulate: counterproductive recruitment of top-down prefrontal-subcortical circuitry in major depression," *Journal of Neuroscience*, vol. 27, no. 33, pp. 8877–8884, 2007.

[14] K. N. Ochsner and J. J. Gross, "Thinking makes it so: a social cognitive neuroscience approach to emotion regulation," in *Handbook of Self-Regulation: Research, Theory, and Applications*, R. F. Baumeister and K. D. Vohs, Eds., pp. 229–255, 2004.

[15] K. McRae, B. Ciesielski, and J. J. Gross, "Unpacking cognitive reappraisal: goals, tactics, and outcomes," *Emotion*, vol. 12, no. 2, pp. 250–255, 2012.

[16] A. K. Y. Mak, Z.-G. Hu, J. X. Zhang, Z.-W. Xiao, and T. M. C. Lee, "Neural correlates of regulation of positive and negative emotions: an fMRI study," *Neuroscience Letters*, vol. 457, no. 2, pp. 101–106, 2009.

[17] M. M. Tugade and B. L. Fredrickson, "Resilient individuals use positive emotions to bounce back from negative emotional experiences," *Journal of Personality and Social Psychology*, vol. 86, no. 2, pp. 320–333, 2004.

[18] E. L. Garland, B. Fredrickson, A. M. Kring, D. P. Johnson, P. S. Meyer, and D. L. Penn, "Upward spirals of positive emotions counter downward spirals of negativity: insights from the broaden-and-build theory and affective neuroscience on the treatment of emotion dysfunctions and deficits in psychopathology," *Clinical Psychology Review*, vol. 30, no. 7, pp. 849–864, 2010.

[19] A. S. Heller, T. Johnstone, A. J. Shackman et al., "Reduced capacity to sustain positive emotion in major depression reflects diminished maintenance of fronto-striatal brain activation," *Proceedings of the National Academy of Sciences of the United States of America*, vol. 106, no. 52, pp. 22445–22450, 2009.

[20] F. A. Huppert, "Positive emotions and cognition developmental, neuroscience and health perspectives," in *Proceedings of the 8th Sydney Symposium*, 2005.

[21] K. N. Ochsner, R. D. Ray, J. C. Cooper, E. R. Robertson, S. Chopra, J. D. E. Gabrieli et al., "For better or for worse: neural systems supporting the cognitive down- and up-regulation of negative emotion," *NeuroImage*, vol. 53, no. 1, pp. 11–20, 2004.

[22] R. D. Ray and D. H. Zald, "Anatomical insights into the interaction of emotion and cognition in the prefrontal cortex," *Neuroscience and Biobehavioral Reviews*, vol. 36, no. 1, pp. 479–501, 2012.

[23] I. A. Cristea, A. S. Tatar, D. Nagy, and D. David, "The bottle is half empty and that's bad, but not tragic: differential effects of negative functional reappraisal," *Motivation and Emotion*, vol. 36, no. 4, pp. 550–563, 2012.

[24] M. N. Shiota and R. W. Levenson, "Effects of aging on experimentally instructed detached reappraisal, positive reappraisal, and emotional behavior suppression," *Psychology and Aging*, vol. 24, no. 4, pp. 890–900, 2009.

[25] M. N. Shiota and R. W. Levenson, "Turn down the volume or change the channel? Emotional effects of detached versus positive reappraisal," *Journal of Personality and Social Psychology*, vol. 103, no. 3, pp. 416–429, 2012.

[26] E. Kross and Ö. Ayduk, "Boundary conditions and buffering effects: does depressive symptomology moderate the effectiveness of self-distancing for facilitating adaptive emotional analysis?" *Journal of Research in Personality*, vol. 43, no. 5, pp. 923–927, 2009.

[27] E. Kross and O. Ayduk, "Making meaning out of negative experiences by self-distancing," *Current Directions in Psychological Science*, vol. 20, no. 3, pp. 187–191, 2011.

[28] E. Kross, D. Gard, P. Deldin, J. Clifton, and O. Ayduk, "'Asking why" from a distance: its cognitive and emotional consequences for people with major depressive disorder," *Journal of Abnormal Psychology*, vol. 121, no. 3, pp. 559–569, 2012.

[29] Y.-L. Wang, Y.-C. Lin, C.-L. Huang, and K.-H. Yeh, "Benefitting from a different perspective: the effect of a complementary matching of psychological distance and habitual perspective on emotion regulation," *Asian Journal of Social Psychology*, vol. 15, no. 3, pp. 198–207, 2012.

[30] C. Lemogne, H. Mayberg, L. Bergouignan et al., "Self-referential processing and the prefrontal cortex over the course of depression: a pilot study," *Journal of Affective Disorders*, vol. 124, no. 1-2, pp. 196–201, 2010.

[31] S. Grimm, C. F. Schmidt, F. Bermpohl et al., "Segregated neural representation of distinct emotion dimensions in the prefrontal cortex—an fMRI study," *NeuroImage*, vol. 30, no. 1, pp. 325–340, 2006.

[32] P. J. Lang, M. M. Bradley, and B. N. Cuthbert, *International Affective Picture System (IAPS): Affective Ratings of Pictures and Instruction Manual*, University of Florida, Gainesville, Fla, USA, 2008.

[33] P. Vrtička, D. Sander, and P. Vuilleumier, "Effects of emotion regulation strategy on brain responses to the valence and social content of visual scenes," *Neuropsychologia*, vol. 49, no. 5, pp. 1067–1082, 2011.

[34] K. McRae, K. N. Ochsner, I. B. Mauss, J. J. D. Gabrieli, and J. J. Gross, "Gender differences in emotion regulation: an fMRI study of cognitive reappraisal," *Group Processes & Intergroup Relations*, vol. 11, no. 2, pp. 143–162, 2008.

[35] S. J. Banks, K. T. Eddy, M. Angstadt, P. J. Nathan, and K. L. Phan, "Amygdala-frontal connectivity during emotion regulation," *Social Cognitive and Affective Neuroscience*, vol. 2, no. 4, pp. 303–312, 2007.

[36] E. P. Duff, R. Cunnington, and G. F. Egan, "REX: response exploration for neuroimaging datasets," *Neuroinformatics*, vol. 5, no. 4, pp. 223–234, 2007.

[37] Y. Liao, X. Huang, Q. Wu, C. Yang, W. Kuang, and M. Du, "Is depression a disconnection syndrome? Meta-analysis of diffusion tensor imaging studies in patients with MDD," *Journal of Psychiatry & Neuroscience*, vol. 38, no. 1, pp. 49–56, 2013.

[38] N. R. Giuliani, K. McRae, and J. J. Gross, "The up- and down-regulation of amusement: experiential, behavioral, and autonomic consequences," *Emotion*, vol. 8, no. 5, pp. 714–719, 2008.

[39] H. K. Sang and S. Hamann, "Neural correlates of positive and negative emotion regulation," *Journal of Cognitive Neuroscience*, vol. 19, no. 5, pp. 776–798, 2007.

[40] J. Lévesque, F. Eugène, Y. Joanette et al., "Neural circuitry underlying voluntary suppression of sadness," *Biological Psychiatry*, vol. 53, no. 6, pp. 502–510, 2003.

[41] M. Beauregard, V. Paquette, and J. Levesque, "Dysfunction in the neural circuitry of emotional self-regulation in major depressive disorder," *Neuroreport*, vol. 17, no. 8, pp. 843–846, 2006.

[42] L. B. Baucom, D. H. Wedell, J. Wang, D. N. Blitzer, and S. V. Shinkareva, "Decoding the neural representation of affective states," *NeuroImage*, vol. 59, no. 1, pp. 718–727, 2012.

[43] A. K. Anderson and N. Sobel, "Dissociating intensity from valence as sensory inputs to emotion," *Neuron*, vol. 39, no. 4, pp. 581–583, 2003.

[44] L. M. Bylsma, B. H. Morris, and J. Rottenberg, "A meta-analysis of emotional reactivity in major depressive disorder," *Clinical Psychology Review*, vol. 28, no. 4, pp. 676–691, 2008.

[45] A. Y. Shestyuk, P. J. Deldin, J. E. Brand, and C. M. Deveney, "Reduced sustained brain activity during processing of positive emotional stimuli in major depression," *Biological Psychiatry*, vol. 57, no. 10, pp. 1089–1096, 2005.

[46] F. C. Murphy, I. Nimmo-Smith, and A. D. Lawrence, "Functional neuroanatomy of emotions: a meta-analysis," *Cognitive, Affective and Behavioral Neuroscience*, vol. 3, no. 3, pp. 207–233, 2003.

[47] D. E. Payer, K. Baicy, M. D. Lieberman, and E. D. London, "Overlapping neural substrates between intentional and incidental down-regulation of negative emotions," *Emotion*, vol. 12, no. 2, pp. 229–235, 2012.

[48] C. Lemogne, P. Delaveau, M. Freton, S. Guionnet, and P. Fossati, "Medial prefrontal cortex and the self in major depression," *Journal of Affective Disorders*, vol. 136, no. 1-2, pp. e1–e11, 2012.

[49] M. Ritchey, F. Dolcos, K. M. Eddington, T. J. Strauman, and R. Cabeza, "Neural correlates of emotional processing in depression: changes with cognitive behavioral therapy and predictors of treatment response," *Journal of Psychiatric Research*, vol. 45, no. 5, pp. 577–587, 2011.

[50] H. L. Urry, C. M. van Reekum, T. Johnstone et al., "Amygdala and ventromedial prefrontal cortex are inversely coupled during regulation of negative affect and predict the diurnal pattern of cortisol secretion among older adults," *Journal of Neuroscience*, vol. 26, no. 16, pp. 4415–4425, 2006.

[51] L. T. Rameson, A. B. Satpute, and M. D. Lieberman, "The neural correlates of implicit and explicit self-relevant processing," *NeuroImage*, vol. 50, no. 2, pp. 701–708, 2010.

[52] T. W. Schmitz and S. C. Johnson, "Relevance to self: a brief review and framework of neural systems underlying appraisal," *Neuroscience and Biobehavioral Reviews*, vol. 31, no. 4, pp. 585–596, 2007.

[53] K. N. Ochsner and J. J. Gross, "Putting the "I" and the "Me" in emotion regulation: reply to Northoff," *Trends in Cognitive Sciences*, vol. 22, no. 2, pp. 126–131, 2005.

[54] C. S. Carter, "The ups and downs of emotion regulation," *Biological Psychiatry*, vol. 65, no. 5, pp. 359–360, 2009.

[55] J. Roelofs, L. Rood, C. Meesters et al., "The influence of rumination and distraction on depressed and anxious mood: a prospective examination of the response styles theory in children and adolescents," *European Child and Adolescent Psychiatry*, vol. 18, no. 10, pp. 635–642, 2009.

[56] M. Mneimne, A. S. Powers, K. E. Walton, D. S. Kosson, S. Fonda, and J. Simonetti, "Emotional valence and arousal effects on memory and hemispheric asymmetries," *Brain and Cognition*, vol. 74, no. 1, pp. 10–17, 2010.

[57] J. M. Spielberg, G. A. Miller, A. S. Engels et al., "Trait approach and avoidance motivation: lateralized neural activity associated with executive function," *NeuroImage*, vol. 54, no. 1, pp. 661–670, 2011.

[58] K. N. Ochsner, S. A. Bunge, J. J. Gross, and J. D. E. Gabrieli, "Rethinking feelings: an fMRI study of the cognitive regulation of emotion," *Journal of Cognitive Neuroscience*, vol. 14, no. 8, pp. 1215–1229, 2002.

[59] B.-T. Lee, S. W. Cho, H. S. Khang et al., "The neural substrates of affective processing toward positive and negative affective pictures in patients with major depressive disorder," *Progress in Neuro-Psychopharmacology and Biological Psychiatry*, vol. 31, no. 7, pp. 1487–1492, 2007.

[60] K. McRae, B. Hughes, S. Chopra, J. D. E. Gabrieli, J. J. Gross, and K. N. Ochsner, "The neural bases of distraction and reappraisal," *Journal of Cognitive Neuroscience*, vol. 22, no. 2, pp. 248–262, 2010.

[61] L. F. van Dillen, D. J. Heslenfeld, and S. L. Koole, "Tuning down the emotional brain: an fMRI study of the effects of cognitive load on the processing of affective images," *NeuroImage*, vol. 45, no. 4, pp. 1212–1219, 2009.

[62] S. L. Warren, L. D. Crocker, J. M. Spielberg, A. S. Engels, M. T. Banich, B. P. Sutton et al., "Cortical organization of inhibition-related functions and modulation by psychopathology," *Frontiers in Human Neuroscience*, vol. 7, article 271, 2013.

[63] H. Shibata and T. Inui, "Brain activity associated with recognition of appropriate action selection based on allocentric perspectives," *Neuroscience Letters*, vol. 491, no. 3, pp. 187–191, 2011.

[64] B. E. Benson, M. W. Willis, T. A. Ketter, A. Speer, T. A. Kimbrell, and M. S. George, "Interregional cerebral metabolic associativity during a continuous performance task (part II): differential alterations in bipolar and unipolar disorders," *Psychiatry Research: Neuroimaging*, vol. 164, no. 1, pp. 30–47, 2008.

[65] R. Veit, V. Singh, R. Sitaram, A. Caria, K. Rauss, and N. Birbaumer, "Using real-time fMRI to learn voluntary regulation of the anterior insula in the presence of threat-related stimuli," *Social Cognitive and Affective Neuroscience*, vol. 7, no. 6, pp. 623–634, 2012.

[66] C. A. Burghy, D. E. Stodola, P. L. Ruttle, E. K. Molloy, J. M. Armstrong, and J. A. Oler, "Developmental pathways to amygdala-prefrontal function and internalizing symptoms in adolescence," *Nature Neuroscience*, vol. 15, no. 12, pp. 1736–1741, 2012.

[67] M. Kovacs, J. Joormann, and I. H. Gotlib, "Emotion (Dys) regulation and links to depressive disorders," *Child Development Perspectives*, vol. 2, no. 3, pp. 149–155, 2008.

[68] E. Davis, E. Greenberger, S. Charles, C. Chen, L. Zhao, and Q. Dong, "Emotion experience and regulation in China and the United States: how do culture and gender shape emotion responding?" *International Journal of Psychology*, vol. 47, no. 3, pp. 230–239, 2012.

[69] J. J. Campos, E. A. Walle, A. Dahl, and A. Main, "Reconceptualizing emotion regulation," *Emotion Review*, vol. 3, no. 1, pp. 26–35, 2011.

[70] A. K. Y. Mak, M. M. C. Wong, S.-H. Han, and T. M. C. Lee, "Gray matter reduction associated with emotion regulation in female outpatients with major depressive disorder: a voxel-based morphometry study," *Progress in Neuro-Psychopharmacology and Biological Psychiatry*, vol. 33, no. 7, pp. 1184–1190, 2009.

Hindawi Publishing Corporation
BioMed Research International
Volume 2014, Article ID 542526, 12 pages
http://dx.doi.org/10.1155/2014/542526

Clinical Study

Does rTMS Alter Neurocognitive Functioning in Patients with Panic Disorder/Agoraphobia? An fNIRS-Based Investigation of Prefrontal Activation during a Cognitive Task and Its Modulation via Sham-Controlled rTMS

Saskia Deppermann,[1] Nadja Vennewald,[2] Julia Diemer,[3] Stephanie Sickinger,[1] Florian B. Haeussinger,[1] Swantje Notzon,[2] Inga Laeger,[2] Volker Arolt,[2] Ann-Christine Ehlis,[1] Peter Zwanzger,[2,4] and Andreas J. Fallgatter[1,5,6]

[1] *Department of Psychiatry and Psychotherapy, University of Tuebingen, Calwerstr 14, 72076 Tuebingen, Germany*
[2] *Mood and Anxiety Disorders Research Unit, Department of Psychiatry and Psychotherapy, University of Muenster, Albert-Schweitzer-Campus 1, Building A9, 48149 Muenster, Germany*
[3] *Department of Clinical Psychology and Psychotherapy, Universitaetsstr 31, 93053 Regensburg, Germany*
[4] *kbo-Inn-Salzach-Hospital, Gabersee 7, 83512 Wasserburg am Inn, Germany*
[5] *Graduate School LEAD, University of Tuebingen, Europastr. 6, 72072 Tuebingen, Germany*
[6] *Cluster of Excellence CIN, University of Tuebingen, Otfried-Mueller-Str. 25, 72076 Tuebingen, Germany*

Correspondence should be addressed to Saskia Deppermann; saskia.deppermann@med.uni-tuebingen.de

Received 4 October 2013; Revised 10 January 2014; Accepted 11 January 2014; Published 18 March 2014

Academic Editor: Qiyong Gong

Objectives. Neurobiologically, panic disorder (PD) is supposed to be characterised by cerebral hypofrontality. Via functional near-infrared spectroscopy (fNIRS), we investigated whether prefrontal hypoactivity during cognitive tasks in PD-patients compared to healthy controls (HC) could be replicated. As intermittent theta burst stimulation (iTBS) modulates cortical activity, we furthermore investigated its ability to normalise prefrontal activation. *Methods*. Forty-four PD-patients, randomised to sham or verum group, received 15 iTBS-sessions above the left dorsolateral prefrontal cortex (DLPFC) in addition to psychoeducation. Before first and after last iTBS-treatment, cortical activity during a verbal fluency task was assessed via fNIRS and compared to the results of 23 HC. *Results*. At baseline, PD-patients showed hypofrontality including the DLPFC, which differed significantly from activation patterns of HC. However, verum iTBS did not augment prefrontal fNIRS activation. Solely after sham iTBS, a significant increase of measured fNIRS activation in the left inferior frontal gyrus (IFG) during the phonological task was found. *Conclusion*. Our results support findings that PD is characterised by prefrontal hypoactivation during cognitive performance. However, verum iTBS as an "add-on" to psychoeducation did not augment prefrontal activity. Instead we only found increased fNIRS activation in the left IFG after sham iTBS application. Possible reasons including task-related psychophysiological arousal are discussed.

1. Introduction

According to DSM-IV, panic disorder (PD) is characterised by the sudden onset of unexpected panic attacks resulting in constant worries about possible reasons and negative consequences of the attacks. Moreover, in the case of comorbid agoraphobia, this eventually leads to behavioural avoidance of situations from which escape might be difficult in case of an attack [1]. On a neurobiological level, functional imaging studies of PD-patients with and without agoraphobia have found hypoactivity of the prefrontal cortex (PFC), paired with hyperactivity of fear relevant brain structures such as the amygdala, suggesting an inadequate inhibition by the PFC in response to anxiety-related stimuli [2–4]. In fact,

hypofrontality of PD-patients has not just been observed in response to emotional stimuli [5], but also during cognitive tasks without any emotional content. For example, in a near-infrared spectroscopy study, Nishimura et al. [6] reported hypoactivation of the left PFC in particular while Ohta et al. [7] found that PD-patients as well as patients with a depressive disorder showed lower bilateral prefrontal activation than healthy controls during a verbal fluency task. Moreover, Nishimura et al. [8] investigated a potential relation between the frequency of panic attacks/agoraphobic avoidance and PFC activation during a cognitive task, indeed finding an association between altered activation patterns in the left inferior prefrontal cortex and panic attacks as well as between the anterior part of the right PFC and the severity of agoraphobic avoidance.

Cortical activation patterns can be selectively modified by means of repetitive transcranial magnetic stimulation (rTMS) via electromagnetic induction [9]. This way, rTMS has been shown to modulate neurotransmitter release [10] and—depending on its stimulation frequency—normalise prefrontal hypoactivity [11]. In fact, even though results are still inconsistent [12], rTMS has been shown to have a moderate antidepressant effect [13, 14]. Within this framework it is of special interest that the method does not just seem to alter affective states but also cognitive functioning [15, 16].

Functional near-infrared spectroscopy (fNIRS) is an imaging method which allows for a less complicated and faster application compared to other imaging methods such as functional magnetic resonance imaging (fMRI) or positron emission tomography (PET) [17]. Especially psychiatric patients with claustrophobic fears benefit from the fact that they merely need to sit in a chair while optodes that emit and receive near-infrared light are attached to their heads [18]. This way, task-related changes in oxygenated and deoxygenated haemoglobin concentrations can be examined. Even though disadvantages such as a relatively low spatial resolution (approximately 3 cm), a limited penetration depth (approximately 2 to 3 cm) [19, 20], and influences of extracranial signals do exist (for a review see [21]), fNIRS has proven to be a useful tool in psychiatric research [22].

Based on these findings and considerations, the goal of the current study was to (1) clarify whether the findings of Ohta et al. [7] concerning prefrontal hypoactivity in PD-patients compared to healthy controls during a cognitive paradigm (verbal fluency task) could be replicated via fNIRS in a larger sample. Also, a sham-controlled rTMS protocol was applied over the time course of three weeks above the left DLPFC to (2) examine whether excitatory rTMS can serve as an adequate tool in order to improve cognitive dysfunction in terms of prefrontal hypoactivation in PD-patients. In this regard, the patients' behavioural performance during the verbal fluency task was also taken into account.

2. Materials and Methods

2.1. Participants. Patients were recruited via the outpatient departments of the two study centres, advertisement in newspapers, as well as the internet and information material sent to local physicians. Exclusion criteria for all participants were age under 18 and over 65 years, pregnancy, and severe somatic disorders (e.g., cardiovascular disease, epilepsy, and neurological disorders). Also, patients fulfilling rTMS contraindications such as ferromagnetic implants or significant abnormalities in routine EEG were excluded. All patients were diagnosed with PD with or without agoraphobia according to DSM-IV-TR criteria [1]. Nonprominent comorbid psychiatric disorders (except for bipolar or psychotic disorder, borderline personality disorder, acute substance abuse disorders, and acute suicidality) were no exclusion criteria. Psychopharmacological treatment was permitted if the dosage had been stable for at least three weeks prior to baseline assessment ($t1$). Benzodiazepines, tricyclic antidepressants (except for Opipramol), and antipsychotics (expect for Quetiapine with maximal dosage of 50 mg) were excluded. Healthy controls who suffered from any axis-I psychiatric disorder (except for specific phobia) or had a family history of psychiatric disorders were excluded. A total of 23 controls and 44 PD-patients, of which 22 were randomised to the sham and 22 to the verum rTMS group, were selected for the study. Groups did not differ with respect to gender, age, years of education, and handedness (Table 1). After a comprehensive study description, written informed consent was obtained. The study was approved by the Ethics Committees of the Universities of Muenster and Tuebingen and all procedures were in accordance with the latest version of the Declaration of Helsinki.

2.2. Design. PD-patients received a total of 15 rTMS applications during three weeks at one of the study centres (Muenster or Tuebingen). Before the first and after the last rTMS-session brain activation was assessed with fNIRS while patients were performing a cognitive task. Between the first and the second fNIRS assessment, all patients received three group sessions of psychoeducation concerning PD. Healthy control subjects attended the two fNIRS measurements but received no rTMS in-between. Enrolment took place between January 2011 and July 2013. Patients and therapists were blinded to rTMS group assignment. This investigation was conducted within the framework of a larger study which included 9 weeks of cognitive behavioral therapy for patients with panic disorder/agoraphobia and additional fNIRS investigations described elsewhere (Deppermann et al., in preparation [23]).

2.3. Psychoeducation. Psychoeducation sessions were held in groups of up to 6 participants and were conducted by trained psychologists, who were supervised regularly by clinical psychotherapists. A state-of-the-art, standardised treatment manual was used [24, 25]. The content of the sessions included information about the pathogenesis of PD and agoraphobia, the vicious cycle of anxiety, somatic components of anxiety, and the sharing of personal experiences among the patients.

Table 1: Sociodemographic sample characteristics.

	Age mean (range)	Gender	Handedness	First language	Years of education mean (SD)	Duration of illness in months mean (range)
Group						
Controls	33.4 (19–64)	14 females 9 males	20 right 3 left	22 German 1 bilingual	12.5 (1.1)	—
Sham	36.3 (22–56)	14 females 8 males	21 right 1 left	19 German 2 bilingual 1 other	12.4 (2.0)	84 (1–336)
Verum	37.6 (19–63)	13 females 9 males	20 right 2 left	19 German 1 bilingual 2 other	12.1 (1.7)	92 (1–372)
Comparisons						
Controls versus Sham	$t_{43} = -0.921$ $P = 0.362$	$\chi^2_1 = 0.037$ $P = 0.848$	$\chi^2_1 = 1.003$ $P = 0.317$	$\chi^2_2 = 1.531$ $P = 0.465$	$t_{33} = -0.234$ $P = 0.816$	—
Controls versus Verum	$t_{43} = -1.148$ $P = 0.257$	$\chi^2_1 = 0.015$ $P = 0.903$	$\chi^2_1 = 0.178$ $P = 0.673$	$\chi^2_2 = 2.198$ $P = 0.333$	$t_{37} = -0.913$ $P = 0.367$	—
Sham versus Verum	$t_{42} = -0.399$ $P = 0.692$	$\chi^2_1 = 0.096$ $P = 0.757$	$\chi^2_1 = 0.358$ $P = 0.550$	$\chi^2_2 = 0.667$ $P = 0.717$	$t_{42} = 0.490$ $P = 0.626$	$t_{42} = -0.290$ $P = 0.773$

SD: standard deviation.

2.4. Verbal Fluency Task (VFT). All subjects were assessed twice within a three-week interval between the first ($t1$) and the second ($t2$) measuring time.

During the measurements participants sat in a comfortable chair and were advised to keep their eyes closed and relax in order to avoid head or body movements. The VFT consisted of a phonological, a semantical and a control task. During the phonological task, subjects were instructed to produce as many nouns as possible beginning with a certain letter, whereas during the semantical task they had to name as many nouns as possible belonging to a certain category while repetitions and proper nouns were supposed to be avoided. During the control task the participants were instructed to repeat the weekdays in a speed that approximately matched the number of recited days to the number of mentioned nouns. The VFT started with a resting state phase of 10 seconds followed by the different tasks and more resting state periods, which lasted 30 seconds each. The sequence of the three tasks and resting phases were repeated three times, each time with a different letter or category. The letters and categories were chosen from the "Regensburger Wortflüssigkeitstest" [26]. Different letters/categories were used at $t1$ and $t2$ and counterbalanced between subjects. During the resting phase, participants were told to relax.

2.5. rTMS. Starting after the first fNIRS measurement, intermittent theta burst stimulation (iTBS, [27]) was applied in the patient group during 15 daily sessions on workdays during three weeks with a figure-of-eight coil (MCF-B65, 2 × 75 mm diameter, $n = 34$, MAGSTIM 9925-00, 2 × 70 mm, $n = 9$) by means of a MagOption/MagPro X100 stimulator (MagVenture, Denmark, $n = 34$) and a MAGSTIM RAPID^2 T/N 3567-23-02 stimulator ($n = 9$), respectively. ITBS was used in order to achieve a facilitating effect on cortex excitability, as this could be demonstrated for the motor cortex, but also for more frontal cortex areas in previous studies [27, 28]. The iTBS protocol consisted of a total of 600 pulses applied in intermittent biphasic bursts at a frequency of 15 pulses per second via 2 second trains, starting every 10 seconds as described by Huang et al. [27]. The time of day for iTBS application did not vary for more than 2 hours from one day to the next. As the circadian rhythm is known to influence cortical excitability [29] the participants' individual resting motor threshold was determined prior to each iTBS session on the left motor cortex and stimulation intensity was set to 80% of this threshold. Stimulation site was F3 (left DLPFC) according to the international 10–20 system for electrode placement [30]. In order to ensure that the site of stimulation stayed constant over all sessions, F3 was drawn onto an individual textile cap for each participant prior to the first session. Additionally, other orientation points as the nasion, the inion, and the auricles were sketched on. While the coil was held tangentially to the scalp forming a 45° angle to the mid-sagittal line of the head (handling pointing in a posterior direction) for verum stimulation, it was flipped away from the scalp in a 90° angle for the sham stimulation. The post-fNIRS measurement ($t2$) was set to be conducted no earlier than 12 hours after the last rTMS-session to avoid the measurement of *acute* rTMS effects.

2.6. fNIRS. Relative temporal changes in oxygenated (O_2Hb) and deoxygenated haemoglobin (HHb) were measured from a 10-second baseline using the ETG-4000 optical topography system (Hitachi Medical Co., Japan). For this purpose, the ETG-4000 uses laser diodes which emit light of two wavelengths (695 ± 20 nm and 830 ± 20 nm) and photodetectors which receive the scattered light intensity. Since the main light absorbers in this setup are the two types of haemoglobin,

changes in measured light intensity between the emitter-detector pairs can be related to haemodynamic changes—which are coupled to neural activation—using a modified Beer-Lambert equation [31]. Altogether the probe set consisted of 16 photodetectors and 17 light emitters arranged in a 3 × 11 fashion with an interoptode distance of 3 cm resulting in 52 distinctive channels with a penetration depth of approximately 2 to 3 cm [19, 20]. The probe set was attached over the participants' prefrontal cortex having the central optode of the lowest row on FPz stretching out towards T3 and T4, respectively, according to the 10–20 international EEG system [32]. The sampling frequency was 10 Hz. The unit used to quantify haemoglobin concentration changes was mmol × mm. Subsequently, the recorded data were averaged over the corresponding blocks and exported into Matlab R2012b (The Math Works Inc., Natick, USA) where they were first corrected for changes in the NIRS signal that were not directly due to functional changes in haemoglobin concentration related to the attended tasks. To this end, frequencies that exceeded 0.05 Hz were removed using a low pass filter and clear technical artefacts (e.g., due to an optode losing contact to the scalp during measurement) were corrected by means of interpolation by replacing the values of the corresponding channels with the values of the circumjacent channels in a Gaussian manner (closer channels were taken more into account). In order to further remove artefacts, due to head movements, a correlation-based signal improvement (CBSI) procedure according to Cui et al. [33] was applied, adjusting the values for each channel by the equation

$$[\text{CBSI}] = 0.5 * \left([\text{O}_2\text{Hb}] - \frac{\text{std}[\text{O}_2\text{Hb}]}{\text{std } [\text{HHb}] * [\text{HHb}]} \right).$$

According to this approach, cortical activation should result in a negative correlation between O_2Hb and HHb concentrations so in case of positive correlations the O_2Hb signal is adjusted. Even though exceptions regarding a strictly negative correlation during brain activation exist [34], Brigadoi et al. [35] showed promising results for this procedure. Finally, the CBSI adjusted signal was once more interpolated in a Gaussian manner by using an inner-subject variance threshold of 4 as an interpolation criterion, assuming that exceeding values were most likely the result of further artefacts. Altogether a total of 5% of all channels were replaced.

After preprocessing, the data were averaged for all three groups within a time frame of 0–45 seconds after the onset of each task. The amplitude integrals in CBSI concentration between 5 and 40 seconds were taken as the basis for statistical analysis as a delay of the haemodynamic response after task onset can be assumed.

2.7. Regions of Interest (ROI). Based on prior studies investigating verbal fluency [6–8, 36, 37], different a priori ROIs were defined. Accordingly, in addition to temporal areas (middle and superior temporal gyrus (MSTG)) and the inferior frontal gyrus (IFG) comprising Broca's area, the DLPFC is also supposed to be critically involved when performing a VFT. Corresponding channels were chosen using a virtual registration procedure as described by Tsuzuki et al. [38], Rorden and Brett [39], and Lancaster et al. [40] (cf. Figure 1).

2.8. Clinical Assessment. PD with or without agoraphobia was diagnosed by experienced clinical psychologists with the German version of the Structured Clinical Interview for DSM-IV, Axis I Disorders (SCID-I [41, 42]). Anxiety was measured with the following questionnaires: *Panic and Agoraphobia Scale* (PAS; [43]), *Hamilton Anxiety Rating Scale* (HAM-A; [44]), and *Cardiac Anxiety Questionnaire* (CAQ; [45, 46]). All questionnaires were completed at $t1$ and $t2$. For all scales, higher scores indicate more severe symptoms.

In case of missing questionnaire items, a last observation carried forward analysis (LOCF) was conducted. If less than 10% of all items were left out, missing values were substituted by the participant's mean on the relevant scale.

2.9. Statistical Analyses. All analyses were conducted with IBM SPSS Statistics 20 and 21, respectively. The sample characteristics were assessed by means of χ^2 tests (gender, handedness, and first language) or t-tests (age, years of education, duration of illness for patients, and questionnaire data for $t1$ and $t2$), directly comparing the experimental groups (active versus sham, sham versus controls, and active versus controls). If numbers for the corresponding categories were below 5, Fisher's exact test was considered instead of asymptotic significance. The effects of patients' blinding regarding rTMS treatment condition were evaluated using binomial tests (test proportion: 0.5) for the subjectively perceived rTMS condition in each patient group, separately. The optimal sample size was determined based on previous studies investigating the effect of high-frequency rTMS on symptom severity in depression (e.g., [47]). The effect size of such a treatment protocol was estimated to approximate 0.5, while power was defined as 80%. The α-level was set to 5%. Since the effect of rTMS protocols in patients suffering from anxiety disorders is still difficult to quantify [48], it was decided to follow a more conservative assessment resulting in a target sample size of $n = 40$ patients.

For baseline assessment, fNIRS-data for all ROIs were analysed by means of analyses of variance (ANOVA) with the between-subject factor group (patients versus controls). The corresponding behavioural performance was analysed accordingly. In order to verify that changes in CBSI concentration were task-related, effects of hemispheric lateralisation were further analysed using a 2 × 3 repeated measurement ANOVA (RM-ANOVA) with the within-subject factors hemisphere (left versus right) and task (semantical versus phonological versus control task). As the factor time was of no relevance within this context, the corresponding data were averaged across the two measurement times. Accordingly, the phonological and semantical task should elicit a left lateralisation in the language relevant ROIs (IFG & MSTG) [36].

To evaluate the effects of rTMS on prefrontal activity, 2×3 RM-ANOVAs for each ROI and cognitive task were conducted (within-subject factor time ($t1$ versus $t2$), between-subject factor group (verum versus sham versus controls)).

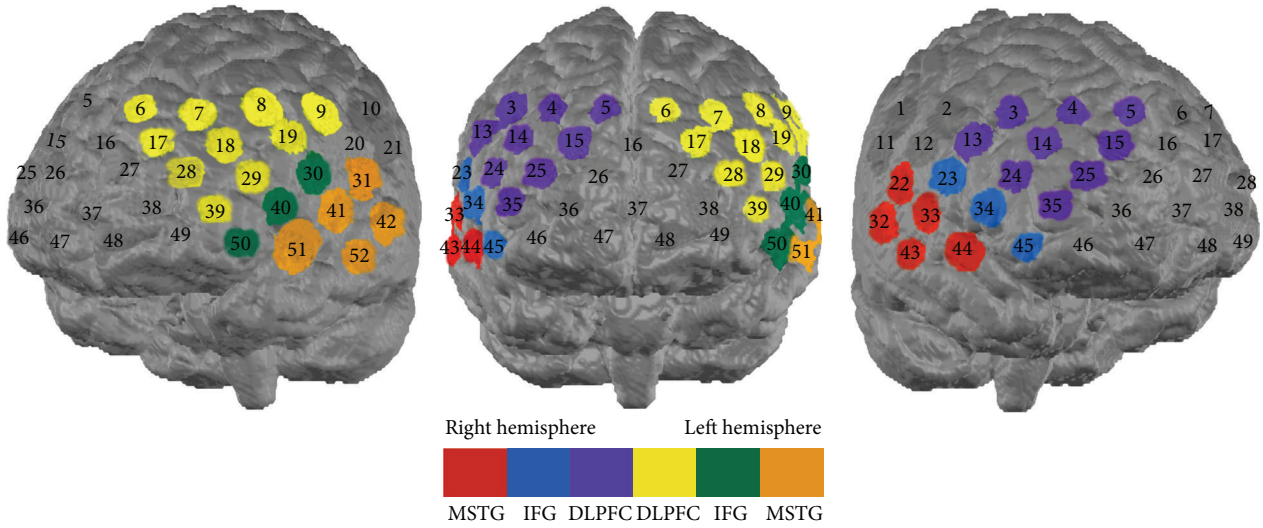

Figure 1: Probe set arrangement with numbers indicating channels. DLPFC: dorsolateral prefrontal cortex, IFG: inferior frontal gyrus, MSTG: middle superior temporal gyrus, color-coded channels were used for analyses.

The total number of produced nouns for the phonological and semantical task was investigated according to the collected fNIRS-data via a 2 × 3 RM-ANOVA with the within-subject factors time ($t1$ versus $t2$) and the between-subject factor group (verum versus sham versus controls). The number of weekdays was not considered in the analysis as it was matched to fit the number of nouns in the other tasks.

In case of violations of the sphericity assumption, the degrees of freedom in the ANOVAs were corrected using the Greenhouse-Geisser or Huynh-Feldt procedure depending on ε ($\varepsilon > 0.75$ Huynh-Feldt, $\varepsilon < 0.75$ Greenhouse-Geisser; see [49]). To avoid α-error accumulation due to multiple testing, the significance level of $\alpha = 0.05$ was adjusted using a Bonferroni-Holm (BH) [50] correction procedure for the ROIs in each hemisphere, separately. Post hoc analysis was conducted by means of two-tailed t-tests for paired and independent samples.

In order to assess the relationship between cortical activation and behavioural performance, correlations between the number of recited words and CBSI-concentration were calculated at $t1$ and $t2$ for each group and task separately by means of Spearman's rho. To further directly consider changes over time, correlations between the differences ($t2$–$t1$) in CBSI concentrations and number of recited words were calculated. For post hoc t-tests and correlations, one-tailed P-values were considered in case of directed hypotheses.

3. Results

3.1. Sample Characteristics. Tables 1 and 2 give an overview of the sociodemographic sample characteristics at baseline and clinical questionnaire data for $t1$ and $t2$. Sociodemographic data did not differ between groups. For the clinical questionnaire data, no significant differences emerged between the sham and verum stimulated group for $t1$. Verum group versus controls and sham group versus controls, respectively, revealed significant differences on all scales in the expected directions (data shown for HAM-A, self-rated PAS, and CAQ, Table 2).

When patients were asked to guess whether they had received active or sham rTMS, 16 patients in the sham group thought that they had been sham stimulated while 5 thought that it had been the active protocol. Fourteen patients in the verum group thought they had obtained the active protocol and 4 said that they received a placebo treatment. Additionally, 5 patients (1 sham, 4 verum) did not reply to the question. For each patient group, these guesses differed significantly from chance (binomial test, sham group: $P = 0.027$ and verum group: $P = 0.031$).

3.2. Behavioural Performance. Table 3 contains means and standard deviations for the number of produced nouns for the phonological as well as the semantical task for each group and each measuring time.

With respect to behavioural data, no significant baseline differences could be found between patients and controls. Further the 2×3 RM-ANOVA revealed no significant changes for either the phonological or the semantical task.

3.3. Prefrontal Activity at Baseline. Because one patient missed $t2$, the fNIRS-data of this subject were excluded from all analyses. Concerning the remaining subjects, significant results were found for all ROIs on both hemispheres for the phonological task (Figure 2) whereby the healthy controls displayed more activation than the patients (left DLPFC: $F_{1,65} = 9.304$, $P = 0.003$, left MSTG: $F_{1,65} = 8.795$, $P = 0.004$, left IFG: $F_{1,65} = 5.279$, $P = 0.025$, right DLPFC: $F_{1,65} = 11.649$, $P = 0.001$, right MSTG: $F_{1,65} = 5.158$, $P = 0.026$, right IFG: $F_{1,65} = 8.130$, $P = 0.006$, all P BH-corrected). For the semantical task significant differences in terms of higher activation in the healthy controls were found only for the DLPFC bilaterally (left DLPFC: $F_{1,65} = 6.189$, $P = 0.015$,

Table 2: Clinical characteristics of all groups, before and after rTMS treatment.

Group	$t1$ HAM-A mean (SD)	$t2$ HAM-A mean (SD)	$t1$ Self-rated PAS mean (SD)	$t2$ Self-rated PAS mean (SD)	$t1$ CAQ mean (SD)	$t2$ CAQ mean (SD)
Controls	3.83 (3.20)[a,b]	2.74 (3.57)[c,d]	0.22 (1.04)[a,b]	0.13 (0.34)[c,d]	0.33 (0.20)[a,b]	0.33 (0.22)[c,d]
Sham	20.3 (7.10)	15.20 (8.81)[e]	20.52 (8.10)	15.34 (8.30)[e]	1.36 (0.51)	1.06 (0.65)[f]
Verum	22.41 (8.97)	18.37 (10.05)[e]	20.76 (7.76)	14.91 (6.90)[f]	1.63 (0.71)	1.20 (0.71)[f]

Over the course of treatment, the degree of assessed symptoms on HAM-A, self-rated PAS, and CAQ significantly declined in the verum and sham stimulated group. However, no significant differences after rTMS-treatment between these two groups occurred. [a]$P < 0.001$ compared with sham rTMS ($t1$); [b]$P < 0.001$ compared with verum rTMS ($t1$); [c]$P < 0.001$ compared with sham rTMS ($t2$); [d]$P < 0.001$ compared with verum rTMS ($t2$); [e]$P < 0.01$ t-test for paired samples; [f]$P < 0.001$ t-test for paired samples; CAQ: cardiac anxiety questionnaire, HAM-A: Hamilton Anxiety Rating Scale, PAS: Panic and Agoraphobia Scale, rTMS: repetitive transcranial magnetic stimulation, SD: standard deviation, $t1$: measuring time 1, and $t2$: measuring time 2.

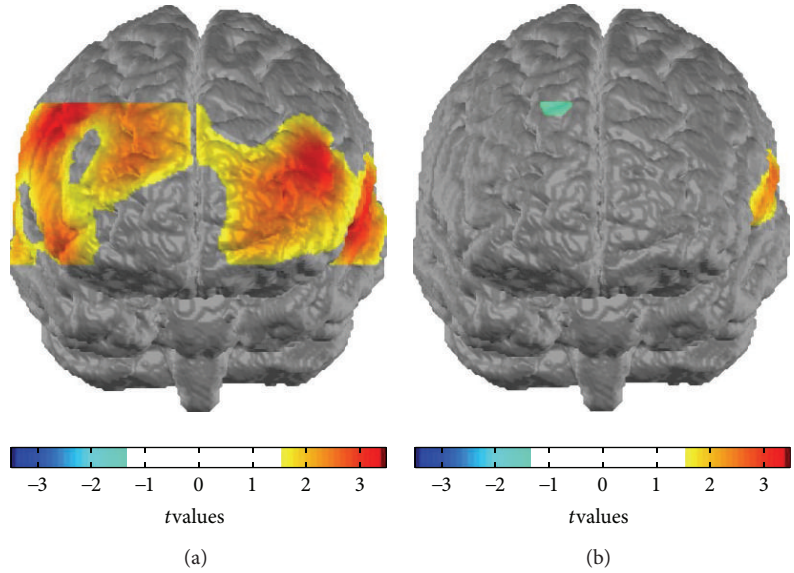

Figure 2: Contrast maps phonological task. Differential CBSI concentration levels contrasted between groups ((a) controls versus PD-patients and (b) verum versus sham) for the phonological task at baseline. Differences in CBSI levels between groups are depicted by means of t-values for each channel, whereby only values for $t \geq 1.7$ are shown.

right DLPFC: $F_{1,65} = 11.176$, $P = 0.001$, all P BH-corrected). For the control task no significant differences were found (Figure 3).

3.4. Effects of Hemispheric Lateralisation. Regarding hemispheric lateralisation effects, the 2 × 3 RM-ANOVA showed a significant main effect for the two language related ROIs IFG ($F_{1,65} = 15.030$, $P < 0.001$ (< 0.0167, BH-corrected)) and MSTG ($F_{1,65} = 8.317$, $P = 0.005$ (< 0.025, BH-corrected)) where activation—as indicated by CBSI concentration—was higher for the left hemisphere. A significant main effect of task was identified for all ROIs (DLPFC: $F_{2,100} = 24.275$ $P < 0.001$ (<0.0167, BH-corrected), MSTG: $F_{2,100} = 55.974$ $P < 0.001$ (<0.025, BH-corrected), and IFG: $F_{2,100} = 61,718$ $P < 0.001$ (<0.05, BH-corrected)). The interaction hemisphere∗task was significant for the IFG ($F_{2,130} = 8.151$, $P < 0.001$ (<0.0167, BH-corrected) and the MSTG ($F_{2,114} = 3.478$, $P = 0.040$ (<0.05, BH-corrected)). Post hoc analyses showed that this was due to a left lateralisation concerning the phonological (IFG, right versus left: $t_{65} = -3.734$, $P < 0.001$ and MSTG, right versus left: $t_{65} = -2.983$, $P = 0.002$) and partly the semantical (IFG, right versus left: $t_{65} = -4.034$, $P < 0.001$) task while there was no significant difference for the control task. Regarding the DLPFC, no significant main effect of hemisphere was found, whereas the interaction hemisphere∗task was significant ($F_{2,130} = 11.040$, $P < 0.001$ (< 0.025, BH-corrected)). For the DLPFC, results were in contrast to the above-mentioned findings with a significant lateralisation effect in terms of increased activation in the right hemisphere for the control task ($t_{65} = 5.072$, $P < 0.001$) but no significant difference for the two active verbal fluency tasks. Differences between tasks were significant for all comparisons for the IFG (right hemisphere: $t_{65} \geq 2.7$, $P \leq 0.005$ and left hemisphere: $t_{65} \geq 3.37$, $P < 0.001$) and left MSTG ($t_{65} \geq 3.322$, $P < 0.001$) with activation during the phonological task > activation during the semantical task > the control task. For the right hemisphere of the DLPFC, activation during the phonological task was also higher than for the semantical task ($t_{65} = 6.083$, $P < 0.001$). For the left DLPFC, participants showed similar activation patterns as for the IFG and left MSTG with respect to the three test tasks

Table 3: Number of produced nouns for phonological and semantical task for $t1$ and $t2$.

Time	Controls		Sham		Verum	
	Phonological mean (SD)	Semantical mean (SD)	Phonological mean (SD)	Semantical mean (SD)	Phonological mean (SD)	Semantical mean (SD)
$t1$	20 (7.6)	37.2 (7.2)	18.4 (7.2)	33.2 (7.4)	16.9 (6.4)	34.3 (7.8)
$t2$	19.7 (7.0)	38.2 (10.1)	19.2 (7.2)	32.5 (7.4)	19.4 (7.8)	35.5 (8.8)

SD: standard deviation, $t1$: measuring time 1, and $t2$: measuring time 2 after 3 weeks.

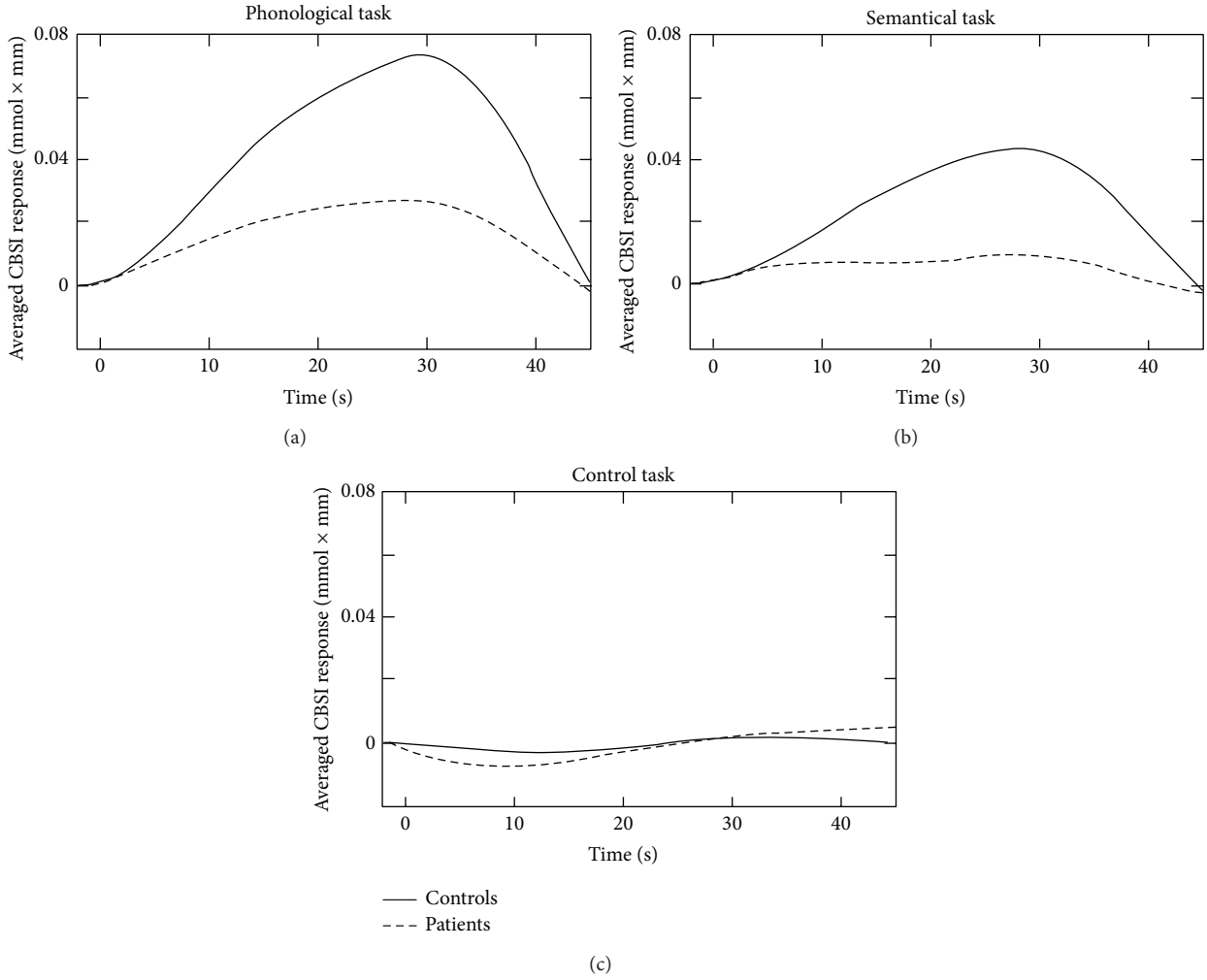

Figure 3: Haemodynamic response function of the left dorsolateral prefrontal cortex at the baseline measurement, averaged over all subjects for each task, separately.

(phonological > semantical > control, for all: $t_{65} \geq 3.114$, $P \leq 0.0015$).

3.5. Effects of rTMS on Prefrontal Activity. For the left DLPFC, the analyses of the phonological task showed a significant main effect of group ($F_{2,63} = 5.32$, $P = 0.007$ (<0.0167, BH-corrected)). Post hoc analyses revealed that this was due to significantly lower cortical activation of patients in the sham ($t_{42} = -2.13$, $P = 0.02$) and verum group ($t_{43} = -2.74$, $P = 0.005$) compared to healthy controls. No significant interaction effect of time and group or main effect of time was found. For the right DLPFC, a significant main effect of group ($F_{2,63} = 5.34$, $P = 0.007$ (<0.0167, BH-corrected)) was found. No significant effect of time or significant interaction effect of time and group existed with respect to the phonological task. Post hoc t-tests displayed similar results as for the left DLPFC. Verum and sham stimulated patients showed a reduced activation compared to healthy controls (for both: $t_{32} \leq -2.348$, $P \leq 0.013$).

For the semantical task, a significant main effect of group was found for the left and the right DLPFC (for both: $F_{2,63} \geq 5.30$, $P \leq 0.007$ (<0.0167, BH-corrected)). For both areas, actively stimulated patients showed a significantly reduced cortical activation compared to healthy controls (left DLPFC: $t_{35} = -2.78$, $P = 0.005$ and right DLPFC: $t_{43} = -2.60$, $P = 0.007$). Also, sham stimulated patients showed significant hypoactivation compared to healthy participants with respect to the right ($t_{38} = -3.19$, $P = 0.002$) and left DLPFC ($t_{34} = -2.316$, $P = 0.014$). No significant main effects of time or significant interactions of time and group were discerned for the left and right DLPFC, respectively. No significant differences between sham and verum stimulated patients existed with regard to the left or right DLPFC for the phonological and semantical task, respectively.

The analyses of the control task for the left and right DLPFC revealed neither significant main effects of group nor significant main effects of time. Also, no significant interaction effects of time and group were found.

For reasons of clarity, solely significant results for the IFG with respect to the three test tasks are depicted in Table 4. For the MSTG, no significant outcomes were found.

3.6. Correlations between fNIRS Data and Behavioural Performance. At baseline, no significant correlations between CBSI concentration and the number of recited words were found for either PD-patients or for the healthy controls. At the second measurement time, a relationship was merely found for the healthy controls in terms of negative correlations for all ROIs, except for the right DLPFC with the number of recited words during the phonological task (left DLPFC: $r = -0.416$, $P = 0.024$, left MSTG: $r = -0.431$, $P = 0.020$, left IFG: $r = -0.452$, $P = 0.015$, right MSTG: $r = -0.534$, $P = 0.004$, right IFG: $r = -0.558$, $P = 0.003$, all P BH-corrected). Regarding changes over time, significant results existed only during the phonological task in the two patients' groups. In this context, an increase in the number of recited words was significantly associated with a decrease in CBSI concentration (resp., vice versa) for the DLPFC (sham, left DLPFC: $r = -0.498$, $P = 0.011$, verum, left DLPFC: $r = -0.485$, $P = 0.011$, verum, right DLPFC: $r = -0.607$, $P = 0.001$, all P BH-corrected). As all correlations were negative, they were only considered explorative, as positive correlations were hypothesized and one-sided tests were conducted.

4. Discussion

The present study aimed to confirm the finding that PD-patients are characterised by prefrontal hypoactivation during cognitive tasks as compared to healthy controls [7]. Moreover, it additionally addressed the question whether a potential hypoactivation of the PFC can be normalised by means of repeated iTBS. Patients with PD were investigated via fNIRS while performing a VFT prior to and after receiving daily prefrontal iTBS application over a time course of three weeks in addition to weekly group sessions of psychoeducation. The VFT-results were compared with those of healthy control subjects.

Regarding our first hypothesis, our results are in line with the above-mentioned findings concerning hypofrontality during cognitive tasks in PD-patients. With respect to our second hypothesis, unexpectedly, an increase in activation over time could only be found for the left IFG in sham stimulated patients.

In more detail, before the start of rTMS treatment, differences in cortical activation (as indicated by CBSI data) between patients and controls were observed for specific task conditions of the VFT. In fact, as predicted by our hypothesis, patients did not differ from controls during the control task but displayed decreased prefrontal activation in all ROIs during the phonological task and partly also during the semantical task. The missing differences during the control task indicate that the differences in CBSI concentration between healthy controls and patients during the two active tasks were indeed due to altered cognitive processing and not to more general effects elicited by the measurement situation. Still, it cannot be excluded that our fNIRS signal may have been affected by components that are not directly related to cognitive processing but still lead to a (task-related) change in blood flow and hence a change of the measured signal. Regarding more general effects that might influence the fNIRS signal, a recent study by Takahashi et al. [51] showed that the verbal fluency task is particularly affected by confounding effects due to stress induced skin blood flow, especially for NIRS channels located over the forehead. In order to verify that we still mainly measured cortical activation, we presumed that lateralisation effects in terms of increased left hemispheric activation should be found for language related areas such as the MSTG and IFG but not for the DLPFC. Further, increases in these two ROIs should only exist for the semantical and phonological but not for the control task. In line with previous studies [36] we could confirm these assumptions and accordingly ascribe our finding mainly to differences in cortical activation.

Contrary to our second hypothesis, no significant changes in prefrontal activation after rTMS treatment could be found in the verum group. In fact, the only significant change was found for the sham group which showed an increase in CBSI concentration in the left IFG during the phonological task. As at first glance these findings are hard to interpret and we further analysed the prefrontal activation patterns in relation to the behavioural performance of healthy controls and the two patients groups.

When regarding only the behavioural data, descriptively, healthy controls could name more nouns than both patients groups; however, this difference was not significant. Further, when associating CBSI concentrations in the different ROIs with the number of recited nouns at baseline, no significant correlations could be revealed for either group. Interestingly, however, at the second measurement time, negative correlations between the behavioural performance and activation patterns in nearly all ROIs existed for the healthy controls. Even though we originally applied one-sided testing (assuming a positive relationship between behavioural performance and cortical activation), we still think that it is worthwhile to give these negative correlations some considerations as they might be helpful for a better understanding of our results.

Table 4: Significant results for the cognitive tasks with respect to the IFG.

ROI	df (df error)	F	P	Verum versus sham	Verum versus controls	Sham versus controls	Paired t-tests
Left IFG-phonological task							
Time × Group	2 (63)	5.23	0.008 (<0.0167, BH-corrected)	$t1$: ns. $t2$: ns.	$t1$: ns. $t2$: ns.	$t1$: S < HC** $t2$: ns.	S: $t1 < t2$* V: ns. HC: ns.

*significant at a significance level of ≤0.05, **significant at a significance level of ≤0.01, BH-corrected: Bonferroni-Holm-corrected, HC: healthy controls, IFG: inferior frontal gyrus, S: sham group, and V: verum group.

Similar to the finding in healthy controls, negative associations between changes in the number of recited nouns from $t1$ to $t2$ and changes in DLPFC activation bilaterally during the phonological task could be found for both patients groups. In order to interpret these results in a meaningful way, it has to be considered that multiple distinct mechanisms might have an influence on the fNIRS signal. Firstly, according to our hypothesis, it can be assumed that a demanding cognitive task leads to an increase in cortical activation which then triggers a certain performance at the behavioural level. In this context, higher cortical activation should lead to a better behavioural performance as it implies that more cognitive resources can be recruited to fulfil the task as well as possible. From another perspective, one could also assume that in subjects with a highly efficient cortical processing (i.e., in case of a subjectively nonchallenging task situation) fewer cognitive resources are needed to achieve good results. In this case, low cortical activation should be associated with high behavioural performance. However, it needs to be kept in mind that the fNIRS signal might not just contain components which are due to cortical activation but might also be influenced by extracranial signal components that relate to peripheral processes such as psychophysiological arousal induced changes in blood flow. In particular, in frontopolar regions, these components have been shown to also trigger an increase in the fNIRS signal due to stress induced vasodilation during a verbal fluency task [51]. In this context, higher CBSI concentrations might then also be associated with a decrease in behavioural performance as it can be presumed that too much psychophysiological arousal should have a negative effect on cognitive functioning. Even though we tried to control for such arousal effects by performing a control task and considering lateralisation effects, we cannot exclude the fact that it still had an effect on our results.

Accordingly, we conclude that we could not find any significant correlations at the baseline measurement time as psychophysiological arousal was probably very high for all participants, hence having confounding effects on the fNIRS signal components due to cortical activation. At the second measurement time, cortical activation should have been the same for the healthy controls while arousal may have decreased for some participants as the situation was more familiar, leading to a reduction in signal intensity and negative correlations with behavioural performance due to improved cognitive function (with reduced arousal). While it cannot be excluded that these negative correlations also imply that the task was not challenging enough for some of the healthy subjects, the study by Takahashi et al. [51] points more in favour of an interpretation in terms of a decrease in psychophysiological arousal. In fact, the authors could show that already a repetition of the verbal fluency task within one measurement could lead to a significant repetition effect by means of a decrease in psychophysiological arousal and associated fNIRS signal intensity.

Concerning the PD-patients, psychophysiological arousal should have also decreased but possibly not as much as in the healthy controls as the measurement situation still represented a typical panic-relevant situation (patients had to sit in a small room with the fNIRS probe set attached to their heads so a sudden escape was not possible). At the same time it can be expected that arousal effects, which are prominent in the frontopolar area of the PFC, also have an effect especially on the DLPFC which cannot be neglected [52]. A possible explanation especially for the influence of DLPFC activation through the frontopolar region is given by Kirilina et al. [53] who found that the vein responsible for arousal effects in the forehead also stretches out to dorsolateral regions. Consequently, apparent effects of a slight decrease in arousal would most likely be expected in the DLPFC, hence explaining the negative correlations between changes in behavioural performance and changes in CBSI concentrations for the patients. Even though correlations between CBSI concentrations and behavioural performance during the semantical task were not significant, it is noteworthy to mention that the direction of the correlations was generally the same, supporting our prior assumptions.

We therefore conclude that healthy controls as well as patients in both groups were generally less affected by psychophysiological arousal during the second measurement time. In this regard, the increase in activation from the first to the second measurement time for the left IFG in the sham group might not be related to an increase in cognitive functioning but might merely represents a more general possibly also arousal related effect. A further reason which might have contributed to the increase in CBSI concentrations after sham iTBS might be given by simple regression towards the mean. In this regard it needs to be considered that sham and verum stimulated patients did not differ significantly in their activation patterns after rTMS application. Instead, sham stimulated patients showed a significantly decreased baseline CBSI concentration in the left IFG compared to healthy controls. All in all, our findings confirm our first

hypothesis that PD-patients show a prefrontal dysfunction that is at least partly independent of panic-related tasks. However, an increase in cortical activation after verum iTBS was not found. Instead, we could accentuate the need to consider task-related arousal induced effects especially when investigating patients with anxiety disorders.

To our knowledge, this is the first controlled study investigating effects of add-on theta burst stimulation (TBS) on prefrontal activation and cognitive functioning in patients with PD/agoraphobia. So far, only a few open studies investigated the effects of TBS on psychiatric symptoms (e.g., [54, 55]).

However, limitations of this study have to be mentioned. The stimulation condition (verum versus sham) was correctly identified by the majority of patients, so one could argue that placebo effects might have affected our results. Possibly, patients exchanged their perceptions about rTMS during the psychotherapy group sessions, as they became acquainted with each other over the course of psychoeducation. For further investigations, we therefore emphasise the need for specialised sham coils which produce a superficial electrical current on the skull, as demonstrated by Rossi et al. [56]. Although in our study sufficient blinding could not be reached, promising results of rTMS in controlled studies with electromagnetic placebo coils could demonstrate specific effects of verum stimulation on psychiatric symptoms (e.g., for PTSD and comorbid depression by Boggio et al. [57]). Referring to the choice of the rTMS-frequency, we used a protocol which is assumed to facilitate motor cortex excitability [27]. Also, a facilitation of frontal activity could be demonstrated. For example, speech repetition accuracy was promoted by intermittent theta burst stimulation of the left posterior inferior frontal gyrus [28]. Nevertheless, rTMS effects seem to be influenced by a wide range of factors, for example, genetic variables or the way of application. Cheeran et al. [58] could demonstrate a significant influence of the brain-derived neurotrophic factor gene (BDNF) on the TBS-efficacy for the primary motor cortex. Also, TBS after-effects seem to hinge on the NMDA-receptor [59]. Further, a study of Gamboa et al. [60] demonstrated reversed iTBS-effects after a prolonged, single application of 1200 instead of 600 stimuli. Taken together, it could be questionable if iTBS consistently facilitates the excitability of stimulated neurons. Moreover, in our study, rTMS was generally applied after psychoeducation sessions. However, an application prior to psychoeducation could have led to a different processing of the afterwards presented information. We therefore suggest that future studies should systematically assess temporal effects of rTMS applications in relation to additional intervention methods. Regarding methodology, we have already discussed the problems that arise from the confounding skin blood flow signal component in the fNIRS data. A possible solution to this—which allows for an even more precise interpretation of the result—might be to measure the skin components selectively by additionally placing optodes with shorter interoptode distances on the probe set [51]. Finally, concerning the diagnostic process, PD/agoraphobia was diagnosed prior to $t1$ with the help of structured clinical interviews. However, the time lag between these interviews and $t1$ was not standardized in our study.

5. Conclusion

This pilot study investigated cortical activation patterns of patients with PD/agoraphobia compared to healthy controls. Further, effects of add-on iTBS on cortical activation and cognitive performance in PD/agoraphobia were analysed. Findings of a baseline cortical hypoactivation could be replicated. However, an increase in cortical activation after verum iTBS could not be supported. Instead we only found increased CBSI concentrations for the left IFG after sham iTBS application. By integrating behavioural performance into our analysis we could attribute this finding to more general effects such as task-related psychophysiological arousal and regression towards the mean. Taken together, our results confirm that PD is characterised by prefrontal hypoactivation. As we could not verify an increase in cortical activation after verum iTBS, further studies that should control for task-related psychophysiological arousal are needed in order to evaluate under which circumstances iTBS might serve as a therapeutic tool in the treatment of PD.

Conflict of Interests

All authors declare no conflict of interests regarding the publication of this paper.

Authors' Contribution

Saskia Deppermann and Nadja Vennewald contributed equally to this work and are therefore both considered as first authors.

Acknowledgments

This study was supported by Grants from the German Federal Ministry of Education and Research (Project no. 01GV0610) as a Subproject of the BMBF Psychotherapy Research Funding Initiative. The authors acknowledge the support by Deutsche Forschungsgemeinschaft and Open Access Publishing Fund of Tuebingen University. Also, they acknowledge the support by Thomas Dresler, Katja Hagen, Agnes Kroczek, Karina Limburg, Florian Metzger, Ramona Täglich, and Sabrina Schneider.

References

[1] American Psychiatric Association, *Diagnostic and Statistical Manual of Mental Disorders*, Text Revision (DSM-IV-TR), American Psychiatric Publishing, 4th edition, 2000.

[2] J. M. Gorman, M. R. Liebowitz, A. J. Fyer, and J. Stein, "A neuroanatomical hypothesis for panic disorder," *The American Journal of Psychiatry*, vol. 146, no. 2, pp. 148–161, 1989.

[3] J. M. Gorman, J. M. Kent, G. M. Sullivan, and J. D. Coplan, "Neuroanatomical hypothesis of panic disorder, revised," *The American Journal of Psychiatry*, vol. 157, no. 4, pp. 493–505, 2000.

[4] T. Dresler, A. Guhn, S. V. Tupak et al., "Revise the revised? New dimensions of the neuroanatomical hypothesis of panic disorder," *Journal of Neural Transmission*, vol. 120, no. 1, pp. 3–29, 2013.

[5] T. Dresler, C. Hindi Attar, C. Spitzer et al., "Neural correlates of the emotional Stroop task in panic disorder patients: an event-related fMRI study," *Journal of Psychiatric Research*, vol. 46, no. 12, pp. 1627–1634, 2012.

[6] Y. Nishimura, H. Tanii, M. Fukuda et al., "Frontal dysfunction during a cognitive task in drug-naive patients with panic disorder as investigated by multi-channel near-infrared spectroscopy imaging," *Neuroscience Research*, vol. 59, no. 1, pp. 107–112, 2007.

[7] H. Ohta, B. Yamagata, H. Tomioka et al., "Hypofrontality in panic disorder and major depressive disorder assessed by multi-channel near-infrared spectroscopy," *Depression and Anxiety*, vol. 25, no. 12, pp. 1053–1059, 2008.

[8] Y. Nishimura, H. Tanii, N. Hara et al., "Relationship between the prefrontal function during a cognitive task and the severity of the symptoms in patients with panic disorder: a multi-channel NIRS study," *Psychiatry Research*, vol. 172, no. 2, pp. 168–172, 2009.

[9] E. M. Wassermann and T. Zimmermann, "Transcranial magnetic brain stimulation: therapeutic promises and scientific gaps," *Pharmacology and Therapeutics*, vol. 133, no. 1, pp. 98–107, 2012.

[10] O. Pogarell, W. Koch, G. Pöpperl et al., "Acute prefrontal rTMS increases striatal dopamine to a similar degree as D-amphetamine," *Psychiatry Research*, vol. 156, no. 3, pp. 251–255, 2007.

[11] A. M. Speer, T. A. Kimbrell, E. M. Wassermann et al., "Opposite effects of high and low frequency rTMS on regional brain activity in depressed patients," *Biological Psychiatry*, vol. 48, no. 12, pp. 1133–1141, 2000.

[12] U. Herwig, A. J. Fallgatter, J. Höppner et al., "Antidepressant effects of augmentative transcranial magnetic stimulation: randomised multicentre trial," *The British Journal of Psychiatry*, vol. 191, pp. 441–448, 2007.

[13] D. J. L. G. Schutter, "Antidepressant efficacy of high-frequency transcranial magnetic stimulation over the left dorsolateral prefrontal cortex in double-blind sham-controlled designs: a meta-analysis," *Psychological Medicine*, vol. 39, no. 1, pp. 65–75, 2009.

[14] D. O. Rumi, W. F. Gattaz, S. P. Rigonatti et al., "Transcranial magnetic stimulation accelerates the antidepressant effect of amitriptyline in severe depression: a double-blind placebo-controlled study," *Biological Psychiatry*, vol. 57, no. 2, pp. 162–166, 2005.

[15] S. S. Cho, E. J. Yoon, J. M. Lee, and S. E. Kim, "Repetitive transcranial magnetic stimulation of the left dorsolateral prefrontal cortex improves probabilistic category learning," *Brain Topography*, vol. 25, no. 4, pp. 443–449, 2012.

[16] K. Yamanaka, B. Yamagata, H. Tomioka, S. Kawasaki, and M. Mimura, "Transcranial magnetic stimulation of the parietal cortex facilitates spatial working memory: near-infrared spectroscopy study," *Cerebral Cortex*, vol. 20, no. 5, pp. 1037–1045, 2010.

[17] L. H. Ernst, S. Schneider, A.-C. Ehlis, and A. J. Fallgatter, "Review: functional near infrared spectroscopy in psychiatry: a critical review," *Journal of Near Infrared Spectroscopy*, vol. 20, no. 1, pp. 93–105, 2012.

[18] F. Irani, S. M. Platek, S. Bunce, A. C. Ruocco, and D. Chute, "Functional near infrared spectroscopy (fNIRS): an emerging neuroimaging technology with important applications for the study of brain disorders," *The Clinical Neuropsychologist*, vol. 21, no. 1, pp. 9–37, 2007.

[19] F. B. Haeussinger, S. Heinzel, T. Hahn, M. Schecklmann, A.-C. Ehlis, and A. J. Fallgatter, "Simulation of near-infrared light absorption considering individual head and prefrontal cortex anatomy: implications for optical neuroimaging," *PLoS ONE*, vol. 6, no. 10, Article ID e26377, 2011.

[20] X. Cui, S. Bray, D. M. Bryant, G. H. Glover, and A. L. Reiss, "A quantitative comparison of NIRS and fMRI across multiple cognitive tasks," *NeuroImage*, vol. 54, no. 4, pp. 2808–2821, 2011.

[21] M. Ferrari and V. Quaresima, "A brief review on the history of human functional near-infrared spectroscopy (fNIRS) development and fields of application," *NeuroImage*, vol. 63, no. 2, pp. 921–935, 2012.

[22] A. C. Ehlis, S. Schneider, T. Dresler, and A. J. Fallgatter, "Application of functional near-infrared spectroscopy in psychiatry," *NeuroImage*, vol. 85, part 1, pp. 478–488, 2014.

[23] S. Deppermann, N. Vennewald, J. Diemer et al., "Neurobiological and clinical effects of NIRS-controlled transcranial magnetic stimulation (rTMS) in patients with panic disorder/agoraphobia during cognitive behavioral therapy," Manuscript in preparation, University of Tuebingen.

[24] J. Margraf and S. Schneider, *Panik Angstanfälle und ihre Behandlung*, Springer, Berlin, Germany, 1990.

[25] S. Schneider and J. Margraf, *Agoraphobie und Panikstörung. Fortschritte der Psychotherapie*, Hogrefe, Göttingen, Germany, 1998.

[26] A. Aschenbrenner, O. Tucha, and K. Lange, *RWT Regensburger Wortflüssigkeits-Test Handanweisung*, Hogrefe, Göttingen, Germany, 2000.

[27] Y.-Z. Huang, M. J. Edwards, E. Rounis, K. P. Bhatia, and J. C. Rothwell, "Theta burst stimulation of the human motor cortex," *Neuron*, vol. 45, no. 2, pp. 201–206, 2005.

[28] J. Restle, T. Murakami, and U. Ziemann, "Facilitation of speech repetition accuracy by theta burst stimulation of the left posterior inferior frontal gyrus," *Neuropsychologia*, vol. 50, no. 8, pp. 2026–2031, 2012.

[29] M. V. Sale, M. C. Ridding, and M. A. Nordstrom, "Factors influencing the magnitude and reproducibility of corticomotor excitability changes induced by paired associative stimulation," *Experimental Brain Research*, vol. 181, no. 4, pp. 615–626, 2007.

[30] U. Herwig, P. Satrapi, and C. Schönfeldt-Lecuona, "Using the international 10-20 EEG system for positioning of transcranial magnetic stimulation," *Brain Topography*, vol. 16, no. 2, pp. 95–99, 2003.

[31] H. Obrig and A. Villringer, "Beyond the visible—imaging the human brain with light," *Journal of Cerebral Blood Flow and Metabolism*, vol. 23, no. 1, pp. 1–18, 2003.

[32] H. Jasper, "The ten-twenty electrode system of the International Federation," *Electroencephalography and Clinical Neurophysiology*, vol. 10, pp. 371–375, 1958.

[33] X. Cui, S. Bray, and A. L. Reiss, "Functional near infrared spectroscopy (NIRS) signal improvement based on negative correlation between oxygenated and deoxygenated hemoglobin dynamics," *NeuroImage*, vol. 49, no. 4, pp. 3039–3046, 2010.

[34] T. Yamamoto and T. Kato, "Paradoxical correlation between signal in functional magnetic resonance imaging and deoxygenated haemoglobin content in capillaries: a new theoretical explanation," *Physics in Medicine and Biology*, vol. 47, no. 7, pp. 1121–1141, 2002.

[35] S. Brigadoi, L. Ceccherini, S. Cutini et al., "Motion artifacts in functional near-infrared spectroscopy: a comparison of motion correction techniques applied to real cognitive data," *NeuroImage*, vol. 85, part 1, pp. 181–191, 2014.

[36] S. V. Tupak, M. Badewien, T. Dresler et al., "Differential prefrontal and frontotemporal oxygenation patterns during phonemic and semantic verbal fluency," *Neuropsychologia*, vol. 50, no. 7, pp. 1565–1569, 2012.

[37] M. Schecklmann, A.-C. Ehlis, M. M. Plichta et al., "Diminished prefrontal oxygenation with normal and above-average verbal fluency performance in adult ADHD," *Journal of Psychiatric Research*, vol. 43, no. 2, pp. 98–106, 2008.

[38] D. Tsuzuki, V. Jurcak, A. K. Singh, M. Okamoto, E. Watanabe, and I. Dan, "Virtual spatial registration of stand-alone fNIRS data to MNI space," *NeuroImage*, vol. 34, no. 4, pp. 1506–1518, 2007.

[39] C. Rorden and M. Brett, "Stereotaxic display of brain lesions," *Behavioural Neurology*, vol. 12, no. 4, pp. 191–200, 2000.

[40] J. L. Lancaster, M. G. Woldorff, L. M. Parsons et al., "Automated Talairach atlas labels for functional brain mapping," *Human Brain Mapping*, vol. 10, no. 3, pp. 120–131, 2000.

[41] M. B. First, R. L. Spitzer, M. Gibbon, and J. B. W. Williams, *Structured Clinical Interview for DSM-IV Axis I Disorders, Clinician Version (SCID-CV)*, American Psychiatric Press, Washington, DC, USA, 1996.

[42] H. Wittchen, U. Wunderlich, S. Gruschwitz, and M. Zaudig, *Strukturiertes Klinisches Interview für DSM-IV: SKID I Interviewheft—Achse 1: Psychische Störungen*, Hogrefe, Göttingen, Germany, 1997.

[43] B. Bandelow, *Panic and Agoraphobia Scale (PAS)*, Hogrefe & Huber, Seattle, Wash, USA, 1997.

[44] H. Hamilton, "Hamilton Anxiety Scale (HAMA)," in *Internationale Skalen für Psychiatrie*, CIPS, Ed., Beltz Test GmbH, Göttingen, Germany, 1996.

[45] G. H. Eifert, R. N. Thompson, M. J. Zvolensky et al., "The cardiac anxiety questionnaire: development and preliminary validity," *Behaviour Research and Therapy*, vol. 38, no. 10, pp. 1039–1053, 2000.

[46] J. Hoyer, S. Helbig, and J. Margraf, *Diagnostik der Angststörungen*, Hogrefe, Göttingen, Germany, 2005.

[47] R. M. Berman, M. Narasimhan, G. Sanacora et al., "A randomized clinical trial of repetitive transcranial magnetic stimulation in the treatment of major depression," *Biological Psychiatry*, vol. 47, no. 4, pp. 332–337, 2000.

[48] S. Pallanti and S. Bernardi, "Neurobiology of repeated transcranial magnetic stimulation in the treatment of anxiety: a critical review," *International Clinical Psychopharmacology*, vol. 24, no. 4, pp. 163–173, 2009.

[49] S. M. Quintana, S. E. Maxwell, S. M. Quintana, and S. E. Maxwell, "A Monte Carlo comparison of seven E-adjustment procedures in repeated measures designs with small sample sizes," *Journal of Educational Statistics*, vol. 19, no. 1, pp. 57–71, 1994.

[50] S. Holm, "A simple sequentially rejective multiple test procedure," *Scandinavian Journal of Statistics*, vol. 6, no. 2, pp. 65–70, 1979.

[51] T. Takahashi, Y. Takikawa, R. Kawagoe, S. Shibuya, T. Iwano, and S. Kitazawa, "Influence of skin blood flow on near-infrared spectroscopy signals measured on the forehead during a verbal fluency task," *NeuroImage*, vol. 57, no. 3, pp. 991–1002, 2011.

[52] F. B. Haeussinger, T. Dresler, S. Heinzel, M. Schecklmann, A. J. Fallgatter, and A. C. Ehlis, "Reconstructing functional near-infrared spectroscopy (fNIRS) signals impaired by extracranialconfounds: an easy-to-use filter method," accepted in *NeuroImage*.

[53] E. Kirilina, A. Jelzow, A. Heine et al., "The physiological origin of task-evoked systemic artefacts in functional near infrared spectroscopy," *NeuroImage*, vol. 61, no. 1, pp. 70–81, 2012.

[54] M. Holzer and F. Padberg, "Intermittent theta burst stimulation (iTBS) ameliorates therapy-resistant depression: a case series," *Brain Stimulation*, vol. 3, no. 3, pp. 181–183, 2010.

[55] A. V. Chistyakov, O. Rubicsek, B. Kaplan, M. Zaaroor, and E. Klein, "Safety, tolerability and preliminary evidence for antidepressant efficacy of theta-burst transcranial magnetic stimulation in patients with major depression," *The International Journal of Neuropsychopharmacology*, vol. 13, no. 3, pp. 387–393, 2010.

[56] S. Rossi, M. Ferro, M. Cincotta et al., "A real electro-magnetic placebo (REMP) device for sham transcranial magnetic stimulation (TMS)," *Clinical Neurophysiology*, vol. 118, no. 3, pp. 709–716, 2007.

[57] P. S. Boggio, M. Rocha, M. O. Oliveira et al., "Noninvasive brain stimulation with high-frequency and low-intensity repetitive transcranial magnetic stimulation treatment for posttraumatic stress disorder," *Journal of Clinical Psychiatry*, vol. 71, no. 8, pp. 992–999, 2010.

[58] B. Cheeran, P. Talelli, F. Mori et al., "A common polymorphism in the brain-derived neurotrophic factor gene (BDNF) modulates human cortical plasticity and the response to rTMS," *The Journal of Physiology*, vol. 586, no. 23, pp. 5717–5725, 2008.

[59] Y.-Z. Huang, R.-S. Chen, J. C. Rothwell, and H.-Y. Wen, "The after-effect of human theta burst stimulation is NMDA receptor dependent," *Clinical Neurophysiology*, vol. 118, no. 5, pp. 1028–1032, 2007.

[60] O. L. Gamboa, A. Antal, V. Moliadze, and W. Paulus, "Simply longer is not better: reversal of theta burst after-effect with prolonged stimulation," *Experimental Brain Research*, vol. 204, no. 2, pp. 181–187, 2010.

Hindawi Publishing Corporation
BioMed Research International
Volume 2014, Article ID 906104, 9 pages
http://dx.doi.org/10.1155/2014/906104

Research Article

Abnormal Early Gamma Responses to Emotional Faces Differentiate Unipolar from Bipolar Disorder Patients

T. Y. Liu,[1,2] Y. S. Chen,[3] T. P. Su,[4,5] J. C. Hsieh,[1,2] and L. F. Chen[1,2]

[1] *Institute of Brain Science, School of Medicine, National Yang-Ming University, Taipei 112, Taiwan*
[2] *Integrated Brain Research Unit, Division of Clinical Research, Department of Medical Research, Taipei Veterans General Hospital, Taipei 112, Taiwan*
[3] *Department of Computer Science, National Chiao Tung University, Hsinchu 300, Taiwan*
[4] *Department of Psychiatry, Taipei Veterans General Hospital, Taipei 112, Taiwan*
[5] *Division of Psychiatry, School of Medicine, National Yang-Ming University, Taipei 112, Taiwan*

Correspondence should be addressed to J. C. Hsieh; jchsieh@ym.edu.tw and L. F. Chen; lfchen@ym.edu.tw

Received 15 October 2013; Revised 30 January 2014; Accepted 1 February 2014; Published 13 March 2014

Academic Editor: Yong He

This study investigates the cortical abnormalities of early emotion perception in patients with major depressive disorder (MDD) and bipolar disorder (BD) using gamma oscillations. Twenty-three MDD patients, twenty-five BD patients, and twenty-four normal controls were enrolled and their event-related magnetoencephalographic responses were recorded during implicit emotional tasks. Our results demonstrated abnormal gamma activity within 100 ms in the emotion-related regions (amygdala, orbitofrontal (OFC) cortex, anterior insula (AI), and superior temporal pole) in the MDD patients, suggesting that these patients may have dysfunctions or negativity biases in perceptual binding of emotional features at very early stage. Decreased left superior medial frontal cortex (smFC) responses to happy faces in the MDD patients were correlated with their serious level of depression symptoms, indicating that decreased smFC activity perhaps underlies irregular positive emotion processing in depressed patients. In the BD patients, we showed abnormal activation in visual regions (inferior/middle occipital and middle temporal cortices) which responded to emotional faces within 100 ms, supporting that the BD patients may hyperactively respond to emotional features in perceptual binding. The discriminant function of gamma activation in the left smFC, right medial OFC, right AI/inferior OFC, and the right precentral cortex accurately classified 89.6% of patients as unipolar/bipolar disorders.

1. Introduction

Mood disorders, including major depressive disorder (MDD) and bipolar disorder (BD), are among the most debilitating diseases worldwide and with a lifetime prevalence estimated about 20.8% [1]. Guidelines from the Diagnostic and Statistical Manual of Mental Disorders, fourth edition (DSM-IV) [2], characterize the manic/hypomanic episodes as an index for distinguishing bipolar from unipolar disorders, but misdiagnosis of bipolar as unipolar could occur particularly when the BD patients come to the hospital in depressive episodes [3, 4]. Identification of disorder biomarkers disclosed from neuroimage researches could improve diagnostic accuracy and clinical treatment outcomes of bipolar disorder [4]. Precious neuroimaging studies have proposed that dysfunction of facial expression perception is one of core impairments in the MDD and BD patients [5–8]. Hence quantitative measurements of neural responses to emotional stimulation may facilitate accurate diagnosis and better treatment outcomes of the MDD and BD patients.

Depressed patients have an attentional bias toward negative stimuli (easier to attract patients' attention) [9], which are more inclined to interpret neutral faces as sad [10, 11]. Stimulation with high arousal levels would activate the negative motivational withdrawal system more strongly than the positive approach system [12], which is called the negativity bias [13]. It implicates that withdrawal from negative stimuli is more critical to survival than approach of pleasant or neutral stimuli [13, 14]. To achieve this goal, humans "early" allocate attentional resources to negatively valenced stimuli in an

efficient way, as proposed in the automatic vigilance model of emotion [15], which leads to delayed attentional disengagement. Hence we speculate that the depression symptoms in mood disorders may associate with their increased negativity bias, which results in dysfunction of early rapid processing of resources allocation.

Implicit emotional paradigms, by which participants attend to judge nonemotional perceptual features (e.g., gender) rather than emotional cues, have been considered an effective way to explore neural substrates of facial emotional processing [16, 17]. Perceptual processing of emotion-laden stimuli engages several critical brain regions, including the amygdala, prefrontal cortex, orbitofrontal cortex (OFC), anterior cingulate cortex (ACC), and anterior insula (AI) [18]. Previous studies showed that the abnormal activity of these regions in patients with affective disorder may be related to their specific symptoms, including anhedonia (easy to be unhappy and sad) and emotional instability [5]. However, there is limited understanding of dysfunction of neurobiological basis underlying "early" emotion perception. The present study aimed at elucidating whether the MDD and BD patients have impaired or biased perception of emotional facial features at very early stage of emotional processing.

The current study measured gamma activity by magnetoencephalography (MEG) and adopted implicit emotional paradigms to investigate early facial emotion perception in BD and MDD patients, compared with healthy controls and to distinguish these two affective disorders by discriminant analyses. Gamma-band responses have been implicated to be a mechanism of perceptual binding and strongly synchronized about 100 ms after sensory processing, reflecting integration processing of perceived features at very early stage [8, 19, 20]. Müller et al. [21] suggests that spatial distribution of gamma oscillations, including limbic, temporal, and frontal cortices may be linked to neural substrates of binding emotional information. Gamma oscillations can provide a potential index to explore regional brain abnormalities of early emotional processing in affective disorders. Previous studies have showed that subcortical and cortical regions activate within 100 ms by high temporal resolution technique, such as event-related potentials (ERPs) and magnetoencephalography (MEG) [22, 23]. Our previous study also demonstrated alterations of gamma activity (50–150 ms) during early emotion processing in the MDD and BD [7]. We in this study further tested that alterations of cortical gamma responses to early perception of emotional facial expression were distinct between the MDD and BD patients, which can be a potential index to differentiate patients with unipolar from bipolar disorders.

2. Materials and Methods

2.1. Subjects. Seventy-two participants were recruited from the Department of Psychiatry at Taipei Veterans General Hospital in this study, including twenty-three MDD patients (mean age 35.96 ± 9.58, nine males), twenty-five BD patients (mean age 36.80 ± 11.38, ten males), and twenty-four age- and gender-matched healthy controls (NC, mean age 36.62 ± 11.36, nine males). The three groups did not show significant differences in age (a one-way ANOVA, $P = 0.961$) and gender (2×3 contingency table analysis, $P = 0.916$). All subjects were right-handed as assessed by the Edinburgh Handedness Inventory. The diagnosis of MDD and BD was confirmed by a structured interview based on the Diagnostic and Statistical Manual for Mental Disorders (DSM-IV) criteria (American Psychiatric Association, 1994). Before MEG data acquisition, psychiatric and mood symptoms of all patients were assessed with the Young Mania Rating Scale (YMRS) and the 17-item Hamilton Rating Scale for Depression (HAMD). For details, see Table 1. The NC subjects underwent the Mini International Neuropsychiatric Interview before participation in the study to confirm the absence of past or current psychiatric symptoms. Each participant signed informed consent forms approved by the Institutional Review Board at Taipei Veterans General Hospital.

2.2. Stimuli and Experimental Design. Face images with duration of 1.5 sec (72 trials for each emotion and four emotions in total, including neutral, sad, happy, and angry faces) were displayed randomly. Visual stimuli were exhibited at the center of a back-projected translucent screen, which was located 100 cm in front of the subject, and subtended 14° (width) by 17° (height) of visual angle. Subjects were instructed to perform a gender discrimination task by lifting their left/right index finger for male/female face images, respectively, while a response cue was displayed. All subjects practiced the test before their MEG signals were recorded.

2.3. MEG and MRI Recordings. Event-related MEG data were recorded by a whole-head 306-channel neuromagnetometer (Vectorview 306, Elekta Neuromag, Finland) with a sampling rate of 1000 Hz and a 0.03~330 Hz bandpass filter. Trials containing deflections exceeding 9000 fT/cm or contaminated by eye movements were excluded for the source analysis. The signal space projection method [24] was applied to remove urban and device interference in the recorded MEG data. The T1-weighted MRI (magnetic resonance images) of each individual was acquired by a 1.5 T GE Signa Excite scanner using an 8-channel phased-array head coil with 3D fast spoiled gradient recalled echo (3D FSPGR, TR = 8.67 ms, TE = 1.86 ms, inversion time = 400 ms, matrix size = $256 \times 256 \times 124$, and voxel size = $1.02 \times 1.02 \times 1.5\,mm^3$). To facilitate precise coregistration of the MEG data and structural MRI, three anatomical landmarks (nasion and left and right preauriculars) were localized with Isotrak 3D digitizer (Polhemus Navigation Sciences, Colchester, Vermont, USA).

2.4. MEG Source Analysis. For each emotion, the noise-free MEG data were filtered at a frequency band of 35 to 55 Hz (gamma). These gamma-band signals were then analyzed through a beamforming method [25] to estimate cortical activity index of emotional evoked responses, which was denoted as the gamma-band activation index (GBAI). The GBAI map with an isotropic voxel size of 4 mm in the whole-brain was obtained by estimating the ratio between estimated signals of the active state (a 30-ms window) and those of the control state (from 300 ms to 200 ms before stimulus

Table 1: Demographic variables for bipolar, major depression, and control groups.

	MDD	BD	NC
Gender (male : female)	9 : 14	11 : 14	9 : 15
Age (years)	35.96 (9.58)	36.80 (11.38)	36.62 (11.36)
Age of onset (years)	26.65 (9.26)	28.80 (9.71)	—
Duration of illness (years)	9.30 (7.64)	7.92 (6.18)	—
Number of manic episodes	—	3.08 (2.34)	—
Number of depressive episodes	4.26 (3.61)	4.12 (2.17)	—
Number of major depressive episodes	2.61 (1.08)	3.00 (1.00)	—
Young Mania Rating Scale (YMRS)	0.77 (1.60)	1.44 (2.02)	—
Hamilton Depression Rating Scale (HAMD)	9.09 (8.22)	6.80 (5.29)	—

Except for the gender variable, all other variables are presented as mean (SD).

onset) for each voxel. This study focused on investigating the difference of brain responses between patients with MDD and BD in emotion processing during the first 100 milliseconds after stimulus onset (from 30 to 120 ms with 5 ms shift).

For group analysis, the individual T1-weighted MRIs were first transformed into the Montreal Neurological Institute (MNI) space (a standard stereotactic space) with an isotropic spatial resolution of 2 mm by the BIRT software [26]. The obtained deformation field was then applied to transform the individual GBAI maps obtained above into the MNI space for further group analysis. A one-way ANOVA ($F(2, 69) = 7.65$, uncorrected $P < 0.001$, cluster size = 100) and two two-sample t-tests ($t(47) = 3.87$ for BD versus NC group, $t(45) = 3.88$ for MDD versus NC group, uncorrected $P < 0.000167$) were conducted at each time point in a voxel-wise manner by using the statistical parametric mapping software (SPM2, http://www.fil.ion.ucl.ac.uk/spm/). The intersection areas between the survived voxels obtained from the ANOVA and t-test analyses were extracted and the mean of GBAI within each area with cluster size ≥30 was calculated for the following correlation and discriminant analyses.

2.5. Correlation and Discriminant Analyses. Pearson correlation coefficients were used to assess the relationship between the abnormal regional GBAIs and symptomatic/demographic data in patient groups. The correlation was determined to be significant at least 10 ms (three continuous maps, e.g., 30, 35, and 40 ms).

Abnormal regional GBAIs of the MDD and BD patients obtained from the above-mentioned source analysis procedure were extracted as possible features for differentiating these two patient groups. A two-stage discriminant analyses were performed to identify distinguishable feature variables (abnormal regional GBAIs) and their weightings by evaluating their contributions in distinguishing patient groups (MDD versus BD). In the first stage, a stepwise linear discriminant procedure was used to select the predictors of the model, which can be best able to distinguish between these two patient groups. At each step, one variable was considered at a time and Wilks' Lambda values of the variables in the model were used to determine this variable to be a predictor or not. The threshold of Wilks' Lambda was set at 0.25 for setting retention in the model, which was based on previous Monte Carlo simulation studies [27]. This procedure iteratively repeated for each variable until there was no further improvement in discriminability of the model.

The second stage was a canonical discriminant analysis which was used to determine the weightings of those variables selected from the first step. The resolved standardized weight of each variable (regional GBAI) reflected its relative discriminating efficiency. The accuracy of the derived discriminant function from the two-stage discriminant analyses was assessed by leave-one-out cross validation for the whole patient cohort. Furthermore, a two-sample t-test was used to test whether the mean values of the discriminant function for the patient groups were different. Finally, a Fisher Exact Test was performed to evaluate the statistical significance of the classification accuracy [28].

3. Results

Overall, both patient groups displayed regional gamma hyperactivity compared to the NC group, but only the MDD patients exhibited the diminished gamma activity, as listed in Table 2. Overall, we found diminished gamma responses at very early time points (30–70 ms after stimulus onset) and elevated gamma responses at later time points (80–115 ms). Figures 1 and 2 showed the brain regions with abnormal gamma activity at peak time points (shown in Table 2) in the MDD and BD patients, respectively.

The MDD patient showed decreased gamma responses to sad and happy faces within 70 ms and increased gamma responses to sad faces around 100 ms, relative to the NC group (Table 2). No significant difference of brain responses to angry or neutral faces was found. The decreased gamma responses to sad faces were in the right anterior insula/inferior OFC (40–70 ms), the right superior temporal pole/parahippocampus (55–70 ms), and the right amygdala (55–65 ms). The hypoactivity responding to happy faces was located in the right superior/medial OFC and left superior medial frontal cortex during 30–40 ms. On the other hand, the right precentral/postcentral cortex (95–115 ms) of the MDD patients was more activated to sad faces, compared to the NCs.

As to the BD patients, only increased responses were found in comparison with the NC group, including the right

Table 2: Between-group differences (patients versus NCs) in neural response to facial expressions during 30–120 ms.

Group difference	Emotion	Brain region	BA	Time (ms)		Coordinate (mm)	$\|t$-value$\|$	Cluster size
				Duration	Peak	x, y, z at peak		
MDD < NC	Sad	R anterior insula/Inferior orbitofrontal cortex	BA47	40–70	60	26, 14, −20	4.94	457
	Happy	R superior temporal pole/parahippocampal cortex	BA38	55–70	60	30, 16, −26	4.7	339
		R amygdala		55–65	55	22, −4, −12	4.47	30
		L superior medial frontal cortex	BA8	30–40	35	−6, 42, 56	4.6	64
		R medial orbitofrontal cortex	BA10/11/32	30–40	35	16, 52, −12	4.46	366
	Angry/neutral	—						
MDD > NC	Sad	R precentral cortex	BA4	95–115	105	22, −24, 62	4.87	217
	Happy/angry/neutral	—						
BD < NC	Sad/happy/angry/neutral	—						
BD > NC	Happy	R middle temporal cortex	BA22	90–100	90	46, −56, 20	4.4	71
	Angry	R middle/inferior occipital cortex	BA18	80–100	95	32, −96, −4	5.15	258
	Sad/neutral	—						

The significant voxels were performed by a one-way ANOVA of three groups (uncorrected $P < 0.001$) and between-group comparisons with a Bonferroni adjustment (uncorrected $P < 0.000167$), all $|t|$ values >3.87. The cluster size denotes the number of voxels and coordinates are in MNI space. BA: Brodmann area; R: right; L: left.

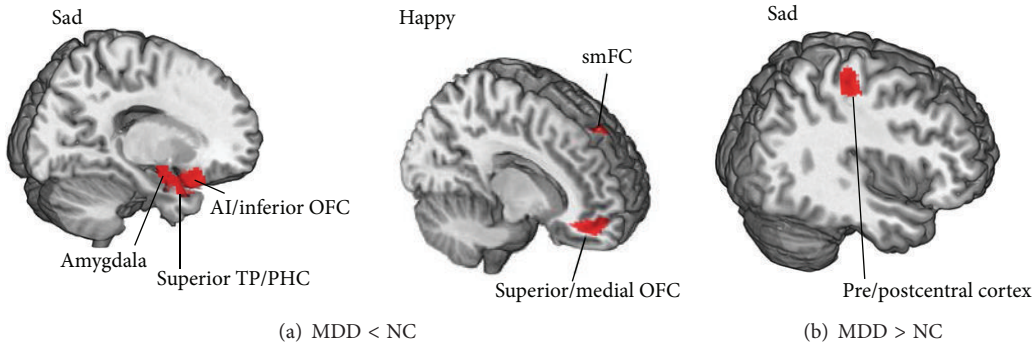

Figure 1: Abnormal regional activity of the MDD patients in early emotion perception at peak time points. Decreased (a) and increased activity (b) in the MDD patients. MDD: major depressive disorder; NC: normal control; AI: anterior insula; OFC: orbitofrontal cortex; TP: temporal pole; PHC: parahippocampus; smFC: superior medial frontal cortex.

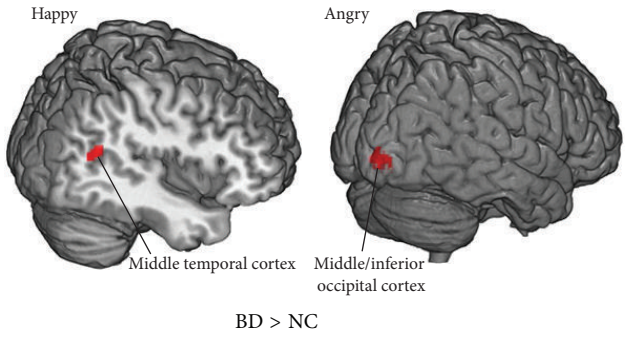

Figure 2: Increased regional activity of the BD patients in early emotion perception at peak time points. BD: bipolar disorder; NC: normal control.

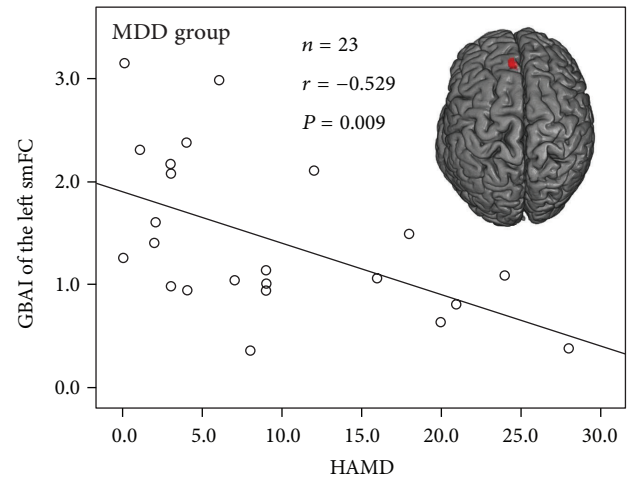

Figure 3: Correlation between HAMD scores and smFC activity of the MDD patients. The HAMD scores of the MDD patients were negatively correlated with the GBAI of the left superior medial frontal cortex ($r = -0.529$, $P = 0.009$ at 35 ms). HAMD: Hamilton Depression Rating Scale; MDD: major depressive disorder; GBAI: gamma-band activation index; smFC: superior medial frontal cortex.

middle temporal cortex (90–100 ms) to happy faces and the right middle/inferior occipital cortex (80–100 ms) to angry faces. (Table 2). No significant difference between the BD and NC groups in response to sad and neutral facial expressions was found.

3.1. Correlation between Abnormal Regional GBAI and Symptomatic Data. The correlations between the abnormal regional GBAIs and the symptomatic and demographic data of the patient groups were assessed. Only the HAMD score of the MDD patients was found to be negatively correlated with the GBAI of the left superior medial frontal cortex ($r = -0.441$, $P = 0.035$ at 30 ms; $r < -0.521$, $P < 0.011$ at 35 and 40 ms), as shown in Figure 3. In the BD patients, no significant correlation between symptomatic/demographic data and abnormal regional GBAIs was found.

3.2. Discriminant Analysis. The stepwise linear discriminant analysis identified four brain regions with the most distinguishing capability between the MDD and BD patients ($F_{4,43} = 9.77$, $P < 0.0001$), including the left superior medial frontal cortex (happy 35 ms), the right medial orbitofrontal cortex (happy 35 ms), the right anterior insula/inferior OFC (sad 60 ms), and the right precentral cortex (sad 105 ms). The outputs of the discriminant functions between these two patient groups were significantly different ($t_{47} = 20.87$, $P < 0.0001$). Figure 4 illustrated the distribution of the discriminant function scores in the MDD (mean = 0.38, se = ±0.32) and BD patients (mean = −3.43, se = ±0.38). The results of leave-one-out cross validation showed that no MDD patient was misclassified and only five out of twenty-five BD patients (80%) were misclassified into the MDD group. Overall, 43 of 48 patients were correctly categorized with a prediction accuracy of 89.6% (Fisher's Exact Test, $P \leq 3.28 \times 10^{-9}$).

4. Discussion

Our results demonstrated the distinct patterns of gamma oscillatory abnormalities in the MDD and BD patients in

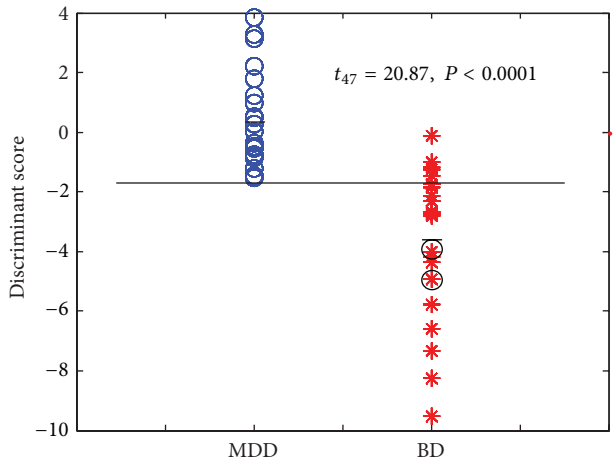

Figure 4: The scatterplots showed individual discriminant function scores of the MDD and BD patients. The black bars illustrated the patient group means. The stepwise discriminant analysis identified four abnormal regional GBAIs of the most discriminating from the MDD (blue circle) and BD (red star) patients ($F_{4,43}$ = 9.77, P < 0.0001) and the function scores were significantly different (t_{47} = 20.87, P < 0.0001). The two BD patients (black circle) were initially diagnosed as the MDD patients. The four abnormal regions include the left superior medial frontal cortex (happy 35 ms), the right medial orbitofrontal cortex (happy 35 ms), the right anterior insula/inferior orbitofrontal cortex (sad 60 ms), and the right precentral cortex (sad 105 ms). MDD: major depressive disorder; BD: bipolar disorder; GBAI: gamma-band activation index.

responses to emotional facial expression during early perceptual processing. The MDD displayed more deficits in the frontal and limbic regions, including amygdala, OFC, and anterior insula, than the BD. Among these regions, the patterns of gamma activation in the left smFC, right mOFC, right AI/inferior OFC, and the right precentral cortex can accurately classify 89.6% of patients into their diagnosed categories.

Notably, in our study there were two BD patients who were initially diagnosed as the MDD patients and then confirmed as the bipolar disorder two weeks later. Our data from the discriminant analyses showed that these two BD patients were correctly classified using their brain signals measured at the first week (the circle marks in Figure 4) although the patients in this study were not drug-naive or drug-free, which could have a confounding effect on the brain signals. These results suggest that the gamma responses to emotional faces can provide a useful objective index to differentiate the BD patients from the MDD patients and may become a potential biomarker to assist in diagnosis.

Our data showed diminished gamma activity at the amygdala, OFC, and insula in response to sad faces during early emotion perception in MDD patients. This finding may unravel three possible neural mechanisms underlying emotion perception in human brain. First, gamma oscillation could be an emotion-evoked oscillation. Being considered as a mechanism of feature binding [11, 12], early sensory-evoked gamma oscillations were reliably found in various modalities [29]. Early visual evoked gamma-band response within 100 ms after stimulation is proposed to be sensitive to attentional and perceptual factors [30]. The finding of the aberrant gamma responses to emotional faces within 100 ms in the present study indicates that human brain integrates emotional facial features in a very effective and rapid way at the early stage of perceptive processing revealed by gamma oscillations.

Second, the frontoinsular cortex as well as amygdala has been reported to be involved in fast processing of salient information obtained from emotional facial features [31]. The amygdala is proposed to be engaged very early (within 100 ms) in processing negative faces as disclosed by neurophysiological studies using MEG [22] and intracranial electroencephalography [23]. Adolphs [32] reported that humans process emotional facial expressions in perception with simple and highly salient features within 120 ms including the amygdala and OFC. Our finding of diminished gamma activity within 100 ms in the amygdala, anterior insula, and OFC in the MDD patients may indicate their impairments or inefficiency in rapid processing or integrating salient emotion.

Finally, the MDD patients were reported to have a negativity bias (easier to attract patients' attention toward negative stimuli) [9], especially toward sad stimuli. We speculated that the negative-affect bias of depressed patients may be associated with the OFC activity in response to sad facial expressions. The OFC, a key region of the top-down facilitation model, is suggested to rapidly extract low spatial frequency components of inputs (at around 50 ms) from visual or subcortical cortices through the magnocellular route to generate possible candidates of objects [33, 34]. Eliminated OFC activity may result in disrupted top-down information processing. Our results of the diminished activity of the OFC within 50 ms in the MDD patients may suggest a neural evidence of top-down modulation of negative-affect bias in the MDD patients while facing a sad expression.

Our data also indicated that the more severe depression symptoms the MDD patients had, the more eliminated the left smFC responses to happy faces were. Our results were in line with the previous studies [6, 35], which also showed the deactivation of the left prefrontal cortex in depressed patients. Mitterschiffthaler et al. [36] also indicated that reduced medial frontal responses to positive valence stimuli in depressed patients were related to abnormalities of positive emotion processing. Our finding suggests that decreased activity in the smFC underlies irregular positive emotion processing in patients with major depression, which may be one of neural substrate candidates related to anhedonia in depression.

In the BD patients, our finding showed elevated activation in visual regions responded to emotional facial expressions at around 100 ms after visual stimulation. In line with our previous findings of the enhanced occipitotemporal gamma oscillations in the BD patients in sensor-space analysis [8], in this study we found the abnormal occipital or temporal regions of the BD patients when they perceived only the happy and angry faces but not the sad and neutral faces. Happy faces consist of more changeable facial features (e.g., mouth) than negative and neutral faces [37]. Extracting the

negative valence from angry expressions is easier than that from sad expressions [38, 39]. Happy and angry faces are high arousal stimuli relative to sad and neutral faces [40, 41]. Hence, the findings of the hyperactivation in the occipital and temporal regions of the BD patients, only to the happy and angry faces but not to the sad and neutral faces, reflect that dysfunction of perceptual processing in the BD patients may be associated with detection of changeable as well as high-arousal facial features. The finding of the hyperactivity of visual regions around 100 ms in the BD patients indicates that the BD patients have altered visual perception of emotional features which may lead to dysfunction of the subsequent cognitive functions.

Other oscillations (theta, alpha, and beta) play different roles for neuronal functions. A review paper [42] summarizes that theta oscillations are a key mechanism of memory processing in the hippocampus (the main brain area related to theta waves); alpha oscillations are related to function of inhibition in the motor cortex; beta oscillations are associated with functions of motor control and attention in cortical structures. Previous studies indicated that high gamma oscillations (>60 Hz) are related to cognitive and perceptual processes [43, 44], but its significance or role remains unclear [45, 46]. On the other hand, low gamma oscillations (30–50 Hz) have been well documented as a crucial mechanism of perceptual binding and object/face representation in numerous human studies [29, 47–49]. The "binding problem" addresses the physiological mechanisms responsible for combining different features in a visual scene to form a coherent percept [29]. The present study focused on investigating the low gamma responses to emotional faces within 100 ms to reveal the dysfunction of perceptual binding in emotional feature processing of the MDD and BD patients.

5. Conclusions

Our results demonstrated that abnormal activation within 100 ms of the MDD patients in the emotion-related regions (amygdala, inferior/medial OFC, AI, and superior temporal pole) responded to emotional facial expressions, which suggests that the MDD patients may have dysfunctions or negativity biases in perceptual binding of salient emotional features at very early stage. In the BD patients, our finding showed that abnormal activation in visual regions (inferior/middle occipital and middle temporal cortices) responded to emotional facial expressions very early within 100 ms, which supports that the BD patients may hyperactively or sensitively respond to emotional features in perceptual binding. Decreased responses to happy faces in the MDD patients at the left smFC were correlated with their serious depression symptoms, which may support that decreased activity in the smFC underlies irregular positive emotion processing in patients with major depression. The discriminant function of four variables, including gamma activation in the left smFC, right mOFC, right AI/inferior OFC, and the right precentral cortex, accurately classified 89.6% of patients as unipolar/bipolar disorders. These findings indicate different impairments of brain regions in the MDD and BD patients during early facial emotional perception and this abnormal regional gamma activity can be a potential index to distinguish these two mood disorders.

Conflict of Interests

The authors declare that there is no conflict of interests regarding the publication of this paper.

Acknowledgments

This study was supported in part by National Science Council (NSC97-2752-B-010-003-PAE and NSC100-2629-B-010-001) and Taipei Veterans General Hospital (V97ER1-001) and Brain Research Center, National Yang-Ming University. The authors thank Chih-Che Chou, Chou-Ming Cheng, and Ying-Chia Lin for their assistance with data collection.

References

[1] R. Kessler, P. Berglund, O. Demler, R. Jin, K. R. Merikangas, and E. E. Walters, "Lifetime prevalence and age-of-onset distributions of DSM-IV disorders in the national comorbidity survey replication," *Archives of General Psychiatry*, vol. 62, no. 6, pp. 593–602, 2005.

[2] A. P. Association and DSM-IV. APATFo, *Diagnostic and Statistical Manual of Mental Disorders: DSM-IV*, Amer Psychiatric, Arlington, Va, USA, 1994.

[3] D. Muzina, D. Kemp, and R. McIntyre, "Differentiating bipolar disorders from major depressive disorders: treatment implications," *Annals of Clinical Psychiatry*, vol. 19, no. 4, pp. 305–312, 2007.

[4] M. L. Phillips and E. Vieta, "Identifying functional neuroimaging biomarkers of bipolar disorder: toward DSM-V," *Schizophrenia Bulletin*, vol. 33, no. 4, pp. 893–904, 2007.

[5] M. L. Phillips, W. C. Drevets, S. L. Rauch, and R. Lane, "Neurobiology of emotion perception II: implications for major psychiatric disorders," *Biological Psychiatry*, vol. 54, no. 5, pp. 515–528, 2003.

[6] N. S. Lawrence, A. M. Williams, S. Surguladze et al., "Subcortical and ventral prefrontal cortical neural responses to facial expressions distinguish patients with bipolar disorder and major depression," *Biological Psychiatry*, vol. 55, no. 6, pp. 578–587, 2004.

[7] J. R. C. D. Almeida, A. Versace, A. Mechelli et al., "Abnormal amygdala-prefrontal effective connectivity to happy faces differentiates bipolar from major depression," *Biological Psychiatry*, vol. 66, no. 5, pp. 451–459, 2009.

[8] T. Y. Liu, J. C. Hsieh, Y. S. Chen, P. C. Tu, T. P. Su, and L. Chen, "Different patterns of abnormal gamma oscillatory activity in unipolar and bipolar disorder patients during an implicit emotion task," *Neuropsychologia*, vol. 50, no. 7, pp. 1514–1520, 2012.

[9] I. H. Gotlib, E. Krasnoperova, D. N. Yue, and J. Joormann, "Attentional biases for negative interpersonal stimuli in clinical depression," *Journal of Abnormal Psychology*, vol. 113, no. 1, pp. 127–135, 2004.

[10] C. Bourke, K. Douglas, and R. Porter, "Processing of facial emotion expression in major depression: a review," *Australian*

and New Zealand Journal of Psychiatry, vol. 44, no. 8, pp. 681–696, 2010.

[11] A. Stuhrmann, T. Suslow, and U. Dannlowski, "Facial emotion processing in major depression: a systematic review of neuroimaging findings," *Biology of Mood & Anxiety Disorders*, vol. 1, pp. 1–17, 2011.

[12] S. E. Taylor, "Asymmetrical effects of positive and negative events: the mobilization-minimization hypothesis," *Psychological Bulletin*, vol. 110, no. 1, pp. 67–85, 1991.

[13] J. T. Cacioppo, W. L. Gardner, and G. G. Berntson, "The affect system has parallel and integrative processing components: form follows function," *Journal of Personality and Social Psychology*, vol. 76, no. 5, pp. 839–855, 1999.

[14] S. Kousta, D. P. Vinson, and G. Vigliocco, "Emotion words, regardless of polarity, have a processing advantage over neutral words," *Cognition*, vol. 112, no. 3, pp. 473–481, 2009.

[15] F. Pratto and O. P. John, "Automatic vigilance: the attention-grabbing power of negative social information," *Journal of Personality and Social Psychology*, vol. 61, no. 3, pp. 380–391, 1991.

[16] H. Critchley, E. Daly, M. Phillips et al., "Explicit and implicit neural mechanisms for processing of social information from facial expressions: a functional magnetic resonance imaging study," *Human Brain Mapping*, vol. 9, no. 2, pp. 93–105, 2000.

[17] J. Scheuerecker, T. Frodl, N. Koutsouleris et al., "Cerebral differences in explicit and implicit emotional processing-an fMRI study," *Neuropsychobiology*, vol. 56, no. 1, pp. 32–39, 2007.

[18] L. Pessoa, "On the relationship between emotion and cognition," *Nature Reviews Neuroscience*, vol. 9, no. 2, pp. 148–158, 2008.

[19] C. Tallon-Baudry, O. Bertrand, F. Peronnet, and J. Pernier, "Induced γ-band activity during the delay of a visual short-term memory task in humans," *Journal of Neuroscience*, vol. 18, no. 11, pp. 4244–4254, 1998.

[20] E. Rodriguez, N. George, J. Lachaux, J. Martinerie, B. Renault, and F. J. Varela, "Perception's shadow: long-distance synchronization of human brain activity," *Nature*, vol. 397, no. 6718, pp. 430–433, 1999.

[21] M. M. Müller, A. Keil, T. Gruber, and T. Elbert, "Processing of affective pictures modulates right-hemispheric gamma band EEG activity," *Clinical Neurophysiology*, vol. 110, no. 11, pp. 1913–1920, 1999.

[22] Q. Luo, T. Holroyd, M. Jones, T. Hendler, and J. Blair, "Neural dynamics for facial threat processing as revealed by gamma band synchronization using MEG," *NeuroImage*, vol. 34, no. 2, pp. 839–847, 2007.

[23] W. Sato, T. Kochiyama, S. Uono et al., "Rapid amygdala gamma oscillations in response to fearful facial expressions," *Neuropsychologia*, vol. 49, no. 4, pp. 612–617, 2011.

[24] M. A. Uusitalo and R. J. Ilmoniemi, "Signal-space projection method for separating MEG or EEG into components," *Medical and Biological Engineering and Computing*, vol. 35, no. 2, pp. 135–140, 1997.

[25] Y. S. Chen, C. Y. Cheng, J. C. Hsieh, and L. F. Chen, "Maximum contrast beamformer for electromagnetic mapping of brain activity," *IEEE Transactions on Biomedical Engineering*, vol. 53, no. 9, pp. 1765–1774, 2006.

[26] J.-X. Liu, Y.-S. Chen, and L.-F. Chen, "Fast and accurate registration techniques for affine and nonrigid alignment of MR brain images," *Annals of Biomedical Engineering*, vol. 38, no. 1, pp. 138–157, 2010.

[27] M. C. Costanza and A. Afifi, "Comparison of stopping rules in forward stepwise discriminant analysis," *Journal of the American Statistical Association*, vol. 74, no. 368, pp. 777–785, 1979.

[28] R. M. Chapman, J. W. McCrary, M. N. Gardner et al., "Brain ERP components predict which individuals progress to Alzheimer's disease and which do not," *Neurobiology of Aging*, vol. 32, no. 10, pp. 1742–1755, 2011.

[29] C. Tallon-Baudry and O. Bertrand, "Oscillatory gamma activity in humans and its role in object representation," *Trends in Cognitive Sciences*, vol. 3, no. 4, pp. 151–162, 1999.

[30] C. S. Herrmann, M. H. J. Munk, and A. K. Engel, "Cognitive functions of gamma-band activity: memory match and utilization," *Trends in Cognitive Sciences*, vol. 8, no. 8, pp. 347–355, 2004.

[31] J. Fan, X. Gu, X. Liu et al., "Involvement of the anterior cingulate and frontoinsular cortices in rapid processing of salient facial emotional information," *NeuroImage*, vol. 54, no. 3, pp. 2539–2546, 2011.

[32] R. Adolphs, "Neural systems for recognizing emotion," *Current Opinion in Neurobiology*, vol. 12, no. 2, pp. 169–177, 2002.

[33] M. Bar, "A cortical mechanism for triggering top-down facilitation in visual object recognition," *Journal of Cognitive Neuroscience*, vol. 15, no. 4, pp. 600–609, 2003.

[34] M. Bar and M. Neta, "The proactive brain: using rudimentary information to make predictive judgments," *Journal of Consumer Behaviour*, vol. 7, no. 4-5, pp. 319–330, 2008.

[35] J. B. Henriques and R. J. Davidson, "Left frontal hypoactivation in depression," *Journal of Abnormal Psychology*, vol. 100, no. 4, pp. 535–545, 1991.

[36] M. T. Mitterschiffthaler, V. Kumari, G. S. Malhi et al., "Neural response to pleasant stimuli in anhedonia: an fMRI study," *NeuroReport*, vol. 14, no. 2, pp. 177–182, 2003.

[37] J. M. Leppänen and J. K. Hietanen, "Positive facial expressions are recognized faster than negative facial expressions, but why?" *Psychological Research*, vol. 69, no. 1-2, pp. 22–29, 2004.

[38] S. Murphy, "The nonconscious discrimination of emotion: evidence for a theoretical distinction between affect and emotion," *Polish Psychological Bulletin*, vol. 32, no. 1, pp. 9–15, 2001.

[39] P. Winkielman, K. C. Berridge, and J. L. Wilbarger, "Unconscious affective reactions to masked happy versus angry faces influence consumption behavior and judgments of value," *Personality and Social Psychology Bulletin*, vol. 31, no. 1, pp. 121–135, 2005.

[40] J. A. Russell and A. Mehrabian, "Evidence for a three-factor theory of emotions," *Journal of Research in Personality*, vol. 11, no. 3, pp. 273–294, 1977.

[41] S. Droit-Volet, S. Brunot, and P. M. Niedenthal, "Perception of the duration of emotional events," *Cognition and Emotion*, vol. 18, no. 6, pp. 849–858, 2004.

[42] P. J. Uhlhaas, C. Haenschel, D. Nikolić, and W. Singer, "The role of oscillations and synchrony in cortical networks and their putative relevance for the pathophysiology of schizophrenia," *Schizophrenia Bulletin*, vol. 34, no. 5, pp. 927–943, 2008.

[43] C. Grützner, P. J. Uhlhaas, E. Genc, A. Kohler, W. Singer, and M. Wibral, "Neuroelectromagnetic correlates of perceptual closure processes," *Journal of Neuroscience*, vol. 30, no. 24, pp. 8342–8352, 2010.

[44] J.-P. Lachaux, N. George, C. Tallon-Baudry et al., "The many faces of the gamma band response to complex visual stimuli," *NeuroImage*, vol. 25, no. 2, pp. 491–501, 2005.

[45] S. Ray and J. H. R. Maunsell, "Different origins of gamma rhythm and high-gamma activity in macaque visual cortex," *PLoS Biology*, vol. 9, no. 4, Article ID e1000610, 2011.

[46] P. J. Uhlhaas, G. Pipa, S. Neuenschwander, M. Wibral, and W. Singer, "A new look at gamma? High- (> 60 Hz) γ-band activity in cortical networks: function, mechanisms and impairment," *Progress in Biophysics and Molecular Biology*, vol. 105, no. 1-2, pp. 14–28, 2011.

[47] C. M. Gray, P. Konig, A. K. Engel, and W. Singer, "Oscillatory responses in cat visual cortex exhibit inter-columnar synchronization which reflects global stimulus properties," *Nature*, vol. 338, no. 6213, pp. 334–337, 1989.

[48] W. Lutzenberger, F. Pulvermüller, T. Elbert, and N. Birbaumer, "Visual stimulation alters local 40-Hz responses in humans: an EEG-study," *Neuroscience Letters*, vol. 183, no. 1-2, pp. 39–42, 1995.

[49] W. Singer and C. M. Gray, "Visual feature integration and the temporal correlation hypothesis," *Annual Review of Neuroscience*, vol. 18, pp. 555–586, 1995.

Hindawi Publishing Corporation
BioMed Research International
Volume 2014, Article ID 196353, 9 pages
http://dx.doi.org/10.1155/2014/196353

Research Article

Fear Processing in Dental Phobia during Crossmodal Symptom Provocation: An fMRI Study

Kevin Hilbert,[1,2] Ricarda Evens,[1,2] Nina Isabel Maslowski,[1,2] Hans-Ulrich Wittchen,[1,2] and Ulrike Lueken[1,2]

[1] *Institute of Clinical Psychology and Psychotherapy, Technische Universität Dresden, Chemnitzer Straße 46, 01187 Dresden, Germany*
[2] *Neuroimaging Center, Technische Universität Dresden, Chemnitzer Straße 46a, 01187 Dresden, Germany*

Correspondence should be addressed to Kevin Hilbert; kevin.hilbert@tu-dresden.de

Received 23 October 2013; Revised 30 January 2014; Accepted 2 February 2014; Published 11 March 2014

Academic Editor: Qiyong Gong

While previous studies successfully identified the core neural substrates of the animal subtype of specific phobia, only few and inconsistent research is available for dental phobia. These findings might partly relate to the fact that, typically, visual stimuli were employed. The current study aimed to investigate the influence of stimulus modality on neural fear processing in dental phobia. Thirteen dental phobics (DP) and thirteen healthy controls (HC) attended a block-design functional magnetic resonance imaging (fMRI) symptom provocation paradigm encompassing both visual and auditory stimuli. Drill sounds and matched neutral sinus tones served as auditory stimuli and dentist scenes and matched neutral videos as visual stimuli. Group comparisons showed increased activation in the insula, anterior cingulate cortex, orbitofrontal cortex, and thalamus in DP compared to HC during auditory but not visual stimulation. On the contrary, no differential autonomic reactions were observed in DP. Present results are largely comparable to brain areas identified in animal phobia, but also point towards a potential downregulation of autonomic outflow by neural fear circuits in this disorder. Findings enlarge our knowledge about neural correlates of dental phobia and may help to understand the neural underpinnings of the clinical and physiological characteristics of the disorder.

1. Introduction

Specific phobia is the most prevalent anxiety disorder and among the most common mental disorders in general [1, 2]. According to DSM IV-TR and DSM-5 criteria, specific phobia is characterized by marked and unreasonable fear towards a specific object or situation which is almost always provoked whenever the phobic stimulus is not avoided [3, 4]. In the last decade, an increasing number of studies investigated the neural substrates of specific phobia, identifying mainly the amygdala, insula, and anterior cingulate cortex (ACC) as core components of the underlying neural network involved in the processing of threat [5, 6]. However, while these results have been proven to be consistent and stable, they are almost exclusively based upon studies investigating the animal subtype of specific phobia, most notably spider phobia. Literature on the other subtypes—blood-injection-injury (BII), situational, natural environment, and other specific phobia—is rare and focuses mostly on BII phobia, which includes dental phobia [7]. Unfortunately, results are more inconsistent here: while some studies reported increased activation in the insula or ACC as well [8, 9], others mainly found differential activation compared to healthy controls in orbitofrontal and prefrontal areas [9–11]. Results also yielded patterns of activation in other areas such as the thalamus [12] or were not indicative of any significant difference between groups in any area [13, 14]. No study so far replicated the finding of amygdala hyperactivation as repeatedly reported for animal phobia.

These diverging findings regarding the notable lack of activation in cortical and subcortical structures involved in the processing of threat were subject to different interpretations. Among others, a dissociation of subjective and physiological fear reactions [14] or altered cognitive control or emotional regulation processes [10, 11] have been proposed. However, methodological causes are possible as well. As pointed out by Köchel et al. [15], fMRI studies to date have

used visual stimuli to induce anxiety without exception. In dental phobics, however, visual stimuli are often less anxiety inducing than stimuli using other sensations [16], which could confound results from studies in BII phobia that often include dental phobics as well [9, 10, 13, 14]. Therefore, inconsistent findings in BII phobia might partly result from the use of stimuli that do not maximally trigger dental fears when investigating group differences in brain activation patterns.

We therefore aimed to further elucidate the influence of stimulus modality on neural fear processing in dental phobics (DP). DP and healthy controls (HC) underwent a symptom provocation paradigm using both auditory and visual stimuli. Autonomic markers (skin conductance) were recorded online. We expected DP not only to show enhanced subjective anxiety towards dental stimuli in general when compared to controls but also to react specifically stronger towards the auditory than visual stimuli. Moreover, we expected stronger autonomic arousal particularly in response to auditory stimuli. On the neural level, we hypothesized DP to show increased brain activation in the amygdala, ACC, insula, thalamus, and orbitofrontal cortex (OFC) compared to HC, particularly during auditory symptom provocation but not during visual phobic stimuli. Based on the finding of a positive relationship between the level of activation in these areas and symptom severity as reflected by subjective and autonomic markers [13, 14], we also expected such a correlation to be present in the current study.

2. Methods

2.1. Subjects. Thirteen dental phobics (DP) and thirteen healthy controls (HC) were recruited from a pool of participants from an online screening. Inclusion criteria were a sum score of 72 or above in the Dental Fear Survey (DFS; indicating moderate to severe dental phobia; [17]) for DP and a sum score of 33 or below (being a score in the lower quartiles) for the HC. Exclusion criteria were fMRI-related exclusion criteria, psychotropic medication less than four weeks prior to assessment, any lifetime neurological disease, or the following current mental disorders (12-month prevalence): bipolar disorder, psychotic disorder, posttraumatic stress disorder, substance dependence, severe major depressive disorder, and comorbid animal type of specific phobia. Psychiatric diagnoses were determined by the Composite International Diagnostic Interview (CIDI; [18]) for DSM IV-TR and confirmed by clinical experts. In total, 2 dental phobics had one comorbid disorder ($n = 1$ panic disorder with agoraphobia, $n = 1$ alcohol abuse) and 4 dental phobics had at least two comorbid disorders ($n = 1$ panic disorder with agoraphobia, $n = 1$ panic disorder without agoraphobia, $n = 1$ agoraphobia without history of panic disorder, $n = 2$ social anxiety disorder, $n = 1$ specific phobia "other" subtype, $n = 1$ eating disorder, $n = 2$ obsessive compulsive disorder, $n = 1$ dysthymia, $n = 1$ conversion disorder, and $n = 1$ dissociative disorder not otherwise specified). HC were free of any DSM IV-TR diagnoses. Additionally, the sample was characterized via questionnaires on depressiveness [19], anxiety sensitivity [20], and broadly defined symptom severity of BII phobia [21]. The study protocol was approved by the ethics committee of the Technische Universität Dresden.

2.2. Experimental Procedure. An fMRI block-design symptom provocation task applying audio and video stimulus materials was programmed on Presentation 12.0 (Neurobehavioral Systems, Albany, CA, USA) software and presented using video goggles (VisuaStim Digital, Northridge, CA, USA). Auditory stimuli comprised a set of 10 dental drill sounds available from a commercial website (http://www.audiosparx.com/) and 10 neutral sinus tone stimuli in different frequencies that were custom made. Sufficient volume was used such that sounds were well discriminated above scanner noise but not uncomfortable for subjects. Visual stimuli comprised a set of 10 previously validated videos [14, 22], depicting anxiety arousing dentist scenes and 10 neutral stimuli matched for information complexity, movements, timing, and background textures. Stimuli were presented for 15 seconds each, separated by a jittered inter-stimulus-interval ranging between 11 to 19 seconds. Thus, there were four conditions in total: dental audio neutral (DAN), dental audio anxiety (DAA), dental video neutral (DVN), and dental video anxiety (DVA). These conditions were presented in pseudorandomized order with no conditions being presented more than two times in a row. Following the fMRI paradigm, all subjects rated all stimuli offline for valence "the picture was negative/neutral/positive," arousal "the picture made me nervous: not at all/very," anxiety "the picture made me anxious: not at all/very," disgust "the picture was disgusting: not at all/very," and pain "the picture made me feel/remember pain: not at all/very" on nine-point Likert scales, similar to earlier studies [13, 14]. During rating, all stimuli were presented in pseudorandomized order as well. Subjective ratings from $n = 2$ subjects ($n = 1$ DP, $n = 1$ HC) were incomplete and therefore excluded from the analysis.

SC responses were recorded online using Ag/AgCl electrodes (MES Medizintechnik, Munich, Germany) affixed to the second phalanx of the nondominant hand's index and middle finger, with isotonic electrode paste (Synapse, Kustomer Kinetics, Arcadia, CA, USA) as contact medium and Brain Vision ExG Amplifier and Brain Vision Recorder (Brain Products, Munich, Germany) as hard- and software. An initial sampling rate of 1000 Hz and 10 sec high-pass and 250 Hz low-pass filters were used with a response criterion of 0.02 μS. The Matlab-based application Ledalab Version 3.4.3 [23, 24] was used for SC data processing, during which the sampling rate was changed to 10 Hz. A continuous decomposition analysis was applied to the data to extract the phasic driver (CDA.SCR) and tonic (CDA.tonic) SC activity within the 1–15 sec time window after stimulus onset. Data were range corrected according to Lykken [25]. SC data from $n = 2$ subjects (DP) were lost due to technical failure.

2.3. Analysis of Demographic, Behavioral, and Physiological Data. Chi-square tests and independent t-tests were applied

to demographic and questionnaire data as appropriate. Ratings were compared between groups for each dimension by repeated-measurement analyses of variance (ANOVAs), with the between-subject factor group (DP; HC) and the within-subject factors stimuli (audio; video) and condition (anxiety; neutral). Testing for normal distribution of SC parameters using Shapiro-Wilk tests indicated a nonnormal distribution of SC data. Therefore, SC data was log transformed at first and then analyzed by repeated-measurement ANOVAs with the between-subject factor group (DP; HC) and the within-subject factors stimuli (audio; video) and condition (anxiety; neutral), for tonic and phasic SC components separately. Pairwise comparisons were employed as post hoc tests. SPSS 20 was used for all analyses, with the level of significance being set at $P < 0.05$.

2.4. fMRI Data Acquisition and Analysis. A 3-Tesla Trio-Tim MRI whole-body scanner (Siemens, Erlangen, Germany) and a 12 channel head coil were used for MRI data collection. Functional images were acquired via T2∗ weighted gradient echo planar imaging (EPI) covering the whole brain (560 volumes, repetition time (TR) 2500 msec, echo time (TE) 25 msec, field of view 192 × 192 mm, and matrix 64 × 64). 44 axial slices were recorded in tilted angle (AC-PC + 30°; interleaved acquisition, no gap, slice thickness 3 mm, and in-plane resolution 3 × 3 mm) to reduce susceptibility artifacts in inferior brain areas [26]. Four dummy volumes were discarded with regard to T1 equilibration effects. The T1 weighted structural reference image was acquired via Magnetization Prepared Rapid Gradient Echo Imaging (MPRAGE; 176 sagittal slices, slice thickness = 1 mm, TE = 2.26 msec, TR = 1900 msec, flip angle = 9°, FOV = 256 × 256 mm^3, and matrix = 256 × 256). Headphones were applied for stimulus presentation, as hearing protection, and to allow communication with the subject. fMRI data were analyzed using SPM8 (Wellcome Trust Centre for Neuroimaging, UCL, London, UK). Images were realigned and unwarped to correct for head movement, applying a fieldmap correction to the EPI time series. Structural and functional images were coregistered, segmented, and normalized to the MNI reference brain (Montreal Neurological Institute, Quebec, Canada). Functional data was upsampled to 2 × 2 × 2 mm voxel size. An 8 mm full-width half-maximum Gaussian kernel was applied for spatial smoothing.

On subject level, four regressors of interest (DAN > BL, DAA > BL, DVN > BL, and DVA > BL) and the six-movement parameters as regressors of no interest were introduced to the general linear model. Results were included in a flexible factorial model for a random effects analysis on group level. The subjects factor, group factor (HC, DP), and stimulus factor (DAN > BL, DAA > BL, DVN > BL, and DVA > BL) were specified and an additional interaction between group and stimulus factors was modeled. The following contrasts were tested: auditory (DAA > DAN) or visual (DVA > DVN) stimulus material, between groups and auditory versus visual stimulus material ((DAA > DAN) > (DVA > DVN)) and vice versa, between groups. As differences between two modalities of the same phobic material might not be of large effect size, a Monte Carlo simulation was used to determine a cluster size-based significance threshold [27]. This approach has been shown to be more sensitive to small effects than the standard 0.05 *familywise error* (FWE) correction, while still being an adequate correction for multiple comparisons [28]. The cluster size was calculated by assuming an individual voxel type I error of $P < 0.001$ and including the study's matrix, slice number, smoothing kernel, and (upsampled) voxel size. 10000 iterations determined a minimum cluster size of 58 consecutive voxels. Since no study investigated the neural correlates of auditory symptom provocation in DP before, an exploratory whole brain analysis was employed. Additionally, a region-of-interest analysis (ROI) was conducted for the amygdala, as the cluster-based significance threshold used here might require too many consecutive voxels for such a rather small structure. Estimated beta values of the insula and OFC were extracted clusterwise via the first eigenvariate and correlated with DFS sum scores and tonic and phasic SCRs towards auditory symptom provocation within the DP. Other estimated beta values were extracted accordingly for illustration.

3. Results

3.1. Sample Characteristics and Behavioral Data. Sample characteristics and clinical data are presented in Table 1. DP rated both auditory and visual stimulus material more negatively than HC (main effect group: valence: $F(1, 22) = 13.514$, $P < 0.01$; arousal: $F(1, 22) = 15.643$, $P < 0.001$; anxiety: $F(1, 22) = 40.550$, $P < 0.001$; disgust: $F(1, 22) = 14.273$, $P < 0.01$; pain: $F(1, 22) = 43.769$, $P < 0.001$). A main effect of stimulus material was detected for pain and valence (valence: $F(1, 22) = 24.324$, $P < 0.001$; pain: $F(1, 22) = 6.020$, $P < 0.05$; all other dimensions above $P > 0.07$), indicating that auditory stimulus material was rated as partially more negative than visual stimulus material. However, this finding was not driven particularly by one of both groups (interaction effect: group ∗ stimulus material: all interactions above $P > 0.07$). Anxiety arousing stimuli were rated as more negative than neutral stimuli (main effect condition: valence: $F(1, 22) = 109.427$, $P < 0.001$; arousal: $F(1, 22) = 59.586$, $P < 0.001$; anxiety: $F(1, 22) = 56.854$, $P < 0.001$; disgust: $F(1, 22) = 40.195$, $P < 0.001$; pain: $F(1, 22) = 69.147$, $P < 0.001$). Post hoc analyses on the group ∗ condition interaction (valence: $F(1, 22) = 17.040$, $P < 0.001$; arousal: $F(1, 22) = 31.930$, $P < 0.001$; anxiety: $F(1, 22) = 33.384$, $P < 0.001$; disgust: $F(1, 22) = 18.146$, $P < 0.001$; pain: $F(1, 22) = 24.458$, $P < 0.001$) indicated that significant group differences were present for anxiety arousing stimuli in all dimensions (all below $P < 0.001$); however, group differences emerged for anxiety and pain dimensions towards neutral stimuli as well (anxiety: $P < 0.05$; pain: $P < 0.05$; all other dimensions above $P > 0.17$). The three-way interaction was not significant (interaction effect: group ∗ stimulus material ∗ condition: all dimensions above $P > 0.05$).

Regarding the physiological data, there was a main effect of stimulus material for CDA.SCR ($F(1, 22) = 5.880$, $P < 0.05$), indicating higher CDA.SCR towards auditory than

Table 1: Sample characteristics. Mean (SD) except where noted.

	HC (n = 13)	DP (n = 13)	chi^2/t (df)	P
Sociodemographic characteristics				
Female sex (n. %)	9 (69.23)	9 (69.23)	—	—
Right-handed (n. %)	13 (100.0)	12 (92.31)	1.040	0.308
Unmarried (n. %)	12 (92.31)	11 (84.62)	0.377	0.539
Nonsmoker (n. %)	12 (92.31)	12 (92.31)	—	—
Age (years)	23.23 (3.19)	24.92 (2.25)	1.562	0.131
Clinical characteristics				
DFS[1]	25.77 (3.37)	79.54 (4.86)	32.788 (24)	<0.001
BDI	3.00 (2.89)	8.62 (9.59)	2.022 (24)	0.054
ASI	14.46 (7.82)	22.15 (12.08)	1.927 (24)	0.066
MQ	7.77 (5.97)	12.69 (6.05)	2.088 (24)	0.048

HC: healthy control group; DP: dental phobia group; DFS: Dental Fear Survey; BDI: Beck Depression Inventory-II; ASI: Anxiety Sensitivity Index; MQ: Mutilation Questionnaire; [1]please note that questionnaire data relate to the date of screening that was used for study inclusion.

visual stimuli. No other significant main effects or interactions emerged (all above $P > 0.05$). Regarding CDA.tonic, there was a nonsignificant trend towards the main effect of group ($F(1, 22) = 3.028$, $P = 0.096$) hinting on a slightly higher tonic SC level in the HC. Beside this trend, no main effects or interactions showed true significance (all above $P > 0.17$). Subjective ratings and physiological data are depicted in Figure 1.

3.2. fMRI Results. Table 2 gives a summary of the whole-brain findings in all contrasts. Direct group comparisons for the auditory stimulus material resulted in significantly increased activation in the ACC, insula, thalamus, inferior frontal gyrus, hippocampus, precuneus, postcentral gyrus, and calcarine sulcus in DP but only in the MCC for HC (see Figure 2). During visual stimulation, considerably less differential brain activation was found, with increased activation in the vermis in the DP being the only significant difference. When finally comparing neural activation during auditory versus visual stimulation between groups, DP showed increased activation in the insula, OFC, and precuneus for auditory versus visual stimuli and in the caudate nucleus for visual versus auditory stimuli. For all contrasts, the ROI approach yielded no additional amygdala activation.

Results of the correlational analyses can be inspected in Table 3. A significant negative correlation emerged between OFC activation during visual stimulation and corresponding CDA.tonic. No other correlations were significant; however, two nonsignificant trends were observed for correlations between insula activation during auditory stimulation and CDA.tonic and between insula activation during visual stimulation and CDA.phasic. Again, a negative correlation was indicated.

4. Discussion

This study investigated the effect of crossmodal phobic stimulus processing on neural correlates in dental phobia. The following main findings were observed: (1) while both auditory and visual dental anxiety stimuli were rated as more aversive from DP versus HC, (2) DP showed increased neural activation under auditory dental anxiety stimuli only in most areas related to phobic fear in the animal subtype (except the amygdala). (3) Despite this activation in neural substrates indicative of threat processing, no differential activation was observed in autonomic arousal markers. Negative correlations between neural and autonomic markers could indicate downregulation of autonomic reactions.

The symptom provocation paradigm applied in this study made use of research on the hierarchy of feared situations in dental phobia [16] and included auditory stimuli in order to find a more powerful and robust trigger for phobic fears in these samples. Subjective ratings confirmed that symptom provocation was successful with both visual and auditory stimulus materials. However, subjective ratings also indicate that auditory and visual stimulus materials differed regarding their pain-inducing quality and subsequent overall valence, with auditory stimuli being more painful and aversive. These results are in line with pain being proposed as the central feared experience in dental phobia [29] and earlier findings in subjective data from our group [14]. As in earlier studies, DP showed no SCR differences compared to HC [13, 14, 30]. However, since pronounced responding towards auditory dental stimuli on a neural level was observed, this finding could indicate a dissociation between autonomic versus subjective and neural reactions as proposed earlier. The significant negative association between those brain regions involved in autonomic control such as the insula (as a trend) and the OFC [31, 32] and SC data may furthermore indicate inhibitory rather than excitatory regulation of autonomic outflow. This observation is also consistent with the often reported fainting response due to a relative vasovagal overshoot in BII phobics [33, 34]. Present findings could partly explain this observation in that subjective and neural elevations of fear may result in downregulation of autonomic reactions.

When comparing neural activation towards auditory versus visual information across groups, a pattern of increased activation in the ACC, insula, thalamus, and OFC was

Table 2: Whole brain analysis on brain activation for group differences.

Group	Region	Side	Voxels	F	P	x	y	z
Stimulus: auditory, between-group: (DAA > DAN)								
DP > HC								
	ACC	L	954	5.91	<0.001	−4	32	22
	Calcarine sulcus	L	100	3.74	<0.001	−14	−62	18
	Hippocampus	L	78	3.94	<0.001	−20	−16	−8
	Insula	L	1858	5.34	<0.001	−30	12	−16
	Insula	R	515	4.48	<0.001	44	−12	10
	Postcentral gyrus	L	60	3.56	<0.001	−32	−42	54
	Precuneus	L	207	3.89	<0.001	−6	−58	46
	Inferior frontal gyrus (pars triangularis)	L	68	4.35	<0.001	−46	48	8
	Inferior frontal gyrus (pars triangularis)	L	76	3.98	<0.001	−50	14	26
	Thalamus	L	212	4.36	<0.001	−6	−8	4
HC > DP								
	MCC	L	107	4.86	<0.001	−12	−26	24
	MCC	R	88	4.29	<0.001	12	−12	30
Stimulus: visual, between-group: (DVA > DVN)								
DP > HC								
	Vermis	R	204	4.30	<0.001	8	−36	−34
HC > DP								
	No differential activation							
Stimulus: auditory versus visual, between-group: (DAA > DAN) > (DVA > DVN)								
DP > HC								
	Insula	L	326	4.93	<0.001	−32	14	−16
	Insula	R	165	4.44	<0.001	48	6	−6
	OFC	L	382	4.92	<0.001	−12	50	−6
	Precuneus	L	64	3.69	<0.001	−14	−58	40
HC > DP								
	No differential activation							
Stimulus: visual versus auditory, between-group: (DVA > DVN) > (DAA > DAN)								
DP > HC								
	Caudate nucleus	R	157	5.05	<0.001	28	−6	24
HC > DP								
	No differential activation							

HC: healthy control group; DP: dental phobia group; DAN: dental auditory neutral stimuli; DAA: dental auditory anxiety stimuli; DVN: dental visual neutral stimuli; DVA: dental visual anxiety stimuli; R: right side; L: left side; voxels: number of voxels per cluster; x, y, and z: MNI coordinates of peak voxel; ACC: anterior cingulate cortex; MCC: middle cingulate cortex; OFC: orbitofrontal cortex; analysis: minimum cluster size = 58; $P < 0.001$.

Table 3: Pearson's correlations between neural activation towards anxiety-inducing stimuli and DFS scores and phasic and tonic skin conductance reactivity in the dental phobia group ($n = 13$).

Brain areas (MNI coordinates)		DFS scores		CDA.SCR		CDA.tonic	
		r	P corr	r	P corr	r	P corr
Insula-L (auditory)	(−32, 14, −16)	−0.252	0.407	0.343	0.301	−0.538	0.088
Insula-L (visual)	(−32, 14, −16)	−0.109	0.722	−0.542	0.085	0.005	0.988
OFC-L (auditory)	(−12, 50, −6)	−0.315	0.294	0.480	0.135	−0.396	0.228
OFC-L (visual)	(−12, 50, −6)	−0.417	0.156	0.095	0.782	−0.642	0.033

DFS: Dental Fear Survey; CDA.SCR: phasic skin conductance reactivity; CDA.tonic: tonic skin conductance reactivity; OFC: orbitofrontal cortex; L: left side.

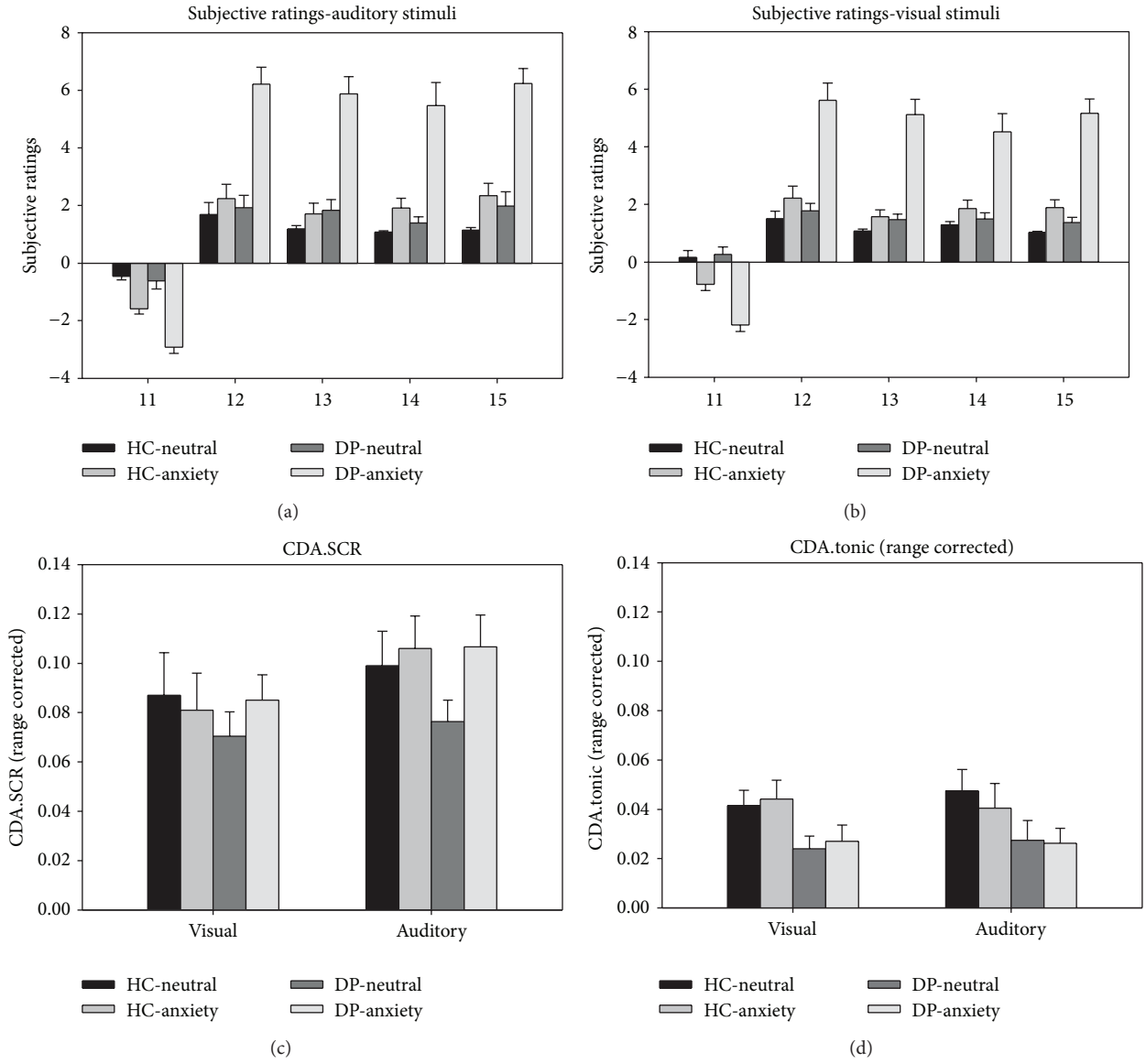

Figure 1: Behavioral data. Upper half: subjective ratings for auditory (a) and visual (b) dental stimuli. Lower half: phasic (CDA.SCR; (c)) and tonic (CDA.tonic; (d)) skin conductance responses. HC: healthy control group; DP: dental phobia group. $^{*}P < 0.05$; $^{**}P < 0.01$; $^{***}P < 0.001$.

detected in DP. This result is also largely overlapping with core areas identified in animal specific phobia [5, 6]. Both ACC and insula were consistently found during phobic stimulus processing [13, 14, 35, 36], and hyperactivity in both structures recedes after successful cognitive-behavioral therapy [37]. Both insula and ACC have been related to threat evaluation processes [36] and anticipatory anxiety [38]. A recent study was also able to demonstrate a strong correlation between ACC and insula activation, albeit only in animal phobia [39]. Both have also been related to the neural response to disgust, being an emotion of particular importance in BII and dental phobia [40], but this seems to be the case for the insula to a greater extent [41]. Most notably, insula and ACC are also crucially involved in pain anticipation [42–44] and modulation of the experience of pain due to the perceived threat or anxiety level [45, 46]. In accordance with the corresponding pain ratings being significantly increased for auditory stimulus material on a subjective level, fear of pain seems to be relevant for the processing of drill sounds.

OFC activation in turn has rarely been investigated in specific phobia samples [47], but increased activation in this area seems to be relatively specific for DP compared to animal phobia [14]. Generally, activation in orbitofrontal and prefrontal gyri in DP has been related to processes of cognitive control and (re-)appraisal, possibly representing a more evaluation based fear response in DP than in animal

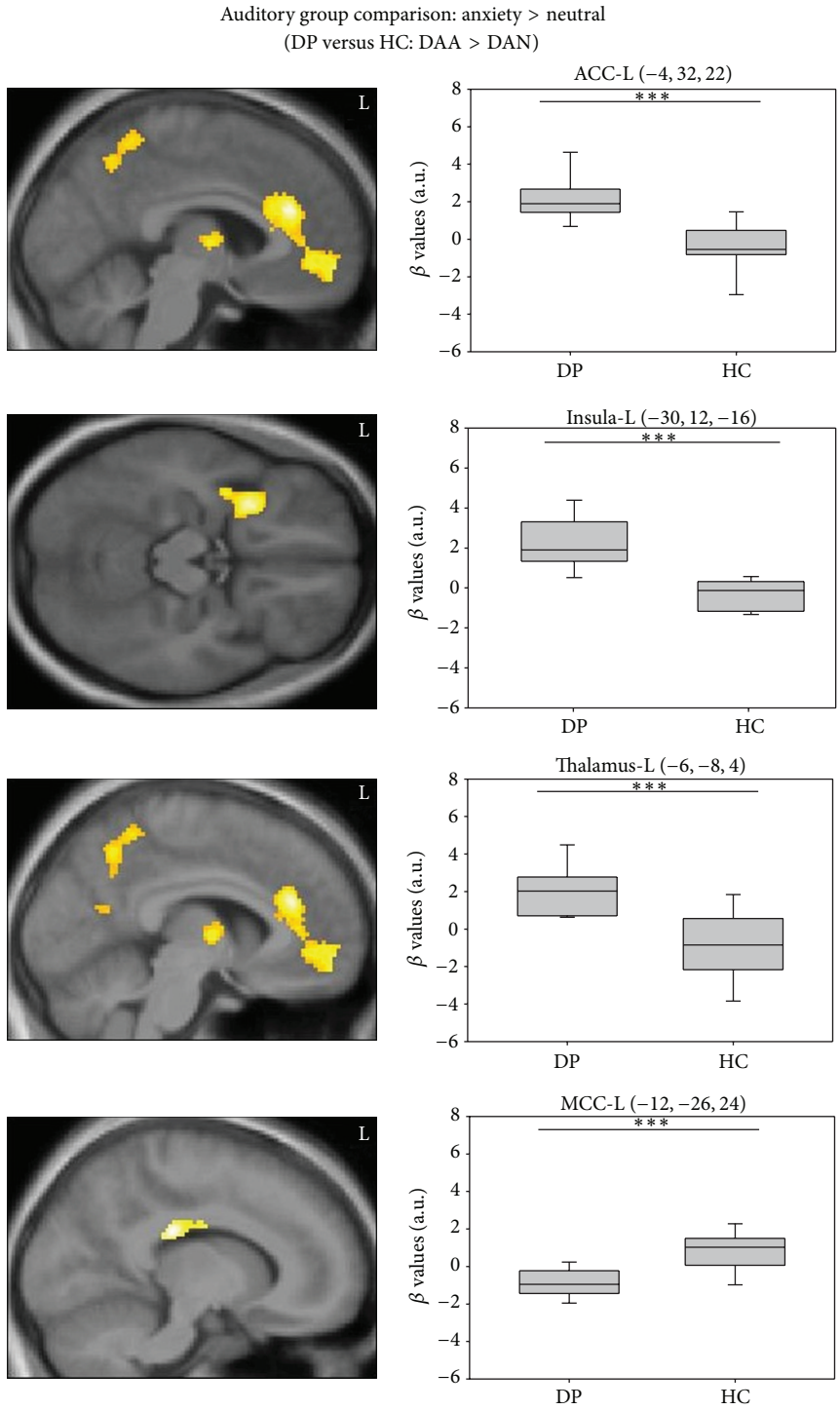

Figure 2: Neural activation patterns of the between-group comparison for auditory stimulus material (DAA > DAN): dental phobics versus healthy controls (upper three) and healthy controls versus dental phobics (below). DP: dental phobia group; HC: healthy control group; ACC: anterior cingulate cortex; MCC: middle cingulate cortex; L: left side; analysis: minimum cluster size = 58; $^{*}P < 0.05$; $^{**}P < 0.01$; $^{***}P < 0.001$.

phobia [9, 10, 14]. Such an evaluation-based response, being based on the sympathetically downregulating OFC rather than on the upregulating amygdala, is also well in line with the interpretation of diminished sympathetic responsiveness outlined above.

Neither the whole-brain nor the ROI approaches found any evidence for amygdala hyperactivation in this study. This lack of differential amygdala activation might be related to the general relevance of BII phobia stimuli applying to healthy subjects as well, as pointed out by Hermann et al. [11].

Additionally, besides contextual reasons, the block design used in this study could also have prevented the detection of amygdala activation [12, 14]. Future studies should combine auditory stimuli with an event-related fMRI task to further investigate whether the amygdala is recruited as well in rapid stimulus processing in DP.

Several limitations should be considered regarding the results of this study: DP were included on the basis of established clinical cut-offs, and future studies are needed to determine whether findings can be generalized to treatment-seeking patient samples. The size of the sample was relatively small, which might limit the ability to detect small scale effects. Additionally, the sample included DP with dental phobia only and DP with comorbid disorders. Due to the small size of both subgroups, an analysis of similarities and differences between these subgroups was omitted. Therefore, it is not clear whether the results of this study were significantly influenced by comorbidity. Furthermore, the study applied a block design that might prevent the finding of activity patterns in rapidly habituating structures.

5. Conclusion

This study aimed to investigate the impact of different stimulus modalities on subjective, autonomic, and neural threat processing in dental phobia. As such, it expands the literature on neural substrates of the disorder by showing evidence for the influence of stimulus modality. Auditory stimulation seems to be a more robust trigger of the neural network subserving threat processing in dental phobia, albeit subjective anxiety was elicited during both visual and auditory symptoms provocation. However, autonomic responding did not parallel neural activation but rather indicated a down-regulation of autonomic outflow. Thus, when investigating the neural correlates of dental phobia, findings may partly depend on the modality of the used stimulus material. If replicated, these findings may help to understand and better distinguish the neural underpinnings and pathophysiology of these different specific phobia subtypes. Additionally, findings may also facilitate the improvement of clinical applications of phobic fear processing, for example, during exposure therapy, in the future.

Conflict of Interests

The following authors report no conflict of interests concerning the content of this paper: Kevin Hilbert, Ricarda Evens, Nina Isabel Maslowski, and Ulrike Lueken. Hans-Ulrich Wittchen has served as a general consultant (nonproduct related) for Pfizer, Organon, Servier, and Essex Pharma and has received grant funding for his institution from Sanofi Aventis, Pfizer, Lundbeck, Novartis, Essex Pharma, Servier, and Wyeth.

Acknowledgments

The authors would like to thank Veronika Stolyar for her support during the collection of the data. They also acknowledge support by the German Research Foundation and the Open Access Publication Funds of the TU Dresden.

References

[1] R. C. Kessler, M. Petukhova, N. A. Sampson, A. M. Zaslavsky, and H. U. Wittchen, "Twelve-month and lifetime prevalence and lifetime morbid risk of anxiety and mood disorders in the United States," *International Journal of Methods in Psychiatric Research*, vol. 21, no. 3, pp. 169–184, 2012.

[2] H. U. Wittchen, F. Jacobi, J. Rehm et al., "The size and burden of mental disorders and other disorders of the brain in Europe 2010," *European Neuropsychopharmacology*, vol. 21, no. 9, pp. 655–679, 2011.

[3] APA, *Diagnostic and Statistical Manual of Mental Disorders*, American Psychiatric Association, Washington, DC, USA, 4 edition, 2000.

[4] APA, *Diagnostic and Statistical Manual of Mental Disorders*, American Psychiatric Publishing, Arlington, Va, USA, 5 edition, 2013.

[5] A. Etkin and T. D. Wager, "Functional neuroimaging of anxiety: a meta-analysis of emotional processing in PTSD, social anxiety disorder, and specific phobia," *American Journal of Psychiatry*, vol. 164, no. 10, pp. 1476–1488, 2007.

[6] L. M. Shin and I. Liberzon, "The neurocircuitry of fear, stress, and anxiety disorders," *Neuropsychopharmacology*, vol. 35, no. 1, pp. 169–191, 2010.

[7] R. T. LeBeau, D. Glenn, B. Liao et al., "Specific phobia: a review of DSM-IV specific phobia and preliminary recommendations for DSM-V," *Depression and Anxiety*, vol. 27, no. 2, pp. 148–167, 2010.

[8] X. Caseras, D. Mataix-Cols, M. V. Trasovares et al., "Dynamics of brain responses to phobic-related stimulation in specific phobia subtypes," *European Journal of Neuroscience*, vol. 32, no. 8, pp. 1414–1422, 2010.

[9] A. Schienle, W. Scharmuller, V. Leutgeb, A. Schafer, and R. Stark, "Sex differences in the functional and structural neuroanatomy of dental phobia," *Brain Structure & Function*, vol. 218, no. 3, pp. 779–787, 2013.

[10] A. Hermann, V. Leutgeb, W. Scharmuller, D. Vaitl, A. Schienle, and R. Stark, "Individual differences in cognitive reappraisal usage modulate the time course of brain activation during symptom provocation in specific phobia," *Biology of Mood & Anxiety Disorders*, vol. 3, no. 1, article 16, 2013.

[11] A. Hermann, A. Schäfer, B. Walter, R. Stark, D. Vaitl, and A. Schienle, "Diminished medial prefrontal cortex activity in blood-injection-injury phobia," *Biological Psychology*, vol. 75, no. 2, pp. 124–130, 2007.

[12] X. Caseras, V. Giampietro, A. Lamas et al., "The functional neuroanatomy of blood-injection-injury phobia: a comparison with spider phobics and healthy controls," *Psychological Medicine*, vol. 40, no. 1, pp. 125–134, 2010.

[13] U. Lueken, K. Hilbert, V. Stolyar, N. Maslowski, K. Beesdo-Baum, and H.-U. Wittchen, "Neural substrates of defensive reactivity in two subtypes of specific phobia," *Social Cognitive & Affective Neuroscience*, 2013.

[14] U. Lueken, J. D. Kruschwitz, M. Muehlhan, J. Siegert, J. Hoyer, and H.-U. Wittchen, "How specific is specific phobia? Different neural response patterns in two subtypes of specific phobia," *NeuroImage*, vol. 56, no. 1, pp. 363–372, 2011.

[15] A. Köchel, M. M. Plichta, A. Schäfer, F. Schöngassner, A. J. Fallgatter, and A. Schienle, "Auditory symptom provocation in dental phobia: a near-infrared spectroscopy study," *Neuroscience Letters*, vol. 503, no. 1, pp. 48–51, 2011.

[16] F. M. D. Oosterink, A. De Jongh, and I. H. A. Aartman, "What are people afraid of during dental treatment? Anxiety-provoking capacity of 67 stimuli characteristic of the dental setting," *European Journal of Oral Sciences*, vol. 116, no. 1, pp. 44–51, 2008.

[17] S. Tönnies, M. Mehrstedt, and I. Eisentraut, "The dental anxiety scale (DAS) and the dental fear survey—two measuring instruments to record dental fears," *Zeitschrift fur Medizinische Psychologie*, vol. 11, pp. 63–72, 2002.

[18] H.-U. Wittchen and H. Pfister, *DIA-X Interview*, Swets & Zeitlinger, Frankfurt, Germany, 1997.

[19] A. T. Beck, R. A. Steer, and G. K. Brown, *Manual for the Beck Depression Inventory*, The Psychological Corporation, San Antonio, Tex, USA, 2 edition, 1996.

[20] S. Reiss, R. A. Peterson, D. M. Gursky, and R. J. McNally, "Anxiety sensitivity, anxiety frequency and the prediction of fearfulness," *Behaviour Research and Therapy*, vol. 24, no. 1, pp. 1–8, 1986.

[21] R. A. Kleinknecht and R. M. Thorndike, "The Mutilation Questionnaire as a predictor of blood/injury fear and fainting," *Behaviour Research and Therapy*, vol. 28, no. 5, pp. 429–437, 1990.

[22] U. Lueken, J. Hoyer, J. Siegert, A. T. Gloster, and H.-U. Wittchen, "Symptom provocation in dental anxiety using cross-phobic video stimulation," *European Journal of Oral Sciences*, vol. 119, no. 1, pp. 61–68, 2011.

[23] M. Benedek and C. Kaernbach, "A continuous measure of phasic electrodermal activity," *Journal of Neuroscience Methods*, vol. 190, no. 1, pp. 80–91, 2010.

[24] M. Benedek and C. Kaernbach, "Decomposition of skin conductance data by means of nonnegative deconvolution," *Psychophysiology*, vol. 47, no. 4, pp. 647–658, 2010.

[25] D. T. Lykken, "Range correction applied to heart rate and to GSR data," *Psychophysiology*, vol. 9, no. 3, pp. 373–379, 1972.

[26] R. Deichmann, J. A. Gottfried, C. Hutton, and R. Turner, "Optimized EPI for fMRI studies of the orbitofrontal cortex," *NeuroImage*, vol. 19, no. 2, pp. 430–441, 2003.

[27] S. D. Slotnick, L. R. Moo, J. B. Segal, and J. Hart Jr., "Distinct prefrontal cortex activity associated with item memory and source memory for visual shapes," *Cognitive Brain Research*, vol. 17, no. 1, pp. 75–82, 2003.

[28] S. D. Slotnick and D. L. Schacter, "A sensory signature that distinguishes true from false memories," *Nature Neuroscience*, vol. 7, no. 6, pp. 664–672, 2004.

[29] M. M. Bradley, T. Silakowski, and P. J. Lang, "Fear of pain and defensive activation," *Pain*, vol. 137, no. 1, pp. 156–163, 2008.

[30] J. Lundgren, U. Berggren, and S. G. Carlsson, "Psychophysiological reactions in dental phobic patients during video stimulation," *European Journal of Oral Sciences*, vol. 109, no. 3, pp. 172–177, 2001.

[31] E. J. Neafsey, "Prefrontal cortical control of the autonomic nervous system: anatomical and physiological observations," *Progress in Brain Research*, vol. 85, pp. 147–166, 1990.

[32] D. Öngür and J. L. Price, "The organization of networks within the orbital and medial prefrontal cortex of rats, monkeys and humans," *Cerebral Cortex*, vol. 10, no. 3, pp. 206–219, 2000.

[33] L. G. Ost, U. Sterner, and I. L. Lindahl, "Physiological responses in blood phobics," *Behaviour Research and Therapy*, vol. 22, no. 2, pp. 109–117, 1984.

[34] B. A. Thyer, J. Himle, and G. C. Curtis, "Blood-injury-illness phobia: a review," *Journal of Clinical Psychology*, vol. 41, no. 4, pp. 451–459, 1985.

[35] J. C. Britton, A. L. Gold, T. Deckersbach, and S. L. Rauch, "Functional MRI study of specific animal phobia using an event-related emotional counting stroop paradigm," *Depression and Anxiety*, vol. 26, no. 9, pp. 796–805, 2009.

[36] T. Straube, H.-J. Mentzel, and W. H. R. Miltner, "Neural mechanisms of automatic and direct processing of phobogenic stimuli in specific phobia," *Biological Psychiatry*, vol. 59, no. 2, pp. 162–170, 2006.

[37] T. Straube, M. Glauer, S. Dilger, H.-J. Mentzel, and W. H. R. Miltner, "Effects of cognitive-behavioral therapy on brain activation in specific phobia," *NeuroImage*, vol. 29, no. 1, pp. 125–135, 2006.

[38] T. Straube, H.-J. Mentzel, and W. H. R. Miltner, "Waiting for spiders: brain activation during anticipatory anxiety in spider phobics," *NeuroImage*, vol. 37, no. 4, pp. 1427–1436, 2007.

[39] X. Caseras, K. Murphy, D. Mataix-Cols et al., "Anatomical and functional overlap within the insula and anterior cingulate cortex during interoception and phobic symptom provocation," *Human Brain Mapping*, vol. 34, no. 5, pp. 1220–1229, 2013.

[40] C. N. Sawchuk, J. M. Lohr, D. H. Westendorf, S. A. Meunier, and D. F. Tolin, "Emotional responding to fearful and disgusting stimuli in specific phobics," *Behaviour Research and Therapy*, vol. 40, no. 9, pp. 1031–1046, 2002.

[41] B. Wicker, C. Keysers, J. Plailly, J.-P. Royet, V. Gallese, and G. Rizzolatti, "Both of us disgusted in my insula: the common neural basis of seeing and feeling disgust," *Neuron*, vol. 40, no. 3, pp. 655–664, 2003.

[42] K. H. Brodersen, K. Wiech, E. I. Lomakina et al., "Decoding the perception of pain from fMRI using multivariate pattern analysis," *NeuroImage*, vol. 63, no. 3, pp. 1162–1170, 2012.

[43] A. Ploghaus, I. Tracey, J. S. Gati et al., "Dissociating pain from its anticipation in the human brain," *Science*, vol. 284, no. 5422, pp. 1979–1981, 1999.

[44] F. Seifert, N. Schuberth, R. De Col, E. Peltz, F. T. Nickel, and C. Maihöfner, "Brain activity during sympathetic response in anticipation and experience of pain," *Human Brain Mapping*, vol. 34, no. 8, pp. 1768–1782, 2013.

[45] C. S. Lin, J. C. Hsieh, T. C. Yeh, S. Y. Lee, and D. M. Niddam, "Functional dissociation within insular cortex: the effect of pre-stimulus anxiety on pain," *Brain Research*, vol. 1493, pp. 40–47, 2013.

[46] K. Wiech, C.-S. Lin, K. H. Brodersen, U. Bingel, M. Ploner, and I. Tracey, "Anterior insula integrates information about salience into perceptual decisions about pain," *Journal of Neuroscience*, vol. 30, no. 48, pp. 16324–16331, 2010.

[47] A. del Casale, S. Ferracuti, C. Rapines et al., "Functional neuroimaging in specific phobia," *Psychiatry Research*, vol. 202, no. 3, pp. 181–197, 2012.

Hindawi Publishing Corporation
BioMed Research International
Volume 2014, Article ID 410472, 9 pages
http://dx.doi.org/10.1155/2014/410472

Research Article

A Preliminary Study of the Influence of Age of Onset and Childhood Trauma on Cortical Thickness in Major Depressive Disorder

Natalia Jaworska,[1,2,3] Frank P. MacMaster,[1,2,3,4] Ismael Gaxiola,[5] Filomeno Cortese,[5] Bradley Goodyear,[1,2,5,6] and Rajamannar Ramasubbu[1,2,5,6]

[1] *Mathison Centre for Mental Health Research & Education, Department of Psychiatry, University of Calgary, TRW Building, 3280 Hospital Drive NW, Calgary, AB, Canada T2N 4Z6*
[2] *Hotchkiss Brain Institute, University of Calgary, 3330 Hospital Drive NW, Calgary, AB, Canada T2N 4N1*
[3] *Alberta Children's Hospital Research Institute, University of Calgary, 2888 Shaganappi Trail NW, Calgary, AB, Canada T3B 6A8*
[4] *Department of Pediatrics, University of Calgary, 2888 Shaganappi Trail NW, Calgary, Canada T3B 6A8*
[5] *The Seaman Family Centre, University of Calgary, Foothills Medical Centre, 1403-29th Street NW, Calgary, AB, Canada T2N 2T9*
[6] *Department of Clinical Neurosciences, University of Calgary, Foothills Medical Centre, 1403-29th Street NW, Calgary, AB, Canada T2N 2T9*

Correspondence should be addressed to Rajamannar Ramasubbu; rramasub@ucalgary.ca

Received 5 November 2013; Revised 17 January 2014; Accepted 21 January 2014; Published 6 March 2014

Academic Editor: Georg Northoff

Background. Major depressive disorder (MDD) neural underpinnings may differ based on onset age and childhood trauma. We assessed cortical thickness in patients who differed in age of MDD onset and examined trauma history influence. *Methods*. Adults with MDD ($N = 36$) and controls (HC; $N = 18$) underwent magnetic resonance imaging. Twenty patients had MDD onset <24 years of age (pediatric onset) and 16 had onset >25 years of age (adult onset). The MDD group was also subdivided into those with ($N = 12$) and without ($N = 19$) physical and/or sexual abuse as assessed by the Childhood Trauma Questionnaire (CTQ). Cortical thickness was analyzed with FreeSurfer software. *Results*. Thicker frontal pole and a tendency for thinner transverse temporal cortices existed in MDD. The former was driven by the pediatric onset group and abuse history (independently), particularly in the right frontal pole. Inverse correlations existed between CTQ scores and frontal pole cortex thickness. A similar inverse relation existed with left inferior and right superior parietal cortex thickness. The superior temporal cortex tended to be thinner in pediatric versus adult onset groups with childhood abuse. *Conclusions*. This preliminary work suggests neural differences between pediatric and adult MDD onset. Trauma history also contributes to cytoarchitectural modulation. Thickened frontal pole cortices as a compensatory mechanism in MDD warrant evaluation.

1. Introduction

Major depressive disorder (MDD) is a common psychiatric disorder with a high burden of disease, yet its neural underpinnings remain elusive. A handful of studies have assessed spatial patterns of cortical thickness in MDD. Interestingly, the regional patterns of cortical thinning in MDD do not perfectly reflect what would be expected from the neuroimaging literature (i.e., cortical thinning is not confined to cognitive and emotive centers; fronto-cortico-limbic structures) [1]. Further, extant literature is not consistent with respect to which cortical regions are typically thicker/thinner in the disorder. This indicates a need for further study with careful attention to factors that may influence cortical thickness in MDD, such as age of disorder onset and past trauma and neglect.

The majority of research on cortical thickness in MDD has focused on assessing elderly depressed individuals (typically defined as >60 years of age; late-life MDD). For instance, one group found no cortical thickness differences between

older depressed females and controls [2]. Similarly, Colloby et al. [3] noted no cortical thickness differences in frontal lobe structures between older individuals with MDD and controls. However, they found a tendency for decreased cortical thickness in MDD in the left frontal pole/pars orbitalis and the right medial orbitofrontal region. In yet another study, Kumar et al. [4] noted a thinner right isthmus in an elderly depressed cohort compared with controls. Another group found that elderly depressed individuals demonstrated thinner cortices in frontal (medial/superior), superior parietal, and inferior temporal regions [5]. Further, treatment nonresponders (versus responders) demonstrated thinner cortices in bilateral posterior cingulate and parahippocampal regions, the left paracentral, pre/cuneus and insular cortices as well as the right medial orbitofrontal, lateral occipital, and superior postcentral cortices [5]. Yet others reported a thinner bilateral dorsolateral prefrontal cortex (DLPFC) and thinner postcentral region in elderly depressed individuals relative to controls. Cortical thinning was also found in the left prefrontal (orbitofrontal, pars triangularis), rostral anterior cingulate, medial/superior temporal, and parietal cortices as well as in the pre/paracentral gyri. Right hemisphere thinning was noted in the pars opercularis, rostral middle frontal, precuneus, and isthmus cortices in elderly individuals with MDD [6]. Finally, cortical thickness in the frontal pole, superior/middle frontal gyrus, orbitofrontal gyrus, and anterior cingulate gyrus was thinner in elderly depressed patients relative to controls [7]. In sum, while some have noted no cortical thickness differences in elderly depressed versus control individuals, others have. Research points to decreased cortical thickness in prefrontal regions, particularly in the orbitofrontal area, in superior/middle frontal aspects (including the DLPFC) as well as para/postcentral regions and the cuneus/isthmus regions in elderly individuals with MDD.

Assessments of cortical thickness in nonelderly adults (i.e., those younger than 60 years of age) with MDD are sparse. Järnum et al. [8] found thinner cortices in MDD patients (middleaged) compared with controls in the orbitofrontal cortex, superior temporal lobe, and insula. Further, depressed nonremitters exhibited a thinner posterior cingulate cortex compared to those in remission. Similarly, another group noted thinner cortices in nonelderly (18–60 years of age) individuals with MDD in the left parahippocampal gyrus, orbitofrontal cortex as well as in the right middle/superior frontal gyri (DLPFC), middle temporal gyrus, and insula [9]. Yet another group noted that depressed adults showed cortical thinning in the bilateral superior/middle frontal gyri, right precentral gyrus (i.e., DLPFC), and right orbitofrontal gyrus. Smaller clusters of cortical thinning existed in the parietal (bilateral inferior parietal regions and left post-central gyrus), temporal (left entorhinal and middle temporal cortex), and occipital lobes (left lateral occipital and lingual gyrus). Regions that were thicker in MDD were the left anterior insula and lateral orbitofrontal gyrus [10]. Recently, van Eijndhoven et al. [11] assessed medication-naïve patients during their first major depressive episode (MDE) or after their first MDE. The medial orbitofrontal cortex was thinner in the MDD patients than in controls. Conversely, the temporal pole and the caudal anterior and posterior cingulate cortices were thicker. This was evident in both currently depressed and recovered patients, suggesting trait-versus state-specific abnormalities. Thus, assessments of nonelderly adults with MDD suggest cortical thinning in the medial orbitofrontal cortex (though lateral regions may be associated with thickening), insula, DLPFC, and the middle temporal cortex—which partially overlap with findings in elderly depressed individuals.

Finally, a handful of groups have assessed cortical thickness in pediatric MDD and found thinner cortices in the right pericalcarine, postcentral, and superior parietal gyri as well as the left supramarginal gyrus. The pediatric MDD cohort (≤18 years of age) exhibited thicker bilateral temporal pole cortices [12], consistent with the results in adults [11]. Additionally, our group observed thicker bilateral middle frontal gyri and left caudal cingulate gyrus in MDD adolescents compared to controls [13].

Potential factors that may contribute to the inconsistency in cortical thickness findings in MDD include the age of the sample examined, medication status, illness severity, sex, and age of MDD onset. The latter is perhaps the most pertinent as later childhood/adolescence is marked by extensive brain changes [14–16]. As such, early MDD onset (i.e., pediatric/adolescent onset) may interfere with normal neurodevelopmental trajectories and manifest as structural abnormalities in adulthood. Further, early MDD onset appears to be associated with increased risk for disorder recurrence, illness burden, and psychiatric comorbidities [14]. This suggests that early MDD onset may be associated with specific neurobiological features. However, few studies have assessed the effect of age of onset on cortical thickness in MDD. A recent study examined the association between age of MDD onset (in this case, early: <24 years; late: >25 years) and cortical thickness [1]. Reductions were found in the DLPFC, pre/postcentral gyri and the lingual gyrus in the early MDD onset group versus controls. Further analyses revealed thicker cortices in the early versus late MDD onset groups in the bilateral posterior cingulate cortex. Conversely, the left parahippocampal, right lingual, right fusiform, and right precuneus gyri were thinner in the early versus the late onset MDD group. Another group assessed elderly depressed patients with earlier (<60 years) and late-life (>60 years) MDD onset and found that the left anterior cingulate was thinner in the late-life onset group [17]. Though preliminary, such data suggest that age of onset may play a role in the spatial distribution of cortical thickness findings in MDD.

Early adverse events increase the possibility of MDD development later in life [18]. Early trauma/maltreatment may interfere with normal brain development. Previous work has reported cortical thickness reductions in maltreated versus nonmaltreated children in the anterior cingulate, superior frontal gyrus, orbitofrontal cortex, left middle temporal regions, and lingual gyrus [19]. Heim et al. [20] also reported widespread cortical thinning as a function of childhood adversity (assessed by the Childhood Trauma Questionnaire (CTQ)). CTQ scores were specifically associated with anterior cingulate gyrus, precuneus, and parahippocampal gyrus cortical thinning. These studies parallel morphometric work

that has noted grey matter density and volumetric reductions in medial/prefrontal regions and cingulate in adults and children with a history of maltreatment/trauma (e.g., physical neglect) [21–26]. These structures have been implicated in emotion regulation and memory processing and tend to exhibit morphometric and functional changes in MDD. Further, this research suggests that maltreatment/trauma is associated with structural modulations persisting into adulthood. To our knowledge, the interaction between age of MDD onset and trauma history on cortical thickness in depression has not been assessed.

As such, this pilot study examined cortical thickness in nonelderly adults (i.e., <60 years of age) with MDD to expand on the relatively scant and inconsistent literature on the matter. Second, we sought to assess whether differences existed in pediatric (<24 years of age) compared with adult MDD onset (>25 years of age) on cortical thickness, in an effort to replicate and expand on previous work. Third, we examined whether differences existed in cortical thickness in depressed adults with childhood sexual and/or physical abuse (sexual + physical abuse group—referred to simply as the abuse group) versus those who experienced no sexual and/or physical abuse but experienced emotional neglect/abuse and/or physical neglect (no sexual + physical abuse group (referred to simply as the non-abuse group); the abuse group also experienced emotional and physical neglect; Table 1). The interaction between age of MDD onset and trauma was also explored.

We expected thinner cortices in orbitofrontal, DLPFC, para-/postcentral, and insular cortices in MDD (versus controls) as well as greater reductions in the pediatric (versus adult) MDD onset group in the DLPFC and posterior inferior temporal regions relative to the adult onset group. Finally, we expected greater thinning in the MDD group with a history of childhood abuse in cortical regions comprising the frontal-limbic network. No directional hypotheses existed regarding age of MDD onset and trauma history due to lack of precedent literature.

2. Methods

2.1. Participants. Thirty-six adults (age range: 19–58 years) with a primary diagnosis of MDD were tested. Clinical diagnoses were made by the study psychiatrist (R.R.) according to the Structured Clinical Interview for DSM (Diagnostic and Statistical Manual of Mental Disorders) IV-TR Diagnoses, Axis I, Patient Version (SCID-IV-I/P) criteria. The Hamilton Rating Scale for Depression ($HAMD_{17}$) was used to assess symptom severity [27], with patients being included if they had an $HAMD_{17}$ score of ≥18. All participants were free of psychotropic medications for a minimum of three weeks at time of neuroimaging. Exclusion criteria included bipolar disorder (BP-I/II or NOS), psychosis history, a clinically significant anxiety disorder, current (<6 months) substance abuse/dependence, neurological disorders, eating disorders, unstable medical condition, and significant suicide risk. Participants with magnetic resonance imaging (MRI) contraindications (e.g., pregnancy, metal implants, and claustrophobia) were also excluded. Twenty patients had MDD onset at <24 years of age (pediatric onset) and 16 patients had MDD onset at >25 years of age (adult onset). Childhood traumatic events were assessed with the Childhood Trauma Questionnaire-Short Form (CTQ-SF) [28]. The CTQ-SF (referred to simply as the CTQ) consists of five subscales with five questions each (range: 1–5): emotional abuse, physical abuse, sexual abuse, emotional neglect, and physical neglect as well as a total score (CTQ_{Total}). For this study, cut-off scores of a minimum of 8 on the physical abuse, physical neglect and sexual abuse subscales, 10 on the emotional abuse subscale, and 15 on the emotional neglect subscale were used. These thresholds are linked with moderate-to-severe levels of abuse and neglect [29]. MDD patients were divided into two groups based on early exposure to physical or sexual abuse: group 1 (abuse group): sexual and/or physical abuse ($N = 12$); group 2 (nonabuse group): no sexual and/or physical abuse (but presence of emotional neglect/abuse and/or physical neglect) ($N = 19$). Most patients who had a history of physical or sexual abuse also experienced some form of emotional maltreatment. Five MDD subjects did not complete the CTQ and were not included in the analyses pertaining to trauma.

Eighteen healthy controls (HCs) without any psychiatric history were also tested; HCs were not included in the cortical thickness analyses regarding trauma history. Informed consent was obtained prior to study initiation in compliance with the Conjoint Health Research Ethics Board at the University of Calgary. Participant characteristics are presented in Tables 1 and 2.

2.2. Magnetic Resonance Imaging (MRI): 3D Image Acquisition. Images were collected at the Seaman Family MR Centre (Foothills Hospital, University of Calgary) with a 3 T General Electric scanner (Signa LX, Waukesha, WI, USA) using a receive-only eight-channel RF head coil. A 3D T1-weighted magnetization prepared rapid acquisition gradient echo (MPRAGE) image was acquired (TR = 8.3 ms; TE = 1.8 ms; flip angle = 20°; voxel size = 0.5 × 0.5 × 1 mm; 1 mm slice thickness; 176 slices).

2.3. Cortical Thickness Analyses. Cortical thickness analyses were carried out using FreeSurfer software (http://surfer.nmr.mgh.harvard.edu/). Detailed procedures on cortical thickness analyses using FreeSurfer have been published [30–33]. In brief, T1-weighted images were intensity-normalized (correcting for magnetic field inconsistencies) and then a skull-stripping procedure was applied to remove extracerebral voxels. A researcher (F.M.-blind to identity/diagnoses) then carried out manual edits to the skull-stripped images. Scans subsequently underwent a segmentation procedure using an estimation of the structure of the grey-white interface. In order to create a smooth spherical representation of the grey-white interface and pial surface, each scan was covered with a triangular tessellation and inflated. Inflated scans were then aligned to FreeSurfer's default reference template via a 2D warp based on cortical folding patterns. Once smoothed using a circularly symmetric Gaussian kernel, sulci and gyri curvature patterns were aligned and the average cortical thickness was measured at each surface point. A uniform

Table 1: Characteristics of MDD onset groups (pediatric/adult MDD onset) and controls.

Characteristics	MDD (overall)	Pediatric MDD onset	Adult MDD onset	HC
N	36	20	16	18
Sex (F/M)	22/14	12/8	10/6	10/8
Age (yrs.)	37.1 ± 11.2	31.5 ± 10.5	44.1 ± 7.7	31.9 ± 9.2
Baseline $HAMD_{17}$	22.1 ± 4.1	20.7 ± 4.1	23.9 ± 3.4	—
Duration of current MDE (yrs.)	5.1 ± 5.4	4.9 ± 5.7	5.4 ± 5.3	—
Time since MDD onset (yrs.)	12.3 ± 9.2	14.4 ± 10.7	9.8 ± 6.3	—
MDD onset (yrs.)	24.8 ± 10.1	17.1 ± 4.8	34.3 ± 5.6	—

HC: healthy controls; $HAMD_{17}$: Hamilton Depression Rating Scale; MDD: major depressive disorder; MDE: major depressive episode; means ± SDs presented.

Table 2: Characteristics of childhood abuse and nonabuse MDD groups.

Characteristics	Nonabuse MDD group	Abuse MDD group
N	19	12
Sex (F/M)	10/9	8/4
Age (yrs.)	36.4 ± 12.6	40.0 ± 9.5
Baseline $HAMD_{17}$	21.2 ± 4.0	24.7 ± 3.9
Duration of current MDE (yrs.)	4.7 ± 5.2	5.4 ± 6.1
Time since MDD onset (yrs.)	11.1 ± 9.4	11.9 ± 9.1
MDD onset (yrs.)	25.3 ± 11.1	28.1 ± 7.3
CTQ_{Total}	51.0 ± 6.1	62.9 ± 11.1
CTQ "neglect" score	39.8 ± 5.6	42.5 ± 6.5
CTQ "abuse" score	11.2 ± 1.1	21.3 ± 6.7

CTQ: Childhood Trauma Questionnaire; CTQ "neglect" score: emotional neglect + physical neglect + emotional abuse; CTQ "abuse" score: physical abuse + sexual abuse; $HAMD_{17}$: Hamilton Depression Rating Scale; MDD: major depressive disorder; MDE: major depressive episode; means ± SDs presented.

surface-based spherical coordinate system was created by transforming the reconstructed surfaces into parameterizable surfaces. An averaging procedure (50 iterations) was applied to smooth the surface and the reconstructed pial surface refined with a deformable surface algorithm. Data was again aligned on a common spherical coordinate system. Cortical thickness was determined by measuring and averaging the distance between the grey-white and pial surfaces [30–33].

2.4. Statistical Analyses. Groups were compared on demographic and clinical indices using one-way analyses of variance (ANOVAs). These analyses were first carried out between the MDD versus HC groups; subsequently, assessments were conducted with three levels (MDD, pediatric onset, adult onset) comprising the group variable. Clinical and demographic features were also compared with one-way ANOVAs between the pediatric and adult onset groups (Table 1).

A multivariate ANOVA (MANOVA) was carried out to assess cortical thickness differences across regions (see Table 1 in Supplementary Material available online at http://dx.doi.org/10.1155/2014/410472) between the MDD and HC groups. The MANOVA was followed by exploratory repeated-measures ANOVAs (rmANOVA; hemisphere as the within- and group (MDD, HC) as the between-subject factor) for each of regional cortical thickness measures (significance set at $P < .01$).

Subsequently, a multivariate analysis of covariance (MANCOVA) was carried out to assess cortical thickness measure differences across regions between the three groups (HC, pediatric onset, and adult onset); age was used as a covariate since it differed in the HC versus the adult and pediatric onset groups (Section 3.2). The MANCOVA was followed by exploratory rmANCOVAs (age as covariate; hemisphere as the within-subject factor; group (HC, pediatric onset, and adult onset) as the between-subject factor) assessing thickness in each cortical region; significance was set at $P < .01$.

One-way ANOVAs were carried out to compare the MDD groups with childhood abuse + neglect versus nonabuse + neglect (i.e., abuse and nonabuse groups, resp.) on pertinent demographic and clinical variables. A MANCOVA was carried out to assess cortical thickness measure differences across regions between the two groups (nonabuse, abuse); $HAMD_{17}$ scores were used as a covariate as they differed between the abuse and nonabuse groups (Section 3.3). This was followed by exploratory rmANCOVAs ($HAMD_{17}$ as covariate; hemisphere as the within-subject factor; group (abuse, non-abuse) as the between-subject factor) assessing thickness in each cortical region; significance was set at $P < .01$.

MANCOVAs ($HAMD_{17}$ scores and age as covariates) were carried out with the two MDD onset (adult, pediatric) and two trauma groups (abuse, nonabuse) as independent variables on cortical thickness measures across regions. Exploratory rmANCOVAs ($HAMD_{17}$ scores and age as covariates; hemisphere as within and groups as between-subject factors) were then carried out for thickness in each cortical region; significance was set at $P < .01$.

Finally, exploratory Spearman's correlations were carried out (for the MDD group) between CTQ_{Total} scores, abuse scores (physical + sexual abuse CTQ scores) and neglect scores (emotional abuse + emotional neglect + physical neglect CTQ scores), and all regional cortical thickness measures; significance was set at $P < .005$. Similarly, correlations were carried out between $HAMD_{17}$ and all regional cortical thickness measures (MDD group only); significance was set at $P < .005$. Unless stated otherwise, means and standard

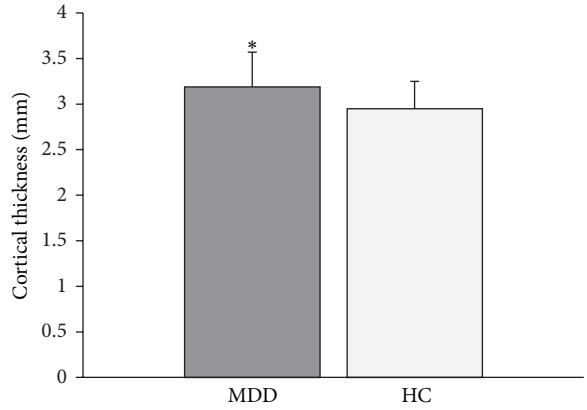

Figure 1: The group with major depressive disorder (MDD) had a thicker frontal pole compared with the healthy control (HC) group ($^*P$ = .01).

deviations (SDs) are presented for all results. All cortical thickness measures are expressed as mm.

3. Results

3.1. Two Group Analyses (HC and MDD). One-way ANOVAs (group (MDD and HCs) as the between-subject factor) revealed no main effect of group on age (Table 1).

The MANOVA (group (HC, MDD) as fixed factor and regions as dependent variables) yielded no main effects of group on cortical thickness. In an effort to replicate previous research, the MANOVA was followed up by exploratory rmANOVA, with hemisphere as the within- and group (MDD, HC) as between-subject factors on cortical thickness (per region). Significance was set at $P < .01$ to minimize false positives and control for multiple comparisons. The main effects of hemisphere, as found by the rmANOVAs, on cortical thickness in various brain regions are listed in Table 3. The rmANOVA revealed a main effect of group (MDD, HC) on frontal pole thickness ($F[1,52] = 7.05$, $P = .01$), with a thicker cortex in the MDD (3.19 ± .38) versus the HC group (2.95 ± .30; Figure 1). A trend for a main effect of group was noted on transverse temporal thickness ($F[1,52] = 6.49$, $P = .014$), with a thinner cortex in the MDD (3.12 ± .17) versus the HC group (3.22 ± .15).

3.2. Three Group Analyses (Adult MDD Onset, Pediatric MDD Onset, and HCs) and Two Group Analyses (Adult and Pediatric MDD Onset). One-way ANOVAs were carried out with group as the independent variable (3 groups: pediatric onset: onset <24 yrs; adult onset: onset >25 yrs; HCs) and age as the dependent variable. A main effect of group existed ($F[2,51] = 9.97$, $P < .001$); follow-up comparisons indicated a difference between the adult MDD onset and both the HC ($P < .001$) and pediatric MDD onset groups ($P < .001$), with the adult onset group being the oldest (Table 1).

Further one-way ANOVAs were carried out between the pediatric versus adult MDD onset groups on other pertinent variables (i.e., $HAMD_{17}$ scores, duration of current MDE, and time since diagnoses). A main effect of group was noted for $HAMD_{17}$ scores ($F[1,34] = 6.50$, $P = .015$), with higher scores in the adult verses the pediatric MDD onset group.

Table 3: Cortical thickness hemispheric differences.

Region (cortical thickness)	Hemisphere effect	P value
Caudal middle frontal cortex	L > R	.003
Entorhinal cortex	L > R	.001
Fusiform cortex	L > R	<.001
Inferior parietal cortex	L > R	.005
Inferior temporal cortex	L > R	<.001
Isthmus cingulate cortex	L > R	<.001
Lingual cortex	R > L	.005
Pars orbitalis cortex	R > L	<.001
Pericalcarine cortex	L > R	.006
Precentral cortex	L > R	.003
Precuneus cortex	R > L	.001
Rostral anterior cingulate cortex	R > L	<.001
Rostral middle frontal cortex	R > L	<.001
Superior frontal cortex	L > R	<.001
Superior parietal cortex	R > L	.001
Superior temporal cortex	L > R	<.001

L: left hemisphere; R: right hemisphere.

The MANCOVA (age as a covariate) yielded no main effect of group (3 groups: HC, adult onset, and pediatric onset) on cortical thickness. However, given the pilot nature of this work, the MANCOVA was followed up with exploratory rmANCOVAs (age as a covariate; hemisphere as the within- and group as the between-subject factor) assessing thickness in each cortical region. Significance was set at $P < .01$. A main effect of hemisphere was noted on cortical thickness in the rostral middle frontal cortex ($F[1,50] = 7.38$, $P = .009$; right > left). A trend for a main effect of group (3 groups) on frontal pole cortex thickness was noted ($F[2,50] = 4.64$, $P = .014$), with a thinner cortex in the HC group (2.93 ± .30) versus the pediatric MDD onset group (3.22 ± .39; $P = .005$).

3.3. Two Group Analyses (MDD Groups: Childhood Abuse Group and Nonabuse Group). One-way ANOVAs were conducted to compare the childhood abuse ($N = 12$) versus non-abuse ($N = 19$) groups on pertinent demographic and

clinical variables (i.e., time since MDD diagnosis, $HAMD_{17}$ scores, current age, age of MDD onset, and duration of current MDE). A main effect of group (neglect, abuse) was found on $HAMD_{17}$ scores ($F[1,29] = 4.21$, $P = .049$), with higher scores in the abuse group. The abuse group also had higher CTQ_{Total} ($F[1,29] = 27.38$, $P < .001$) and, expectedly, abuse scores ($F[1,29] = 42.04$, $P < .001$) than the nonabuse group (Table 2).

The MANCOVA, with group (nonabuse, abuse) as the independent variable, was carried out on cortical thickness measures ($HAMD_{17}$ scores were the covariate)—no main group effect on cortical thickness existed. Exploratory rmANOVAs (group as between- and hemisphere as within-subject factors, $HAMD_{17}$ as the covariate) yielded no significant results, apart from a weak trend for a main effect of group ($F[1,28] = 3.26$, $P = .082$) on frontal pole cortical thickness. This trend was followed up with univariate ANOVAs assessing frontal pole thickness in each hemisphere ($HAMD_{17}$ as covariate). A trend for main effect of group on right frontal pole cortex thickness ($F[1,28] = 4.20$, $P = .05$) was found, with a thicker cortex in the abuse ($3.36 \pm .37$) versus the nonabuse group ($3.10 \pm .25$).

An inverse correlation was found between left precuneus cortex thickness ($r = -.57$, $P < .001$, $N = 31$) as well as right middle temporal cortex thickness ($r = -.59$, $P < .001$, $N = 31$) and CTQ_{Total} scores. Similarly, an inverse correlation existed between both left ($r = -.51$, $P = .003$, $N = 31$) and right ($r = -.54$, $P = .002$, $N = 31$) frontal pole cortex thickness and CTQ_{Total} scores. An inverse correlation also existed between right frontal pole cortex thickness and "abuse" scores ($r = -.50$, $P = .004$, $N = 31$). An inverse relation existed between left inferior parietal cortex thickness ($-.59$, $P < .001$, $N = 31$) as well as right superior parietal cortex thickness ($-.53$, $P = .002$, $N = 31$) and "neglect" scores.

Finally, Chi-square tests revealed no significant difference in the proportion of the pediatric versus adult MDD onset individuals in either the abuse or nonabuse groups. MANCOVAs ($HAMD_{17}$ scores and age as covariates) were carried out with the two MDD onset (adult and pediatric) and two childhood trauma groups (abuse and nonabuse) as the independent variables on cortical thickness measures. No main group effects or interactions were found. Exploratory rmANOVAs ($HAMD_{17}$ scores and age as covariates; hemisphere as with- and groups as between-subject factors; significance was set at $P < .01$) yielded a trend for an onset group × childhood trauma group interaction for superior temporal cortex thickness ($F[1,25] = 5.98$, $P = .022$), with pairwise comparisons indicating a trend for a difference in cortical thickness between the pediatric ($N = 8$; $2.59 \pm .14$) and adult ($N = 8$; $2.77 \pm .14$) MDD onset groups with childhood abuse ($P = .02$). For frontal pole thickness, an onset group × childhood trauma group × hemisphere interaction trend existed ($F[1,25] = 5.07$, $P = .033$). Pairwise comparisons indicated a trend for a difference ($P = .026$) in right frontal pole cortical thickness between the abuse ($N = 8$; $3.01 \pm .15$) and nonabuse ($N = 8$; $3.42 \pm .41$) groups in the adult MDD onset cohort.

4. Discussion

In brief, this pilot study aimed to contribute to existing literature on cortical thickness in depressed adults in two ways. First, we sought to clarify the effect of age of MDD onset on spatial cortical thickness patterns. Second, we investigated the role of childhood trauma, in the form of abuse or nonabuse history (though both groups experienced neglect), on cortical thickness in MDD and its interaction with age of disorder onset. We found thicker frontal pole cortices in the MDD versus HC group. Conversely, a tendency for a thinner transverse temporal cortex existed in MDD. With respect to age of onset, clinically, the adult versus pediatric onset group exhibited higher $HAMD_{17}$ scores. The pediatric onset group had a thicker frontal pole cortex than HCs. In comparisons of MDD groups with childhood abuse versus nonabuse history (the abused group also exhibited neglect and had higher CTQ_{Total} scores), the abuse group had greater $HAMD_{17}$ scores. A tendency for a thicker cortex was noted in the abuse versus nonabuse group in the right frontal pole. Inverse correlations existed between the left precuneus, right middle temporal as well as bilateral frontal pole cortical thickness, and CTQ_{Total} scores. Inverse relations were also noted between right frontal pole cortex thickness and CTQ abuse scores as well as between the left inferior and right superior parietal cortex thickness and CTQ neglect scores. Finally, the superior temporal cortex tended to be thinner in the pediatric versus adult onset groups with childhood abuse. Additionally, the right frontal pole cortex tended to be thinner in the abuse versus nonabuse groups in the adult onset group.

The role of the frontal poles in MDD (and outside the context of the disorder) is not well understood. Neuroimaging studies suggest that frontal poles play a role in "cognitive branching" (i.e., flexibility) as they are activated when performing several subgoals while keeping in mind another (main) goal. Though a handful of functional MRI (fMRI) studies have implicated frontal pole activity in response to antidepressant interventions [34, 35], few morphometric studies of the frontal poles in MDD exist. Much of the work linking the frontal poles with depression stems from stroke research, where greater depression severity has been associated with increased lesion proximity to the frontal poles [36].

Unlike Sheline et al. [7], we noted thicker frontal pole cortices in MDD versus HCs. However, since their sample consisted of late-life depressed individuals while ours was comprised of relatively young-to-middle aged adults, the results may not be directly comparable. They also found that thinner frontal pole cortices existed in patients who did not achieve remission compared to those who did. Given that greater frontal pole cortical thickness in our study was driven by the pediatric onset group, it is feasible that these individuals may have been more likely to be treatment responders (versus the adult onset group). However, as response was not assessed in the current study (though this represents a worthy future direction), this interpretation is speculative. Further, because the pediatric onset group was characterized by lower $HAMD_{17}$ scores than the adult onset

group, thicker frontal pole cortices may reflect a neurocompensatory/adaptive mechanism in the disorder. Neurocompensatory mechanisms are more likely during adolescence, which is a period associated with extensive brain plasticity [14–16]. Additionally, the right frontal pole cortex tended to be thinner in the abuse versus nonabuse groups in the adult MDD onset group suggesting that more pronounced trauma might make the brain susceptible to the neural consequences associated with a psychiatric condition in adulthood.

Few studies have assessed (or reported on) the significance of the transverse temporal cortex (Heschl's gyrus) in MDD. One fMRI study found greater right Heschl's gyrus activation during an emotive processing/attention control task in individuals with a family history of depression versus those without a family history [37], suggesting that the region may play some role in MDD. However, postmortem examinations yielded no differences in neural or glial cell density or cortical thickness in the Heschl's gyrus between individuals with MDD and HCs [38]. Another group found volumetric reductions in the superior temporal gyrus (not Heschl's gyrus specifically) in recovered depressed participants [39], which is somewhat consistent with our observed trend for a thinner transverse temporal cortex in MDD. We also noted a tendency for a thinner superior temporal cortex in the pediatric versus adult onset groups with childhood abuse suggesting that abuse during critical neurodevelopmental periods may influence cytoarchitecture within this region.

Childhood maltreatment is strongly associated with increased risk for psychiatric disorder development [22]. By extension, neural abnormalities associated with trauma/maltreatment may increase psychiatric disorder vulnerability. Previous work has reported reduced cortical thickness and volume in maltreated versus nonmaltreated children in the anterior cingulate, superior frontal gyrus, and orbitofrontal cortex [19, 25]. Similarly, childhood emotional maltreatment and physical neglect were associated with reductions in medial prefrontal cortex volumes in adults [21, 22]. Nondepressed subjects with a family history of MDD and a history of emotional abuse exhibited smaller DLPFC, medial prefrontal, and anterior cingulate cortices than controls [23]. Yet another group found that decreased cingulate volume in individuals with MDD was related to abuse history [5]. Finally, Dannlowski et al. [24] reported reduced grey matter volumes in regions including the orbitofrontal cortex and anterior cingulate gyrus in adults with high CTQ scores. The above indicates that prefrontal, anterior cingulate cortex, and lateral temporal regions (areas implicated in MDD) tend to be rather consistently affected by maltreatment/trauma. Further, research suggests that maltreatment/trauma is associated with structural damage that persists into adulthood. These results mimic our findings of an inverse relation between cortical thickness in the frontal poles, precuneus, and middle temporal regions and CTQ_{Total} scores as well as inverse relations between abuse scores and left inferior and right superior parietal cortical thickness.

The primary limitation of this study was its exploratory nature as well as the small sample size, specifically when groups were split by abuse/nonabuse history. Assessments of interactions between age of MDD onset and childhood trauma (i.e., 2×2 group comparisons) on cortical thickness—though highly novel—were statistically underpowered. Further, in an effort to correct for multiple comparisons and decrease false positive rates, we included covariates when appropriate; inclusion of covariates further decreases power. Due to these limitations, it was not feasible to meaningfully explore the influence of sex on cortical thickness in this study, which may have been informative. In a similar vein, although we attempted to correct for multiple comparisons by adjusting our significance level, true corrections (e.g., Bonferroni) were not applied, though this should be done in comparable future work. As such, our findings and conclusions should be treated as preliminary and with caution, warranting further replication and expansion with a larger sample size.

Briefly, the focal future direction of this work is to assess cortical thickness in a large sample of well-characterized depressed individuals in terms of their trauma history and MDD onset age in order to disambiguate the contributions of these factors in influencing cortical cytoarchitecture in MDD. Greater clarity is needed to better understand the multiple, likely interacting, factors that contribute to altered cortical thickness patterns in MDD. Assessments of such well-characterized samples over time (versus cross-sectionally) would also allow us to gain better insight regarding the neurodevelopmental processes across the lifespan in the context of depression.

Conflict of Interests

The authors declare that there is no conflict of interests regarding the publication of this paper.

Acknowledgment

This study was partly supported by an investigator-initiated grant from Astra Zeneca awarded to Dr. Rajamannar Ramasubbu and the Cuthbertson and Fischer Chair (Dr. Frank P. MacMaster).

References

[1] W. Truong, L. Minuzzi, C. N. Soares et al., "Changes in cortical thickness across the lifespan in major depressive disorder," *Psychiatry Research*, vol. 214, no. 3, pp. 204–211, 2013.

[2] P. C. M. P. Koolschijn, N. E. M. van Haren, H. G. Schnack, J. Janssen, H. E. Hulshoff Pol, and R. S. Kahn, "Cortical thickness and voxel-based morphometry in depressed elderly," *European Neuropsychopharmacology*, vol. 20, no. 6, pp. 398–404, 2010.

[3] S. J. Colloby, M. J. Firbank, A. Vasudev, S. W. Parry, A. J. Thomas, and J. T. O'Brien, "Cortical thickness and VBM-DARTEL in late-life depression," *Journal of Affective Disorders*, vol. 133, no. 1-2, pp. 158–164, 2011.

[4] A. Kumar, O. Ajilore, A. Zhang, D. Pham, and V. Elderkin-Thompson, "Cortical thinning in patients with late-life minor depression," *The American Journal of Geriatric Psychiatry*, 2013.

[5] R. S. Mackin, D. Tosun, S. G. Mueller et al., "Patterns of reduced cortical thickness in late-life depression and relationship to psychotherapeutic response," *The American Journal of Geriatric Psychiatry*, vol. 21, pp. 794–802, 2013.

[6] H. K. Lim, W. S. Jung, K. J. Ahn et al., "Regional cortical thickness and subcortical volume changes are associated with cognitive impairments in the drug-naive patients with late-onset depression," *Neuropsychopharmacology*, vol. 37, no. 3, pp. 838–849, 2012.

[7] Y. I. Sheline, B. M. Disabato, J. Hranilovich et al., "Treatment course with antidepressant therapy in late-life depression," *The American Journal of Psychiatry*, vol. 169, pp. 1185–1193, 2012.

[8] H. Järnum, S. F. Eskildsen, E. G. Steffensen et al., "Longitudinal MRI study of cortical thickness, perfusion, and metabolite levels in major depressive disorder," *Acta Psychiatrica Scandinavica*, vol. 124, no. 6, pp. 435–446, 2011.

[9] G. Wagner, C. C. Schultz, K. Koch, C. Schachtzabel, H. Sauer, and R. G. Schlosser, "Prefrontal cortical thickness in depressed patients with high-risk for suicidal behavior," *Journal of Psychiatric Research*, vol. 46, pp. 1449–1455, 2012.

[10] P.-C. Tu, L.-F. Chen, J.-C. Hsieh, Y.-M. Bai, C.-T. Li, and T.-P. Su, "Regional cortical thinning in patients with major depressive disorder: a surface-based morphometry study," *Psychiatry Research*, vol. 202, no. 3, pp. 206–213, 2012.

[11] P. van Eijndhoven, G. van Wingen, M. Katzenbauer et al., "Paralimbic cortical thickness in first-episode depression: evidence for trait-related differences in mood regulation," *The American Journal of Psychiatry*, vol. 170, no. 12, pp. 1477–1486, 2013.

[12] E. Fallucca, F. P. MacMaster, J. Haddad et al., "Distinguishing between major depressive disorder and obsessive-compulsive disorder in children by measuring regional cortical thickness," *Archives of General Psychiatry*, vol. 68, no. 5, pp. 527–533, 2011.

[13] S. C. N. Reynolds, N. Jaworska, L. M. Langevin, and F. P. MacMaster, *Cortical Thickness in Youth with Major Depressive Disorder*, 2013.

[14] J. Kaufman, A. Martin, R. A. King, and D. Charney, "Are child-, adolescent-, and adult-onset depression one and the same disorder?" *Biological Psychiatry*, vol. 49, no. 12, pp. 980–1001, 2001.

[15] T. Paus, "Structural maturation of neural pathways in children and adolescents: in vivo study," *Science*, vol. 283, no. 5409, pp. 1908–1911, 1999.

[16] M. Arain, M. Haque, L. Johal et al., "Maturation of the adolescent brain," *Neuropsychiatric Disease and Treatment*, vol. 9, pp. 449–461, 2013.

[17] B. M. Disabato, C. Morris, J. Hranilovich et al., "Comparison of brain structural variables, neuropsychological factors, and treatment outcome in early-onset versus late-onset late-life depression," *The American Journal of Geriatric Psychiatry*, 2013.

[18] K. M. Scott, D. R. Smith, and P. M. Ellis, "Prospectively ascertained child maltreatment and its association with DSM-IV mental disorders in young adults," *Archives of General Psychiatry*, vol. 67, no. 7, pp. 712–719, 2010.

[19] P. A. Kelly, E. Viding, G. L. Wallace et al., "Cortical thickness, surface area, and gyrification abnormalities in children exposed to maltreatment: neural markers of vulnerability?" *Biological Psychiatry*, vol. 74, no. 11, pp. 845–852, 2013.

[20] C. M. Heim, H. S. Mayberg, T. Mletzko, C. B. Nemeroff, and J. C. Pruessner, "Decreased cortical representation of genital somatosensory field after childhood sexual abuse," *The American Journal of Psychiatry*, vol. 170, pp. 616–623, 2013.

[21] A.-L. van Harmelen, M.-J. van Tol, N. J. A. van der Wee et al., "Reduced medial prefrontal cortex volume in adults reporting childhood emotional maltreatment," *Biological Psychiatry*, vol. 68, no. 9, pp. 832–838, 2010.

[22] T. Frodl, E. Reinhold, N. Koutsouleris, M. Reiser, and E. M. Meisenzahl, "Interaction of childhood stress with hippocampus and prefrontal cortex volume reduction in major depression," *Journal of Psychiatric Research*, vol. 44, no. 13, pp. 799–807, 2010.

[23] A. Carballedo, D. Lisiecka, A. Fagan et al., "Early life adversity is associated with brain changes in subjects at family risk for depression," *The World Journal of Biological Psychiatry*, vol. 13, pp. 569–578, 2012.

[24] U. Dannlowski, A. Stuhrmann, V. Beutelmann et al., "Limbic scars: long-term consequences of childhood maltreatment revealed by functional and structural magnetic resonance imaging," *Biological Psychiatry*, vol. 71, no. 4, pp. 286–293, 2012.

[25] S. A. de Brito, E. Viding, C. L. Sebastian et al., "Reduced orbitofrontal and temporal grey matter in a community sample of maltreated children," *Journal of Child Psychology and Psychiatry*, vol. 54, pp. 105–112, 2013.

[26] N. V. Malykhin, R. Carter, K. M. Hegadoren, P. Seres, and N. J. Coupland, "Fronto-limbic volumetric changes in major depressive disorder," *Journal of Affective Disorders*, vol. 136, no. 3, pp. 1104–1113, 2012.

[27] M. Hamilton, "Development of a rating scale for primary depressive illness," *The British Journal of Social and Clinical Psychology*, vol. 6, no. 4, pp. 278–296, 1967.

[28] D. P. Bernstein, J. A. Stein, M. D. Newcomb et al., "Development and validation of a brief screening version of the Childhood Trauma Questionnaire," *Child Abuse and Neglect*, vol. 27, no. 2, pp. 169–190, 2003.

[29] M. M. Grant, C. Cannistraci, S. D. Hollon, J. Gore, and R. Shelton, "Childhood trauma history differentiates amygdala response to sad faces within MDD," *Journal of Psychiatric Research*, vol. 45, no. 7, pp. 886–895, 2011.

[30] A. M. Dale, B. Fischl, and M. I. Sereno, "Cortical surface-based analysis: I. Segmentation and surface reconstruction," *NeuroImage*, vol. 9, no. 2, pp. 179–194, 1999.

[31] B. Fischl and A. M. Dale, "Measuring the thickness of the human cerebral cortex from magnetic resonance images," *Proceedings of the National Academy of Sciences of the United States of America*, vol. 97, no. 20, pp. 11050–11055, 2000.

[32] B. Fischl, M. I. Sereno, and A. M. Dale, "Cortical surface-based analysis: II. Inflation, flattening, and a surface-based coordinate system," *NeuroImage*, vol. 9, no. 2, pp. 195–207, 1999.

[33] B. Fischl, M. I. Sereno, R. B. Tootell, and A. M. Dale, "High-resolution intersubject averaging and a coordinate system for the cortical surface," *Human Brain Mapping*, vol. 8, pp. 272–284, 1999.

[34] G. S. Dichter, J. N. Felder, and M. J. Smoski, "The effects of brief behavioral activation therapy for depression on cognitive control in affective contexts: an fMRI investigation," *Journal of Affective Disorders*, vol. 126, no. 1-2, pp. 236–244, 2010.

[35] J. Wu, M. S. Buchsbaum, J. C. Gillin et al., "Prediction of antidepressant effects of sleep deprivation by metabolic rates in the ventral anterior cingulate and medial prefrontal cortex," *American Journal of Psychiatry*, vol. 156, no. 8, pp. 1149–1158, 1999.

[36] K. Narushima, J. T. Kosier, and R. G. Robinson, "A reappraisal of poststroke depression, intra- and inter-hemispheric lesion location using meta-analysis," *Journal of Neuropsychiatry and Clinical Neurosciences*, vol. 15, no. 4, pp. 422–430, 2003.

[37] F. Amico, A. Carballedo, D. Lisiecka, A. J. Fagan, G. Boyle, and T. Frodl, "Functional anomalies in healthy individuals with a first degree family history of major depressive disorder," *Biology of Mood & Anxiety Disorders*, vol. 2, article 1, 2012.

[38] D. Cotter, D. Mackay, S. Frangou, L. Hudson, and S. Landau, "Cell density and cortical thickness in Heschl's gyrus in schizophrenia, major depression and bipolar disorder," *British Journal of Psychiatry*, vol. 185, pp. 258–259, 2004.

[39] T. Takahashi, M. Yücel, V. Lorenzetti et al., "An MRI study of the superior temporal subregions in patients with current and past major depression," *Progress in Neuro-Psychopharmacology and Biological Psychiatry*, vol. 34, no. 1, pp. 98–103, 2010.

Hindawi Publishing Corporation
BioMed Research International
Volume 2014, Article ID 691505, 11 pages
http://dx.doi.org/10.1155/2014/691505

Research Article

Reduced Amygdala Volume Is Associated with Deficits in Inhibitory Control: A Voxel- and Surface-Based Morphometric Analysis of Comorbid PTSD/Mild TBI

B. E. Depue,[1,2] J. H. Olson-Madden,[3,4] H. R. Smolker,[1] M. Rajamani,[3] L. A. Brenner,[3,4] and M. T. Banich[1,2]

[1] *Institute of Cognitive Science, University of Colorado at Boulder, Boulder, CO 80309, USA*
[2] *Department of Psychology and Neuroscience, University of Colorado at Boulder, Boulder, CO 80309, USA*
[3] *VISN 19 Mental Illness Research Education and Clinical Center, Denver, CO 80220, USA*
[4] *University of Colorado Denver, Anschutz Medical Campus, Aurora, CO 80045, USA*

Correspondence should be addressed to B. E. Depue; depue@colorado.edu

Received 4 November 2013; Accepted 11 January 2014; Published 3 March 2014

Academic Editor: John A. Sweeney

A significant portion of previously deployed combat Veterans from Operation Enduring Freedom and Operation Iraqi Freedom/Operation New Dawn (OEF/OIF/OND) are affected by comorbid posttraumatic stress disorder (PTSD) and mild traumatic brain injury (mTBI). Despite this fact, neuroimaging studies investigating the neural correlates of cognitive dysfunction within this population are almost nonexistent, with the exception of research examining the neural correlates of diagnostic PTSD or TBI. The current study used both voxel-based and surface-based morphometry to determine whether comorbid PTSD/mTBI is characterized by altered brain structure in the same regions as observed in singular diagnostic PTSD or TBI. Furthermore, we assessed whether alterations in brain structures in these regions were associated with behavioral measures related to inhibitory control, as assessed by the Go/No-go task, self-reports of impulsivity, and/or PTSD or mTBI symptoms. Results indicate volumetric reductions in the bilateral anterior amygdala in our comorbid PTSD/mTBI sample as compared to a control sample of OEF/OIF Veterans with no history of mTBI and/or PTSD. Moreover, increased volume reduction in the amygdala predicted poorer inhibitory control as measured by performance on the Go/No-go task, increased self-reported impulsivity, and greater symptoms associated with PTSD. These findings suggest that alterations in brain anatomy in OEF/OIF/OND Veterans with comorbid PTSD/mTBI are associated with both cognitive deficits and trauma symptoms related to PTSD.

1. Introduction

Posttraumatic stress disorder (PTSD) affects a significant percentage (e.g., 10–30%) of deployed combat Veterans (i.e., Operation Enduring Freedom and Operation Iraqi Freedom/Operation New Dawn (OEF/OIF/OND); [1, 2]). Similarly, a significant percent (e.g., 15–25%) of OEF/OIF Veterans are also affected by traumatic brain injury (TBI; [3, 4]), particularly mild TBI (mTBI). Therefore, estimates of comorbidity are as high as 42% [3–5]. One factor cited for the increase in the rise of comorbidity is the presence of implemented explosive devices (IEDs; [6]). Neuroimaging research indicates that individuals with PTSD exhibit abnormalities in the hippocampal/amygdalar complex [7, 8] and regions putatively responsible for regulation of them. That is the ventromedial prefrontal cortex (vmPFC) and the subgenual anterior cingulate cortex (sgACC) [8, 9]. Likewise, individuals with TBI that experience direct impact or blast wave trauma exhibit damage to the brain in these same regions, most significantly the vmPFC/sgACC [10–12]. The localization of injury associated with TBI may result from inner-cranial wave physics [13] and the presence of boney protuberances on the inner surface of the skull near the orbital and anterior temporal lobes [14, 15] makes the vmPFC/sgACC and amygdalar complex vulnerable. Therefore, it is not surprising that a vast anatomical and functional

neuroimaging literature exists that focuses on or indicates results relating either PTSD or TBI to these brain regions. However, in comparison, there is a paucity of literature examining the neuroanatomical deficits in comorbid PTSD/TBI.

Neuroimaging studies examining comorbid PTSD/TBI are almost nonexistent, perhaps, because of an old but common notion that an amnesic TBI event was "protective" towards developing PTSD [16]. This idea has been largely reversed in the last 20 years by studies investigating the prevalence of cooccurring PTSD/TBI, which indicate increased rates of PTSD among individuals with a TBI when compared to individuals who have never had a brain injury [17, 18]. Furthermore, recent indications suggest that an occurrence of TBI may even render individuals more susceptible to PTSD [6, 17]. The few neuroimaging studies investigating comorbid PTSD/TBI indicate glucose hypometabolism in the cerebellum and medial temporal lobe [19] and increases in hemosiderin deposits (iron deposits related to hemorrhaging) linked to increases in TBI symptoms [20].

However, neuroimaging studies conducted on individuals with PTSD consistently indicate both functional and anatomical alterations in the vmPFC/sgACC, striatum, thalamus, and amygdalar/hippocampal complex (for reviews/meta-analyses see [21–24]). Functional studies show alterations in a multitude of brain regions, although being able to detect altered engagement likely depends on the tasks employed. As such, there are inconsistencies in reported results with both hyper- and hypoactivation observed in the aforementioned regions [25, 26]. However, anatomical studies consistently indicate reductions in amygdalar/hippocampal complex and the vmPFC/sgACC volume and represent the most replicated findings among individuals with PTSD, when compared to controls ([27–31].) Dysfunction in the vmPFC/sgACC—amygdalar/hippocampal complex pathways is suggested to be functionally associated with decreased control or regulation over fear/threat related stimuli and conditioning [25].

Compared to PTSD, the neuroimaging literature is less abundant concerning TBI, particularly mild TBI, and studies tend to focus more on anatomical measures (e.g., diffusion tensor imaging (DTI), morphometry) rather than function, possibly due to the condition acutely causing tissue damage [32]. Mirroring morphometric studies in PTSD, volumetric reductions in the amygdalar/hippocampal complex, and the vmPFC/sgACC occur in individuals with TBI as compared to controls [33–36]. Historically, TBI has been linked to impaired executive function, such that individuals with a TBI perform worse on tasks designed to tap executive or cognitive control processes (thought to primarily involve the PFC) than individuals without TBI [37, 38]. However, many of these studies involve individuals with moderate and severe TBI, rather than mTBI [39]. Therefore, it is unclear whether persistent executive dysfunction is also compromised among those with mTBI [5, 40].

Regardless of the paucity of neuroimaging studies examining individuals with comorbid PTSD/TBI studies, a reasonable estimate is that disruption in neural circuitry of comorbid PTSD/TBI likely involves constituent elements observed within singular diagnosis of PTSD and TBI individually. The most consistent and replicated findings common to both of these populations are anatomical alterations in the vmPFC/sgACC and amygdalar/hippocampal complex. Consistent with these anatomical findings, diagnostically comorbid PTSD/TBI is associated with deficient inhibitory control [41, 42]. Inhibitory control is ubiquitously described under the rubric of executive function as the ability to "hold back" or inhibit a prepotent response and its dysfunction is usually associated with impulsive symptomatology [43]. While anatomical findings indicate that regions of the brain underlying inhibitory control are compromised in both PTSD and TBI, it is unclear whether symptoms related to PTSD or TBI are more indicative of these inhibitory control deficits in comorbid PTSD/TBI.

While specific symptoms and diagnostic criteria associated with PTSD and TBI have been associated with amygdalar/hippocampal complex hyperactivity and reduced volume [22, 25, 44, 45]) as well as vmPFC/sgACC hypoarousal and decreased volume [25, 31, 46], however, there have been few anatomical neuroimaging investigations of the basic underlying cognitive processes that may be disrupted, without using emotional or fear-related stimuli. Knowledge of these more general cognitive processes and the associated alterations in anatomy is important in order to design more effective interventions. For example, it is thought that alterations in the putative fear conditioning/extinction circuitry (vmPFC/sgACC-amygdala) reflect poor inhibitory control. However, investigations, using tasks designed to tap inhibitory control by a means not associated with fear and/or threat, are lacking. One notable exception is a study by Falconer and colleagues [47] who investigated inhibitory control in individuals diagnosed with PTSD using a Go/No-go paradigm. Compared to controls, individuals with PTSD had decreased right inferior PFC activity and increased striatal activity, suggesting decreased activity in the neural mechanisms of inhibitory control. More research investigating inhibitory control as a cognitive or behavioral construct is needed to determine whether inhibitory systems are specifically linked to fear or threat related stimuli are altered in individuals with PTSD or whether they are generally compromised. Additionally, because deficits in inhibitory control are related to both PTSD and TBI, understanding the specific context in which inhibitory control is deficient may lend insight into dysfunctional neural mechanisms that are associated with the specific diagnoses.

In order to increase our understanding of the neural underpinnings of inhibitory control deficits in comorbid PTSD/mTBI, we investigated several questions. First, we investigated whether anatomical differences in previously deployed OEF/OIF/OND combat Veterans with comorbid PTSD/mTBI were consistent with either singular diagnostic (a) PTSD and/or (b) mTBI or they were perhaps more severe due to comorbidity, as compared to previously deployed OEF/OIF combat Veterans without PTSD or mTBI diagnoses. Because the extant literature covering both diagnostic groups indicates disruptions in general fear circuitry, we expected to find decreased anatomical volume within (a) vmPFC/sgACC and the (b) hippocampus/amygdalar complex. Second, we

examined the degree to which performance on a task of inhibitory control that does not involve fearful or threatening stimuli, the Go/No-go task, was predicted by anatomical alterations. Finally, we examined the degree to which self-report of impulsivity and symptoms related to PTSD or mTBI are associated with anatomical alterations. Based on the extant literature, we hypothesized that individuals with PTSD/mTBI would show reduced volume in vmPFC/sgACC and amygdalar/hippocampal regions as compared to controls. Moreover, we predicted that anatomical alterations would predict behavioral measures. More specifically, we expected that decreased volume in these regions in individuals with comorbid PTSD/mTBI, but not controls, would be associated with decreased inhibitory control on the Go/No-go task, and with self-reported measures of impulsivity.

2. Methods

Twenty-one previously deployed OEF/OIF/OND combat Veterans with comorbid PTSD/mTBI diagnoses (20 males) and 17 OEF/OIF/OND previously deployed combat veteran controls without PTSD or mTBI (14 males) took part in the study. One individual (male) from the control group was excluded for MRI head movement leaving an N of 21 and 16, respectively. Recruitment was primarily accomplished through fliers circulated in the Denver area. All individuals were required to provide consent, which was approved through the Colorado Multiple Institutional Review Board. Individuals were compensated for their participation. Demographic information regarding age, gender, race, and years of education was obtained.

2.1. Recruitment

Inclusion Criteria. Inclusion criteria include (1) population between the ages of 18–45, (2) at least one OEF/OIF/OND deployment, and (3) population currently receiving or eligible to receive physical and/or mental health care through the VA Eastern Colorado Health Care System.

Exclusion Criteria. Exclusion criteria include (1) history of other significant neurological diseases (other than mild TBI for the appropriate group) as assessed by interview and chart review; (2) history or diagnosis of lifetime moderate or severe TBI for the PTSD/mTBI group, or any history of TBI for the non-TBI group, as assessed by interview and chart review; (3) history or diagnosis of nonactive duty-related mild TBI or PTSD disorder as assessed by interview and/or chart review; (4) diagnosis of schizophrenia or bipolar I disorder as assessed by administration of the Structured Clinical Interview for the DSM IV (SCID; [48]); (5) Computerized Assessment of Response Bias (CARB) [49] performance categorized as very poor effort, poor effort, or symptom exaggerator; (6) problematic drinking behavior that consistently exceeds recommended drinking limits per day, for example, diagnosis of alcohol abuse disorder or alcohol dependence disorder per the SCID, or five or more alcoholic drinks per day, four out of seven days per week for the previous two weeks; (7) use of illicit substance(s) more than five times in the two weeks before enrollment; (8) inability to read the informed consent document or adequately respond to questions regarding the informed consent procedure; (9) contraindication to having an MRI; and (10) Veterans who have previously enrolled in other VA studies which administer identical or similar instruments to this study.

Diagnostic Criteria/Measures. We used the Computerized Assessment of Response Bias (CARB) to assess performance and determine effort, the Shipley 2 Institute of Living Scale to measure premorbid level of functioning [50]. To assess impulsivity we used the Barratt Impulsivity Scale [51]. Alcohol and Substance use was measured by the SCID [48]. To diagnose PTSD we used the SCID and we also assessed PTSD symptom severity using the Trauma Symptom Inventory (TSI; [52]). To diagnose TBI we used the Ohio State University Traumatic Brain Injury Identification Method (OSU TBI-ID) structured clinical interview, which allows for interrogation of mTBI symptoms [53]; if the participant had a TBI, it must have been a mild TBI from active duty. Though severity of TBI by the OSU TBI-ID is mostly determined according to loss or alteration of conciousness, the following criteria was used to determine TBI severity: (1) mild TBI: A TBI with normal structural imaging, 0–30 minutes of loss of consciousness (LOC), a moment and up to 24 hours of alteration of consciousness/mental state (AOC), 0-1 day of or posttraumatic amnesia (PTA), or a best available Glascow Coma Scale Score (GCS) of 13–15 recorded within the 24 hours of the injury event, (2) moderate TBI: A TBI with normal or abnormal structural imaging, >30 min and <24 hours of LOC, >24 hours of AOC, >1 and <7 days of PTA, or a GCS score of 9–12, and (3) severe TBI: A TBI with normal or abnormal structural imaging, >24 hours of LOC, >24 hours of AOC, >7 days of PTA, or a GCS score < 9.

Inhibitory Control. To assess inhibitory control we used a standard Go/No-go task [54]. Participants were required to press the response button with the right index finger for each letter that appeared on the screen except for the letter X. The task consisted of three blocks of 120 trials each. Each letter, approximately 2.5 cm in size, appeared for 500 milliseconds with an interstimulus interval of 2000 ms. The letter "X" occurred on 20% of all trials ($n = 72$), which were presented randomly throughout the run. Other letters were randomly selected from the alphabet. Performance measures on the Go/No-go task were mean reaction time for correct go trials, errors of omission, and errors of commission.

2.2. Neuroimaging Acquisition

Structural. All structural MRI images were acquired using a Philips 1.5-Tesla Achieva 16-channel MR scanner located at the Denver Veterans Affairs Medical Center. An eight-channel headcoil was used for radiofrequency transmission and reception. Foam padding was placed around the head, within the head coil, to limit head motion during the scan. Structural images were obtained via a T1-weighted 3D TFE in 160 sagittal slices. Imaging parameters were as follows:

echo time (T_E) = 3.2 ms., repetition time (T_R) = 7100 ms, flip angle = 8.0°, field of view (FoV) = 240 mm, and voxel size = 1.0 × 1.03 × 1.0 mm. Scan parameters were consistent for all imaging sessions.

2.3. Neuroimaging Analysis

Voxel-Based Morphometry (VBM). All VBM analyses were performed using the FSL-VBM toolbox and follow the processing pipeline put forth by Ashburner and Friston [55] and Good et al. [56]. First, the raw T1-weighted images were brain-extracted using the FSL default BET brain extraction process, which strips the skull and removes any nonbrain tissue from the image using the FAST4 tool. The resulting GM images were then aligned to MNI152 standard space using the affine registration tool FLIRT, followed by nonlinear registration using FNIRT. The resulting images were averaged to create a study-specific template, to which the native GM images were then nonlinearly reregistered using FNIRT. The registered partial volume images were then modulated (to correct for local expansion and contraction) by dividing the Jacobian of the warp field. The modulated segmented images were then smoothed with an isotropic Gaussian kernel with a sigma of 2, yielding full-width half-maximum (FWHM) 2 × 2.3 mm = 4.6 mm FWHM. The resulting subject-specific GM probability maps were input into a general linear model (GLM) evaluating group differences between all voxels of GM, using whole-brain GM volume as a nuisance covariate. One-sample t-tests for group contrasts were performed using the Threshold-Free Cluster Enhancement (TFCE) method, which detects clusters of contiguous voxels without first setting an arbitrary statistical cut-off (e.g., $Z > 2.58$) and controls the familywise error (FWE) rate at $P < 0.05$. Each contrast underwent 5000 permutations. Randomize produces corrected 1-p maps, which we used to mask t-score maps for all figures. Figures of statistical maps were created using FSLview.

Surface-Based Morphometry (SBM). Automated segmentation of the bilateral amygdala and hippocampus was performed using FIRST (FSL v4.0.1) which uses a Bayesian probabilistic approach. The shape and appearance models in FIRST are constructed from a library of manually segmented images. The manually generated labels are parameterized as surface meshes and then modeled as a point distribution. Using the learned models, FIRST searches through shape deformations that are linear combinations of the modes of variation to find the most probable shape instance given the observed intensities from the input image. Using T1 images, the segmentation was performed with two-stage affine transformation to standard space of MNI 152 at 1 mm resolution [57, 58]. The first stage utilized a standard 12 degrees of freedom registration to the template and the second stage applied 12 degrees of freedom registration using an MNI152 subcortical mask to exclude voxels outside the subcortical regions. Boundary voxels were thresholded at $s = 2$ and $s = 3$, along with the recommended number of modes (iterations) for the hippocampus (30) and amygdala (50). All processes of segmentation were then visually inspected to assess boundaries by two independent raters for each of the two boundary thresholded training sets ($s = 2$, $s = 3$). Because $s = 2$ yielded a more conservative boundary threshold that included the amygdala and hippocampus proper, while minimizing neocortical tissue, ventricles, and white matter, this data set was selected for final analyses. One-sample t-tests for group contrasts were performed using the Threshold-Free Cluster Enhancement (TFCE) method, which detects clusters of contiguous voxels without first setting an arbitrary statistical cut-off (e.g., $Z > 2.58$) and controls the familywise error (FWE) rate at $P < 0.05$. Each contrast underwent 5000 permutations. Randomize produces corrected 1-p maps, which we used to mask t-score maps for all figures. Figures of statistical maps were created using FSLview.

Multiple Regression. To perform multiple regression we used a two-stage procedure as outlined in Hastie et al. [59]. We first used penalized regression using LASSO [60] to perform subset variable/feature selection. Subsequently, because LASSO can over penalize highly collinear variables, we then performed an ordinary least squares (OLS) best model multiple regression on the subset of selected variables/features taken from LASSO to obtain beta estimates, regression coefficients, and determinants of explained variance.

3. Results

3.1. Demographic and Behavioral Measures. There were no significant differences between the groups in demographic characteristics (Table 1). Significant group differences emerged for previous alcohol use ($P < 0.005$), indicating that the PTSD/mTBI group had higher proportions of alcohol use. Significant group differences emerged for the Barratt Impulsivity Scale (Barratt) in the subcomponents of attention, perseveration, and self-control ($P = 0.0002$, $P = 0.01$, and $P = 0.001$, resp.), indicating that the PTSD/mTBI group exhibited higher proportions or more impulsivity than the control group. Group differences also arose in the Trauma Symptom Inventory in the three subcomponents linked to SCID PTSD diagnostic criteria (Intrusive Experiences, Defensive Avoidance, and Dissociation; all three $P < 0.0001$), indicating that the PTSD/mTBI group exhibited higher proportions or more symptoms associated with PTSD than the control group. Group differences were also found in the Shipley 2 Abstraction and Composite A score ($P = 0.004$, $P = 0.006$, resp.), indicating that the PTSD/mTBI group exhibited lower premorbid functioning as compared to the control group.

3.2. Inhibitory Control. Go/No-go behavior indicated a significant group difference in errors of commission ($t^{2,35} = 2.61$, $P = 0.009$), with individuals with PTSD/mTBI ($M = 15.14$, SE = 1.82) who made more errors of commission than controls ($M = 9.25$, SE = 1.25). Errors of omission (EO) and reaction time (RT) did not significantly differ between the two groups (PTSD/mTBI, EO = 5.3, RT = 373.62 ms.; controls, EO = 4.4, RT = 409.77 ms., $P = 0.78$, $P = 0.21$, resp.).

Table 1: Demographic and self-report information for the PTSD/TBI and control group. Numbers represent % (N) or median (range) in self-report measures. Fisher's exact or Wilcoxon rank sum test were used for all P values.

Characteristic	Control ($n = 16$)	TBI/PTSD ($n = 21$)	P value
Gender			0.57
Male	87.5% (14)	95.2% (20)	
Female	12.5% (2)	4.8% (1)	
Age	28.0 (24–45)	29.0 (23–43)	0.62
Race			0.37
Caucasian	75.0% (12)	90.5% (19)	
Other	25.0% (4)	9.5% (2)	
Years of education	15.5 (12–18)	14.5 (11–22)	0.14
Alcohol use			0.005
No history	81.3% (13)	38.1% (8)	
Past history of abuse	12.5% (2)	9.5% (2)	
Past history of dependence	6.3% (1)	52.4% (11)	
Substance use			0.60
No history	87.5% (14)	71.4% (15)	
Past history of abuse	6.3% (1)	9.5% (2)	
Past history of dependence	6.3% (1)	19.1% (4)	
Most severe TBI from deployment of related TBI			
Alteration of consciousness		38.1% (8)	
Loss of conscious < 5 minutes		52.4% (11)	
Loss of conscious 5 minutes to 30 minutes		9.5% (2)	
Number of symptoms from most recent injury		5 (0–9)	
Barratt Impulsivity Scale			
Attention	8.5 (5–15)	14 (9–19)	0.0002
Cognitive instability	5 (3–10)	6 (3–12)	0.16
Motor	14 (11–22)	15 (12–25)	0.11
Perseverance	7.5 (4–11)	9 (6–14)	0.01
Self-control	9 (6–16)	14 (6–22)	0.001
Cognitive complexity	10 (6–17)	12 (6–20)	0.09
Trauma Symptom Inventory			
Intrusive Experiences (IE)	45 (42–61)	75 (58–87)	<0.0001
Defensive Avoidance (DA)	44 (41–63)	67 (49–79)	<0.0001
Dissociation (DIS)	47 (41–55)	64 (47–98)	<0.0001
Shipley 2 Institute of Living Scale			
Vocabulary score	112 (99–121)	108 (86–121)	0.18
Abstraction score	108 (84–122)	93 (59–122)	0.004
Composite A score	112.5 (90–125)	99 (79–118)	0.006

3.3. Neuroimaging. Whole brain VBM analyses controlling for overall GM volume revealed significant group differences in the bilateral anterior amygdala, such that the PTSD/mTBI group showed reduced volume, as compared to the control group ($P < 0.05$ TFCE corrected, 5000 permutations; see methods for a full description; Figure 1(a)). Because VBM analyses can be susceptible to incorrect registration and differences in individual cortical folding patterns [61], we also performed SBM on the amygdala to potentially corroborate our findings. SBM analyses mirrored our VBM analyses, indicating significant group differences in the bilateral anterior amygdala ($P < 0.05$ TFCE corrected, 5000 permutations; see methods for a full description; Figure 1(b)).

Next, to determine whether the volumetric differences in the amygdala are related to behavioral performance, we extracted an individual's left and right amygdala volume based on the SBM analyses and regressed it with Go/No-go errors of commission and omission, as well as RT, controlling for overall GM volume. Analyses revealed that errors of commission significantly related to volume in the left amygdala, such that increased errors of commission were predicted by decreased volume of the left amygdala, in the

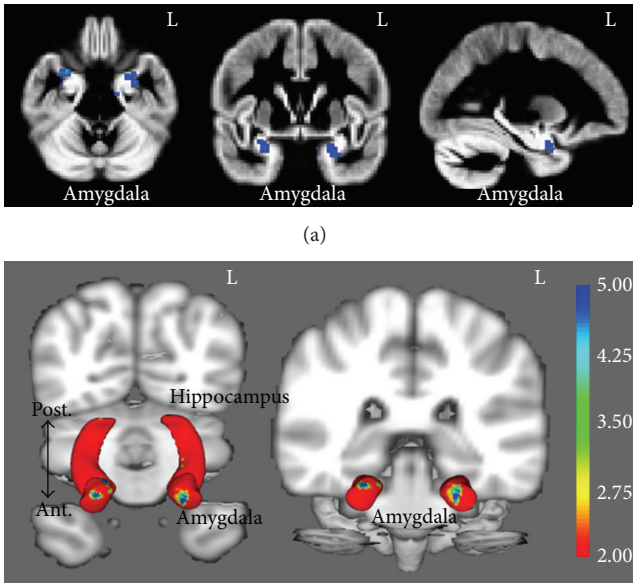

Figure 1: (a) shows whole-brain VBM analyses indicating significant group differences in the bilateral anterior amygdala (L = left). (b) shows SBM analyses of the amygdala and hippocampus indicating significant group differences in the anterior amygdala (post. = posterior, ant. = anterior). Color scale represents t values for the group comparison.

PTSD/mTBI group, but not the control group ($F^{1,20} = 7.81$, $P = 0.01$, $R^2 = 0.30$; Figures 2(1(a)) and 2(2(a))).

We then determined whether the volume of the left and right amygdala was associated with impulsivity (Barratt), premorbid functioning (Shipley 2), and symptoms related to PTSD (Trauma Symptom Inventory) or TBI (OSU TBI-ID form), controlling for overall GM volume. Regression analyses revealed that an increased cognitive instability subcomponent of the Barratt Impulsivity Scale was predicted by decreased volume of the left amygdala in the PTSD/mTBI group, but not the control group ($F^{1,20} = 5.41$, $P = 0.03$, $R^2 = 0.23$; Figures 2(1(b)) and 2(2(b))). Decreases of cognitive function as measured by Composite A of the Shipley 2 was associated with decreased volume of the right hippocampus in the PTSD/mTBI group but not the control group ($F^{1,20} = 4.60$, $P = 0.04$, $R^2 = 0.20$; Figures 2(1(c)) and 2(2(c))). Increased scores on the Defensive Avoidance subscale of the Trauma Symptom Inventory were associated with decreased right amygdala volume in the PTSD/TBI group, but not the control group ($F^{1,20} = 4.84$, $P = 0.04$, $R^2 = 0.17$; Figures 2(1(d)) and 2(2(d))). No relationship between amygdalar volume and symptoms of mTBI was noted.

With regard to hippocampal volume, our VBM and SBM analyses revealed no significant differences. We also tested the difference between the regression parameter estimates of amygdala volume with the behavioral variables and hippocampal volume with the behavioral variables, respectively. The differences in parameter estimates for amygdala volume and behavioral variables were all significantly different than those for hippocampal volume and behavioral variables, indicating that our findings are specific to amygdala volume (cognitive instability: $Z = 2.05$, $P = 0.04$; Shipley A: $Z = -2.23$, $P = 0.03$; Defensive Avoidance: $Z = 2.49$, $P = 0.01$).

As a summary analysis, we ran feature selection and multiple regression with left amygdala volume and multiple regression with trauma symptoms examining the sets of variables within the PTSD/mTBI group that best predicted (1) left amygdala volume (as it was found to be associated with motor inhibition and impulsivity) and (2) trauma symptoms related to PTSD (as they were the symptoms related to amygdala volume). Feature selection and multiple regression examining decreases in left amygdala volume were best predicted by a model indicating significant contributions of independent variance from both (a) increases in commission errors from Go/No-go performance and (b) increases in the cognitive instability subcomponent of the Barratt Impulsivity Scale $F^{2,19} = 5.94$, $P = 0.02$, $R^2 = 0.34$; standardized coefficients are presented in Figure 2(3(a)). Feature selection and multiple regression examining increases in trauma symptoms related to PTSD were best predicted by a model indicating significant contributions of independent variance from (a) increases in the cognitive instability subcomponent of the Barratt Impulsivity Scale, (b) decreases in right amygdala volume, and (c) decreases of cognitive function of in Composite A of the Shipley 2 $F^{3,18} = 4.17$, $P = 0.04$, $R^2 = 0.33$; standardized coefficients are presented in Figure 2(3(b)).

4. Discussion

The current study is the first, to our knowledge, in its approach to examine both voxel- and surface-based morphometry in a comorbid diagnostic group of individuals with PTSD/mTBI. Furthermore, it is novel in demonstrating that inhibitory control, as assessed through the Go/No-go task, is linked to known abnormalities in brain morphometry in PTSD/mTBI, namely, decreased amygdala volume. Decreased amygdala volume also was associated with increased impulsivity (Barratt Impulsivity Scale), a known indicator of deficits in inhibitory control. Both increased errors of commission and impulsivity contributed independent variance predicting decreases in amygdala volume. Furthermore, decreased amygdala volume was related to increases in trauma symptoms related to PTSD, but not mTBI symptoms (Trauma Inventory Scale, OSU TBI-ID, resp.). And finally, decreased amygdala volume, increased impulsivity, and decreased cognitive functioning assessed by the Shipley 2 Composite A contributed independent variance predicting increases in trauma symptoms related to PTSD.

While neuroimaging literature suggests that both singular diagnostic PTSD and TBI are related to decreases in the vmPFC/sgACC and amygdalar/hippocampal complex volume, our results indicate that comorbid diagnosis of PTSD/mTBI shows the same decreases in amygdala volume. Our analysis using VBM indicating reductions in anterior amygdala volume was corroborated by our analysis using SBM. The combination of VBM and SBM is an important analysis step considering that voxel-based morphometric

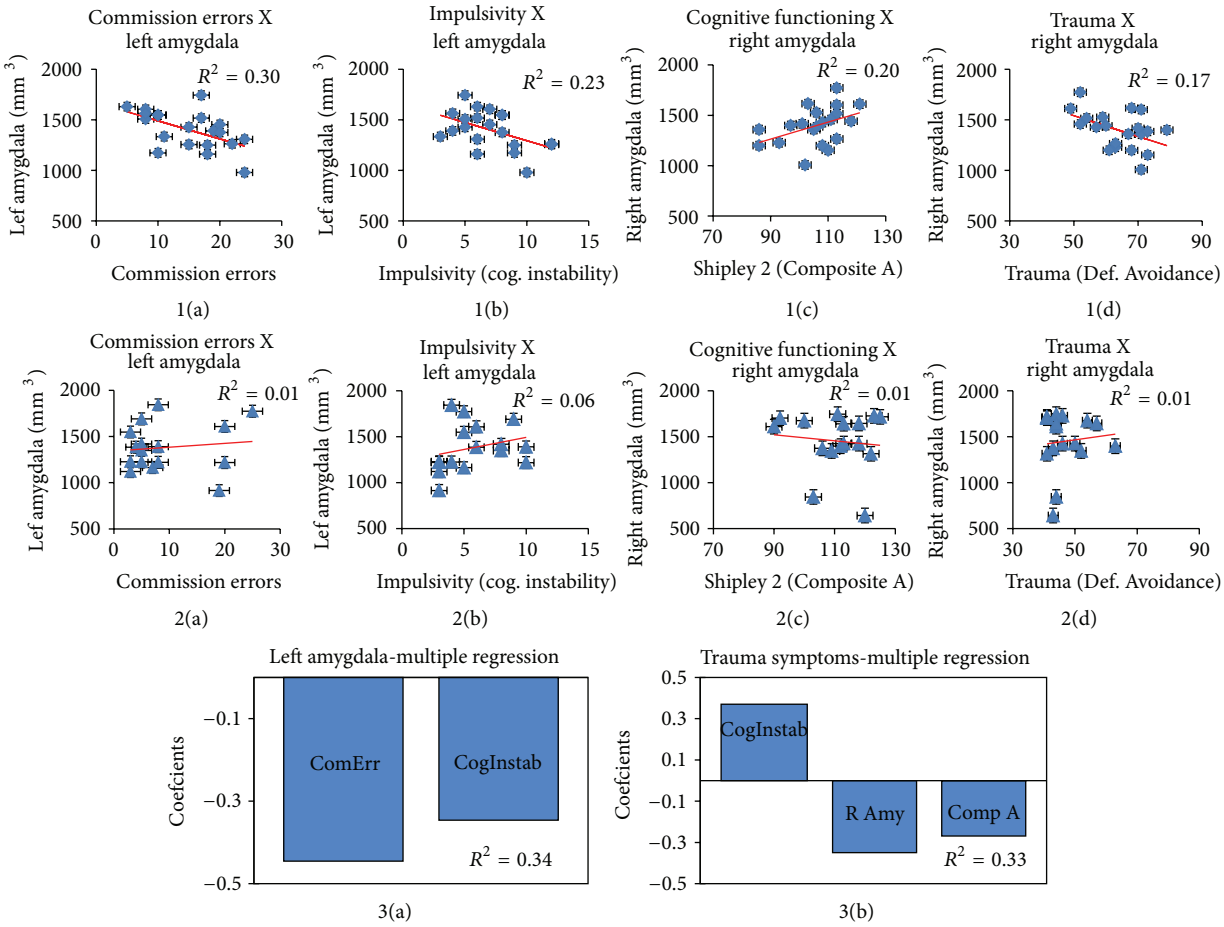

FIGURE 2: 1(a)–1(d) show significant regression from the PTSD/mTBI group, while 2(a)–2(d) show the nonsignificant regression in the control group. 1(a)-2(a) show the relationship between commission errors and left amygdala volume (mm^3); 1(b)-2(b) show relationship between impulsivity (subscale of cognitive instability, Barratt Impulsivity Scale) and left amygdala volume (mm^3); 1(c)-2(c) show the relationship between cognitive functioning (Shipley 2 Composite A score) and right amygdala volume (mm^3); 1(d)-2(d) show the relationship between trauma (Trauma Symptom Inventory subscale of Defensive Avoidance) and right amygdala volume (mm^3). 3(a) shows the standardized coefficients for the multiple regression with left amygdala volume (ComErr = commission errors; CogInstab = the cognitive instability subcomponent of the Barratt Impulsivity Scale). 3(b) shows the standardized coefficients for the multiple regression with trauma symptoms (CogInstab = the cognitive instability subcomponent of the Barratt Impulsivity Scale, R Amy = right amygdala volume mm^3; Comp A = Shipley 2 Composite A score). The multiple regression with left amygdala volume and multiple regression with trauma symptoms were controlled for whole brain grey matter volume.

studies have been shown to be susceptible to misregistration and individual cortical folding differences [61]. Utilizing both approaches and obtaining convergent findings enable us to be more confident in our results.

Although we found no group differences in the vmPFC/sgACC and the hippocampus, this null effect can potentially be attributed to a myriad of different factors. First, reductions of vmPFC/sgACC volume have been linked to TBI [62], but it is unclear how the severity of a TBI affects brain damage. Because individuals with a moderate or severe TBI were excluded from the current study, we may have less power to detect abnormalities in the vmPFC/sgACC. Additionally, mTBI has been linked to increased vulnerability of developing PTSD symptoms [6, 17], such that it may not be the long-term effects of mTBI, but rather a predisposition to developing PTSD in our sample that was detected. Future research is needed to determine whether there is a pattern whereby certain brain regions are not affected at low levels of severity of TBI, while other regions are affected more uniformly across levels of severity and the nature of mTBI predisposing individuals to PTSD. Second, while reductions in hippocampal volume have been replicated in a large number of studies examining PTSD, numerous studies also fail to replicate this finding [63, 64]. In particular, studies have suggested that only certain subpopulations (dependent on trauma type) show reductions in hippocampal volume [65]. Lastly, variation exists in the control samples used across these studies. One of the largest differences affecting results is likely because of the inclusion of either combat deployed or noncombat deployed military personnel. Because our

study used previously combat deployed military OEF/OIF Veterans, differences between the current groups may be harder to detect than between PTSD/TBI and a nonmilitary control group. Future research is needed to determine whether simply the experience of combat deployment affects brain morphometry. For instance, combat deployment in general may relate to increased stress and subsequently affect the hippocampus through stress induced glucocorticoid release [66].

The current study analyzed multiple measures related to symptoms of both PTSD and mTBI. We indicate that deficits in inhibitory control, highly related to PTSD and TBI, are associated with decreases in amygdala volume in the PTSD/mTBI but not the control group. This relationship was significant in the PTSD/mTBI but not control group as indicated through regressions with errors of commission from the Go/No-go task, which also indicated significant group differences. Increased impulsivity, which has also been shown to be related to deficits in inhibitory control and performance on the Go/No-go task, also showed an association with decreased amygdala volume in the PTSD/mTBI but not control group. The Shipley 2 was used as a proxy for IQ, and therefore our best premorbid indicator of cognitive functioning. However, group differences emerged in both Abstraction and Composite A subscales, indicating that the PTSD/mTBI group exhibited decreased cognitive functioning. An individual's score on the Composite A subscale was also related to amygdala volume, such that decreased cognitive function were related to decreases in amygdala volume, in the PTSD/mTBI but not control group. We acknowledge that there are multiple interpretations regarding the Shipley 2 in the context of the current study (a) that the Shipley 2 is sensitive to the premorbid cognitive functioning of the individual, or (b) that the Shipley 2 is actually measuring cognitive impairment sequelae of PTSD and/or mTBI, or (3) some combination of the previous two interpretations. The current results are consistent with the literature suggesting that premorbid decreases in IQ may predispose individuals to PTSD [67]; however, it is notable that abstraction can be considered an executive function, which is known to be affected by both PTSD and TBI. Continued research is needed to determine the contribution of premorbid deficits and sequelae of individuals with PTSD and/or TBI as it relates to cognitive and executive function. The culmination of the findings from these multiple measures suggests that deficient inhibitory control is related to decreases in amygdala volume and may be more related to trauma associated with PTSD, rather than mTBI symptoms. The location of VBM and more importantly SBM findings in the anterior amygdala provide further interpretation of deficient inhibitory control as it relates to PTSD/mTBI.

Often the amygdala is treated as a functionally homogeneous region, but both animal and human research investigating nonpsychiatric populations suggests there may be dissociations of function along either a ventral-dorsal or anterior-posterior axis [68]. The ventral-dorsal axis has been linked to numerous functional dissociations including sensory input versus sensory output [69], impulsivity versus aggression [68], and fear conditioning (via input to the hippocampus) versus fear response [70], respectively. These dissociations are most likely attributed to the locality of two of the major amygdalar nuclei groups, the basolateral nuclei (BLA) and the central nuclei (CE). In humans, the BLA corresponds to the anterior or ventral segment of amygdala, while the CE is localized to the posterior or dorsal region of the amygdala [71]. The BLA is the set of nuclei in which multimodal sensory information converges [69]. This information is then processed and relayed to the CE nuclei group responsible for affecting physiological response via output to the brainstem, insula, and somatosensory cortex [70]. This well-established circuitry has been linked to fear extinction in which inhibitory cell groups (intercalated cell masses) positioned between the BLA and CE can reduce fear response via excitatory input from the vmPFC, which in turn decreases information flow to the CE nuclei group and fear mediated physiological response is lessened or abolished [69]. Therefore, our findings, indicating decreases specific to anterior amygdala volume, can likely be interpreted as abnormal morphometry associated with the BLA and as such may be linked to problems with multimodal sensory input. Problems with sensory input may lead to overprocessing of irrelevant stimuli and lead to increased anxiety and impulsive behavior [72–74]. Indeed, our results are consistent with this previous interpretation as we found that Go/No-go task, impulsivity, and trauma symptoms were linked to the anterior amygdala. Of course, it is not clear how reduced volume in this region is associated with sensory input specifically; however, it provides an interesting focus for future research.

The current study employed a standard cognitive task (Go/No-go), as opposed to using a symptom provocation task (e.g., script-driven imagery, processing of threat-related stimuli). Understandably, while most neuroimaging research regarding PTSD uses symptom provocation studies, it is also important to determine whether deficits in inhibitory function can be found under nonemotional conditions. The results of the current study suggest more general inhibitory control deficits in PTSD/mTBI individuals, consistent with the findings of Falconer et al., [47] in PTSD individuals. Therefore, future research using standard cognitive tasks may help to determine whether the neural systems affecting these populations are "generally" dysfunctional or whether they exhibit deficits only under certain conditions (e.g., threat/fear stimuli). Such information will likely be helpful to provide additional insights into how to develop more effective interventions.

While the current study uses multiple neuroimaging analysis techniques (i.e., VBM, SBM) and linear regression to indicate relationships between PTSD/mTBI symptoms and impairments, there are limitations that should be acknowledged. First, the sample size is relatively small for individual difference analyses, even though we first selected regions that exhibited group differences. Therefore, our findings are in need of replication. Second, we only included individuals with a mild but not moderate or severe TBI, which may have reduced our power to detect differences based on mTBI symptoms. Currently, it is unclear how TBI symptoms relate to differences in volume of specific brain regions. Third, our control population had trauma symptoms which have been

shown to be linked to anatomical changes [75]; therefore, future studies need to determine the effect of trauma in isolation from diagnostic disorders. Fourth, our findings regarding increased impulsivity and the relation to decreased amygdala volume are based on the Barratt Impulsivity Scale, a self-report measure, which can lead to social desirability biases. Therefore, future research is needed to also investigate the relationship between impulsivity and amygdala volume with more biological indices of impulsivity. And last, we used a comorbid diagnostic group (i.e., PTSD/mTBI) to determine the relationships between brain morphometry and behavior/symptoms. Although this was the goal of the current study, future studies should examine the differences within a comorbid diagnostic group, in comparison to singular diagnostic groups (i.e., PTSD only, TBI only) to help fully decipher brain morphometry and the relationship to specific symptom profiles.

In sum, the current study has provided novel findings indicating abnormal anterior amygdala morphometry in comorbid PTSD/TBI, as compared to controls, as assessed by both voxel- and surface-based morphometric analyses. The group level reduction in amygdala volume was then shown to predict individual differences within the PTSD/mTBI group in errors of commission, impulsivity, cognitive function, and symptoms related to PTSD but not mTBI. Therefore, abnormalities in the anterior amygdala may provide a specific neural region that can be examined as it relates to deficits in inhibitory control, which may help identify biomarkers related more to PTSD, rather than mTBI in comorbid diagnostic groups.

Disclaimer

The views expressed in this paper are those of the authors and do not necessarily represent the official policy or position of the Department of Veterans Affairs or the US Government.

Conflict of Interests

The authors declare that there is no conflict of interests regarding the publication of this paper.

Acknowledgment

Support for this project was provided by the Colorado Traumatic Brain Injury Trust Fund Program.

References

[1] S. Dolan, S. Martindale, J. Robinson et al., "Neuropsychological sequelae of PTSD and TBI following war deployment among OEF/OIF veterans," *Neuropsychology Review*, vol. 22, no. 1, pp. 21–34, 2012.

[2] C. W. Hoge, C. A. Castro, S. C. Messer, D. McGurk, D. I. Cotting, and R. L. Koffman, "Combat duty in Iraq and Afghanistan, mental health problems, and barriers to care," *New England Journal of Medicine*, vol. 351, no. 1, pp. 13–22, 2004.

[3] C. W. Hoge, C. A. Castro, S. C. Messer, D. McGurk, D. I. Cotting, and R. L. Koffman, "Combat duty in Iraq and Afghanistan, mental health problems, and barriers to care," *U.S. Army Medical Department Journals*, 2008.

[4] C. W. Hoge, D. McGurk, J. L. Thomas, A. L. Cox, C. C. Engel, and C. A. Castro, "Mild traumatic brain injury in U.S. soldiers returning from Iraq," *New England Journal of Medicine*, vol. 358, no. 5, pp. 453–463, 2008.

[5] H. G. Belanger, T. Kretzmer, R. Yoash-Gantz, T. Pickett, and L. A. Tupler, "Cognitive sequelae of blast-related versus other mechanisms of brain trauma," *Journal of the International Neuropsychological Society*, vol. 15, no. 1, pp. 1–8, 2009.

[6] G. A. Elder and A. Cristian, "Blast-related mild traumatic brain injury: mechanisms of injury and impact on clinical care," *Mount Sinai Journal of Medicine*, vol. 76, no. 2, pp. 111–118, 2009.

[7] D. W. Hedges and F. L. M. Woon, "Premorbid brain volume estimates and reduced total brain volume in adults exposed to trauma with or without posttraumatic stress disorder: a meta-analysis," *Cognitive and Behavioral Neurology*, vol. 23, no. 2, pp. 124–129, 2010.

[8] A. Karl, M. Schaefer, L. S. Malta, D. Dörfel, N. Rohleder, and A. Werner, "A meta-analysis of structural brain abnormalities in PTSD," *Neuroscience and Biobehavioral Reviews*, vol. 30, no. 7, pp. 1004–1031, 2006.

[9] L. M. Shin, C. I. Wright, P. A. Cannistraro et al., "A functional magnetic resonance imaging study of amygdala and medial prefrontal cortex responses to overtly presented fearful faces in posttraumatic stress disorder," *Archives of General Psychiatry*, vol. 62, no. 3, pp. 273–281, 2005.

[10] C. L. Mac Donald, A. M. Johnson, D. Cooper et al., "Detection of blast-related traumatic brain injury in U.S. military personnel," *New England Journal of Medicine*, vol. 364, no. 22, pp. 2091–2100, 2011.

[11] S. R. Sponheim, K. A. McGuire, S. S. Kang et al., "Evidence of disrupted functional connectivity in the brain after combat-related blast injury," *NeuroImage*, vol. 54, no. 1, pp. S21–S29, 2011.

[12] T. L. S. Benzinger, D. Brody, S. Cardin et al., "Blast-related brain injury: imaging for clinical and research applications: report of the 2008 st. louis workshop," *Journal of Neurotrauma*, vol. 26, no. 12, pp. 2127–2144, 2009.

[13] P. A. Taylor and C. C. Ford, "Simulation of blast-induced early-time intracranial wave physics leading to traumatic brain injury," *Journal of Biomechanical Engineering*, vol. 131, no. 6, p. 61007, 2009.

[14] Y. Toyama, T. Kobayashi, Y. Nishiyama, K. Satoh, M. Ohkawa, and K. Seki, "CT for acute stage of closed head injury," *Radiation Medicine*, vol. 23, no. 5, pp. 309–316, 2005.

[15] C. Imielinska, A. Przekwas, and X. G. Tan, "Multi-scale visual analysis of trauma injury," *Information Visualization*, vol. 5, no. 4, pp. 279–289, 2006.

[16] N. S. King, "PTSD and traumatic brain injury: folklore and fact?" *Brain Injury*, vol. 22, no. 1, pp. 1–5, 2008.

[17] R. A. Mayou, J. Black, and B. Bryant, "Unconsciousness, amnesia and psychiatric symptoms following road traffic accident injury," *British Journal of Psychiatry*, vol. 177, pp. 540–545, 2000.

[18] A. I. Greenspan, A. Y. Stringer, V. L. Phillips, F. M. Hammond, and F. C. Goldstein, "Symptoms of post-traumatic stress: intrusion and avoidance 6 and 12 months after TBI," *Brain Injury*, vol. 20, no. 7, pp. 733–742, 2006.

[19] E. R. Peskind, E. C. Petrie, D. J. Cross et al., "Cerebrocerebellar hypometabolism associated with repetitive blast exposure mild traumatic brain injury in 12 Iraq war Veterans with persistent post-concussive symptoms," *NeuroImage*, vol. 54, no. 1, pp. S76–S82, 2011.

[20] L. A. Brenner, S. E. Ladley-O'Brien, J. E. F. Harwood et al., "An exploratory study of neuroimaging, neurologic, and neuropsychological findings in veterans with traumatic brain injury and/or posttraumatic stress disorder," *Military Medicine*, vol. 174, no. 4, pp. 347–352, 2009.

[21] R. A. Lanius, R. Bluhm, U. Lanius, and C. Pain, "A review of neuroimaging studies in PTSD: heterogeneity of response to symptom provocation," *Journal of Psychiatric Research*, vol. 40, no. 8, pp. 709–729, 2006.

[22] S. L. Rauch, L. M. Shin, and E. A. Phelps, "Neurocircuitry models of posttraumatic stress disorder and extinction: human neuroimaging research—past, present, and future," *Biological Psychiatry*, vol. 60, no. 4, pp. 376–382, 2006.

[23] A. N. Simmons and S. C. Matthews, "Neural circuitry of PTSD with or without mild traumatic brain injury: a meta-analysis," *Neuropharmacology*, vol. 62, no. 2, pp. 598–606, 2012.

[24] R. Patel, R. N. Spreng, L. M. Shin, and T. A. Girard, "Neurocircuitry models of posttraumatic stress disorder and beyond: a meta-analysis of functional neuroimaging studies," *Neuroscience & Biobehavioral Reviews*, vol. 36, no. 9, pp. 2130–3142, 2012.

[25] L. M. Shin, S. P. Orr, M. A. Carson et al., "Regional cerebral blood flow in the amygdala and medial prefrontal cortex during traumatic imagery in male and female Vietnam veterans with PTSD," *Archives of General Psychiatry*, vol. 61, no. 2, pp. 168–176, 2004.

[26] R. A. Lanius, P. C. Williamson, M. Densmore et al., "Neural correlates of traumatic memories in posttraumatic stress disorder: a functional MRI investigation," *American Journal of Psychiatry*, vol. 158, no. 11, pp. 1920–1922, 2001.

[27] N. Kitayama, V. Vaccarino, M. Kutner, P. Weiss, and J. D. Bremner, "Magnetic resonance imaging (MRI) measurement of hippocampal volume in posttraumatic stress disorder: a meta-analysis," *Journal of Affective Disorders*, vol. 88, no. 1, pp. 79–86, 2005.

[28] M. E. Smith, "Bilateral hippocampal volume reduction in adults with post-traumatic stress disorder: a meta-analysis of structural MRI studies," *Hippocampus*, vol. 15, no. 6, pp. 798–807, 2005.

[29] S. L. Rauch, L. M. Shin, E. Segal et al., "Selectively reduced regional cortical volumes in post-traumatic stress disorder," *NeuroReport*, vol. 14, no. 7, pp. 913–916, 2003.

[30] K. Kasai, H. Yamasue, M. W. Gilbertson, M. E. Shenton, S. L. Rauch, and R. K. Pitman, "Evidence for acquired pregenual anterior cingulate gray matter loss from a twin study of combat-related posttraumatic stress disorder," *Biological Psychiatry*, vol. 63, no. 6, pp. 550–556, 2008.

[31] S. H. Woodward, D. G. Kaloupek, C. C. Streeter, C. Martinez, M. Schaer, and S. Eliez, "Decreased anterior cingulate volume in combat-related PTSD," *Biological Psychiatry*, vol. 59, no. 7, pp. 582–587, 2006.

[32] I. Cernak, A. C. Merkle, V. E. Koliatsos et al., "The pathobiology of blast injuries and blast-induced neurotrauma as identified using a new experimental model of injury in mice," *Neurobiology of Disease*, vol. 41, no. 2, pp. 538–551, 2011.

[33] M. Ariza, R. Pueyo, M. D. M. Matarín et al., "Influence of APOE polymorphism on cognitive and behavioural outcome in moderate and severe traumatic brain injury," *Journal of Neurology, Neurosurgery and Psychiatry*, vol. 77, no. 10, pp. 1191–1193, 2006.

[34] L. Himanen, R. Portin, H. Isoniemi, H. Helenius, T. Kurki, and O. Tenovuo, "Cognitive functions in relation to MRI findings 30 years after traumatic brain injury," *Brain Injury*, vol. 19, no. 2, pp. 93–100, 2005.

[35] F. Tomaiuolo, G. A. Carlesimo, M. Di Paola et al., "Gross morphology and morphometric sequelae in the hippocampus, fornix, and corpus callosum of patients with severe non-missile traumatic brain injury without macroscopically detectable lesions: A T1 weighted MRI study," *Journal of Neurology, Neurosurgery and Psychiatry*, vol. 75, no. 9, pp. 1314–1322, 2004.

[36] R. F. Mollica, I. K. Lyoo, M. C. Chernoff et al., "Brain structural abnormalities and mental health sequelae in south Vietnamese ex-political detainees who survived traumatic head injury and torture," *Archives of General Psychiatry*, vol. 66, no. 11, pp. 1221–1232, 2009.

[37] A. Serino, E. Ciaramelli, A. Di Santantonio, S. Malagù, F. Servadei, and E. Làdavas, "Central executive system impairment in traumatic brain injury," *Brain Injury*, vol. 20, no. 1, pp. 23–32, 2006.

[38] B. C. McDonald, L. A. Flashman, and A. J. Saykin, "Executive dysfunction following traumatic brain injury: neural substrates and treatment strategies," *NeuroRehabilitation*, vol. 17, no. 4, pp. 333–344, 2002.

[39] T. W. McAllister, M. B. Sparling, L. A. Flashman, and A. J. Saykin, "Neuroimaging findings in mild traumatic brain injury," *Journal of Clinical and Experimental Neuropsychology*, vol. 23, no. 6, pp. 775–791, 2001.

[40] H. G. Belanger, T. Kretzmer, R. D. Vanderploeg, and L. M. French, "Symptom complaints following combat-related traumatic brain injury: relationship to traumatic brain injury severity and posttraumatic stress disorder," *Journal of the International Neuropsychological Society*, vol. 16, no. 1, pp. 194–199, 2010.

[41] L. A. Brenner, H. Terrio, B. Y. Homaifar et al., "Neuropsychological test performance in soldiers with blast-related mild TBI," *Neuropsychology*, vol. 24, no. 2, pp. 160–167, 2010.

[42] R. A. Bryant, "Acute stress disorder as a predictor of posttraumatic stress disorder: a systematic review," *The Journal of Clinical Psychiatry*, vol. 72, no. 2, pp. 233–239, 2011.

[43] A. Miyake, N. P. Friedman, M. J. Emerson, A. H. Witzki, A. Howerter, and T. D. Wager, "The unity and diversity of executive functions and their contributions to complex "frontal lobe" tasks: a latent variable analysis.," *Cognitive Psychology*, vol. 41, no. 1, pp. 49–100, 2000.

[44] J. D. Bremner, M. Vythilingam, E. Vermetten et al., "MRI and PET study of deficits in hippocampal structure and function in women with childhood sexual abuse and posttraumatic stress disorder," *American Journal of Psychiatry*, vol. 160, no. 5, pp. 924–932, 2003.

[45] M. W. Gilbertson, M. E. Shenton, A. Ciszewski et al., "Smaller hippocampal volume predicts pathologic vulnerability to psychological trauma," *Nature Neuroscience*, vol. 5, no. 11, pp. 1242–1247, 2002.

[46] H. Yamasue, K. Kasai, A. Iwanami et al., "Voxel-based analysis of MRI reveals anterior cingulate gray-matter volume reduction in posttraumatic stress disorder due to terrorism," *Proceedings of the National Academy of Sciences of the United States of America*, vol. 100, no. 15, pp. 9039–9043, 2003.

[47] E. Falconer, R. Bryant, K. L. Felmingham et al., "The neural networks of inhibitory control in posttraumatic stress disorder," *Journal of Psychiatry and Neuroscience*, vol. 33, no. 5, pp. 413–422, 2008.

[48] R. L. Spitzer, J. B. W. Williams, M. Gibbon, and M. B. First, *Structured Clinical Interview for DSM-IV (SCID)*, Biometrics Research, New York, NY, USA, 1995.

[49] L. M. Allen, R. L. Conder, P. Green, and D. R. Cox, *CARB'97 Manual For the Computerized Assessment of Response Bias*, CogniSyst, Durham, NC, USA, 1997.

[50] J. H. Patton, M. S. Stanford, and E. S. Barratt, "Factor structure of the Barratt Impulsiveness Scale," *Journal of Clinical Psychology*, vol. 51, no. 6, pp. 768–774, 1995.

[51] R. A. Zachary and W. C. Shipley, *Shipley Institute of Living Scale: Revised Manual*, WPS, Western Psychological Services, 1986.

[52] J. Briere, *Trauma Symptom Inventory*, Psychological Assessment Resources, Odessa, Fla, USA, 1996.

[53] J. D. Corrigan and J. Bogner, "Initial reliability and validity of the Ohio state university TBI identification method," *Journal of Head Trauma Rehabilitation*, vol. 22, no. 6, pp. 318–329, 2007.

[54] J. N. Epstein, B. J. Casey, S. T. Tonev et al., "ADHD- and medication-related brain activation effects in concordantly affected parent-child dyads with ADHD," *Journal of Child Psychology and Psychiatry and Allied Disciplines*, vol. 48, no. 9, pp. 899–913, 2007.

[55] J. Ashburner and K. J. Friston, "Voxel-based morphometry—the methods," *NeuroImage*, vol. 11, no. 6, pp. 805–821, 2000.

[56] C. D. Good, I. Johnsrude, J. Ashburner, R. N. A. Henson, K. J. Friston, and R. S. J. Frackowiak, "Cerebral asymmetry and the effects of sex and handedness on brain structure: a voxel-based morphometric analysis of 465 normal adult human brains," *NeuroImage*, vol. 14, no. 3, pp. 685–700, 2001.

[57] M. W. Woolrich, S. Jbabdi, B. Patenaude et al., "Bayesian analysis of neuroimaging data in FSL," *NeuroImage*, vol. 45, no. 1, pp. S173–S186, 2009.

[58] R. A. Morey, F. Dolcos, C. M. Petty et al., "The role of trauma-related distractors on neural systems for working memory and emotion processing in posttraumatic stress disorder," *Journal of Psychiatric Research*, vol. 43, no. 8, pp. 809–817, 2009.

[59] T. Hastie, R. Tibshirani, and J. Friedman, *Linear Methods For Regression*, Springer, New York, NY, USA, 2009.

[60] R. Tibshirani, "Regression shrinkage and selection via the lasso: a retrospective," *Journal of the Royal Statistical Society B*, vol. 73, no. 3, pp. 273–282, 2011.

[61] F. L. Bookstein, "'voxel-based morphometry' should not be used with imperfectly registered images," *NeuroImage*, vol. 14, no. 6, pp. 1454–1462, 2001.

[62] B. B. Bendlin, M. L. Ries, M. Lazar et al., "Longitudinal changes in patients with traumatic brain injury assessed with diffusion-tensor and volumetric imaging," *NeuroImage*, vol. 42, no. 2, pp. 503–514, 2008.

[63] O. Bonne, D. Brandes, A. Gilboa et al., "Longitudinal MRI study of hippocampal volume in trauma survivors with PTSD," *The American Journal of Psychiatry*, vol. 158, no. 8, pp. 1248–1251, 2001.

[64] M. D. De Bellis, J. Hall, A. M. Boring, K. Frustaci, and G. Moritz, "A pilot longitudinal study of hippocampal volumes in pediatric maltreatment-related posttraumatic stress disorder," *Biological Psychiatry*, vol. 50, no. 4, pp. 305–309, 2001.

[65] H. Winter and E. Irle, "Hippocampal volume in adult burn patients with and without posttraumatic stress disorder," *American Journal of Psychiatry*, vol. 161, no. 12, pp. 2194–2200, 2004.

[66] R. M. Sapolsky, H. Uno, C. S. Rebert, and C. E. Finch, "Hippocampal damage associated with prolonged glucocorticoid exposure in primates," *Journal of Neuroscience*, vol. 10, no. 9, pp. 2897–2902, 1990.

[67] R. J. McNally and L. M. Shin, "Association of intelligence with severity of posttraumatic stress disorder symptoms in Vietnam combat veterans," *American Journal of Psychiatry*, vol. 152, no. 6, pp. 936–938, 1995.

[68] A. Gopal, E. Clark, A. Allgair et al., "Dorsal/ventral parcellation of the amygdala: relevance to impulsivity and aggression," *Psychiatry Research*, vol. 211, no. 1, pp. 24–30, 2013.

[69] S. Royer, M. Martina, and D. Paré, "An inhibitory interface gates impulse traffic between the input and output stations of the amygdala," *Journal of Neuroscience*, vol. 19, no. 23, pp. 10575–10583, 1999.

[70] R. G. Phillips and J. E. LeDoux, "Differential contribution of amygdala and hippocampus to cued and contextual fear conditioning," *Behavioral Neuroscience*, vol. 106, no. 2, pp. 274–285, 1992.

[71] P. J. Whalen, L. M. Shin, S. C. McInerney, H. Fischer, C. I. Wright, and S. L. Rauch, "A functional MRI study of human amygdala responses to facial expressions of fear versus anger," *Emotion*, vol. 1, no. 1, pp. 70–83, 2001.

[72] A. Etkin, K. C. Klemenhagen, J. T. Dudman et al., "Individual differences in trait anxiety predict the response of the basolateral amygdala to unconsciously processed fearful faces," *Neuron*, vol. 44, no. 6, pp. 1043–1055, 2004.

[73] M. Davis, D. Rainnie, and M. Cassell, "Neurotransmission in the rat amygdala related to fear and anxiety," *Trends in Neurosciences*, vol. 17, no. 5, pp. 208–214, 1994.

[74] C. A. Winstanley, D. E. H. Theobald, R. N. Cardinal, and T. W. Robbins, "Contrasting roles of basolateral amygdala and orbitofrontal cortex in impulsive choice," *Journal of Neuroscience*, vol. 24, no. 20, pp. 4718–4722, 2004.

[75] S. Lui, L. Chen, L. Yao, Y. Xiao, Q. Z. Wu, J. R. Zhang et al., "Brain structural plasticity in survivors of a major earthquake," *Journal of Psychiatry and Neuroscience*, vol. 38, no. 3, pp. 120244–120244, 2013.

Hindawi Publishing Corporation
BioMed Research International
Volume 2014, Article ID 860658, 8 pages
http://dx.doi.org/10.1155/2014/860658

Research Article

Diffusion Tensor Imaging Studies on Chinese Patients with Social Anxiety Disorder

Changjian Qiu,[1] Chunyan Zhu,[1,2] Jingna Zhang,[3,4] Xiaojing Nie,[1] Yuan Feng,[1] Yajing Meng,[1] Ruizhi Wu,[1] Xiaoqi Huang,[5] Wei Zhang,[1] and Qiyong Gong[5]

[1] *Mental Health Center, West China Hospital of Sichuan University, Chengdu 610041, China*
[2] *The Seventh People's Hospital of Hangzhou, Hangzhou 310013, China*
[3] *Key Laboratory for Neuroinformation of Ministry of Education, School of Life Science and Technology, University of Electronic Science and Technology of China, Chengdu 610054, China*
[4] *Department of Medical Image, College of Biomedical Engineering, Third Military Medical University, Chongqing 400038, China*
[5] *Huaxi MR Research Center (HMRRC), Department of Radiology, West China Hospital of Sichuan University, West China School of Medicine, Chengdu 610041, China*

Correspondence should be addressed to Xiaoqi Huang; julianahuang@163.com and Wei Zhang; weizhang27@163.com

Received 20 October 2013; Revised 6 January 2014; Accepted 29 January 2014; Published 3 March 2014

Academic Editor: Yong He

The aim of this study was to explore white-matter disruption in social anxiety disorder (SAD) patients by using diffusion tensor imaging (DTI) and to investigate the relationship between cerebral abnormalities and the severity of the symptoms. Eighteen SAD patients and age- and gender-matched healthy controls were recruited. DTI scans were performed to measure fractional anisotropy (FA) and apparent diffusion coefficient (ADC) for each subject. We used voxel-based analysis to determine the differences of FA and ADC values between the two groups with two-sample t-tests. The SAD patient showed significantly decreased FA values in the white matter of the left insula, left inferior frontal gyrus, left middle temporal gyrus, and left inferior parietal gyrus and increased ADC values in the left insula, bilateral inferior frontal gyrus, bilateral middle temporal gyrus, and left inferior parietal gyrus. In SAD patients, we observed a significant negative correlation between FA values in the left insula and the total LSAS scores and a positive correlation between the ADC values in the left inferior frontal gyrus and the total LSAS scores. Above results suggested that white-matter microstructural changes might contribute to the neuropathology of SAD.

1. Introduction

Social anxiety disorder (SAD) is a marked and persistent fear of social or performance situations in which the person is exposed to unfamiliar people or to possible scrutiny by others. The situations provoke intense anxiety symptoms in the patients, which are often experienced as somatic symptoms, and, as a result, the individuals may avoid social situations. SAD can be particularly disabling in some patients, leading to reduced likelihood of employment, social isolation, functional disability, and dissatisfaction with life and health [1]. Data obtained by the National Comorbidity Survey indicate that the adult lifetime prevalence of SAD is 13.3% [2]. Recent research also indicated that the 12-month prevalence rate of SAD was 2.48%~7.9% and that the lifetime prevalence was about 3.8%~14.4% [3, 4]. The highly comorbid nature of SAD, which often occurs along with depression, panic disorder, and alcohol abuse, is well established [5, 6].

To date, there is no clear neuroanatomical model for SAD; however, an increasing amount of the neuroscience literature is being devoted to social functioning. The previous functional magnetic resonance imaging (fMRI) studies on SAD found altered brain function in SAD within the medial prefrontal cortex and the limbic regions which formed the corticolimbic circuits, including the amygdala, hippocampus, and insula [7–11]. The amygdala, as a part of the corticolimbic circuits, plays a critical role in learning about environmental predictors of threat and in attention and facial emotions in SAD [12]. Its ability to control fear responses to threatening

stimuli was regulated by the hippocampus and medial prefrontal cortex [13]. In addition, the insular cortex is a pivotal structure in the greater limbic lobe and plays a role in diverse functions linked to emotion and memory [14]. However, a better understanding of the neurobiology of SAD would require investigations at the microstructure or anatomical connectivity level, especially in patients not yet exposed to psychotherapy or psychiatric medications.

Diffusion tensor imaging (DTI), which is a recently developed MRI technique, allows for the examination of the integrity of the white-matter microstructure and, thus, serves as an important tool for mapping the anatomical connectivities in humans [15]. DTI measures the directionality and coherence of water diffusion (as reflected by the degree of anisotropy), which provides an estimate of the axonal organization in the brain [16]. The indices used to interpret DTI data were fractional anisotropy (FA) and the apparent diffusion coefficient (ADC). FA values reflect the directionality and coherence of water self-diffusion. Tissues with highly regular fibers have high anisotropy, whereas those with less regular fibers have low anisotropy. Consequently, FA values serve as a quantitative indicator of white-matter coherence or integrity, with lower values signifying decreased structural connectivity in white matter. The ADC values reflect the degree of apparent water diffusivity. Tissues without obstacles (such as cerebrospinal fluid (CSF)) have high water diffusivity, whereas those with obstacles (such as white matter) have low water diffusivity. To date, the use of DTI in the examination of white-matter tracts in SAD patients has been limited. Therefore, the aim of the current study was to explore the differences in the white-matter connectivity in SAD patients and healthy controls by using DTI. In addition, the current study also explored the relation between the severity of SAD symptoms and abnormalities in the white matter.

2. Methods and Materials

2.1. Subjects. The subjects were 18 adult patients with SAD (according to the DSM-IV criteria) who were recruited from the Outpatient Clinic of the West China Hospital. All subjects were interviewed using the Structured Clinical Interview for DSM-IV criteria Patient Version (SCID-I/P) [17], with additional probes from the self-administered Liebowitz social anxiety scale (LSAS) [18]. All SAD patients were right handed and had LSAS scores ≥38 without psychiatric comorbidities or other medical conditions. None of the patients had received any pharmacological and/or psychotherapeutic treatment. Eighteen healthy controls (HCs), matched for age, sex, handedness, and education, were recruited from the local area by poster advertisement and screened using the SCID-I/P to rule out the presence of current diagnosis or past history of SAD/other axis I psychiatric disorders/axis II antisocial or borderline personality disorders and had LSAS less than 38.

The exclusion criteria for SAD patients and HCs were as follows: (1) any current or past serious medical or neurological illness, including neurologic (Tourette's syndrome, Huntington's disease, Parkinson's disease, encephalitis, stroke, aneurysms, tumors, central nervous system infections, degenerative brain diseases, or trauma), pulmonary, cardiac, renal, hepatic, endocrine, or metabolic (including dehydration) disorders; prior psychosurgery or contraindications to MR scanning, including metal implants, pregnancy, or severe claustrophobia; (2) a current diagnosis or past history of other axis I psychiatric disorders; (3) axis II antisocial or borderline personality disorders (identified using the Structured Clinical Interview for DSM-IV criteria); (4) a history of drug dependence or abuse; (5) a history of psychiatric illness in first-degree relatives.

The study procedure and the involved risks were explained to the subjects; all the subjects gave their written informed consent according to the protocol approved by the ethics committee.

2.2. Image Acquisition. All MRI scans were performed using a 3.0 Tesla GE Signa scanner with an eight-channel phased-array head coil. A board-certified neuroradiologist reviewed the scans and found no gross abnormalities in any of the subjects. The DTI was performed using a single-shot echo-planar technique with 15 motion-probing gradient orientations. The key data acquisition parameters for the DTI scan were as follows: TR = 12000 ms; TE = 73.9 ms; flip angle = 90; imaging matrix = 128 × 128; field of view (FOV) = 24 × 24 cm^2; slice thickness = 3 mm; number of slices = 50; slice gap = 0 mm; number of diffusion gradient directions = 15; b = 0 and 1000 s/mm^2; total scan time = 6 min and 47 s.

2.3. Image Processing. The FA and ADC maps were obtained using DTI-Studio (Department of Radiology, Johns Hopkins University School of Medicine, Baltimore, MD, USA; available at http://cmrm.med.jhmi.edu). Image analysis was performed using SPM2 software (developed at the Wellcome Department of Imaging Neuroscience, Institute of Neurology, University College London), which was run on MATLAB7.0 (Mathworks, Sherborn, MA). Spatial normalization is an essential preprocessing step in SPM-based analysis. The contrast settings of the FA and ADC maps differ from those of the T1-weighted and T2-weighted template images provided by SPM2. Thus, the FA and ADC templates specific for this study were created using data from all the participants. Each $b = 0$ image in the native space was standardized using the T2 template supplied with the SPM2 software, and the normalization parameter was applied to the respective $b = 0$, FA, and ADC maps. The normalized maps were smoothed with a 6 mm full width at half-maximum (FWHM) isotropic Gaussian kernel, and the mean images ($b = 0$ template, FA template, and ADC template) were created. Then, all the FA and ADC maps in native space were transformed into stereotactic space by registering each image with the customized FA and ADC templates.

2.4. Statistical Analysis. Differences between the demographic variables of the 2 groups were examined using independent-group t-tests. Two-sample t-tests were performed for each voxel of the FA and ADC values across the entire brain. In these analyses, the statistical threshold was defined

Table 1: Demographic characteristics (mean ± SD) of subjects.

	SAD ($N = 18$)	HC ($N = 18$)	t (df = 34)	P
Age	22.72 ± 3.85	21.78 ± 3.90	0.73	0.47
Gender	12 M/6 F	12 M/6 F	—	—
Education	14.11 ± 1.53	14.05 ± 2.04	0.09	0.927
Duration	49.22 ± 40.17			
Total LSAS	54.11 ± 11.90	19.50 ± 8.50	10.04	0.000

SAD: social anxiety disorder; HC: healthy control; M: male; F: female.
Educational background was measured according to the years of education.
The severity of social anxiety was measured using the Liebowitz social anxiety scale.
Duration: the time from the beginning of the first episode to the time of assessment (measured in months).

Table 2: Differences between the FA and ADC values of the SAD patients and HCs.

Anatomical region	Talairach coordinates at the center of the cluster			Cluster sizes	t value
	x	y	z		
Lower FA					
Inferior frontal gyrus (L)	−51	10	12	66	3.5212
Insula (L)	−36	4	−5	114	3.4206
Inferior parietal gyrus (L)	−42	−35	39	226	4.1552
Middle temporal gyrus (L)	−57	−23	−2	164	3.3456
Higher ADC					
Inferior frontal gyrus (L)	−50	11	18	173	4.8080
Inferior frontal gyrus (R)	59	21	27	81	3.6572
Insula (L)	−38	−4	−10	78	3.1251
Inferior parietal gyrus (L)	−44	−37	42	382	4.3239
Middle temporal gyrus (L)	−40	3	−24	443	4.4674
Middle temporal gyrus (R)	50	−37	−2	758	4.5024

as a t value above 2.44 ($P < 0.01$, uncorrected). We used MarsBar (http://marsbar.sourceforge.net) for extracting the FA and ADC values in the ROIs (region of interest) by two steps: firstly, ROIs were defined as regions in which the FA and ADC values of the SAD patients were abnormal from two-sample t-tests with a cluster size bigger than 50; secondly, values were extracted from FA or ADC map of each SAD patient separately and investigated the correlations between ROIs' FA and ADC values and the score of LSAS in the SAD patients. Correlations were calculated using Pearson's correlation analysis, and a P value less than 0.05 was considered significant.

3. Results

Age, sex, handedness, and education did not differ significantly between the SAD patients and the HCs (Table 1). In comparison to the HCs, the SAD patients had decreased FA values in the white matter of the left insula, left inferior frontal gyrus, left middle temporal gyrus, and left inferior parietal gyrus (Figure 1; Table 2). The SAD patients also showed increased ADC values in the left and right inferior frontal gyrus, left and right middle temporal gyrus, left inferior parietal gyrus, and left insula (Figure 2; Table 2). In addition, we found a negative correlation between the decreased FA values in the left insula and the total LSAS scores of the SAD patients ($r = -0.504$, $P = 0.033$) and a trend of negative correlation between FA values and the left inferior frontal gyrus ($r = -0.414$, $P = 0.087$); there was a positive correlation between the increased ADC values in the left inferior frontal gyrus and the total LSAS scores of the SAD patients ($r = 0.558$, $P = 0.016$) (Figure 3).

4. Discussion

Few studies have examined the brain white matter in SAD patients. The preliminary findings provided evidence of abnormal white-matter microstructure in SAD patients, as inferred from the DTI results. Specifically, the findings of this study were as follows: (1) the SAD patients showed decreased FA values in the left insula, left inferior frontal gyrus, left middle temporal gyrus, and left inferior parietal gyrus and a negative correlation between the decreased FA values in the left insula and the total LSAS scores; (2) the SAD patients also showed increased ADC values in the left insula, left and right inferior frontal gyrus, left and right middle temporal gyrus, and left inferior parietal gyrus and a positive correlation between the increased ADC values in the left inferior frontal gyrus and the total LSAS scores.

These findings corroborate the findings of prior studies, which reported functional abnormalities in the corticolimbic circuits of SAD patients [8–10]. In this study, significant

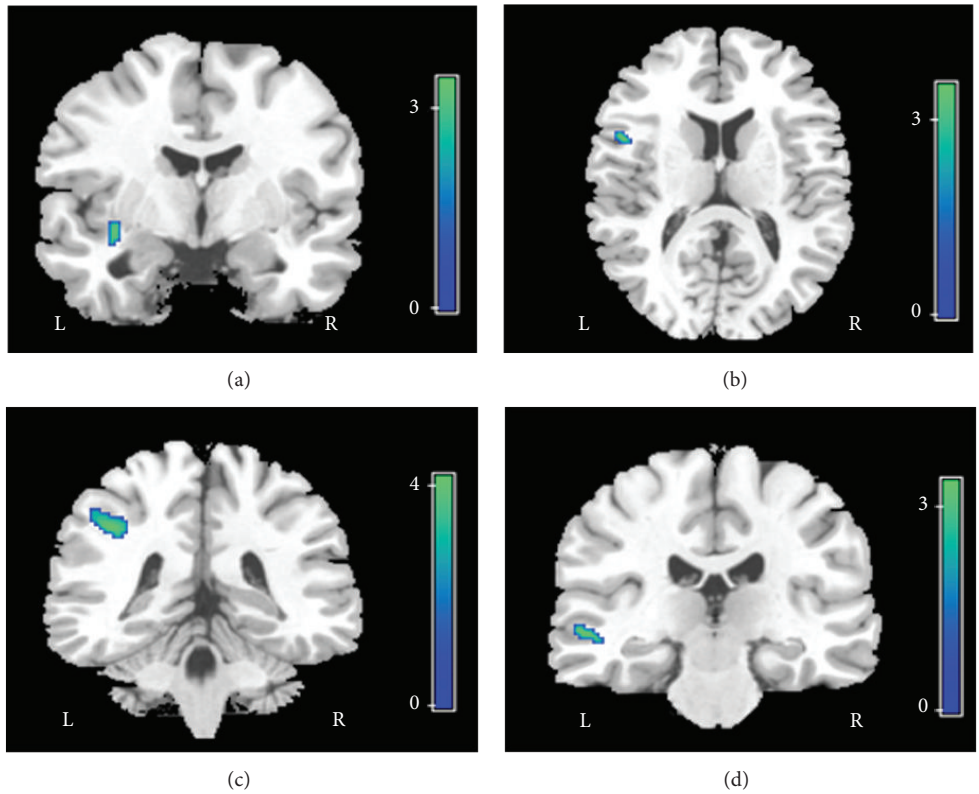

Figure 1: Four clusters of significantly decreased FA values in the left insula cortex (a), left inferior frontal gyrus (b), left inferior parietal gyrus (c), and left middle temporal gyrus (d) in the SAD patient group, in comparison to the corresponding values of the HCs. The clusters are superimposed onto the images from a representative T1-weighted MRI study in Montreal Neurological Institute (MNI) space (Courtesy of MRIcro, Chris Rorden).

white-matter abnormalities were observed on both sides of the frontal cortex of the subjects with SAD. A recent study on SAD conducted using social anxiety imagery condition showed several regions of altered regional cerebral blood flow (rCBF)/activation [19]. Changes in rCBF/activation were also noted following pharmacotherapy. A recent PET study showed that the anticipatory anxiety in SAD subjects was associated with decreased bilateral frontal activation [20]. Another recent SAD study revealed a significant positive correlation between the resting perfusion values and the total LSAS scores at the left frontal cortex [21]. A review of the role of the medial frontal cortex (MFC) in social cognition by Amodio and Frith [22] suggests that the anterior rostral MFC plays a role in social cognition by integrating the afferents from the posterior rostral MFC (involved in the monitoring of action) and the orbitofrontal cortex (involved in the monitoring of reward or punishment). The medial prefrontal cortex is hypothesized to play a role in the inhibition or extinction of excessive corticolimbic activity in patients with anxiety disorders [23]. If this is the case, then frontal findings from this study may indicate dysfunction in the cortical regions of the SAD patients, which contribute directly to the etiology of SAD.

The insula is associated with strong emotional responses, such as disgust [24, 25] as well as the representation of visceral sensation [26], and might play a role in several anxiety disorders [27]. In this study, the FA and ADC values in the left insula of the SAD patients were significantly lower and higher, respectively, than the corresponding values in the HCs. In addition, this result was also strengthened by the independent finding of a correlation between the total LSAS score and FA value in the SAD group. Insula activation results for SAD patients were found to be different from those for the HCs, which paralleled the results of previous studies [10, 28]. Interestingly, there is evidence that brain activation in response to threatening faces in SAD patients differs greatly from the activation in HCs when facial emotional expressions are task irrelevant, which suggests an automatic processing of facial anger cues in SAD patients [10]. The functional and structural abnormalities in SAD patients may affect their social cognitive processing circuits. We speculated that insula abnormalities were one of the neurobiological mechanisms. In addition, a recent study found that if the anterior insula participated in anticipatory processing [29], then abnormalities in the white matter of the insula may be interpreted as neural mechanism for symptom of anticipatory anxiety in SAD patients.

Our study reported abnormalities in the white matter of the middle temporal gyrus and inferior parietal gyrus in subjects with SAD. Many studies have revealed that, in the temporal cortex of monkeys and humans, the temporoparietal junction, which is located primarily in the superior temporal sulcus (STS) region, is activated by movements of the eyes, mouth, hands, and body, suggesting that this junction is

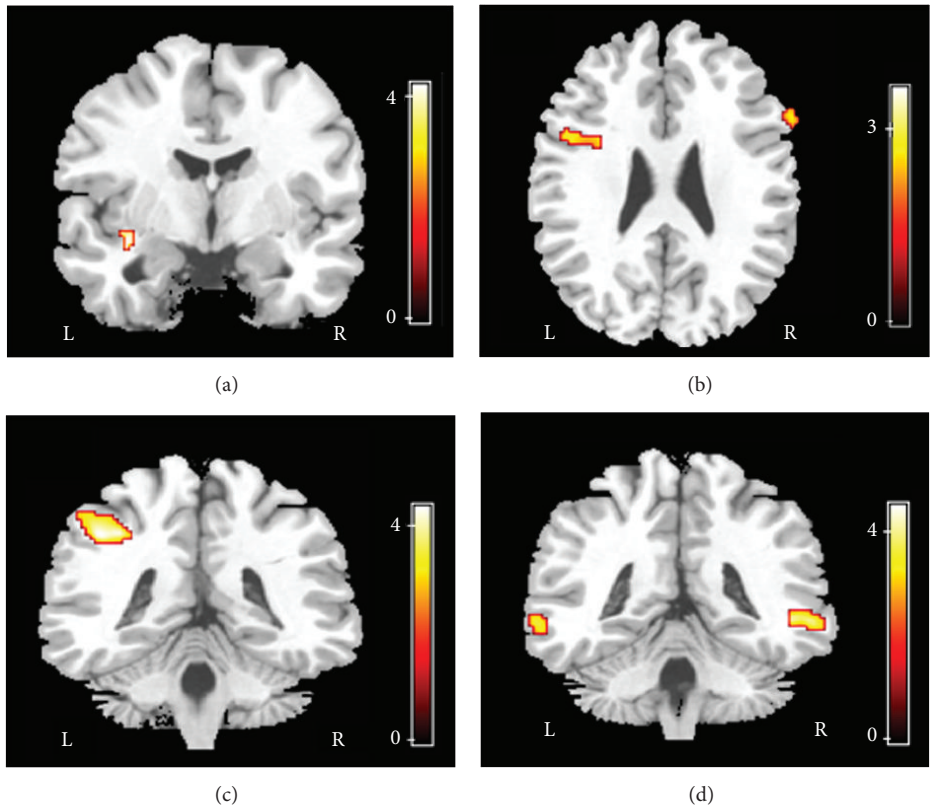

Figure 2: Six clusters of significantly increased ADC values in the left insula (a), left and right inferior frontal gyrus (b), left inferior parietal gyrus (c), and left and right middle temporal gyrus (d) of the SAD patient group, in comparison to the corresponding values of the HCs. The clusters are superimposed on the images from a representative T1-weighted MRI study in MNI space (Courtesy of MRIcro, Chris Rorden).

involved in the analysis of biological motion [25, 30]. STS, the core system perceptual area, has been associated with the perception of expression [31, 32], the evaluation of the intentions and personality traits of others [32, 33], and, more generally, the social evaluation of others [34]. Face recognition and analysis of facial expression form an important part of everyday interactions among humans. Previous studies have suggested that SAD patients show biased processing of emotional expressions and personality traits, resulting in the fear of social interaction [35, 36]. A significant behavioral effect while processing socially relevant stimuli, face processing in particular, has been shown in previous studies. Specifically, behavioral studies have reported that SAD patients tend to judge neutral faces negatively [37], remember critical faces better than accepting ones [38], and scan faces with a different pattern of eye movements than that used by the HCs [36]. These results suggest that SAD view still images of faces with a negative or wary attitude. Straube et al. found that in a comparison of angry versus neutral faces in an implicit task, activation of the STS region in the SAD patients was stronger than that in the HCs [10]. These results suggest a specific pattern of activity in the different parts of the distributed neural system for face perception in SAD patients. Abnormalities in the above-mentioned neuroanatomical regions may supply the neurobiological basis for biased processing of information in SAD patients.

It is particularly interesting that all of significantly decreased FA regions occurred in the left hemisphere including the left insula cortex, left inferior frontal gyrus, left inferior parietal gyrus, and left middle temporal gyrus in the SAD patient group. The possible lateralization of emotion was found in brain structures, such as the frontal cortex, the amygdala, and insular cortex in a previous meta-analysis of neuroimaging studies [39]. Our results were also consistent with recent functional neuroimaging studies showing an overall lateralization of cortex and limbic system activations to the left hemisphere, particularly for corticolimbic circuits [40]. Further studies specifically designed to examine whether the lateralization of the function and structure exists and how it works in SAD patients would be helpful to clarify the disease etiology.

The current study had a number of limitations. Firstly, the patient group was interviewed using the Structured Clinical Interview for the Diagnosis of Axis-I Disorders, but they were not classified into general SAD or specific SAD groups. Secondly, while the 2 groups of subjects were comparable with respect to age, gender, and level of education, the comparability of the 2 groups for other potentially confounding factors, such as socioeconomic status, was not assessed. Finally, it needs to be noted that this study used a low significance threshold for a whole-brain, voxel-wise analysis ($P < 0.01$ uncorrected). Although this situation was not ideal, we believed

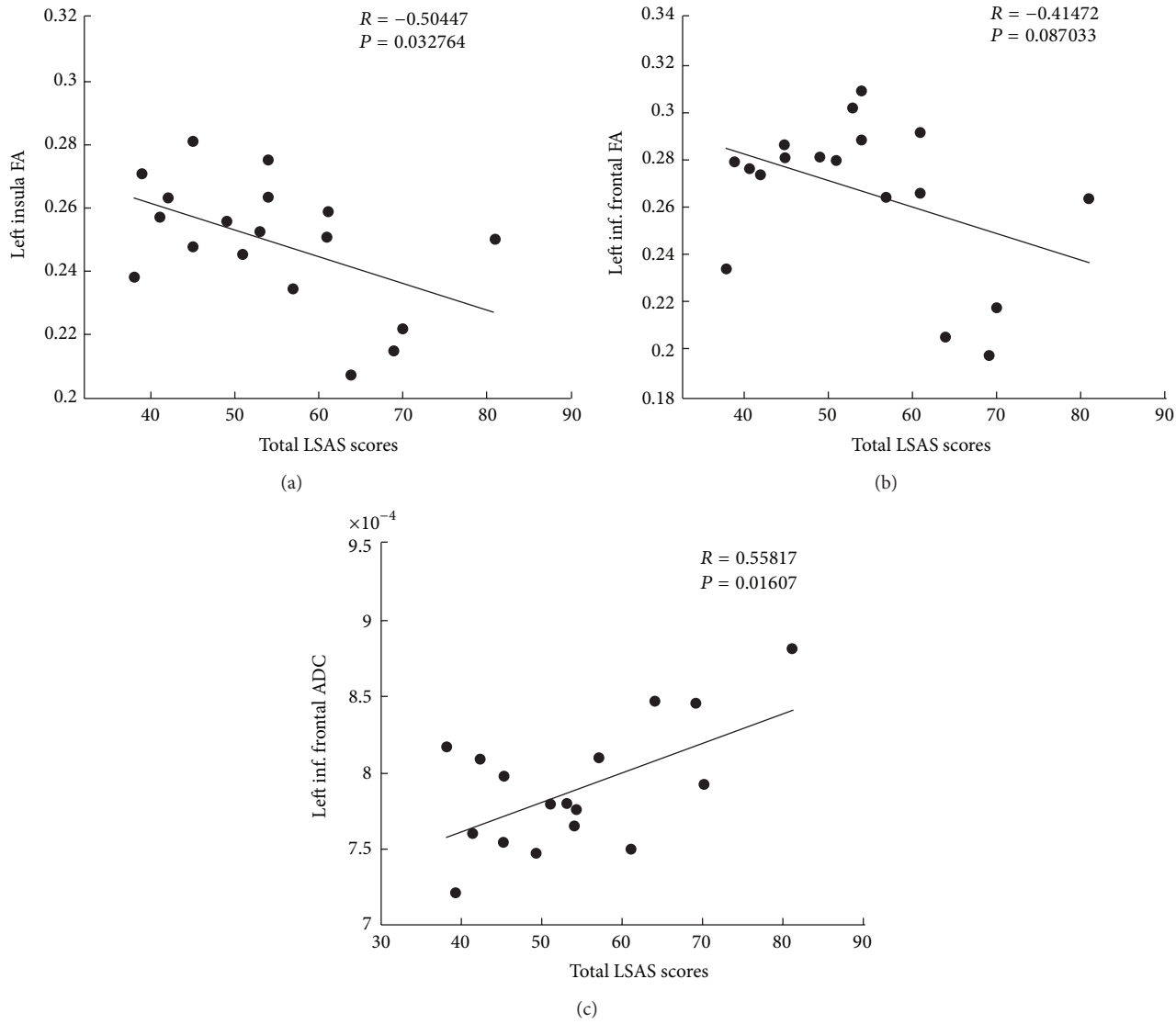

Figure 3: (a) A cluster in the left insula region with a significant negative correlation between the FA values and the total LSAS scores. (b) A cluster in the left inferior frontal region with a trend of a negative correlation between the FA values and total LSAS scores. (c) A cluster in the left inferior frontal region with a significant positive correlation between the ADC values and the total LSAS scores.

that we were still able to perform a comparison of 2 reasonably well-defined groups. The emphasis in this analysis was to maximize sensitivity and to use a less strict threshold so as to avoid overlooking significant findings. Future studies with larger sample size may help to see whether there would be more robust result for SAD patients concerning white-matter abnormalities. Despite these limitations, we believe that our findings will contribute to the growing literature on the imaging studies of anxiety disorders.

5. Conclusion

This study showed several brain-lobe abnormalities in the white matter of the SAD patient group. These findings were parallel to those of previous studies that showed functional abnormalities in these regions; the findings were also consistent with the hypothesized role of these regions in the modulation of excessive limbic activity in anxiety disorders. The left insula and the left inferior frontal gyrus in SAD patients showed a significant correlation between the total LSAS score and the FA or ADC values, which may point to the defective perception of self and others in these patients. Future studies with tractography would provide more information referring to the disruption of corticolimbic circuits in SAD patients.

Conflict of Interests

The authors declare that there is no conflict of interests regarding the publication of this paper.

Authors' Contribution

Changjian Qiu and Chunyan Zhu have equal contribution to this paper.

Acknowledgments

This research was partially supported by the State Important Basic Research Development Program (Program no. 2008CB517407), the National Natural Science Foundation of China (Grant no. 81171488), and the National Key Technologies R&D Program (Program no. 2012BAI01B03). The authors thank all the subjects who participated in this study. They also thank the MRI Laboratory of the West China Hospital for processing the fMRI data.

References

[1] H.-U. Wittchen and E. Beloch, "The impact of social phobia on quality of life," *International Clinical Psychopharmacology*, vol. 11, supplement 3, pp. 15–23, 1996.

[2] T. H. Ollendick and D. R. Hirshfeld-Becker, "The developmental psychopathology of social anxiety disorder," *Biological Psychiatry*, vol. 51, no. 1, pp. 44–58, 2002.

[3] J. Sareen and M. Stein, "A review of the epidemiology and approaches to the treatment of social anxiety disorder," *Drugs*, vol. 59, no. 3, pp. 497–509, 2000.

[4] R. G. Heimberg, "Assessment and diagnosis of social phobia in the clinic and the community," *Psychological Medicine*, vol. 33, no. 4, pp. 583–588, 2003.

[5] W. D. Shields, "Effects of epilepsy surgery on psychiatric and behavioral comorbidities in children and adolescents," *Epilepsy and Behavior*, vol. 5, supplement 3, pp. S18–S24, 2004.

[6] V. Cramer, S. Torgersen, and E. Kringlen, "Quality of life and anxiety disorders: A Population Study," *Journal of Nervous and Mental Disease*, vol. 193, no. 3, pp. 196–202, 2005.

[7] A. Etkin and T. D. Wager, "Functional neuroimaging of anxiety: a meta-ana lysis of emotional processing in PTSD, social anxiety disorder, and specific phobia," *American Journal of Psychiatry*, vol. 164, no. 10, pp. 1476–1488, 2007.

[8] R. E. Cooney, L. Y. Atlas, J. Joormann, F. Eugène, and I. H. Gotlib, "Amygdala activation in the processing of neutral faces in social anxiety disorder: is neutral really neutral?" *Psychiatry Research*, vol. 148, no. 1, pp. 55–59, 2006.

[9] K. L. Phan, D. A. Fitzgerald, P. J. Nathan, and M. E. Tancer, "Association between amygdala hyperactivity to harsh faces and severity of social anxiety in generalized social phobia," *Biological Psychiatry*, vol. 59, no. 5, pp. 424–429, 2006.

[10] T. Straube, I.-T. Kolassa, M. Glauer, H.-J. Mentzel, and W. H. R. Miltner, "Effect of task conditions on brain responses to threatening faces in social phobics: an event-related functional magnetic resonance imaging study," *Biological Psychiatry*, vol. 56, no. 12, pp. 921–930, 2004.

[11] F. Schneider, U. Weiss, C. Kessler et al., "Subcortical correlates of differential classical conditioning of aversive emotional reactions in social phobia," *Biological Psychiatry*, vol. 45, no. 7, pp. 863–871, 1999.

[12] D. G. Amaral, "The primate amygdala and the neurobiology of social behavior: implications for understanding social anxiety," *Biological Psychiatry*, vol. 51, no. 1, pp. 11–17, 2002.

[13] R. Yehuda and J. LeDoux, "Response variation following trauma: a translational neuroscience approach to understanding PTSD," *Neuron*, vol. 56, no. 1, pp. 19–32, 2007.

[14] B. P. Shelley and M. R. Trimble, "The insular lobe of reil-its anatamico-functional, behavioural and neuropsychiatric attributes in humans—a review," *World Journal of Biological Psychiatry*, vol. 5, no. 4, pp. 176–200, 2004.

[15] K. O. Lim and J. A. Helpern, "Neuropsychiatric applications of DTI—a review," *NMR in Biomedicine*, vol. 15, no. 7-8, pp. 587–593, 2002.

[16] S. Mori and J. Zhang, "Principles of diffusion tensor imaging and its applications to basic neuroscience research," *Neuron*, vol. 51, no. 5, pp. 527–539, 2006.

[17] M. B. First, B. Gibbon, R. L. Spitzer et al., SCID-I/P(Structureed Clinical Interview for DSM-IV axis I disorders, research version for patients), 1996.

[18] D. M. Fresco, M. E. Coles, R. G. Heimberg et al., "The Liebowitz Social Anxiety Scale: a comparison of the psychometric properties of self-report and clinician-administered formats," *Psychological Medicine*, vol. 31, no. 6, pp. 1025–1035, 2001.

[19] C. D. Kilts, J. E. Kelsey, B. Knight et al., "The neural correlates of social anxiety disorder and response to pharmacotherapy," *Neuropsychopharmacology*, vol. 31, no. 10, pp. 2243–2253, 2006.

[20] M. Tillfors, T. Furmark, I. Marteinsdottir, and M. Fredrikson, "Cerebral blood flow during anticipation of public speaking in social phobia: A PET Study," *Biological Psychiatry*, vol. 52, no. 11, pp. 1113–1119, 2002.

[21] J. M. Warwick, P. Carey, G. P. Jordaan, P. Dupont, and D. J. Stein, "Resting brain perfusion in social anxiety disorder: a voxel-wise whole brain comparison with healthy control subjects," *Progress in Neuro-Psychopharmacology and Biological Psychiatry*, vol. 32, no. 5, pp. 1251–1256, 2008.

[22] D. M. Amodio and C. D. Frith, "Meeting of minds: the medial frontal cortex and social cognition," *Nature Reviews Neuroscience*, vol. 7, no. 4, pp. 268–277, 2006.

[23] J. LeDoux, "Fear and the brain: where have we been, and where are we going?" *Biological Psychiatry*, vol. 44, no. 12, pp. 1229–1238, 1998.

[24] M. L. Phillips, A. W. Young, C. Senior et al., "A specific neural substrate for perceiving facial expressions of disgust," *Nature*, vol. 389, no. 6650, pp. 495–498, 1997.

[25] B. Wicker, C. Keysers, J. Plailly, J.-P. Royet, V. Gallese, and G. Rizzolatti, "Both of us disgusted in My insula: the common neural basis of seeing and feeling disgust," *Neuron*, vol. 40, no. 3, pp. 655–664, 2003.

[26] H. D. Critchley, S. Wiens, P. Rotshtein, A. Öhman, and R. J. Dolan, "Neural systems supporting interoceptive awareness," *Nature Neuroscience*, vol. 7, no. 2, pp. 189–195, 2004.

[27] M. P. Paulus and M. B. Stein, "An insular view of anxiety," *Biological Psychiatry*, vol. 60, no. 4, pp. 383–387, 2006.

[28] J. Sareen, D. W. Campbell, W. D. Leslie et al., "Striatal function in generalized social phobia: A Functional Magnetic Resonance Imaging Study," *Biological Psychiatry*, vol. 61, no. 3, pp. 396–404, 2007.

[29] K. L. Lovero, A. N. Simmons, J. L. Aron, and M. P. Paulus, "Anterior insular cortex anticipates impending stimulus significance," *NeuroImage*, vol. 45, no. 3, pp. 976–983, 2009.

[30] F. Castelli, F. Happé, U. Frith, and C. Frith, "Movement and mind: a functional imaging study of perception and interpretation of complex intentional movement patterns," *NeuroImage*, vol. 12, no. 3, pp. 314–325, 2000.

[31] A. D. Engell and J. V. Haxby, "Facial expression and gaze-direction in human superior temporal sulcus," *Neuropsychologia*, vol. 45, no. 14, pp. 3234–3241, 2007.

[32] J. S. Winston, R. N. A. Henson, M. R. Fine-Goulden, and R. J. Dolan, "fMRI-adaptation reveals dissociable neural representations of identity and expression in face perception," *Journal of Neurophysiology*, vol. 92, no. 3, pp. 1830–1839, 2004.

[33] M. I. Gobbini, A. C. Koralek, R. E. Bryan, K. J. Montgomery, and J. V. Haxby, "Two takes on the social brain: a comparison of theory of mind tasks," *Journal of Cognitive Neuroscience*, vol. 19, no. 11, pp. 1803–1814, 2007.

[34] T. Allison, A. Puce, and G. McCarthy, "Social perception from visual cues: role of the STS region," *Trends in Cognitive Sciences*, vol. 4, no. 7, pp. 267–278, 2000.

[35] F. Saboonchi, L.-G. Lundh, and L.-G. Öst, "Perfectionism and self-consciousness in social phobia and panic disorder with agoraphobia," *Behaviour Research and Therapy*, vol. 37, no. 9, pp. 799–808, 1999.

[36] K. Horley, L. M. Williams, C. Gonsalvez, and E. Gordon, "Face to face: visual scanpath evidence for abnormal processing of facial expressions in social phobia," *Psychiatry Research*, vol. 127, no. 1-2, pp. 43–53, 2004.

[37] E. C. Winton, D. M. Clark, and R. J. Edelmann, "Social anxiety, fear of negative evaluation and the detection of negative emotion in others," *Behaviour Research and Therapy*, vol. 33, no. 2, pp. 193–196, 1995.

[38] F. Saboonchi, L.-G. Lundh, and L.-G. Öst, "Perfectionism and self-consciousness in social phobia and panic disorder with agoraphobia," *Behaviour Research and Therapy*, vol. 37, no. 9, pp. 799–808, 1999.

[39] T. D. Wager, K. L. Phan, I. Liberzon, and S. F. Taylor, "Valence, gender, and lateralization of functional brain anatomy in emotion: a meta-analysis of findings from neuroimaging," *NeuroImage*, vol. 19, no. 3, pp. 513–531, 2003.

[40] A. Hahn, P. Stein, C. Windischberger et al., "Reduced resting-state functional connectivity between amygdala and orbitofrontal cortex in social anxiety disorder," *NeuroImage*, vol. 56, no. 3, pp. 881–889, 2011.

Hindawi Publishing Corporation
BioMed Research International
Volume 2014, Article ID 374828, 7 pages
http://dx.doi.org/10.1155/2014/374828

Research Article

Surface-Based Regional Homogeneity in First-Episode, Drug-Naïve Major Depression: A Resting-State fMRI Study

Hui-Jie Li,[1] Xiao-Hua Cao,[2] Xing-Ting Zhu,[1,3] Ai-Xia Zhang,[2] Xiao-Hui Hou,[1,3] Yong Xu,[2] Xi-Nian Zuo,[1] and Ke-Rang Zhang[2]

[1] *Laboratory for Functional Connectome and Development, Magnetic Resonance Imaging Research Center, Key Laboratory of Behavioral Science, Institute of Psychology, Chinese Academy of Sciences, No. 16 Lincui Road, Chaoyang District, Beijing 100101, China*
[2] *Department of Psychiatry, First Hospital of Shanxi Medical University, No. 85 Jiefang South Road, Taiyuan 030001, China*
[3] *University of Chinese Academy of Sciences, Beijing 100049, China*

Correspondence should be addressed to Xi-Nian Zuo; zuoxn@psych.ac.cn and Ke-Rang Zhang; krzhang_sxmu@vip.163.com

Received 5 November 2013; Revised 15 January 2014; Accepted 19 January 2014; Published 25 February 2014

Academic Editor: Qiyong Gong

Background. Previous volume-based regional homogeneity (ReHo) studies neglected the intersubject variability in cortical folding patterns. Recently, surface-based ReHo was developed to reduce the intersubject variability and to increase statistical power. The present study used this novel surface-based ReHo approach to explore the brain functional activity differences between first-episode, drug-naïve MDD patients and healthy controls. *Methods.* Thirty-three first-episode, drug-naïve MDD patients and 32 healthy controls participated in structural and resting-state fMRI scans. MDD patients were rated with a 17-item Hamilton Rating Scale for Depression prior to the scan. *Results.* In comparison with the healthy controls, MDD patients showed reduced surface-based ReHo in the left insula. There was no increase in surface-based ReHo in MDD patients. The surface-based ReHo value in the left insula was not significantly correlated with the clinical information or the depressive scores in the MDD group. *Conclusions.* The decreased surface-based ReHo in the left insula in MDD may lead to the abnormal top-down cortical-limbic regulation of emotional and cognitive information. The surface-based ReHo may be a useful index to explore the pathophysiological mechanism of MDD.

1. Introduction

Major depressive disorder (MDD) is characterized by cognitive deficits, functional disability, and pervasive negative feelings, such as sadness, anxiety, dysphoria, anhedonia, sleep abnormalities, and feelings of worthlessness [1]. MDD patients have deficits in emotional self-regulation and are prone to negative emotion bias toward life events [2]. Researchers have used behavioral, neurochemical, and electrophysiological approaches to explore the pathophysiology of depression, but the mechanisms of pathophysiology are still unclear.

Most recently, resting-state fMRI (RFMRI) has been widely used to study the functional brain abnormalities of MDD, given the highly synchronous nature of spontaneous low-frequency oscillations (0.01–0.08 Hz) in motor cortices [3]. Of the many RFMRI approaches, regional homogeneity (ReHo) has attracted substantial attention in research studies. ReHo employs Kendall's coefficient of concordance (KCC) to measure the functional coherence of a given voxel with its nearest voxels in a voxelwise analysis; it assumes that the spontaneous neural activity of a given voxel is similar to its neighbors [4–6]. ReHo reflects the temporal homogeneity of the regional blood oxygen level dependent (BOLD) signal. Thus, an abnormal ReHo may be related to changes in temporal spontaneous neural activity of a certain region [4].

Various studies explored spontaneous brain activity in MDD with the volume-based ReHo approach. The MDD group included medicated and unmedicated patients and showed decreased ReHo mainly in the frontal and limbic lobes and the basal ganglia [7]. Given that the MDD group included some medicated patients, the results could not

exclude a potential medication effect. Two other studies explored the ReHo in treatment-resistant depression (TRD) patients and found that TRD patients showed lower ReHo in the left insula, the superior temporal gyrus, the inferior frontal gyrus, the posterior fusiform gyrus, the superior parietal lobule, and the precuneus [8, 9]. In these two studies, all of the patients were medicated and treatment-resistant; thus, the medication may have contributed to the results. Our previous study investigated the ReHo in 15 first-episode, drug-naïve MDD patients, 15 first-degree relatives, and 15 healthy controls; the results revealed that both MDD patients and the first-degree relatives showed decreased ReHo in the right insula and the left cerebellum [10]. Two other studies investigated first-episode and drug-naïve MDD patients and reported decreased ReHo in the left thalamus, the left temporal lobe, the left cerebellar posterior lobe, and the bilateral occipital lobe [11] and increased ReHo in the fusiform gyrus and the bilateral superior frontal gyrus in comparison with healthy controls [12].

These previous ReHo studies on MDD are based on the 3-dimensional volume-based calculation. Although volume-based activation maps have been used widely to date, this approach neglected the intersubject variability in cortical folding patterns. Therefore, some anatomical regions could not accurately match the same location in the standard template. While under the cortical surface space, the anatomical regions could occupy the same place, reduce the intersubject variability, and increase statistical power [13–15]. Recently, a volume-based ReHo computation was transplanted into a 2-dimensional variant with cortical surface-based fMRI analysis; the surface-based ReHo was found to have moderate to high intersession and intrasession test-retest reliability [16].

In the present study, using this relatively new surface-based ReHo approach, we aimed to explore whether the surface-based ReHo could be an effective biomarker of MDD. We recruited first-episode and drug-naïve patients to exclude a potential medication effect. Moreover, we also aimed to investigate the relationships between the ReHo and the clinical variables in the MDD group.

2. Methods

2.1. Participants. Thirty-two patients with MDD from 17 to 60 years of age were recruited from the inpatient and outpatient units in the Department of Psychiatry, First Hospital of Shanxi Medical University. All of the patients were diagnosed with a Chinese version of the Modified Structured Clinical Interview for DSM-IV for patient version (SCID-I/P) [17] by two trained clinical psychiatrists. All MDD patients were drug-naïve and in their first episode of illness (the first time they experienced a depressive episode). These patients had no history of other major psychiatric illness, neurological illness, head injury, and alcohol or drug abuse. MDD patients were rated with a 17-item Hamilton Rating Scale for Depression (HRSD) before the imaging scan.

Thirty-three age-, gender-, and education-matched healthy controls were recruited by advertisements. They were interviewed with the Structured Clinical Interview for DSM-IV for nonpatient version (SCID-I/NP). All healthy controls were free of depression or other psychiatric or neurological illness and had no history of head injury and alcohol or drug abuse.

All MDD patients and healthy controls were right-handed. Written informed consent was obtained from each participant. The Medical Research Ethics Committee of the First Hospital of Shanxi Medical University approved this study.

2.2. Data Acquisition. Participants were scanned by the 3.0T Siemens Trio scanner. During the scanning, participants laid supine in the scanner with their heads fixed with foam pads to decrease head motion and reduce scanner noise. They were informed to close their eyes and remain awake while moving as little as possible. The scanning sessions included the following: (i) three-dimensional T1-weighted whole-brain images: 3D-MPRAGE sequence, TR/TE = 2300/2.95 ms, 160 slices, thickness/gap = 1.2/0.6 mm, FOV = 226 × 240 mm, matrix = 240 × 256, and flip angle = 9° and (ii) the resting-state fMRI image: echo planar imaging (EPI) pulse sequence, 32 slices, TR/TE = 2000/30 ms, thickness/gap = 3/1 mm, matrix = 64 × 64, FOV = 240 × 240 mm, flip angle = 90°, and 212 volumes.

2.3. Data Preprocessing. The Connectome Computation System (CCS: http://lfcd.psych.ac.cn/ccs.html) carries all steps of preprocessing both the structural and functional image preprocessing [16]. The structural image processing included the following steps: (1) the MR image denoise with a spatially adaptive nonlocal means filter [18, 19], (2) reconstruction of cortical surface, (3) segmentation of the cerebrospinal fluid (CSF), white matter (WM), and gray matter (GM) volumetric structures, (4) estimation of a triangular mesh tessellation over the GM-WM boundary and the mesh deformation to produce a smooth representation of the GM-WM interface (white surface) and the GM-CSF interface (pial surface) spatial normalization from individual native space to *fsaverage* stereotaxic space, (5) correction of topological defect on the surface, (6) inflation of individual surface mesh into a sphere, and (7) estimation of the deformation between the resulting spherical mesh and a common spherical coordinate system. The functional image preprocessing included (1) drop of the first five volumes, (2) slice timing correction, (3) 3D motion correction, (4) 4D global mean-based intensity normalization (mean intensity: 10,000), (5) nuisance regression (the WM and CSF mean time series and the Friston-24 motion time series) [20], (6) band-pass filtering (0.01–0.1 Hz), (7) removal of linear and quadratic trends, (8) coregistration between individual structural and functional images by the GM-WM boundary-based registration (BBR) algorithm [21], and (9) projection of the individual preprocessed 4D RFMRI time series onto a standard cortical surface *fsaverage5*.

Following the preprocessing, a data quality control procedure (QCP) was conducted. The QCP of structural images included visual head motion inspection, tissue segmentation, and pial and white surface reconstruction.

The QCP of functional images included steps of checking of the minimal cost of coregistration (mcBBR) and the root mean square of framewise displacement (rmsFD) http://lfcd.psych.ac.cn/ccs/QC.html.

2.4. Surface-Based ReHo Analysis. Surface-based ReHo analysis was performed with the CCS. Details of the analysis can be found in our recent study [16]. The individual preprocessed R-FMRI data was projected into the *fsaverage5* (FREESURFER 5.1) surface space. For each vertex of the surface space, the corresponding coordinates were computed in anatomical and functional space, and then the trilinear interpolation was used to interpolate the fMRI values [16]. Surface-based ReHo was calculated by Kendall's coefficient of concordance of the time series of a given vertex with those of its nearest neighbors. This computational procedure was repeated for all vertices in surfaces of both hemispheres to produce vertexwise KCC-ReHo surface maps, which are denoted 2-dimensional ReHo (2dReHo). When 7 nearest neighbors were used to explore the 2dReHo, we call it 2dReHo. Moreover, we also used a broader range of 19 neighbors to calculate 2dReHo and named it 2dReHo2. The individual 2dReHo maps were smoothed with a Gaussian kernel of 6 mm full-width half-maximum for subsequent statistical analyses.

2.5. Statistical Analysis. Unpaired two-sample t-tests were performed to compare age and years of education. A chi-square test was used to compare the gender ratio between the two groups. Voxelwise one-way ANCOVA tests (covariates: age, sex, years of education, mcBBR, and rmsFD) were performed to explore the 2dReHo differences between the MDD and healthy controls. The Pearson correlation coefficients between each vertex on the surface and demographic and clinical variables were calculated. We employed a cluster-level familywise error (FWE) correction for multiple comparisons [22]. Specifically, given a vertexwise statistical parameter map, a vertexwise P value (i.e., uncorrected $P < 0.01$) was first assigned to form clusters across the entire hemisphere. Based upon the distribution of spatial extents of the survived clusters, an implicit cluster size or extent was generated to achieve the final corrected P value (here, $P < 0.05$) for controlling the FWE.

3. Results

3.1. Participants. Participants' characteristics are shown in Table 1. The two groups were matched by age, gender ratio, and years of education. Moreover, age at illness onset, illness duration, and HRSD score of MDD patients are also included in Table 1.

3.2. Surface-Based ReHo Differences between MDD and Healthy Controls. Across the cortical surface, no significant differences were found between the MDD patients and healthy controls for the global mean ReHo or ReHo2 (Table 1). Moreover, MDD patients had a significant decrease in ReHo and ReHo2 in the left insula when compared with healthy controls (Figure 1). There was no increase in ReHo or ReHo2 in MDD patients.

3.3. Correlation Analysis. For MDD group, there were no significant correlations between age/years of education with left insula ReHo values (age: $P = 0.26$ and $P = 0.26$ for ReHo and ReHo2; years of education: $P = 0.81$ and $P = 0.68$ for ReHo and ReHo2, resp.). Moreover, no significant correlations were found between the left insula ReHo values and the patients' age at illness onset ($P = 0.24$ and $P = 0.25$), illness duration ($P = 0.90$ and $P = 0.99$), or the HRSD total score ($P = 0.41$ and $P = 0.43$).

We also calculated the correlations between global ReHo values and the age and years of education. For MDD group, no significant correlations were found between age/yeas of education and global ReHo values (age: $P = 0.36$ and $P = 0.44$ for ReHo and ReHo2; years of education: $P = 0.43$ and $P = 0.40$ for ReHo and ReHo2). For healthy control group, there were also no significant correlations between age/years of education and global ReHo values (age: $P = 0.25$, $P = 0.29$ for ReHo and ReHo2; years of education: $P = 0.72$, $P = 0.72$ for ReHo and ReHo2).

4. Discussion

To the best of our knowledge, this is the first study of surface-based ReHo in MDD. The present results reveal that MDD patients show decreased surface-based ReHo in the left insula; no significant correlations were found between the surface-based ReHo value in the left insula and the clinical characteristics of MDD.

The present surface-based ReHo results are more concise and partly supported by previous volume-based ReHo studies in MDD [8, 10]. Our previous volume-based ReHo study found that first-episode, drug-naïve MDD patients had decreased volume-based ReHo in the right insula cortex [10]. Different approaches may be the main reason for the differences across studies. Moreover, the participants and the scanning parameters were also different. The present results are supported by a recent meta-analysis of resting-state brain activity in MDD [23]. This meta-analysis included resting-state fMRI studies analyzed by volume-based ReHo and independent component analysis, as well as several PET studies of MDD; the results revealed that MDD patients had lower brain activity in left insula in comparison with healthy controls [23].

Located among the frontal, temporal, and parietal lobe and limbic regions, insula cortex is considered as an integration center of external events and internal cognitive processing [24, 25] and plays important role in various emotional and cognitive functions [26]. Compared with healthy controls, MDD patients had decreased activation in the left insula in a series of emotion-related tasks [27–29]. Recent RFMRI studies also reported decreased functional connectivity between the left insula and the bilateral amygdala [30] and the insula cortex and the subgenual anterior cingulate cortex [31] in MDD patients. Another RFMRI study further revealed that nonrefractory depression

Table 1: Participants information.

	MDD (N = 33)	Health control (N = 32)	P
Age (years)	34.18 (10.96)	34.56 (9.92)	0.88[a]
Gender (male/female)	13/20	13/19	0.92[b]
Yeas of education	13.18 (3.09)	13.72 (2.93)	0.48[a]
Illness onset age	33.91 (10.92)		
Illness duration (month)	6.02 (6.25)		
HRSD	20.16 (3.22)		
mcBBR	0.59	0.60	0.82[a]
rmsFD (mm)[c]	0.14	0.14	0.55[a]
Global ReHo	0.67	0.66	0.51[a]
Global ReHo2	0.52	0.52	0.63[a]

MDD: major depressive disorder; HRSD: Hamilton Rating Scale for Depression. The values in brackets are standard deviations.
[a]Obtained by two-sample t-test. [b]Obtained by chi-square test; [c]rmsFD is the root mean square of the framewise displacement for in-scanner head motion.

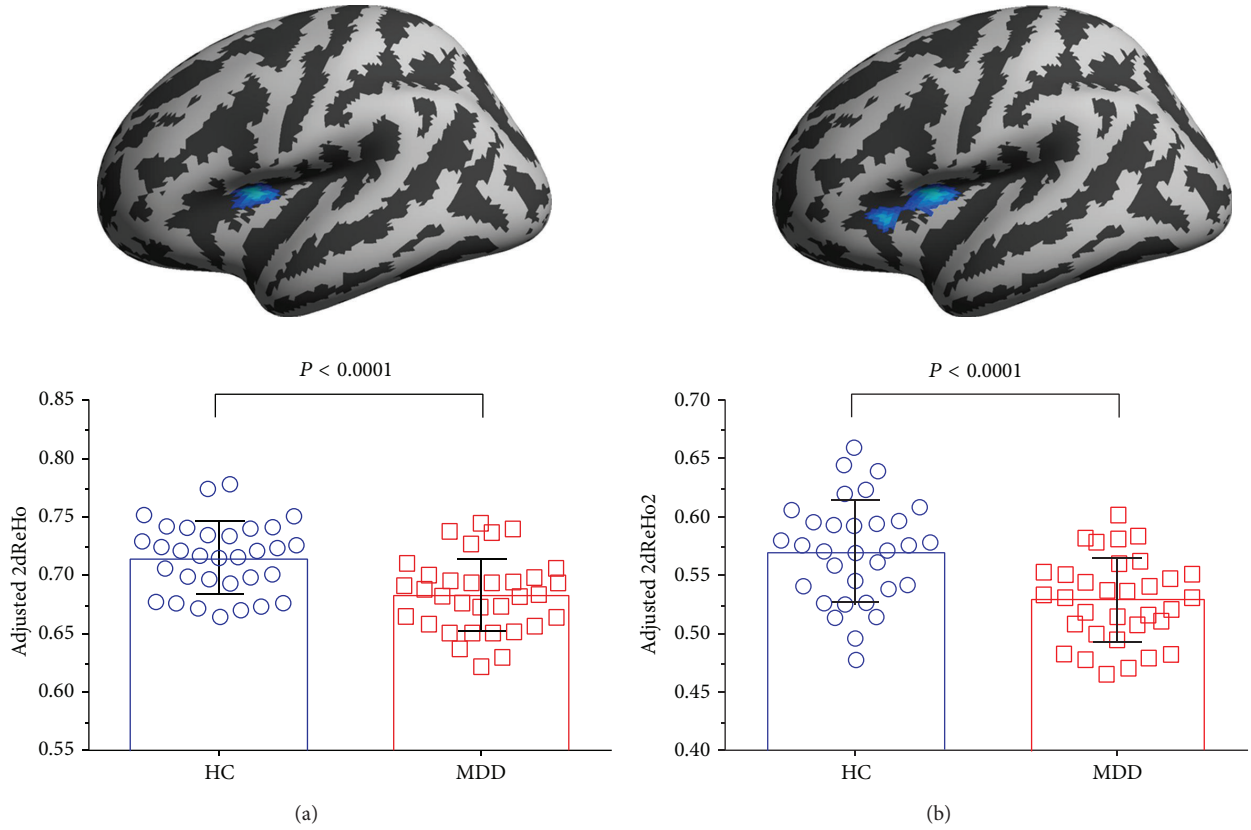

Figure 1: MDD patients showed lower vertexwise functional homogeneity in left insula ((a) 2dReHo and (b) 2dReHo2) compared to healthy controls.

was associated with decreased functional connectivity in the limbic-striatal-pallidal-thalamic circuits, of which the insula is an important part [32]. A recent meta-analysis focusing on cortical-subcortical interactions in emotion demonstrated that the insula is activated across all basic and social emotions [33]. Two other reviews also highlighted the insula as an important region involved in emotional processing and the affective symptoms in MDD [34, 35]. Following a systematic review of the role of the insula cortex in MDD, researchers proposed that, due to the neuroanatomical connections, the insula might also be part of the frontolimbic network [36]; this network plays a very important role in emotion regulation. The decreased activity in the insula cortex of MDD may lead to somatic complaints, emotional dysfunctions, and the negative bias in explaining life events [31]. The abnormal activity of the corticolimbic network leads to the disruptions of top-down processing, which is thought to mediate pervasive emotions of sadness and negative affect in MDD patients.

Recent neuroanatomical and neurochemical studies reveal that the insula cortex plays an important role in the pathophysiology of MDD. MDD patients show significantly

reduced volume [37] and cortical thickness [38] in the insula cortex. A voxel-based morphometry meta-analysis supports evidence that the clinical high-risk populations for psychosis show reduced gray matter in the left insula [39]. MDD patients also show lower fractional anisotropy in the left insula compared to healthy controls [40]. Several positron emission tomography (PET) studies found that MDD patients showed increased 5-HTT binding potential [41], decreased binding of the metabotropic glutamate receptor [42], and lower rCBF levels [43] in the insula cortex compared to healthy controls.

The correlation analysis shows that the surface-based ReHo value in the left insula cortex was not significantly correlated with the clinical variables and the depressive symptoms. Of the previous volume-based ReHo studies in MDD, only one study reported correlations between the ReHo value in the right insula and the severity of anxiety [7]; several other studies did not find significant correlations between the ReHo values and the clinical variables, as well as the HRSD score in first-episode and drug-naïve MDD [10], early-onset and late-onset drug-naïve MDD [12], TRD [8], and late-life depression [44]. The structural imaging studies also provided inconsistent results. No significant correlations were found between insula volume and the severity of depressive symptoms [37], while significant correlations were reported between the insula cortex and the Beck Depression Inventory, the Hamilton Depression Rating Scale, and the Snaith-Hamilton Pleasure Scale in MDD patients [45]. Together with these correlation results, the correlations between the ReHo values in the potential biomarker regions and the depressive symptoms still require further exploration.

Although the present study focused on the surface-based ReHo, we also analyzed the volume-based ReHo in the same cohort of participants. With the same covariates (age, sex, years of education, mcBBR, and rmsFD) and the same statistical criteria (corrected, $Z = 2.3$, $P < 0.05$), we found no significant clusters between MDD and healthy controls with volume-based ReHo approach. Some technical and methodological reasons may result in the differences between surface- and volume-based ReHo approaches. Firstly, the volume-based ReHo measures local signal synchronization in both gray and white matter, while the surface-based ReHo measures mostly the gray matter local synchronization signals. Therefore, the volume-based ReHo may include some artificial signals from white matter. Secondly, for 2dReHo and 3dReHo, although we try to keep the same length of neighbors for a certain vertices or voxel, the number of neighbors is different; the 2dReHo1 and 2dReHo2 calculation recruits 6 and 19 neighbors, respectively, while the 3dReHo recruits 26 neighbors. Moreover, the mask templates are different (MNI 152 3 mm standard volume for 3dReHo, while *fsaverage5* 4 mm resolution standard space for 2dReHo). These factors may influence the results in some degree. Thirdly, on the cortical surface, the intersubject variability in anatomy and the intersubject registration in both brain structure and function may be estimated more accurately [16]. Finally, previous volume-based neuroimaging studies consider that some subcortical regions (amygdala and thalamus) play important role in emotional circuit [46, 47]; however, the present surface-based ReHo only investigates the cortical regions; therefore it cannot reveal the differences in subcortical regions between healthy controls and MDD.

Although the present surface-based ReHo revealed interesting results, this study also had several limitations. First, previous findings suppose that MDD patients show deficits in the prefrontal-amygdala-pallidostriatal-mediothalamic mood regulating circuit [46, 47]. Given that the present surface-based ReHo approach focuses only on the cortical cortex, we did not examine the surface-based ReHo in the subcortical cortex, which are important regions of the mood regulating circuit. Second, the present study did not include neuropsychological tasks, specifically, the emotion processing related tasks. Including these tasks may help to determine whether the first-episode, drug-naïve MDD patients show deficits in the corresponding behavioral levels.

In conclusion, the present study revealed decreased surface-based ReHo in the left insula in MDD patients. The abnormal activity in the left insula may lead to the abnormal top-down cortical-limbic regulation of the emotional and cognitive based information. Moreover, no significant correlations were found between the surface-based ReHo value in the left insula and the age, years of education, age of illness onset, illness duration, and HRSD score in MDD patients.

Conflict of Interests

The authors declare that there is no conflict of interests regarding the publication of this paper.

Acknowledgments

This work was supported by the Natural Science Foundation of China (31000465, 81171409, 81000583, 30971054, and 81171290) and the Hundred Talents Program and the Key Research Program (KSZD-EW-TZ-002, XNZ) of Chinese Academy of Sciences.

References

[1] American Psychiatric Association, *Diagnostic and Statistical Manual of Mental Disorders*, American Psychiatric Press, Washington, DC, USA, 4th edition, 2000.

[2] G. J. Siegle, S. R. Steinhauer, M. E. Thase, V. A. Stenger, and C. S. Carter, "Can't shake that feeling: event-related fMRI assessment of sustained amygdala activity in response to emotional information in depressed individuals," *Biological Psychiatry*, vol. 51, no. 9, pp. 693–707, 2002.

[3] B. Biswal, F. Z. Yetkin, V. M. Haughton, and J. S. Hyde, "Functional connectivity in the motor cortex of resting human brain using echo-planar MRI," *Magnetic Resonance in Medicine*, vol. 34, no. 4, pp. 537–541, 1995.

[4] Y. Zang, T. Jiang, Y. Lu, Y. He, and L. Tian, "Regional homogeneity approach to fMRI data analysis," *NeuroImage*, vol. 22, no. 1, pp. 394–400, 2004.

[5] Y. Liu, K. Wang, C. YU et al., "Regional homogeneity, functional connectivity and imaging markers of Alzheimer's disease: a review of resting-state fMRI studies," *Neuropsychologia*, vol. 46, no. 6, pp. 1648–1656, 2008.

[6] D. K. Shukla, B. Keehn, and R. A. Müller, "Regional homogeneity of fMRI time series in autism spectrum disorders," *Neuroscience Letters*, vol. 476, no. 1, pp. 46–51, 2010.

[7] Z. Yao, L. Wang, Q. Lu, H. Liu, and G. Teng, "Regional homogeneity in depression and its relationship with separate depressive symptom clusters: a resting-state fMRI study," *Journal of Affective Disorders*, vol. 115, no. 3, pp. 430–438, 2009.

[8] W. B. Guo, X. L. Sun, L. Liu et al., "Disrupted regional homogeneity in treatment-resistant depression: a resting-state fMRI study," *Progress in Neuro-Psychopharmacology and Biological Psychiatry*, vol. 35, no. 5, pp. 1297–1302, 2011.

[9] Q. Z. Wu, D. M. Li, W. H. Kuang et al., "Abnormal regional spontaneous neural activity in treatment-refractory depression revealed by resting-state fMRI," *Human Brain Mapping*, vol. 32, no. 8, pp. 1290–1299, 2011.

[10] Z. Liu, C. Xu, Y. Xu et al., "Decreased regional homogeneity in insula and cerebellum: a resting-state fMRI study in patients with major depression and subjects at high risk for major depression," *Psychiatry Research*, vol. 182, no. 3, pp. 211–215, 2010.

[11] D. H. Peng, K. D. Jiang, Y. R. Fang et al., "Decreased regional homogeneity in major depression as revealed by resting-state functional magnetic resonance imaging," *Chinese Medical Journal*, vol. 124, no. 3, pp. 369–373, 2011.

[12] J. D. Chen, F. Liu, G. L. Xun et al., "Early and late onset, first-episode, treatment-naive depression: same clinical symptoms, different regional neural activities," *Journal of Affective Disorders*, vol. 143, no. 1–3, pp. 56–63, 2012.

[13] B. D. Argall, Z. S. Saad, and M. S. Beauchamp, "Simplified intersubject averaging on the cortical surface using SUMA," *Human Brain Mapping*, vol. 27, no. 1, pp. 14–27, 2006.

[14] B. Fischl, M. I. Sereno, R. B. Tootell, and A. M. Dale, "High-resolution intersubject averaging and a coordinate system for the cortical surface," *Human Brain Mapping*, vol. 8, no. 4, pp. 272–284, 1999.

[15] B. Fischl, N. Rajendran, E. Busa et al., "Cortical folding patterns and predicting cytoarchitecture," *Cerebral Cortex*, vol. 18, no. 8, pp. 1973–1980, 2008.

[16] X. N. Zuo, T. Xu, L. Jiang et al., "Toward reliable characterization of functional homogeneity in the human brain: preprocessing, scan duration, imaging resolution and computational space," *Neuroimage*, vol. 65, pp. 374–386, 2013.

[17] M. B. First, R. L. Spitzer, and M. Gibbon, *Structured Clinical Interview for DSM-IV Axis 1 Disorder*, Biometrics Research Department, New York State Psychiatric Institute, New York, NY, USA, 1995.

[18] X. X. Xing, Y. L. Zhou, J. S. Adelstein, and X. N. Zuo, "PDE-based spatial smoothing: a practical demonstration of impacts on MRI brain extraction, tissue segmentation and registration," *Magnetic Resonance Imaging*, vol. 29, no. 5, pp. 731–738, 2011.

[19] X. N. Zuo and X. X. Xing, "Effects of non-local diffusion on structural MRI preprocessing and default network mapping: statistical comparisons with isotropic/anisotropic diffusion," *PLoS ONE*, vol. 6, no. 10, Article ID e26703, 2011.

[20] C. G. Yan, R. C. Craddock, X. N. Zuo, Y. F. Zang, and M. P. Milham, "Standardizing the intrinsic brain: towards robust measurement of inter-individual variation in 1000 functional connectomes," *Neuroimage*, vol. 80, pp. 246–262, 2013.

[21] D. N. Greve and B. Fischl, "Accurate and robust brain image alignment using boundary-based registration," *NeuroImage*, vol. 48, no. 1, pp. 63–72, 2009.

[22] J. L. Bernal-Rusiel, M. Atienza, and J. L. Cantero, "Determining the optimal level of smoothing in cortical thickness analysis: a hierarchical approach based on sequential statistical thresholding," *NeuroImage*, vol. 52, no. 1, pp. 158–171, 2010.

[23] S. Kuhn and J. Gallinat, "Resting-state brain activity in schizophrenia and major depression: a quantitative meta-analysis," *Schizophrenia Bulletin*, vol. 39, no. 2, pp. 358–365, 2013.

[24] M. M. Mesulam and E. J. Mufson, "Insula of the old world monkey. I. Architectonics in the insulo-orbito-temporal component of the paralimbic brain," *Journal of Comparative Neurology*, vol. 212, no. 1, pp. 1–22, 1982.

[25] E. J. Mufson and M. M. Mesulam, "Insula of the old world monkey. II. Afferent cortical input and comments on the claustrum," *Journal of Comparative Neurology*, vol. 212, no. 1, pp. 23–37, 1982.

[26] J. R. Augustine, "Circuitry and functional aspects of the insular lobe in primates including humans," *Brain Research Reviews*, vol. 22, no. 3, pp. 229–244, 1996.

[27] B. T. Lee, C. Seong Whi, K. Hyung Soo et al., "The neural substrates of affective processing toward positive and negative affective pictures in patients with major depressive disorder," *Progress in Neuro-Psychopharmacology and Biological Psychiatry*, vol. 31, no. 7, pp. 1487–1492, 2007.

[28] J. D. Townsend, N. K. Eberhart, S. Y. Bookheimer et al., "FMRI activation in the amygdala and the orbitofrontal cortex in unmedicated subjects with major depressive disorder," *Psychiatry Research*, vol. 183, no. 3, pp. 209–217, 2010.

[29] M. W. Schlund, G. Verduzco, M. F. Cataldo, and R. Hoehn-Saric, "Generalized anxiety modulates frontal and limbic activation in major depression," *Behavioral and Brain Functions*, vol. 8, article 8, 2012.

[30] I. M. Veer, C. F. Beckmann, M. J. van Tol et al., "Whole brain resting-state analysis reveals decreased functional connectivity in major depression," *Frontiers in Systems Neuroscience*, vol. 4, article 41, 2010.

[31] K. R. Cullen, D. G. Gee, B. Klimes-Dougan et al., "A preliminary study of functional connectivity in comorbid adolescent depression," *Neuroscience Letters*, vol. 460, no. 3, pp. 227–231, 2009.

[32] S. Lui, Q. Wu, L. Qiu et al., "Resting-state functional connectivity in treatment-resistant depression," *The American Journal of Psychiatry*, vol. 168, no. 6, pp. 642–648, 2011.

[33] H. Kober, L. F. Barrett, J. Joseph, E. Bliss-Moreau, K. Lindquist, and T. D. Wager, "Functional grouping and cortical-subcortical interactions in emotion: a meta-analysis of neuroimaging studies," *NeuroImage*, vol. 42, no. 2, pp. 998–1031, 2008.

[34] A. Stuhrmann, T. Suslow, and U. Dannlowski, "Facial emotion processing in major depression: a systematic review of neuroimaging findings," *Biology of Mood & Anxiety Disorders*, vol. 1, no. 1, article 10, 2011.

[35] P. B. Fitzgerald, A. R. Laird, J. Maller, and Z. J. Daskalakis, "A meta-analytic study of changes in brain activation in depression," *Human Brain Mapping*, vol. 29, no. 6, pp. 683–695, 2008.

[36] D. Sliz and S. Hayley, "Major depressive disorder and alterations in insular cortical activity: a review of current functional magnetic imaging research," *Frontiers in Human Neuroscience*, vol. 6, article 323, 2012.

[37] T. Takahashi, M. Yücel, V. Lorenzetti et al., "Volumetric MRI study of the insular cortex in individuals with current and past major depression," *Journal of Affective Disorders*, vol. 121, no. 3, pp. 231–238, 2010.

[38] H. Järnum, S. F. Eskildsen, E. G. Steffensen et al., "Longitudinal MRI study of cortical thickness, perfusion, and metabolite levels in major depressive disorder," *Acta Psychiatrica Scandinavica*, vol. 124, no. 6, pp. 435–446, 2011.

[39] P. Fusar-Poli, S. Borgwardt, A. Crescini et al., "Neuroanatomy of vulnerability to psychosis: a voxel-based meta-analysis," *Neuroscience and Biobehavioral Reviews*, vol. 35, no. 5, pp. 1175–1185, 2011.

[40] X. Liu, Y. Wang, H. Liu, Z. Liu, and W. Zhou, "Diffusion tensor imaging and resting state functional magnetic resonance imaging on young patients with major depressive disorder," *Journal of Central South University*, vol. 35, no. 1, pp. 25–31, 2010.

[41] D. M. Cannon, M. Ichise, D. Rollis et al., "Elevated serotonin transporter binding in major depressive disorder assessed using positron emission tomography and [11C]DASB, comparison with bipolar disorder," *Biological Psychiatry*, vol. 62, no. 8, pp. 870–877, 2007.

[42] A. Deschwanden, B. Karolewicz, A. M. Feyissa et al., "Reduced metabotropic glutamate receptor 5 density in major depression determined by [11C]ABP688 PET and postmortem study," *The American Journal of Psychiatry*, vol. 168, no. 7, pp. 727–734, 2011.

[43] H. Hanada, J. Imanaga, A. Yoshiiwa et al., "The value of ethyl cysteinate dimer single photon emission computed tomography in predicting antidepressant treatment response in patients with major depression," *International Journal of Geriatric Psychiatry*, vol. 28, no. 7, pp. 756–765, 2013.

[44] F. Liu, M. Hu, S. Wang et al., "Abnormal regional spontaneous neural activity in first-episode, treatment-naive patients with late-life depression: a resting-state fMRI study," *Progress in Neuro-Psychopharmacology & Biological Psychiatry*, vol. 39, no. 2, pp. 326–331, 2012.

[45] R. Sprengelmeyer, J. D. Steele, B. Mwangi et al., "The insular cortex and the neuroanatomy of major depression," *Journal of Affective Disorders*, vol. 133, no. 1-2, pp. 120–127, 2011.

[46] W. C. Drevets, "Functional neuroimaging studies of depression: the anatomy of melancholia," *Annual Review of Medicine*, vol. 49, pp. 341–361, 1998.

[47] H. S. Mayberg, "Limbic-cortical dysregulation: a proposed model of depression," *Journal of Neuropsychiatry and Clinical Neurosciences*, vol. 9, no. 3, pp. 471–481, 1997.

Hindawi Publishing Corporation
BioMed Research International
Volume 2014, Article ID 706157, 9 pages
http://dx.doi.org/10.1155/2014/706157

Research Article

Neuroanatomical Classification in a Population-Based Sample of Psychotic Major Depression and Bipolar I Disorder with 1 Year of Diagnostic Stability

Mauricio H. Serpa,[1,2] Yangming Ou,[3] Maristela S. Schaufelberger,[1,2] Jimit Doshi,[3] Luiz K. Ferreira,[1,2] Rodrigo Machado-Vieira,[2,4] Paulo R. Menezes,[5] Marcia Scazufca,[6] Christos Davatzikos,[3] Geraldo F. Busatto,[1,2] and Marcus V. Zanetti[1,2,4]

[1] *Laboratory of Psychiatric Neuroimaging (LIM-21), Department and Institute of Psychiatry, Faculty of Medicine, University of São Paulo, Dr. Ovídio Pires de Campos Street, 3rd Floor, LIM-21, Nuclear Medicine Center, 05403-010 São Paulo, SP, Brazil*
[2] *Center for Interdisciplinary Research on Applied Neurosciences (NAPNA), Nuclear Medicine Center, University of São Paulo, Dr. Ovídio Pires de Campos Street, 3rd Floor, LIM-21, Nuclear Medicine Center, 05403-010 São Paulo, SP, Brazil*
[3] *Section of Biomedical Image Analysis (SBIA), Department of Radiology, University of Pennsylvania, 3600 Market Street, Suite 380, Philadelphia, PA 19104, USA*
[4] *Laboratory of Neuroscience (LIM-27), Department and Institute of Psychiatry, Faculty of Medicine, University of São Paulo, Dr. Ovídio Pires de Campos Street, 3rd Floor, LIM-27, Institute of Psychiatry, 05403-010 São Paulo, SP, Brazil*
[5] *Department of Preventive Medicine, Faculty of Medicine, University of São Paulo, 455 Dr. Arnaldo Avenue, 01246-903 São Paulo, SP, Brazil*
[6] *Laboratory of Psychopharmacology and Clinical Psychophysiology (LIM-23), Department and Institute of Psychiatry, Faculty of Medicine, University of São Paulo, Dr. Ovídio Pires de Campos Street, Ground Floor, LIM-23, Institute of Psychiatry, 05403-010 São Paulo, SP, Brazil*

Correspondence should be addressed to Mauricio H. Serpa; mauricio.serpa@hc.fm.usp.br

Received 3 October 2013; Revised 10 December 2013; Accepted 10 December 2013; Published 19 January 2014

Academic Editor: John A. Sweeney

The presence of psychotic features in the course of a depressive disorder is known to increase the risk for bipolarity, but the early identification of such cases remains challenging in clinical practice. In the present study, we evaluated the diagnostic performance of a neuroanatomical pattern classification method in the discrimination between psychotic major depressive disorder (MDD), bipolar I disorder (BD-I), and healthy controls (HC) using a homogenous sample of patients at an early course of their illness. Twenty-three cases of first-episode psychotic mania (BD-I) and 19 individuals with a first episode of psychotic MDD whose diagnosis remained stable during 1 year of followup underwent 1.5 T MRI at baseline. A previously validated multivariate classifier based on support vector machine (SVM) was employed and measures of diagnostic performance were obtained for the discrimination between each diagnostic group and subsamples of age- and gender-matched controls recruited in the same neighborhood of the patients. Based on T1-weighted images only, the SVM-classifier afforded poor discrimination in all 3 pairwise comparisons: BD-I versus HC; MDD versus HC; and BD-I versus MDD. Thus, at the population level and using structural MRI only, we failed to achieve good discrimination between BD-I, psychotic MDD, and HC in this proof of concept study.

1. Introduction

Mood disorders share a large number of clinical and neurobiological features. The nonspecificity and variability of symptoms over time are frequent causes of misdiagnosis in patients with bipolar disorder (BD) [1, 2]. Although more frequent in BD, psychotic symptoms may be present in some patients with major depressive disorder (MDD) [3]. Nevertheless, epidemiological studies have shown that

patients presenting depressive episodes with psychotic features are at increased risk for developing BD [2, 4]. Thus, a medical tool that reliably differentiates patients with psychotic MDD from BD at an early stage of the illness would be highly useful to aid psychiatrists to improve diagnostic accuracy and, consequently, treatment response and prognosis in the clinical practice.

Neuroanatomical pattern classification is a relative new technique that holds promise in solving diagnosis and outcome issues in psychiatry [5]. This new method for brain image analysis allows voxelwise between-group comparisons and classification of scans at an individual basis [5, 6]. Given the multivariate nature of their statistical approach, and the possibility to employ both linear and nonlinear analysis models, these techniques afford improved sensitivity to uncover complex morphological brain differences in comparison to other voxelwise methods [7]. Moreover, once the pattern of abnormalities which better discriminates two groups is defined, this morphological signature can be used to classify images at an individual basis, and measures of diagnostic accuracy (DA) can be obtained [5, 6].

Up until now, a limited number of magnetic resonance imaging (MRI) studies have investigated the usefulness of pattern classification methods in the evaluation of affective disorders, producing variable results. Most studies implemented functional MRI (fMRI) to investigate neuroanatomical classifiers in groups of depressed patients and healthy controls (HC). Such studies have shown diagnostic accuracies (DA) as higher as 82% [8–12]. Regarding BD, investigations are still scarce. In a fMRI study, Costafreda et al. [13] applied a classifier based on support vector machine (SVM) in the discrimination between BD versus schizophrenia (SZ) versus HC and found that SZ were more correctly identified (AD = 92%) than BD (AD = 79%). Three fMRI studies investigated the use of pattern classification approaches to discriminate depressive BD and MDD [14–16]. Although two of those studies [15, 16] have shown good DA (up to 90% in Grotegerd et al. [15]), Mourão-Miranda et al. [14] have found no statistically significant DA to discriminate MDD from depressive BD.

Few studies have investigated the usefulness of pattern classification methods based on structural MRI in mood disorders, with inconsistent results. Liu et al. [17] found that MDD patients with and without resistance to pharmacological treatment could be discriminated from each other, as well as from HC, with fair accuracies as higher as 82%. In a sample of drug-naïve patients with MDD submitted to MRI scans before starting antidepressant treatment, Gong et al. [18] found that grey matter (GM) could discriminate patients from HC with suboptimal DA of 67% (refractory MDD) and 76% (nonrefractory MDD); white matter (WM) was statistically significant only for discriminating nonrefractory patients, with DA of up to 84%. Investigating whole-brain structural neuroanatomy as a diagnostic biomarker, Costafreda et al. [19] obtained a modest DA of 67.6% in the discrimination between MDD patients and HC using a SVM-based classifier. Qiu et al. [20] studied a group of drug-näive patients presenting a first-episode of MDD ($n = 32$) versus HC ($n = 32$) with a SVM classifier and different combinations of morphometric features. The authors reported overall modest classification accuracies ranging from 50% to 78% depending on the combination of features employed [20]. Only one morphometric MRI study has applied pattern classification techniques in BD, comparing two independent samples of patients with BD type I (BD-I) versus HC [21]. The authors found modest DA of up to 73% in the differentiation between BD-I patients versus HC when the classification was performed with the GM and 78% for the analysis based on the WM. However, the two samples were composed of chronic medicated patients, and such results should be interpreted with caution.

Differences in the pipelines for image processing, feature extraction/dimensionality reduction, and pattern recognition methods might at least partly account for the discrepancies observed across studies using pattern classification techniques in neuropsychiatric disorders [6]. Another potential factor associated to this variability of results is the widespread adoption of unsystematic single-diagnosis approach for the definition of the groups under study, which limits the validity of the categories that will be informed to the classifier [22]. An additional issue that might also contribute for the heterogeneity of findings is the occurrence of selection bias. In this regard, it is relevant to note that none of the investigations of affective disorders employing neuroanatomical pattern classification to date have employed population-based approaches. In population-based studies, epidemiological methods are used to identify and recruit representative samples of cases and demographically matched controls from the same, circumscribed geographical area. The use of such designs reduces selection biases by ensuring that control individuals truly represent the population from which the cases came from [23, 24].

To the best of our knowledge, no study to date has investigated the diagnostic performance of a neuroanatomical classifier in the discrimination of patients with a first-episode of mania from individuals presenting their first-episode of psychotic MDD. Moreover, most studies evaluating pattern classification methods in mood disorders to date have used fMRI, which has a of relatively complex implementation and is less available in the clinical practice when compared to 1.5 T structural MRI.

In this proof of concept morphometric MRI study, a sample of individuals with first-episode of psychotic mania (BD-I) and psychotic MDD and a group of demographically matched controls were recruited from the same defined geographical area using an epidemiologic approach. All subjects were followed up naturalistically over a 1-year period, with reinterviews carried out for diagnostic confirmation. A support-vector machine (SVM) classifier was employed to ascertain how distinguishable are BD-I with psychotic features and psychotic MDD at the time of first-presentation using the widely available T1-weighted MRI data. The SVM method applied here has been used in a number of previous investigations of neuropsychiatric disorders, showing consistent results [25–27].

2. Materials and Methods

2.1. Participants and Design. Patients fulfilling Diagnostic and Statistical Manual for Mental Disorders, 4th edition, (DSM-IV) [28] criteria for a first-episode of mania (BD-I) or a first-episode of psychotic unipolar depression (psychotic MDD) were selected from a large sample of first-episode psychosis individuals who took part in a population-based case-control study investigating the incidence of psychotic disorders in a circumscribed region of São Paulo city, as previously described [29, 30]. In the original epidemiological investigation, cases were identified by active surveillance of all people that made contact for the first time with the mental healthcare services for that region between 2002 and 2005 due to a DSM-IV defined psychotic disorder, regardless of its severity (both outpatients and inpatients were recruited), duration of illness, or compliance to treatment. Patients with psychotic disorders due to a general medical condition or substance-induced psychosis were excluded. The research team provided general guidance to patients but they were referenced to treatment at the health services located in the geographical region where they lived. Both patients and controls were reinterviewed after 1 year of followup for clinical assessment and diagnostic confirmation.

Other inclusion criteria for both cases and controls were (a) current age between 18 and 50 years; (b) residence for 6 months or more in defined geographic areas of São Paulo. The exclusion criteria consisted of (a) history of head injury with loss of consciousness; (b) presence of neurological disorders or any organic disorders that could affect the central nervous system; (c) moderate or severe mental retardation; and (d) contraindications for MRI scanning.

In the present investigation, we included the cases diagnosed as having a first-episode of psychotic mania or a first-episode of psychotic MDD according to the Structured Clinical Interview for DSM-IV (SCID) [31] at the time of initial evaluation and who have shown diagnostic stability (i.e., BD-I and MDD diagnoses) over the 1 year of followup. At baseline, 24 cases initially fulfilled criteria for BD-I with psychotic features (23 for first-episode of mania and 1 for psychotic bipolar depression), and 25 for first-episode of psychotic MDD. Over the follow-up period, from the 25 cases of psychotic MDD initially identified, 3 patients were reclassified as BD-I after presenting manic episodes, 2 as schizoaffective disorder, and 1 as delusional disorder. Thus, the final sample of affective disorders after the 1-year diagnostic reevaluation was formed by the following groups: 27 cases of BD-I (of whom 23 entered the study due to a first-episode of mania) and 19 individuals with psychotic MDD whose diagnosis remained stable over the 1-year follow-up period after the first-episode. Details about the other psychosis cases not included in the present investigation can be found elsewhere [30, 32].

In order to obtain a population-based sample of controls, next-door neighbors matched for age (within five years) and gender with the patients were initially screened to exclude the presence of psychotic symptoms using the Psychosis Screening Questionnaire [33] and interviewed with the SCID for the assessment of other psychiatric disorders. This approach resulted in an initial pool of 94 psychosis-free epidemiological controls eligible for the neuroimaging investigation [32].

Aiming at selecting homogeneous control samples to be used by the classifier against the patients, subsamples of HC (free of any Axis I disorder other than specific phobia, including lifetime substance misuse) matched for gender, age and handedness with psychotic BD-I and MDD subgroups were drawn from the total pool of controls. The matching was performed individually when possible, respecting the following hierarchical rank: gender, age, (within a 2-year range), and handedness. Moreover, as it has been shown that the larger the control sample, the higher the statistical power to detect between-group morphometric abnormalities in MRI studies [23, 34], we tried to select as many controls as possible for each comparison. Therefore, the following pairwise comparisons were carried out:

(i) first-episode psychotic mania (BD-I) ($n = 23$) versus matched HC ($n = 33$);

(ii) first-episode psychotic MDD ($n = 19$) versus matched HC ($n = 38$).

(iii) first-episode psychotic mania (BD-I) ($n = 23$) versus psychotic MDD ($n = 19$).

Local ethics committees approved the study, and all subjects provided informed written consent.

2.2. Clinical Assessment Scales. Both patients and controls were screened for substance use with the Alcohol Use Disorders Identification Test (AUDIT) [35] and the South Westminster Questionnaire [36]; when appropriate, diagnoses of substance use disorders was made using the SCID. A general medical history, including medication use, was obtained directly with each participant or with his/her relatives and also through reviewing of medical records.

All clinical assessment tools, including the SCID, were administered to the participants both at baseline and at the 1-year follow-up evaluation.

2.3. Neuroimaging Data Acquisition and Analysis. Imaging data were acquired using two identical MRI scanners (1.5 T GE Signa scanner, General Electric, Milwaukee, WI, USA). Exactly the same acquisition protocols were used (a T1-SPGR sequence providing 124 contiguous slices, voxel size = 0.86 × 0.86 × 1.5 mm, TE = 5.2 ms, TR = 21.7 ms, flip angle = 20, FOV = 22 cm, matrix = 256 × 192 pixels). For the three pairwise comparisons conducted here, the number of subjects (%) acquired using Scanner number 1 are 13 (56.5%) BD-I versus 24 (72.7%) matched HC ($\chi^2 = 1.59$, df = 1, $P = 0.208$); 10 (52.6%) psychotic MDD versus 25 (65.8%) matched HC ($\chi^2 = 0.92$, df = 1, $P = 0.336$); and 13 (56.5%) BD-I versus 10 (52.6%) psychotic MDD ($\chi^2 = 0.064$, df = 1, $P = 0.801$).

All images were visually inspected by an experienced radiologist with the purpose of identifying artifacts during image acquisition and the presence of silent gross brain

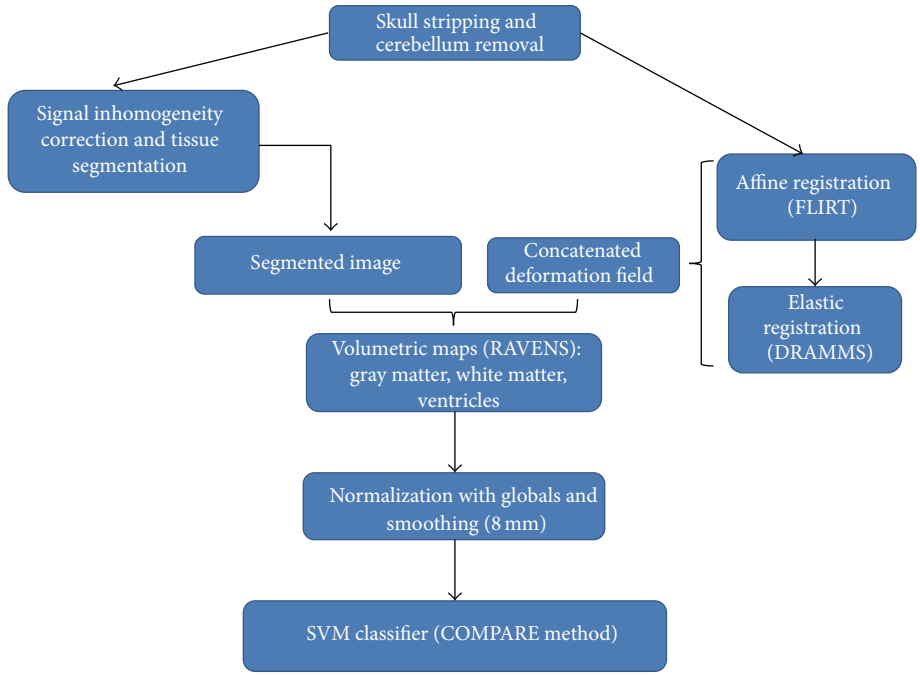

Figure 1: Routine employed for the processing and analysis of T1-weighted MRI images.

lesions. Five participants have been excluded from the original neuroimaging investigation on first-episode psychosis from which our sample was drawn due to motion artifacts [30].

The processing and analysis of the structural MRI dataset was performed using a routine previously described by our group [6]. Figure 1 summarizes the pipeline of image processing and analysis employed here.

Initially, the T1-weighted images were preprocessed as follows: skull-stripping; manual removal of the cerebellum in order to improve the tissue segmentation of the temporal lobe; and correction for signal inhomogeneities. The images were subsequently segmented into their 3 principal brain tissue compartments (GM, WM, and cerebrospinal fluid space) through an automated routine. Images were then spatially registered to a Montreal Neurological Institute (MNI) single-subject brain template through two steps (Figure 1). Firstly, an affine transformation was performed using the FLIRT (FMRIB's Linear Image Registration Tool) tool of the FSL (FMRIB Software Library, http://www.fmrib.ox.ac.uk/fsl/flirt) in order to align the major brain structures to the MNI template and also to correct for differences in head positioning. Secondly, a robust method for elastic registration called Deformable Registration via Attribute Matching and Mutual-Saliency weighting (DRAMMS) [37] was employed. The deformation field resulting from the spatial registration of each T1-weighted image to the MNI template was applied to the segmented images in order to generate mass-preserved volumetric maps, named Regional Analysis of Volumes Examined in Normalized Space (RAVENS) maps of the GM, WM, and cerebrospinal fluid compartments [38]. An automated algorithm was used to isolate the cerebral ventricles (lateral ventricles and third ventricle) from the remaining cerebrospinal fluid space, resulting in a ventricular RAVENS map. In the RAVENS maps, the tissue density reflects the amount of tissue present in each subject's image at a given location, after mapping to the standardized template space [38]. Thus, a region of decreased density indicates a reduced volume in this structure, for example. Lastly, the RAVENS maps (GM, WM, and ventricles) were corrected for the total brain volume (given by the sum of all voxels of brain tissue and cerebrospinal fluid space) and smoothed with 8 mm Gaussian kernels.

The GM, WM, and ventricular RAVENS maps were used as inputs for a previously described and validated SVM-based pattern classifier named Classification of Morphological Patterns Using Adaptive Regional Elements (COMPARE) [7] (https://www.rad.upenn.edu/sbia/software/index.html#compare). In this method, voxelwise correlations between RAVENS maps and group membership are used to identify voxels that are candidates to be useful for intergroup discrimination. To achieve the necessary dimensionality reduction, a watershed segmentation algorithm is then used to group voxels into regional clusters and to identify the most relevant features to classification (group discrimination) [7]. This approach also works as an initial feature selection step, reducing the initial dimensionality of the data from millions of variables to a relatively small set of regional volumetric measurements, which the subsequent classifier can handle successfully. In order to improve the spatial consistency of the watershed-derived regional volumetric elements and also to minimize the inclusion of voxels not relevant for the classification (which might reduce the discriminative power), the degree of agreement among all features in its spatial neighborhood is computed by an intraclass correlation coefficient, and a region-growing method based

on the Pearson correlation coefficient is employed [7]. Here, the voxel with the highest discriminative power in each watershed-derived region is first selected, and the neighboring voxels are included as long as their inclusion will not decrease the discriminative power of the regional feature. Finally, a feature-selection technique based on SVM criteria is used to select a subset of the top-ranked features that optimizes the performance of the classifier, constituting the "morphological signature" of each group under study which is used by the classifier [7]. The COMPARE classifier, then, employs a nonlinear SVM method to assign a class label to each image under study (individual classification of the MRI scans) through a Gaussian radial basis function kernel.

Although other theoretical frameworks for pattern recognition analyses are available [10, 21], SVM with sufficient dimensionality reduction is currently one of the most widely employed pattern classification models in the study of neuropsychiatric disorders [5, 6]. SVM is a powerful pattern classification method that works to find a line or "decision boundary" that better separates two groups [39]. This boundary may be depicted either by a hyperplane—in the case of linear classifiers—or by a more general hypersurface—when a nonlinear SVM is used—in the high-dimensional feature space where the vectors representing each brain under study are projected [39]. Differently from other hyperplane-based classifiers, however, the SVM focuses its analysis on those brains (or vectors) that are more closely located to or on the hypersurface separating the two groups, which are called the "support vectors," maximizing the distance between the nearest vectors of the two groups. Thus, a SVM classifier inherently focuses on subtle between-group morphological differences and not on gross differences that are easily identifiable [39].

For each of the two-group comparisons, the diagnostic performance of the COMPARE classifier was estimated using the leave-one-out crossvalidation (LOOCV) method. In each LOOCV experiment, one subject was first selected as a testing subject, and the remaining subjects were used for the entire adaptive regional feature extraction, feature selection, and training procedure. Then, the classification result on the testing subject using the trained SVM classifier was compared with the ground-truth class label, to evaluate the classification performance. By repeatedly leaving each subject out as a testing subject, we obtained the average classification rate from all of these LOOCV experiments [7].

After LOOCV, high-dimensional spatial maps of the brain regions that constitute the patterns of brain tissue distributions characteristics of the three SVMs were generated by COMPARE as previously described and validated [7]. This spatial feature map shows how frequently a particular region/feature was selected during all the LOOCV tests, displaying regional brain volume changes as one follows the path of the abnormality score from positive (patient-like) to negative (control-like). A scale ranging from 0 to 1 is set for each region, reflecting the relative importance for between-group discriminations based on the LOOCV experiments [7]. It is important to notice, however, that the discriminative morphological pattern generated by the classifier reflects a set of brain regions needed for between-group classification, but not necessarily all areas of regional brain volume differences between the groups under study.

2.4. ROC Curve Analysis. The classification scores obtained by the COMPARE analyses were evaluated using a *receiver operating characteristic* (ROC) curve aiming to visualize the diagnostic performance of the classifier in each of the pairwise comparisons and to calculate the area under the curve (AUC).

Indices of diagnostic performance such as DA (overall classification rate), sensitivity, specificity, positive predictive value (PPV), and negative predictive value (NPV) were calculated using a 2×2 contingency table. In the ROC curves, the individual Z scores obtained by the SVM classifier were plotted in a graph according to the true positive rate (y-axis, corresponding to the sensitivity measure) versus false positive rate (x-axis, corresponding to 1-specificity) generated in the group classification [40]. This procedure allowed us to adjust the threshold used by the SVM classifier according to the desired sensitivity/specificity relationship. We will report herein the sensitivity and specificity values observed when the highest classification accuracy was achieved.

The AUC measure of a classifier is equivalent to the probability that the classifier will rank a randomly chosen (truly) positive diagnosis higher than a randomly chosen negative diagnosis [40]. Thus, the AUC provides an estimate of the discriminative power of the classifier for a given condition, regardless of both the chosen threshold (classifier's score which separates the 2 groups under study) and the sample size of each group.

3. Results

3.1. Demographic and Clinical Details. Demographic and clinical data for the psychotic BD-I and MDD groups, as well as for the two subsamples of matched controls are summarized in Table 1.

More patients with psychotic MDD were using antipsychotic and antidepressant agents at the day of MRI scanning relative to the BD-I group, whereas more individuals with BD-I were taking mood stabilizers. Also, 3 MDD patients were left-handed, whereas all BD-I individuals were right-handed (Table 1).

3.2. Diagnostic Performance of the Classifier. Table 2 shows the measures of diagnostic performance for the three pairwise comparisons: psychotic BD-I versus controls, psychotic MDD versus controls, and psychotic BD-I versus psychotic MDD. The ROC curves for each of these comparisons are depicted in Figures 2, 3, and 4 (resp.).

The SVM classifier attained poor discrimination in the pairwise comparisons between first-episode of psychotic mania versus controls (DA = 66.1%) (Table 2 and Figure 2), and first-episode of psychotic MDD versus controls (DA = 59.6%) (Table 2 and Figure 3). The direct comparison between the BD-I and MDD groups also resulted in a classification rate near to chance (DA = 54.76%) (Table 2 and Figure 4).

Table 1: Demographic and clinical information for patients with first-episode of psychotic mania (BD-I), psychotic major depression (MDD), and subsamples of matched healthy controls (HC).

	BD-I ($n = 23$)	HC 1 ($n = 33$)	MDD ($n = 19$)	HC 2 ($n = 38$)	Statistical tests (BD-I versus MDD)
Age (mean ± SD)	27.09 ± 8.87	27.55 ± 6.41	29.05 ± 8.34	29.66 ± 7.92	$t = 0.734$, df = 40, $P = 0.467$
Gender (number of males; %)	9 (39.1%)	13 (39.4%)	4 (21.1%)	8 (21.1%)	$\chi^2 = 1.59$, df = 1, $P = 0.207$
Handedness (number of right-handed; %)	23 (100%)	32 (97.0%)	16 (84.2%)	35 (92.1%)	**$\chi^2 = 3.91$, df = 1, $P = 0.048$**
Substance misuse[a]	7 (30.4%)	—	3 (15.8%)	—	
Duration of illness (days; mean ± sd)	184.5 ± 130.7	—	250.8 ± 205.7	—	Mann-Whitney test, $P = 0.441$
Duration of untreated psychosis (days; mean ± sd)	44.3 ± 57.2	—	43.0 ± 48.3	—	Mann-Whitney test, $P = 0.595$
Medication use at the MRI (n; %)					
Antipsychotics	10 (43.5%)	—	15 (78.9%)	—	**$\chi^2 = 5.43$, df = 1, $P = 0.020$**
Mood stabilizers[b]	12 (52.2%)	—	4 (21.1%)	—	**$\chi^2 = 4.27$, df = 1, $P = 0.039$**
Antidepressants	1 (4.3%)	—	10 (52.6%)	—	**$\chi^2 = 12.54$, df = 1, $P < 0.001$**

BD-I: bipolar I disorder (FE mania); MDD: major depressive disorder; HC 1: subsample of healthy controls selected for the comparison with BD-I patients; HC 2: subsample of healthy controls selected for the comparison with patients with psychotic MDD; MRI: magnetic resonance imaging.
[a]Number of patients with a positive diagnosis of DSM-IV substance use disorder (prevalence).
[b]Lithium, carbamazepine, and/or sodium valproate/divalproex.
We have set in bold the results that present statistical difference.

Table 2: Diagnostic performance of the SVM classifier in the individual discrimination of cases of BD-I and MDD with psychotic features versus controls.

Pairwise comparison	AUC[a]	Accuracy	Morphological features[b]	Sensitivity	Specificity	PPV	NPV
Psychotic BD-I ($n = 23$) × Matched controls ($n = 33$)	0.61	66.1%	99	39.1%	84.8%	64.3%	66.6%
Psychotic MDD ($n = 19$) × Matched controls ($n = 38$)	0.44	59.6%	80	31.6%	73.7%	37.5%	68.3%
Psychotic BD-I ($n = 23$) × Psychotic MDD ($n = 19$)	0.52	54.76%	53	57.9%	52.1%	50.0%	60.0%

BD-I: bipolar I disorder (first-episode mania); MDD: major depressive disorder; PPV: positive predictive value; NPV: negative predictive value.
[a]Area under the curve; [b]number of morphological features used for the best classification rate (accuracy).

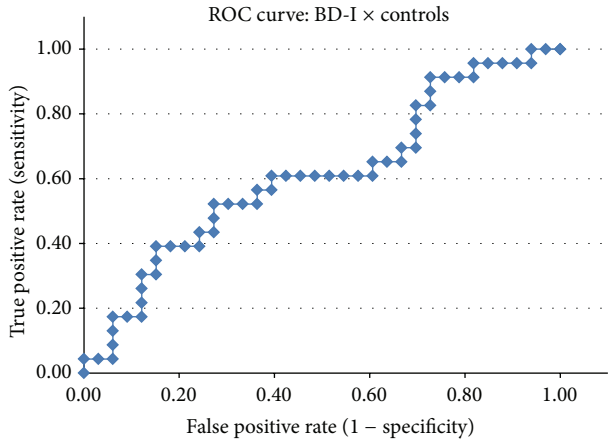

Figure 2: ROC curve for the comparison between bipolar I disorder (BD-I) individuals and healthy controls.

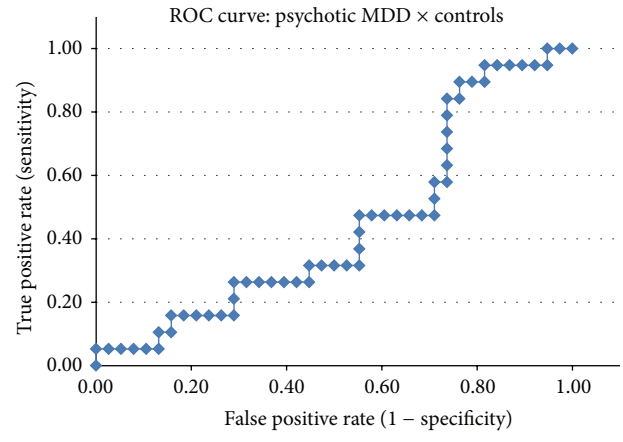

Figure 3: ROC curve for the comparison between patients with psychotic major depressive disorder (MDD) and healthy controls.

4. Discussion

To our knowledge, the present study is the first to apply a SVM classifier to conventional structural (T1-weighted) MRI data of first-episode patients with BD-I and psychotic MDD using an epidemiologic approach to recruit both patients and controls.

In regard to the individual classification of patients with BD-I (first-episode of psychotic mania) and psychotic MDD, the negative results obtained suggest that neuroanatomical

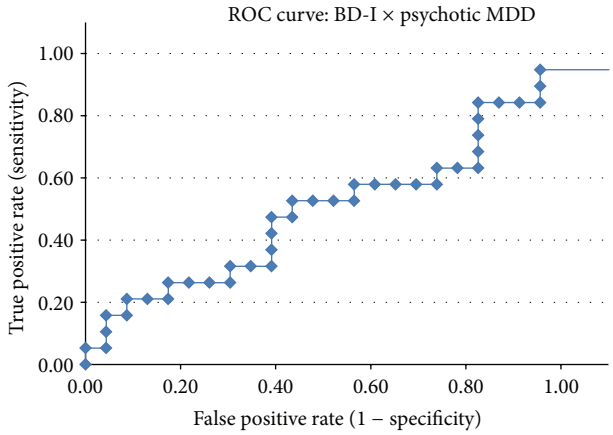

Figure 4: ROC curve for the direct comparison between patients with psychotic bipolar I disorder (BD-I) and psychotic major depressive disorder (MDD).

pattern classifiers based solely on structural MRI images possess poor diagnostic power to discriminate BD-I and psychotic MDD cases from controls, as well as from each other, at least at an early course of their illnesses. The fact that a relatively high number of morphological features were used for each pairwise classification (i.e., 53, 80, and 99) compared to previous studies using the same method but achieving better between-group discrimination reinforces this notion. That is, the classifier failed to find a specific pattern that affords good separation between the study groups and each of these features contributes very little to the classification analyses.

Congruently with our results, the few studies with structural MRI and neuroanatomical pattern classifiers in mood disorders published to date have achieved lower DA than fMRI studies [17–21]. Also, the literature on structural MRI investigations of BD has consistently shown a great variability of findings, including many negative studies and low reproducibility even across the different meta-analyses published so far [41–43]. Thus, it is conceivable that such inhomogeneity denotes that structural brain abnormalities in mood disorders remain very subtle to be detected by current neuroimaging techniques and cannot provide a reliable frame to automated classification methods. Conversely, recent studies using neuroanatomical pattern classifiers to evaluate fMRI datasets of previously medicated patients with chronic depressive disorders have shown promising results [8, 10], which suggests that functional neuroimaging measures might afford better discrimination of mood disorders cases than structural MRI. Nonetheless, incipient results of fMRI studies that attempted to discriminate BD from MDD using pattern classifiers are conflicting [14–16].

The adequate selection of relevant features for between-group discrimination is one important methodological step of neuroanatomical pattern classification studies [7, 44]. However, the stability of the model generated by the classifier and how generalizable this model is to the full range of patients suffering with a given disorder in the general population relies heavily on an adequate sample size [45] and also on the method employed for recruitment of cases and controls for the study [6, 46]. Population-based designs are likely to reduce selection biases by ensuring that control individuals represent the population from which the cases came from, therefore providing a valid estimate of the exposure of interest in that population [6, 23, 46, 47]. This is particularly important for the aim of developing a neuroimaging tool to aid in diagnostic and prognosis evaluations in clinical psychiatric practice, as "real world" patients present with a range of clinical comorbidities (such as substance use disorders) and variable disease courses [6, 46]. In this regard, it is interesting to notice that our group has previously used the COMPARE classifier in the first-episode SZ arm of the original population-based investigation from where the present samples of affective patients were drawn [6]. In that study, we found an overall modest DA of 73.4% in the individual discrimination between first-episode SZ ($n = 62$) and HC ($n = 62$), which is lower than the DA reported by most preliminary studies that have applied neuroanatomical classifiers in samples of SZ patients selected in academic institutions [6] but similar to that reported in the large, representative SZ sample recruited by Nieuwenhuis et al. [45].

There are a number of methodological limitations that should be weighted in the interpretation of our results. Firstly, a significant proportion of our BD-I and MDD patients (43.5% and 78.9%, resp.) were using antipsychotic medication at the day of MRI scanning. Although the time of such exposure was relatively short, it is known that antipsychotic treatment is associated with both GM and WM reductions [41, 48] and, thus, might have influenced our results. Secondly, comorbid substance abuse or dependence is another important confounding variable in the assessment of regional brain volumes [32] and the fact that a substantial proportion of the patients enrolled in our study presented a positive history of substance misuse could have limited the sensitivity of the classifier to identify morphometric abnormalities specifically associated with BD-I and psychotic MDD diagnoses. Nevertheless, substance misuse is pervasive in mood disorders, and a useful classifier should discriminate patients despite such comorbidity. Finally, the size of the BD-I and psychotic MDD groups may have been insufficiently large to avoid the risk of type II errors. Thus, more studies with larger samples of BD and psychotic MDD patients are needed in order to further confirm the results observed in this proof of concept investigation.

5. Conclusion

Neuroanatomical pattern classification is a recent method that affords individual classification of brain measures and, thus, is considered promising for developing a tool to improve diagnostic accuracy in the psychiatric practice. However, in the present structural MRI study, the diagnostic performance of such method in the discrimination between psychotic MDD, BD-I, and HC was limited. New studies preferably with larger samples are warranted to further confirm that classifiers based solely on structural MRI scans do not

achieve satisfactory discrimination of individuals with mood disorders.

Conflict of Interests

The authors declare to have no conflicts of interest pertaining to the present work.

Acknowledgments

We acknowledge the contribution of Professors Robin M. Murray and Philip K. McGuire in the design of the original study that generated MRI data for the present investigation. Such previous investigation was supported with funding from the Wellcome Trust, UK, and Fundação de Amparo à Pesquisa do Estado de São Paulo (FAPESP), Brazil (no. 2003/13627-0). Marcus V. Zanetti is funded by FAPESP, Brazil (no. 2013/03905-4). Geraldo F. Busatto, Paulo R. Menezes, and Marcia Scazufca are partially funded by CNPq-Brazil.

References

[1] P. Salvatore, R. J. Baldessarini, H. M. Khalsa et al., "Predicting diagnostic change among patients diagnosed with first-episode DSM-IV-TR major depressive disorder with psychotic features," *The Journal of Clinical Psychiatry*, vol. 74, no. 7, pp. 723–731, 2013.

[2] Y. T. Xiang, L. Zhang, G. Wang et al., "Sociodemographic and clinical features of bipolar disorder patients misdiagnosed with major depressive disorder in China," *Bipolar Disorders*, vol. 15, no. 2, pp. 199–205, 2013.

[3] O. Owoeye, T. Kingston, P. J. Scully et al., "Epidemiological and clinical characterization following a first psychotic episode in major depressive disorder: comparisons with schizophrenia and bipolar I disorder in the Cavan-Monaghan First Episode Psychosis Study (CAMFEPS)," *Schizophrenia Bulletin*, vol. 39, no. 4, pp. 756–765, 2013.

[4] J.-M. Azorin, J. Angst, A. Gamma et al., "Identifying features of bipolarity in patients with first-episode postpartum depression: findings from the international BRIDGE study," *Journal of Affective Disorders*, vol. 136, no. 3, pp. 710–715, 2012.

[5] S. Klöppel, A. Abdulkadir, C. R. Jack Jr., N. Koutsouleris, J. Mourão-Miranda, and P. Vemuri, "Diagnostic neuroimaging across diseases," *NeuroImage*, vol. 61, no. 2, pp. 457–463, 2012.

[6] M. V. Zanetti, M. S. Schaufelberger, J. Doshi et al., "Neuroanatomical pattern classification in a population-based sample of first-episode schizophrenia," *Progress in Neuro-Psychopharmacology and Biological Psychiatry*, vol. 43, pp. 116–125, 2013.

[7] Y. Fan, D. Shen, R. C. Gur, R. E. Gur, and C. Davatzikos, "COMPARE: classification of morphological patterns using adaptive regional elements," *IEEE Transactions on Medical Imaging*, vol. 26, no. 1, pp. 93–105, 2007.

[8] C. H. Fu, J. Mourao-Miranda, S. G. Costafreda et al., "Pattern classification of sad facial processing: toward the development of neurobiological markers in depression," *Biological Psychiatry*, vol. 63, no. 7, pp. 656–662, 2008.

[9] R. C. Craddock, P. E. Holtzheimer III, X. P. Hu, and H. S. Mayberg, "Disease state prediction from resting state functional connectivity," *Magnetic Resonance in Medicine*, vol. 62, no. 6, pp. 1619–1628, 2009.

[10] T. Hahn, A. F. Marquand, A.-C. Ehlis et al., "Integrating neurobiological markers of depression," *Archives of General Psychiatry*, vol. 68, no. 4, pp. 361–368, 2011.

[11] L.-L. Zeng, H. Shen, L. Liu et al., "Identifying major depression using whole-brain functional connectivity: a multivariate pattern analysis," *Brain*, vol. 135, no. 5, pp. 1498–1507, 2012.

[12] Y. Yu, H. Shen, L. L. Zeng, Q. Ma, and D. Hu, "Convergent and divergent functional connectivity patterns in schizophrenia and depression," *PLoS ONE*, vol. 8, no. 7, Article ID e68250, 2013.

[13] S. G. Costafreda, C. H. Fu, M. Picchioni et al., "Pattern of neural responses to verbal fluency shows diagnostic specificity for schizophrenia and bipolar disorder," *BMC Psychiatry*, vol. 11, article 18, 2011.

[14] J. Mourão-Miranda, J. R. Almeida, S. Hassel et al., "Pattern recognition analyses of brain activation elicited by happy and neutral faces in unipolar and bipolar depression," *Bipolar Disorders*, vol. 14, no. 4, pp. 451–460, 2012.

[15] D. Grotegerd, T. Suslow, J. Bauer et al., "Discriminating unipolar and bipolar depression by means of fMRI and pattern classification: a pilot study," *European Archives of Psychiatry and Clinical Neuroscience* , vol. 263, no. 2, pp. 119–131, 2013.

[16] J. R. Almeida, J. Mourao-Miranda, H. J. Aizenstein et al., "Pattern recognition analysis of anterior cingulate cortex blood flow to classify depression polarity," *The British Journal of Psychiatry*, vol. 203, pp. 310–311, 2013.

[17] F. Liu, W. Guo, D. Yu et al., "Classification of different therapeutic responses of major depressive disorder with multivariate pattern analysis method based on structural MR scans," *PLoS ONE*, vol. 7, no. 7, Article ID e40968, 2012.

[18] Q. Gong, Q. Wu, C. Scarpazza et al., "Prognostic prediction of therapeutic response in depression using high-field MR imaging," *NeuroImage*, vol. 55, no. 4, pp. 1497–1503, 2011.

[19] S. G. Costafreda, C. Chu, J. Ashburner, and C. H. Fu, "Prognostic and diagnostic potential of the structural neuroanatomy of depression," *PLoS ONE*, vol. 4, no. 7, Article ID e6353, 2009.

[20] L. Qiu, X. Huang, J. Zhang et al., "Characterization of major depressive disorder using a multiparametric classification approach based on high resolution structural images," *Journal of Psychiatry & Neuroscience*, vol. 38, no. 5, Article ID 130034, 2013.

[21] V. Rocha-Rego, J. Jogia, A. F. Marquand, J. Mourao-Miranda, A. Simmons, and S. Frangou, "Examination of the predictive value of structural magnetic resonance scans in bipolar disorder: a pattern classification approach," *Psychological Medicine*, 2013.

[22] R. Uher and M. Rutter, "Basing psychiatric classification on scientific foundation: problems and prospects," *International Review of Psychiatry*, vol. 24, no. 6, pp. 591–605, 2012.

[23] D. A. Grimes and K. F. Schulz, "Compared to what? finding controls for case-control studies," *The Lancet*, vol. 365, no. 9468, pp. 1429–1433, 2005.

[24] W. Lee, J. Bindman, T. Ford et al., "Bias in psychiatric case-control studies: literature survey," *The British Journal of Psychiatry*, vol. 190, pp. 204–209, 2007.

[25] C. Davatzikos, D. Shen, R. C. Gur et al., "Whole-brain morphometric study of schizophrenia revealing a spatially complex set of focal abnormalities," *Archives of General Psychiatry*, vol. 62, no. 11, pp. 1218–1227, 2005.

[26] N. Koutsouleris, E. M. Meisenzahl, C. Davatzikos et al., "Use of neuroanatomical pattern classification to identify subjects in at-risk mental states of psychosis and predict disease transition," *Archives of General Psychiatry*, vol. 66, no. 7, pp. 700–712, 2009.

[27] J. B. Toledo, X. Da, P. Bhatt et al., "Alzheimer's disease neuroimaging initiative. Relationship between plasma analytes and SPARE-AD defined brain atrophy patterns in ADNI," *PLoS ONE*, vol. 8, no. 2, Article ID e55531, 2013.

[28] American Psychiatric Association, *Diagnostic and Statistical Manual of Mental Disorders (DSM-IV)*, APA, Washington, DC, USA, 4th edition, 1994.

[29] P. R. Menezes, M. Scazufca, G. Busatto, L. M. Coutinho, P. K. McGuire, and R. M. Murray, "Incidence of first-contact psychosis in São Paulo, Brazil," *The British Journal of Psychiatry*, vol. 191, supplement, pp. s102–s106, 2007.

[30] M. S. Schaufelberger, F. L. Duran, J. M. Lappin et al., "Grey matter abnormalities in Brazilians with first-episode psychosis," *The British Journal of Psychiatry*, vol. 191, supplement, pp. s117–s122, 2007.

[31] M. B. First, R. L. Spitzer, M. Gibbon, and J. B. W. Williams, *Structured Clinical Interview for DSM-IV Axis I Disorders, Patient Edition (SCID-I/P)*, Biometrics Research, New York State Psychiatry Institute, New York, NY, USA, 1995.

[32] R. R. Colombo, M. S. Schaufelberger, L. C. Santos et al., "Voxelwise evaluation of white matter volumes in first-episode psychosis.," *Psychiatry Research*, vol. 202, pp. 198–205, 2012.

[33] P. E. Bebbington and T. Nayani, "The psychosis screening questionnaire," *International Journal of Methods in Psychiatric Research*, vol. 5, no. 1, pp. 11–19, 1995.

[34] G. S. Pell, R. S. Briellmann, C. H. Chan, H. Pardoe, D. F. Abbott, and G. D. Jackson, "Selection of the control group for VBM analysis: influence of covariates, matching and sample size," *NeuroImage*, vol. 41, no. 4, pp. 1324–1335, 2008.

[35] J. B. Saunders, O. G. Aasland, T. F. Babor, J. R. de la Fuente, and M. Grant, "Development of the alcohol use disorders identification test (AUDIT): WHO collaborative project on early detection of persons with harmful alcohol consumption-II," *Addiction*, vol. 88, no. 6, pp. 791–804, 1993.

[36] P. R. Menezes, S. Johnson, G. Thornicroft et al., "Drug and alcohol problems among individuals with severe mental illnesses in South London," *The British Journal of Psychiatry*, vol. 168, pp. 612–619, 1996.

[37] Y. Ou, A. Sotiras, N. Paragios, and C. Davatzikos, "DRAMMS: deformable registration via attribute matching and mutual-saliency weighting," *Medical Image Analysis*, vol. 15, no. 4, pp. 622–639, 2011.

[38] D. Shen and C. Davatzikos, "Very high-resolution morphometry using mass-preserving deformations and HAMMER elastic registration," *NeuroImage*, vol. 18, no. 1, pp. 28–41, 2003.

[39] Z. Lao, D. Shen, Z. Xue, B. Karacali, S. M. Resnick, and C. Davatzikos, "Morphological classification of brains via high-dimensional shape transformations and machine learning methods," *NeuroImage*, vol. 21, no. 1, pp. 46–57, 2004.

[40] C. E. Metz, "Receiver operating characteristic analysis: a tool for the quantitative evaluation of observer performance and imaging systems," *Journal of the American College of Radiology*, vol. 3, no. 6, pp. 413–422, 2006.

[41] E. Bora, A. Fornito, M. Yücel, and C. Pantelis, "Voxelwise meta-analysis of gray matter abnormalities in bipolar disorder," *Biological Psychiatry*, vol. 67, no. 11, pp. 1097–1105, 2010.

[42] B. Hallahan, J. Newell, J. C. Soares et al., "Structural magnetic resonance imaging in bipolar disorder: an international collaborative mega-analysis of individual adult patient data," *Biological Psychiatry*, vol. 69, no. 4, pp. 326–335, 2011.

[43] S. Selvaraj, D. Arnone, D. Job et al., "Grey matter differences in bipolar disorder: a meta-analysis of voxel-based morphometry studies," *Bipolar Disorders*, vol. 14, no. 2, pp. 135–145, 2012.

[44] A. Caprihan, G. D. Pearlson, and V. D. Calhoun, "Application of principal component analysis to distinguish patients with schizophrenia from healthy controls based on fractional anisotropy measurements," *NeuroImage*, vol. 42, no. 2, pp. 675–682, 2008.

[45] M. Nieuwenhuis, N. E. van Haren, H. E. Hulshoff Pol, W. Cahn, R. S. Kahn, and H. G. Schnack, "Classification of schizophrenia patients and healthy controls from structural MRI scans in two large independent samples," *NeuroImage*, vol. 61, no. 3, pp. 606–612, 2012.

[46] P. Walsh, M. Elsabbagh, P. Bolton, and I. Singh, "In search of biomarkers for autism: scientific, social and ethical challenges," *Nature Reviews Neuroscience*, vol. 12, no. 10, pp. 603–612, 2011.

[47] S. Wacholder, "Design issues in case-control studies," *Statistical Methods in Medical Research*, vol. 4, no. 4, pp. 293–309, 1995.

[48] B.-C. Ho, N. C. Andreasen, S. Ziebell, R. Pierson, and V. Magnotta, "Long-term antipsychotic treatment and brain volumes: a longitudinal study of first-episode schizophrenia," *Archives of General Psychiatry*, vol. 68, no. 2, pp. 128–137, 2011.

Hindawi Publishing Corporation
BioMed Research International
Volume 2014, Article ID 180468, 7 pages
http://dx.doi.org/10.1155/2014/180468

Research Article

Long-Term Effects of Postearthquake Distress on Brain Microstructural Changes

Atsushi Sekiguchi,[1,2] Yuka Kotozaki,[3] Motoaki Sugiura,[2,4] Rui Nouchi,[3,4] Hikaru Takeuchi,[5] Sugiko Hanawa,[2] Seishu Nakagawa,[2] Carlos Makoto Miyauchi,[2,6] Tsuyoshi Araki,[3] Atsushi Sakuma,[2,7] Yasuyuki Taki,[1,5,8] and Ryuta Kawashima[2,3,5]

[1] *Division of Medical Neuroimage Analysis, Department of Community Medical Supports, Tohoku Medical Megabank Organization, Tohoku University, 4-1 Seiryo-machi, Aoba-ku, Sendai 980-8575, Japan*
[2] *Department of Functional Brain Imaging, Institute of Development, Aging and Cancer (IDAC), Tohoku University, 4-1 Seiryo-machi, Aoba-ku, Sendai 980-8575, Japan*
[3] *Department of Advanced Brain Science, Smart Ageing International Research Center, IDAC, Tohoku University, 4-1 Seiryo-machi, Aoba-ku, Sendai 980-8575, Japan*
[4] *International Research Institute of Disaster Science, Tohoku University, 4-1 Seiryo-machi, Aoba-ku, Sendai 980-8575, Japan*
[5] *Division of Developmental Cognitive Neuroscience, IDAC, Tohoku University, 4-1 Seiryo-machi, Aoba-ku, Sendai 980-8575, Japan*
[6] *Graduate Schools for Law and Politics, The University of Tokyo, 7-3-1 Hongo, Bunkyo-ku, Tokyo 113-0033, Japan*
[7] *Department of Psychiatry, Tohoku University Graduate School of Medicine, 1-1 Seiryo-machi, Aoba-ku, Sendai 980-8574, Japan*
[8] *Department of Nuclear Medicine and Radiology, IDAC, Tohoku University, 4-1 Seiryo-machi, Aoba-ku, Sendai 980-8575, Japan*

Correspondence should be addressed to Atsushi Sekiguchi; asekiguchi@idac.tohoku.ac.jp

Received 3 October 2013; Revised 15 December 2013; Accepted 16 December 2013; Published 14 January 2014

Academic Editor: Qiyong Gong

Stressful events can have both short- and long-term effects on the brain. Our recent investigation identified short-term white matter integrity (WMI) changes in 30 subjects soon after the Japanese earthquake. Our findings suggested that lower WMI in the right anterior cingulum (Cg) was a pre-existing vulnerability factor and increased WMI in the left anterior Cg and uncinate fasciculus (Uf) after the earthquake was an acquired sign of postearthquake distress. However, the long-term effects on WMI remained unclear. Here, we examined the 1-year WMI changes in 25 subjects to clarify long-term effects on the WMI. We found differential FAs in the right anterior Cg, bilateral Uf, left superior longitudinal fasciculus (SLF), and left thalamus, suggesting that synaptic enhancement and shrinkage were long-term effects. Additionally, the correlation between psychological measures related to postearthquake distress and the degree of WMI alternation in the right anterior Cg and the left Uf led us to speculate that temporal WMI changes in some subjects with emotional distress occurred soon after the disaster. We hypothesized that dynamic WMI changes predict a better prognosis, whereas persistently lower WMI is a marker of cognitive dysfunction, implying the development of anxiety disorders.

1. Introduction

Stressful events have both short- and long-term effects on the brain [1, 2]. Acute and chronic stress-induced brain microstructural changes have been observed in prefrontal areas in rodents [3]. Recent human studies identified white matter microstructural changes due to stress using diffusion tensor imaging (DTI) methods [4] in subjects with post-traumatic stress disorder (PTSD) [5–8] as well as healthy survivors of a disaster [9]. These studies revealed lower white matter integrity (WMI) in several brain regions, including the cingulum (Cg) and uncinate fasciculus (Uf), in subjects who developed PTSD [5–8] (i.e., long-term effect) and in individuals soon after a disaster [9] (i.e., short term effect).

However, because these previous studies employed cross-sectional designs, longitudinal WMI changes within individuals remained unclear.

Our previous longitudinal investigation unveiled the causal relationships between WMI changes and psychological distress soon after a disaster [10]. In our previous study, we collected DTI data from a group of healthy subjects before the Japanese earthquake (pre). Then, we recruited 30 subjects (male/female = 24/6, age = 21.0 ± 1.6 yr, range = 19 to 25 yr) from this group and examined results from DTI and from psychological measures related to postearthquake distress 3 to 4 months after the earthquake (post) to examine short-term effects. We found that lower WMI in the right anterior Cg before the earthquake was a preexisting vulnerability factor for postearthquake distress, and that increased WMI in the left anterior Cg and Uf after the earthquake was an acquired sign of post-earthquake distress [10].

In the current study, we examined WMI changes in subjects from the previous investigation 1 year later (followup) [10]. We tried to identify WMI changes that occurred in early (pre to post) and late (post to followup) phases after this stressful life event and investigated when and where these WMI changes occurred. In particular, we focused on the prognosis of FA changes in the right anterior Cg and the left anterior Cg and Uf, which were identified as a preexisting vulnerability factor and an acquired sign of post-earthquake distress, respectively.

2. Materials and Methods

2.1. Subjects. All subjects participated in our previous investigation [10, 11]. Of the 30 subjects in our previous DTI study [10], we rerecruited 25 subjects (male/female = 19/6, age = 21.7 ± 1.4 yr) and assessed their structural DTI results one year after the earthquake. We screened for neuropsychiatric disorders using the Mini International Neuropsychiatric Interview (M.I.N.I.) [12, 13]. Handedness was assessed using the Edinburgh Handedness Inventory [14]. All subjects provided written informed consent before participating in the current study, which examined the possible effects of psychological trauma on brain structure, in accordance with the Declaration of Helsinki [15]. The M.I.N.I. confirmed that no subject had any history of psychiatric illness including PTSD and no subjects were exposed to life-threatening experiences due to the earthquake or tsunami. The current study was approved by the Ethics Committee of Tohoku University.

2.2. Psychological Evaluations. All participants were interviewed by trained psychologists using the Japanese version of the clinician-administered PTSD scale (CAPS) structured interview [16, 17]. In accordance with the M.I.N.I., no subject was diagnosed as having PTSD. Levels of anxiety and depression were evaluated using the State-Trait Anxiety Inventory (STAI) [18, 19] and the Center for Epidemiologic Studies Depression Scale (CES-D) [20, 21]. Psychological traits related to resilience in response to stressful life events were assessed using the Japanese version of the Posttraumatic Growth Inventory (PTGI-J) [22, 23] and the Japanese version of the Rosenberg Self-Esteem Scale [24, 25]. All psychological measures were assessed at 3 to 4 months (post) and at 1 year (followup) after the earthquake.

2.3. Image Acquisition. All MRI data were acquired with a 3-T Philips Intera Achieva scanner. The diffusion-weighted data were acquired using a spin-echo EPI sequence (TE = 55 ms, FOV = 22.4 cm, $2 \times 2 \times 2\,mm^3$ voxels, 60 slices). The diffusion weighting was isotropically distributed along 32 directions (b value = $1{,}000\,s/mm^2$). Additionally, a dataset with no diffusion weighting (b value = $0\,s/mm^2$; b0 image) was acquired. The total scan time was 7 min 17 s. Then, fractional anisotropy (FA) values were calculated from the collected images. This information is of particular interest when making inferences regarding white matter microstructural properties, as diffusion is faster along axons than in the perpendicular direction. Consequently, diffusion in white matter is anisotropic (i.e., diffusion rates in different directions are unequal). By contrast, isotropic diffusion is equally fast in all directions. FA in each voxel was used as a measure of the degree of diffusion anisotropy. FA varies between 0 and 1, with 0 representing isotropic diffusion and 1 representing diffusion occurring entirely in one direction. After DTI image acquisition, FA map images were calculated from DTI using software preinstalled on the Philips MR console.

2.4. Preprocessing of Diffusion Imaging Data. Preprocessing and data analysis were performed using statistical Parametric Mapping software (SPM5; Wellcome Department of Cognitive Neurology, London, UK) implemented in MATLAB (MathWorks, Natick, MA, USA). First, our original b0 image template was created as follows. Using the affine and nonlinear spatial normalization algorithm, the b0 images from the pre-earthquake scans of all subjects in this study were spatially normalized to the SPM5 T2 template, which is based on averages taken from 152 brains from the Montreal Neurological Institute database. Then, we calculated a mean image of the normalized b0 images as our original b0 image template. Using the affine and nonlinear spatial normalization algorithm, the b0 image of each participant was normalized to our original b0 image template. Before normalization of the FA map, the postearthquake FA maps were coregistered with the pre-earthquake FA maps from each subject. Then, using the parameter for this affine and nonlinear normalization procedure, an FA map image of each participant was spatially normalized to yield images with $2 \times 2 \times 2$ mm voxels and spatially smoothed using a Gaussian kernel of 10 mm FWHM. The resulting maps representing FA were then subjected to the group regression analysis described below.

2.5. Statistical Analysis. Differences in FA between before the earthquake (pre), 3-4 months after the earthquake (post), and 1 year after the earthquake (followup) were compared using analysis of covariance (ANCOVA) in SPM5. The analysis was performed with sex and period between MR acquisition and the earthquake as additional covariates. Differential FA between time periods was detected as a main effect (pre/post/followup) using F-contrasts in SPM. The significance level was set at $P = 0.05$, corrected for multiple comparisons (voxel-level family-wise error) and $k > 10$ to

Table 1: Psychological measures.

	Post	Followup	P value
CAPS (total)	6.6 ± 9.6	1.6 ± 2.9	0.04
CES-D score	12.1 ± 10.6	10.7 ± 9.3	n.s.
STAI scores			
State	44.1 ± 11.8	39.2 ± 10.4	n.s.
Trait	42.7 ± 9.6	43.2 ± 11.2	n.s.
Self-esteem	32.8 ± 8.2	32.8 ± 8.9	n.s.
PTGI-J (total)	33.8 ± 18.9	34.3 ± 19.3	n.s.

Values are shown as mean ± standard deviation.
CAPS: clinician-administered PTSD scale, CES-D: center for epidemiologic studies depression scale, STAI: state-trait anxiety inventory, and PTGI-J: Japanese version of the posttraumatic growth inventory.

Table 2: MNI coordinates, voxel sizes, F values, and P values for results of the SPM analyses.

Brain region	MNI coordinates			k (voxels)	F values	P values (FWE)
	x	y	z			
Rt anterior Cg	26	52	14	55	21.68	0.002
Rt Uf	8	46	−22	10	19.38	0.007
Lt Uf	−32	44	−6	72	33.49	0.000
Lt SLF	−28	−18	22	63	24.21	0.001
Lt thalamus	−10	−22	10	23	17.96	0.017

MNI: montreal neurological institute, Rt: right, Lt: left, Cg: cingulum, Uf: uncinate fasciculus, and SLF: superior longitudinal fissure.

suppress the possibility of small clusters arising by chance. Additionally, to check for structural changes between each period (pre versus post, pre versus followup, and post versus followup), paired t-tests were performed for each cluster identified as a main effect in the ANCOVA. Finally, to ascertain the 1-year prognosis of FA changes as a preexisting vulnerability factor and as an acquired sign of postearthquake distress, *post hoc* correlation analysis was performed including the scores for postearthquake distress (e.g., CAPS and STAI-state at post) and FA changes from pre to followup in the right anterior Cg (i.e., a preexisting vulnerability factor at Pre) as well as from post to followup in the left anterior Cg and Uf (i.e., an acquired sign at Post) within the clusters detected by the ANCOVA.

All FA tests were performed using an absolute threshold of FA >0.2 [26], such that if a voxel anywhere in the brain had an FA value >0.2 in all subjects, that voxel was included in the analysis. This measure was used because FA is more susceptible to errors arising from partial volumes [27], and this FA cut-off value allowed us to dissociate white matter structure from other tissue [28].

3. Results

As for psychological measures, the CAPS total score significantly recovered between post and followup (6.6 ± 11.2 to 1.6 ± 2.9, $P < 0.05$). Scores on STAI-state (44.1 ± 11.4 to 39.2 ± 10.4, n.s.), STAI-trait (42.7 ± 9.6 to 43.2 ± 11.2, n.s.), CES-D (12.1 ± 10.6 to 10.7 ± 9.3, n.s.), Rosenberg self-esteem scale (32.8 ± 8.2 to 32.8 ± 8.9, n.s.), and PTGI-J (33.8 ± 18.9 to 34.3 ± 19.3, n.s.) were not significantly changed from post to followup (Table 1).

We found differential FAs to be a significant main effect of time period (pre/post/followup) in the right anterior Cg, bilateral Uf, left superior longitudinal fasciculus (SLF), and the thalamus (Table 2, Figure 1). *post hoc* correlation analyses revealed a significant positive correlation between the FA changes in the right anterior Cg from pre to followup and CAPS scores at post (Spearman's Rho = 0.414, $P = 0.039$, Figure 2(a)) and a significant negative correlation between the FA changes in the left Uf from post to followup and STAI-state scores at post ($r = -0.440$, $P = 0.028$, Figure 2(b)).

4. Discussion

To the best of our knowledge, this is the first longitudinal study to track microstructural changes in the brain at three time points: before, a short time after, and a long time after a disaster. We found differential FA at each time point in the right anterior Cg, bilateral Uf, left SLF, and left thalamus. According to the results of additional comparisons, we categorized the data according to the following three types of FA changes: normalization from initial FA changes in the right anterior Cg and right Uf (Figures 1(a) and 1(b)), sustained FA changes from the early phase in the left Uf (Figure 1(c)), and FA changes appearing during the late phase in the left SLF and thalamus (Figures 1(d) and 1(e)).

Increased or decreased WMI both a short and a long time after a disaster is likely to be due to synaptic enhancement and shrinkage, respectively. Biologically, synaptic enhancement or shrinkage has been observed in altered white matter following stress [3]. These changes are caused by hyper-secretion of glucocorticoids, a stress hormone [29]. The effects of stress hormones on the brain are observed as an inverse

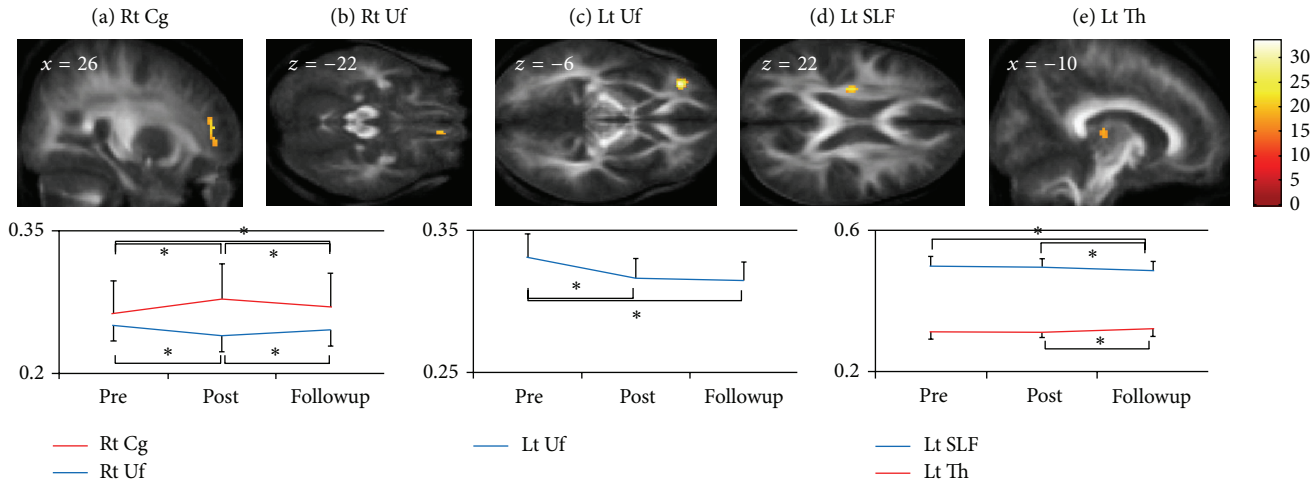

Figure 1: (a) FA in the right anterior Cg was significantly increased from pre to post ($P < 0.05$, paired t-test) and from pre to followup ($P < 0.05$, paired t-test), but it was significantly decreased from post to followup ($P < 0.05$, paired t-test). (b) FA in the right Uf was significantly decreased from pre to post ($P < 0.05$, paired t-test), but it was significantly increased from post to followup ($P < 0.05$, paired t-test). (c) FA in the left Uf was significantly decreased from pre to post ($P < 0.05$, paired t-test) and from pre to followup ($P < 0.05$, paired t-test). (d) FA in the left SLE was significantly decreased from pre to followup ($P < 0.05$, paired t-test) and from post to followup ($P < 0.05$, paired t-test). (e) FA in the left Th was significantly increased from post to followup ($P < 0.05$, paired t-test). These FA changes are illustrated by the plots at the bottom: vertical axes represent FA at peak voxels in each cluster, and horizontal axes indicate time periods. Error bars represent standard deviations. Colored bars represent F values. FA: fractional anisotropy; Rt: right; Lt: left; Cg: cingulum; Uf: uncinate fasciculus; SLE: superior longitudinal fasciculus; Th: thalamus.

U shape, depending on dose and time [30]. Additionally, stress-induced structural and functional alterations have been shown to be reversible, at least in the prefrontal cortex [31, 32]. In the context of these considerations, we assumed that FA changes in the right anterior Cg were consistent with the aforementioned concept and that increased FA in the thalamus and decreased FA in the Uf and SLF reflected the rising and falling components, respectively, of the inverse U-shaped curve that characterizes such changes.

The results of correlation analyses and our previous findings [10] led us to speculate that, in some subjects, the WMI changes reflected normalization after initial changes. Such reversible WMI changes are congruent with the aforementioned biological conceptualizations [30–32]. As discussed below, we interpreted such WMI changes as not only signs of recovery from emotional distress shortly after a disaster but also as predictors of a better prognosis for subjects with more pronounced psychological responses to a stressful event, namely, following two cases.

First, the WMI changes in the left Uf identified in some subjects who reported distress indicated that recovery from emotional distress is possible following a stressful event. Our previous study demonstrated that the WMI was greater in the left Uf after the earthquake as compared with before the earthquake and was positively correlated with state anxiety levels, suggesting that the increased WMI in the left Uf was an acquired sign of emotional distress soon after a disaster [10]. In the present study, the WMI in the left Uf decreased from soon after (Post) to one year after (followup) the earthquake in subjects who had had higher state anxiety levels soon after the earthquake (Post). The Uf, which is also involved in emotional processing [33], is a principal white matter tract that connects the orbitofrontal cortex (OFC) and limbic regions, including the amygdala and the anterior temporal cortices [34, 35]. Neural responses in the OFC are preferentially enhanced, along with those in the amygdala, during extinction [36] and this relationship is crucial to the voluntary regulation of emotion [37]. Taking the functional roles of the Uf into account, the current results suggest that WMI in the Uf, which was elevated soon after the earthquake, reflecting the requirements of emotional regulation related to postearthquake stress, declined 1 year after the earthquake.

Next, the WMI changes in the right anterior Cg in some subjects who reported subclinical PTSD symptoms also suggested that a stressful event would strengthen structural connectivity, particularly in vulnerable subjects. The anterior Cg bundle is a part of the principal white matter tract in the Papez circuit, which includes the ACC and the amygdala [38]. Reduced WMI in the anterior Cg is frequently reported in patients with anxiety disorders such as PTSD [6–8, 39], social anxiety disorder (SAD) [40], and generalized anxiety disorder (GAD) [41] and in healthy subjects with high trait anxiety [42, 43]. It has been suggested that reduced WMI in the Cg represents dysfunctional emotion processing in such patients [6–8, 39–41]. Our previous study revealed that lower WMI in the right anterior Cg was a preexisting vulnerability factor for emotional distress soon after a disaster [10]. The current results showing the positive correlation between increased WMI in the right anterior Cg and CAPS scores demonstrated that those who had more PTSD symptoms

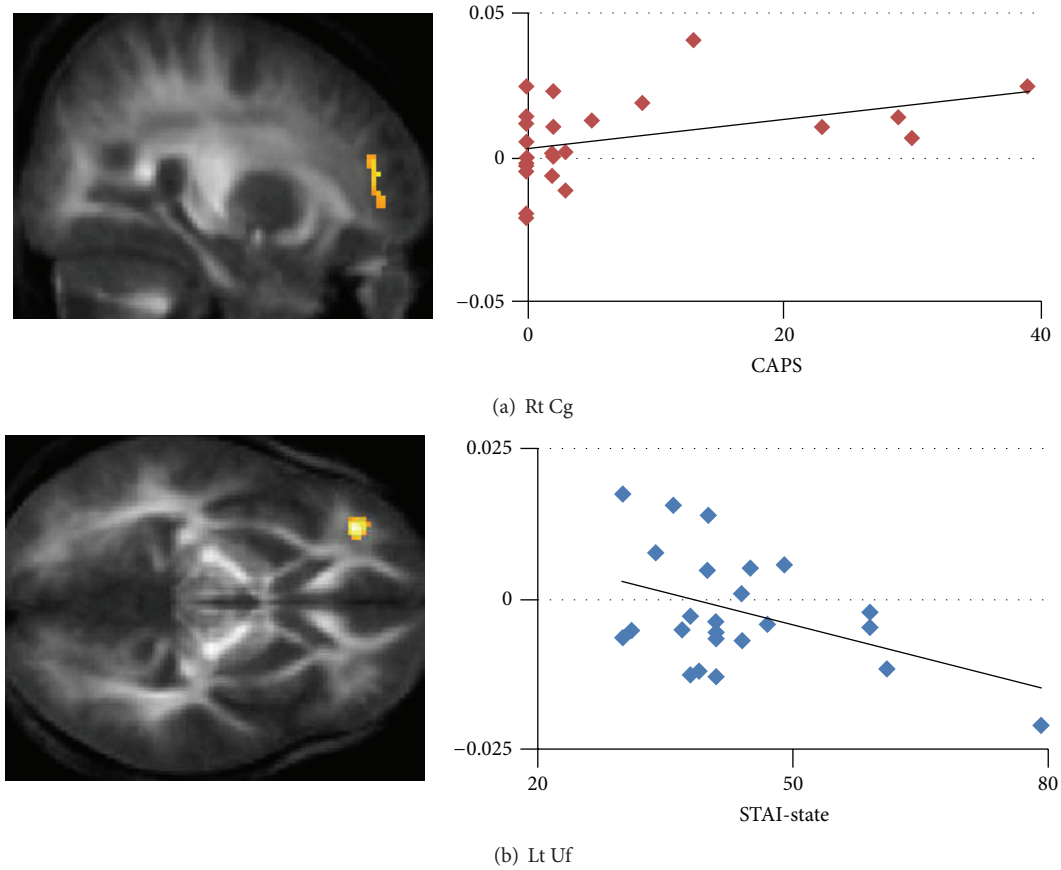

Figure 2: (a) CAPS scores were positively associated with FA changes from pre to followup in the right anterior Cg (Spearman's Rho = 0.414, $P = 0.039$), and (b) STAI-state scores were positively associated with FA changes from post to followup in the left Uf ($r = -0.440$, $P = 0.028$), as illustrated by the scatter plots on the right. Vertical axes represent FA changes at peak voxels in each cluster, and horizontal axes indicate (a) CAPS scores and (b) STAI-state scores. FA: fractional anisotropy; Rt: right; Lt: left; Cg: cingulum; Uf: uncinate fasciculus.

soon after the earthquake displayed increased structural connectivity in the anterior Cg from before to 1 year after the earthquake. Furthermore, although depression and anxiety levels did not improve from 3-4 months after to 1 year after the earthquake, none of the subjects in this study developed clinical PTSD. Together, the findings suggest that dynamic WMI changes in the Cg predict a better prognosis, whereas persistently lower WMI represents cognitive dysfunction, implying the development of anxiety disorders (e.g., PTSD, SAD, and GAD).

White matter changes due to maturation and/or aging should be taken into account when interpreting the results, because this study did not include a control group, which is a limitation of this study. This is particularly problematic with respect to interpreting WMI changes, such as the increased WMI in the thalamus and the decreased WMI in the SLF, without evaluating their correlation with psychological measures. A recent study that investigated WMI changes due to maturation and/or aging revealed that peak FAs in the Cg, Uf, and SLF were observed in subjects older than the age range of our subjects (19 to 25 yr) [44]. Another study reported increased FA in thalamic radiations with age [45]. In contrast, another recent study investigating longitudinal FA changes at younger ages found that FA in the Uf decreased by almost half in subjects ranging in age from 19 to 25 [46]. Thus, decreased WMI in the SLF is unlikely to have occurred in our subjects, whereas it is difficult to reject the possibility that our finding of the increased WMI in the thalamus is a result of maturation. Nevertheless, the interpretation of WMI changes, such as the increased WMI in the Cg and the decreased WMI in the Uf, and their correlation with psychological measures are less problematic. We believe that the current study provides sufficient evidence of the short- and long-term effects on the brain microstructure despite the absence of a control group.

5. Conclusions

The present followup DTI study showed the long lasting effects of stressful events on brain microstructure. Our findings suggest that microstructures within the brain change due to stress and recovery. We assumed that brain microstructural changes due to stressful life events were not static but dynamic through life. Recently, the alteration of functional and structural connectivity, including regions adjacent to the Cg and the Uf, was reported in subjects soon after a disaster

[47, 48]. Therefore, further longitudinal investigations using multimodal approaches are necessary to examine whether the stress-induced alterations in brain structure are reversible.

Conflict of Interests

The authors declare that they have no conflict of interests.

Authors' Contribution

All authors contributed to the concept and design of the study. Atsushi Sekiguchi, Yuka Kotozaki, Motoaki Sugiura, Tsuyoshi Araki, Sugiko Hanawa, Seishu Nakagawa, and Carlos Makoto Miyauchi contributed to data acquisition. Atsushi Sekiguchi, Motoaki Sugiura, Yuka Kotozaki, Rui Nouchi, Hikaru Takeuchi, Tsuyoshi Araki, Yasuyuki Taki, and Ryuta Kawashima contributed to the data analysis and interpretation. Atsushi Sekiguchi, Motoaki Sugiura, Rui Nouchi, Hikaru Takeuchi, Tsuyoshi Araki, Yasuyuki Taki, and Ryuta Kawashima provided statistical expertise. Atsushi Sekiguchi wrote the paper. Motoaki Sugiura, Rui Nouchi, Hikaru Takeuchi, Yasuyuki Taki, and Ryuta Kawashima reviewed/revised the paper. All authors discussed the results and commented on the paper. All authors gave their final approval for the paper to be submitted.

Acknowledgments

The authors thank their study participants, the psychological test examiners, and all of their colleagues at the Institute of Development, Aging, and Cancer and at Tohoku University for their support. Atsushi Sekiguchi was supported by a Grant for Special Project Research from the International Research Institute of Disaster Science, a grant-in-Aid for Young Scientists (B) (KAKENHI 24790653) from the Ministry of Education, Culture, Sports, Science, and Technology, and grants-in-Aid for Scientific Research (H24-seishin-wakate014) from the Ministry of Health, Labor, and Welfare in Japan.

References

[1] G. A. Van Wingen, E. Geuze, E. Vermetten, and G. Fernández, "Perceived threat predicts the neural sequelae of combat stress," *Molecular Psychiatry*, vol. 16, no. 6, pp. 664–671, 2011.

[2] G. A. Van Wingen, E. Geuze, E. Vermetten, and G. Fernández, "The neural consequences of combat stress: long-term follow-up," *Molecular Psychiatry*, vol. 17, no. 2, pp. 116–118, 2012.

[3] M. Popoli, Z. Yan, B. S. McEwen, and G. Sanacora, "The stressed synapse: the impact of stress and glucocorticoids on glutamate transmission," *Nature Reviews Neuroscience*, vol. 13, no. 1, pp. 22–37, 2012.

[4] D. Le Bihan, "Looking into the functional architecture of the brain with diffusion MRI," *Nature Reviews Neuroscience*, vol. 4, no. 6, pp. 469–480, 2003.

[5] O. Abe, H. Yamasue, K. Kasai et al., "Voxel-based diffusion tensor analysis reveals aberrant anterior cingulum integrity in posttraumatic stress disorder due to terrorism," *Psychiatry Research*, vol. 146, no. 3, pp. 231–242, 2006.

[6] L. Zhang, Y. Zhang, L. Li et al., "Different white matter abnormalities between the first-episode, treatment-naive patients with posttraumatic stress disorder and generalized anxiety disorder without comorbid conditions," *Journal of Affective Disorders*, vol. 133, no. 1, pp. 294–299, 2011.

[7] S. J. Kim, D.-U. Jeong, M. E. Sim et al., "Asymmetrically altered integrity of cingulum bundle in posttraumatic stress disorder," *Neuropsychobiology*, vol. 54, no. 2, pp. 120–125, 2007.

[8] M. J. Kim, I. K. Lyoo, S. J. Kim et al., "Disrupted white matter tract integrity of anterior cingulate in trauma survivors," *NeuroReport*, vol. 16, no. 10, pp. 1049–1053, 2005.

[9] L. Chen, S. Lui, Q.-Z. Wu et al., "Impact of acute stress on human brain microstructure: an MR diffusion study of earthquake survivors," *Human Brain Mapping*, vol. 34, no. 2, pp. 367–373, 2013.

[10] A. Sekiguchi, M. Sugiura, Y. Taki et al., "White matter microstructural changes as vulnerability factors and acquired signs of post-earthquake distress," *PLoS ONE*, vol. 9, no. 1, Article ID e83967, 2014.

[11] A. Sekiguchi, M. Sugiura, Y. Taki et al., "Brain structural changes as vulnerability factors and acquired signs of post-earthquake stress," *Molecular Psychiatry*, vol. 18, no. 5, pp. 618–623, 2013.

[12] D. V. Sheehan, Y. Lecrubier, K. H. Sheehan et al., "The Mini-international neuropsychiatric interview (M.I.N.I.): the development and validation of a structured diagnostic psychiatric interview for DSM-IV and ICD-10," *The Journal of Clinical Psychiatry*, vol. 59, 20, pp. 22–33, 1998.

[13] T. Otsubo, K. Tanaka, R. Koda et al., "Reliability and validity of Japanese version of the mini-international neuropsychiatric interview," *Journal of Psychiatry and Clinical Neurosciences*, vol. 59, no. 5, pp. 517–526, 2005.

[14] R. C. Oldfield, "The assessment and analysis of handedness: the Edinburgh inventory," *Neuropsychologia*, vol. 9, no. 1, pp. 97–113, 1971.

[15] "Declaration of helsinki," *Law, Medicine & Health Care*, vol. 19, pp. 264–265, 1991.

[16] D. D. Blake, F. W. Weathers, L. M. Nagy et al., "The development of a clinician-administered PTSD scale," *Journal of Traumatic Stress*, vol. 8, no. 1, pp. 75–90, 1995.

[17] N. Asukai and A. Nishizono-Maher, "The Japanese version of clinician-administered PTSD scale," Tokyo Institute of Psychiatry, Tokyo, Japan, 1998.

[18] C. Spielberger, R. Gorsuch, R. Lushene, P. Vagg, and G. Jacobs, *Manual for the State-Trait Anxiety Inventory*, Consulting Psychologists Press, Palo Alto, Calif, USA, 1983.

[19] K. Nakazato and T. Mizuguchi, "How to use STAI," Sankyoubou, Kyoto, Japan, 1982.

[20] L. S. Radloff, "The CES-D scale: a self-report depression scale for research in the general population," *Applied Psychological Measurement*, vol. 1, no. 3, pp. 385–401, 1977.

[21] S. Shima, T. Shikano, T. Kitamura, and M. Asai, "New self-rated scale for depression," *Japanese Journal of Clinical Psychiatry*, vol. 27, pp. 717–723, 1985 (Japanese).

[22] R. G. Tedeschi and L. G. Calhoun, "The posttraumatic growth inventory: measuring the positive legacy of trauma," *Journal of Traumatic Stress*, vol. 9, no. 3, pp. 455–471, 1996.

[23] K. Taku, L. G. Calhoun, R. G. Tedeschi, V. Gil-Rivas, R. P. Kilmer, and A. Cann, "Examining posttraumatic growth among Japanese university students," *Anxiety, Stress and Coping*, vol. 20, no. 4, pp. 353–367, 2007.

[24] M. Rosenberg, *Society and the Adolescent Self-Image*, Princeton University Press, Princeton, NJ, USA, 1965.

[25] M. Yamamoto, Y. Matsui, and Y. Yamanari, "Substructure of self-recognition," *Japanese Journal of Educational Psychology*, vol. 30, pp. 64–68, 1982.

[26] J. Albrecht, P. R. Dellani, M. J. Müller et al., "Voxel based analyses of diffusion tensor imaging in Fabry disease," *Journal of Neurology, Neurosurgery & Psychiatry*, vol. 78, no. 9, pp. 964–969, 2007.

[27] A. Pfefferbaum and E. V. Sullivan, "Increased brain white matter diffusivity in normal adult aging: relationship to anisotropy and partial voluming," *Magnetic Resonance in Medicine*, vol. 49, no. 5, pp. 953–961, 2003.

[28] D. H. Salat, D. S. Tuch, D. N. Greve et al., "Age-related alterations in white matter microstructure measured by diffusion tensor imaging," *Neurobiology of Aging*, vol. 26, no. 8, pp. 1215–1227, 2005.

[29] R. M. Sapolsky, "Glucocorticoids and hippocampal atrophy in neuropsychiatric disorders," *Archives of General Psychiatry*, vol. 57, no. 10, pp. 925–935, 2000.

[30] M. Joëls, "Corticosteroid effects in the brain: U-shape it," *Trends in Pharmacological Sciences*, vol. 27, no. 5, pp. 244–250, 2006.

[31] J. J. Radley, A. B. Rocher, W. G. M. Janssen, P. R. Hof, B. S. McEwen, and J. H. Morrison, "Reversibility of apical dendritic retraction in the rat medial prefrontal cortex following repeated stress," *Experimental Neurology*, vol. 196, no. 1, pp. 199–203, 2005.

[32] C. Liston, B. S. McEwen, and B. J. Casey, "Psychosocial stress reversibly disrupts prefrontal processing and attentional control," *Proceedings of the National Academy of Sciences of the United States of America*, vol. 106, no. 3, pp. 912–917, 2009.

[33] H. T. Ghashghaei and H. Barbas, "Pathways for emotion: interactions of prefrontal and anterior temporal pathways in the amygdala of the rhesus monkey," *Neuroscience*, vol. 115, no. 4, pp. 1261–1279, 2002.

[34] H. T. Ghashghaei, C. C. Hilgetag, and H. Barbas, "Sequence of information processing for emotions based on the anatomic dialogue between prefrontal cortex and amygdala," *NeuroImage*, vol. 34, no. 3, pp. 905–923, 2007.

[35] U. Ebeling and D. V. Cramon, "Topography of the uncinate fascicle and adjacent temporal fiber tracts," *Acta Neurochirurgica*, vol. 115, no. 3-4, pp. 143–148, 1992.

[36] J. A. Gottfried and R. J. Dolan, "Human orbitofrontal cortex mediates extinction learning while accessing conditioned representations of value," *Nature Neuroscience*, vol. 7, no. 10, pp. 1144–1152, 2004.

[37] K. N. Ochsner and J. J. Gross, "The cognitive control of emotion," *Trends in Cognitive Sciences*, vol. 9, no. 5, pp. 242–249, 2005.

[38] M. B. Hamner, J. P. Lorberbaum, and M. S. George, "Potential role of the anterior cingulate cortex in PTSD: review and hypothesis," *Depression and Anxiety*, vol. 9, no. 1, pp. 1–14, 1999.

[39] N. Schuff, Y. Zhang, W. Zhan et al., "Patterns of altered cortical perfusion and diminished subcortical integrity in posttraumatic stress disorder: an MRI study," *NeuroImage*, vol. 54, no. 1, pp. S62–S68, 2011.

[40] V. Baur, A. B. Brühl, U. Herwig et al., "Evidence of frontotemporal structural hypoconnectivity in social anxiety disorder: a quantitative fiber tractography study," *Human Brain Mapping*, vol. 34, no. 2, pp. 437–446, 2011.

[41] J. M. Hettema, B. Kettenmann, V. Ahluwalia et al., "Pilot multimodal twin imaging study of generalized anxiety disorder," *Depression and Anxiety*, vol. 29, no. 3, pp. 202–209, 2012.

[42] M. J. Kim and P. J. Whalen, "The structural integrity of an amygdala-prefrontal pathway predicts trait anxiety," *Journal of Neuroscience*, vol. 29, no. 37, pp. 11614–11618, 2009.

[43] V. Baur, J. Hänggi, and L. Jäncke, "Volumetric associations between uncinate fasciculus, amygdala, and trait anxiety," *BMC Neuroscience*, vol. 13, no. 1, article 4, 2012.

[44] C. Lebel, M. Gee, R. Camicioli, M. Wieler, W. Martin, and C. Beaulieu, "Diffusion tensor imaging of white matter tract evolution over the lifespan," *NeuroImage*, vol. 60, no. 1, pp. 340–352, 2012.

[45] B. D. Peters, P. R. Szeszko, J. Radua et al., "White matter development in adolescence: diffusion tensor imaging and meta-analytic results," *Schizophrenia Bulletin*, vol. 38, no. 6, pp. 1308–1317, 2012.

[46] C. Lebel and C. Beaulieu, "Longitudinal development of human brain wiring continues from childhood into adulthood," *Journal of Neuroscience*, vol. 31, no. 30, pp. 10937–10947, 2011.

[47] S. Lui, X. Huang, L. Chen et al., "High-field MRI reveals an acute impact on brain function in survivors of the magnitude 8.0 earthquake in China," *Proceedings of the National Academy of Sciences of the United States of America*, vol. 106, no. 36, pp. 15412–15417, 2009.

[48] S. Lui, L. Chen, L. Yao et al., "Brain structural plasticity in survivors of a major earthquake," *Journal of Psychiatry & Neuroscience*, vol. 38, no. 6, Article ID 120244, pp. 381–387, 2013.

Hindawi Publishing Corporation
BioMed Research International
Volume 2013, Article ID 635131, 8 pages
http://dx.doi.org/10.1155/2013/635131

Research Article

GRIN2B Gene and Associated Brain Cortical White Matter Changes in Bipolar Disorder: A Preliminary Combined Platform Investigation

Carissa Nadia Kuswanto,[1] Min Yi Sum,[1] Christopher Ren Zhi Thng,[2] Yi Bin Zhang,[3] Guo Liang Yang,[4] Wieslaw Lucjan Nowinski,[4] Yih Yian Sitoh,[5] Chian Ming Low,[3,6] and Kang Sim[1,7]

[1] *Research Division, Institute of Mental Health, 10 Buangkok View, Singapore 539747*
[2] *NUS High School of Mathematics and Science, 10 Clementi Avenue 1, Singapore 129957*
[3] *Department of Pharmacology, Yong Loo Lin School of Medicine, National University of Singapore, 1E Kent Ridge Road, Singapore 119228*
[4] *Biomedical Imaging Laboratory, Singapore Bioimaging Consortium, Agency for Science, Technology and Research, 11 Biopolis Way, Singapore 138667*
[5] *Department of Neuroradiology, National Neuroscience Institute, 11 Jalan Tan Tock Seng, Singapore 308433*
[6] *Department of Anesthesia, Yong Loo Lin School of Medicine, National University of Singapore, 1E Kent Ridge Road, Singapore 119228*
[7] *Department of General Psychiatry, Institute of Mental Health/Woodbridge Hospital, 10 Buangkok View, Singapore 539747*

Correspondence should be addressed to Kang Sim; kang_sim@imh.com.sg

Received 9 October 2013; Revised 4 December 2013; Accepted 5 December 2013

Academic Editor: Qiyong Gong

Abnormalities in glutamate signaling and glutamate toxicity are thought to be important in the pathophysiology of bipolar disorder (BD). Whilst previous studies have found brain white matter changes in BD, there is paucity of data about how glutamatergic genes affect brain white matter integrity in BD. Based on extant neuroimaging data, we hypothesized that GRIN2B risk allele is associated with reductions of brain white matter integrity in the frontal, parietal, temporal, and occipital regions and cingulate gyrus in BD. Fourteen patients with BD and 22 healthy controls matched in terms of age, gender and handedness were genotyped using blood samples and underwent diffusion tensor imaging. Compared to G allele, brain FA values were significantly lower in BD patients with risk T allele in left frontal region ($P = 0.001$), right frontal region ($P = 0.002$), left parietal region ($P = 0.001$), left occipital region ($P = 0.001$), right occipital region ($P < 0.001$), and left cingulate gyrus ($P = 0.001$). Further elucidation of the interactions between different glutamate genes and their relationships with such structural, functional brain substrates will enhance our understanding of the link between dysregulated glutamatergic neurotransmission and neuroimaging endophenotypes in BD.

1. Introduction

Glutamate (Glu) is an excitatory neurotransmitter that is involved in important neural processes such as synaptic plasticity, neuronal development, and toxicity [1, 2]. Several studies have suggested that the abnormalities in glutamatergic function and signaling pathways through the *N*-methyl-D-aspartate (NMDA) receptors are involved in the pathophysiology of bipolar disorder (BD), a debilitating psychiatric illness characterized by alternating and often recurring episodes of mania or hypomania and depression [1, 3–6]. It was previously thought that mood stabilisers such as lithium and valproate exert their neuroprotective effects through reducing NMDA receptor-induced excitotoxicity [4–6]. Within the glutamatergic receptor, the NR2B subunit is a critical structural and functional component of the NMDA receptor. Encoded by the GRIN2B gene, which is located at 12p12 and 419 kb in size, this subunit is expressed in the

cortical and medial temporal parts of the brain, striatum, and olfactory bulb [7, 8]. Earlier studies have explored the relationship between GRIN2B gene and BD [9–12]. A genetic study of Italian patients with BD found linkage to marker D12S364 at locus 12p12 within the GRIN2B gene [9]. Another study of 440 single-nucleotide polymorphisms (SNPs) from 64 candidate genes among Ashkenazi Jewish case-parent trios with bipolar I disorder noted the aforementioned association of GRIN2B with BD [10], and this was confirmed by a follow up study [11]. Genetic association studies have shown significant association between the 3′UTR region of GRIN2B and BD with psychotic symptoms [13] and number of hospitalization due to mania [14]. Recently, a positive association between GRIN2B gene and BD was also reported in Han Chinese patients with BD [12].

Understanding the impact of specific glutamatergic pathways on brain substrates in BD are important for several reasons. First, it can determine particular brain regions associated with and affected by the glutamatergic genetic signals. Second, multiplatform approaches such as genetic-imaging paradigms can clarify and highlight pathophysiological mechanisms underlying BD [15]. Third, this can subsequently foster targeted multimodality investigations involving structural, functional, and chemical neuroimaging tools. Fourth, there is also suggestion that glutamatergic genes including GRIN2B are involved in oligodendrocyte survival through common stress related signaling pathways [16]. Furthermore, previous diffusion tensor imaging studies had implicated abnormalities in brain white matter regions including frontal, parietal brain regions and cingulum in BD [17].

In the context of scant extant studies examining the impact of glutamatergic genetic signals on brain structural abnormalities in BD, we aimed to investigate the relationship of GRIN2B gene and brain white matter (WM) changes in patients with BD using diffusion tensor imaging. Based on extant neuroimaging data, we hypothesized that GRIN2B risk allele is associated with brain cortical white matter abnormalities involving reductions of white matter integrity in the frontal, parietal and temporal, and occipital regions and cingulate gyrus in BD.

2. Method

2.1. Participants. All subjects gave written informed consent to participate in the study after a detailed explanation of the study procedures. Fourteen patients suffering from BD were recruited from the Institute of Mental Health, Singapore. All diagnoses were made by a psychiatrist (K.S.) using information obtained from the existing medical records, clinical history, mental status examination, interviews with the patients, and their significant spouses or relatives as well as the administration of the Structured Clinical Interview for DSM-IV disorders-Patient Version (SCID-I/P) [18]. Participants with a history of significant neurological illness such as seizure disorder, head trauma, and cerebrovascular accidents were excluded. Furthermore, no subject met DSM-IV criteria for alcohol or other substance abuse in the preceding 3 months. The patients were maintained on a stable dose of antipsychotic medication for at least two weeks prior to the recruitment and did not have their medication withdrawn for the purpose of the study. Another twenty two age- and gender-matched healthy controls (HC) were screened using the Structured Clinical Interview for DSM-IV disorders—Nonpatient Version (SCID-I/NP)—[19] and deemed not to suffer from any Axis 1 psychiatric disorder and had no history of any major neurological, medical illnesses, substance abuse or psychotropic medication use. They were recruited from the staff population at the hospital as well as from the community by advertisements. This study was approved by the Institutional Review Boards of the Institute of Mental Health, Singapore, as well as the National Neuroscience Institute, Singapore.

2.2. Genotyping Procedure. PCR was performed according to Ohtsuki et al. [20] with slight modifications. Isolated genomic DNA was amplified in 25 μL amplification mixture: 2 ng genomic DNA, 0.2 μM of each primer, 0.5 mM of dNTPs, 0.625 U GoTaq DNA polymerase (Promega, USA), 5 μL GoTaq PCR buffer, and sterile milliQ water. The cycling conditions were initial denaturation at 95 degree celsius for 2 min followed by 40 cycles with a profile of 95 degree celsius for 1 min, 59 degree celsius for 1 min, 72 degree celsius for 1 min, and a final extension at 72 degree celsius for 5 min. Amplicons (rs890G/T) were separated by electrophoresis on 1.7% agarose gel, excised, purified (Qiagen Gel Extraction Kit) and sequenced.

2.3. Brain Imaging Acquisition. Brain imaging was performed using a 3-Tesla whole body scanner (Philips Achieva, Philips Medical System, Eindhoven, The Netherlands) with a SENSE head coil at the National Neuroscience Institute, Singapore. High-resolution T1-weighted Magnetization Prepared Rapid Gradient Recalled Echo (MPRAGE) was required (TR = 7.2 s; TE = 3.3 ms; flip angle = 8°). Each T1-weighted volume consisted of 180 axial slices of 0.9 mm thickness with no gap (field of view, 230 mm × 230 mm; acquisition matrix, 256 × 256 pixels). For DTI, single-shot echo-planar diffusion tensor images were obtained (TR = 3725 ms; TE = 56 ms; flip angle = 90°, b = 800 s/mm^2) with 15 different nonparallel directions (b = 800 sec/mm^2) and the baseline image without diffusion weighting (b = 0 sec/mm^2). The acquisition matrix was 112 × 109 pixels with a field of view of 230 mm × 230 mm, which was zero-filled to 256 × 256 pixels. A total of 42 axial slices of 3.0 mm thickness were acquired parallel to anterior-posterior commissure line. The T1-weighted and DTI data were sequentially acquired in a single session scan time without position change. Stability of a high signal to noise ratio was assured through a regular automated quality control procedure.

2.4. Image Processing. The structural MRI images were converted from the scanned images into the Analyze format, which were further processed using the Free Surfer software package (Athinoula A. Martinos Center for Biomedical Imaging, Massachusetts General Hospital, Harvard University,

Table 1: Demographic and clinical characteristics of participants.

Characteristics	BD ($n = 14$)	HC ($n = 22$)	Test statistic	P
Age[a], years	36.9 (12.2)	32.7 (12.3)	$t = -0.986$	.331
Gender[b]				
Males	10 (71.4)	11 (50.0)	$\chi^2 = 1.616$	.204
Females	4 (28.6)	11 (50.0)		
Education[a], years	11.4 (2.3)	14.1 (2.3)	$t = 0.662$	<0.05
Age at onset[a], years	32.3 (13.5)	—	—	—
Duration of psychiatric illness[a], years	4.07 (5.62)	—	—	—
Duration of untreated illness[a], years	0.25 (0.34)	—	—	—
Medication				
Lithium	7	—	—	—
Valproate	7			

[a]Mean (S.D.).
[b]Mean (%).
BD: patients with bipolar disorder; HC: healthy controls.

http://surfer.nmr.mgh.harvard.edu/). The software reformats each brain volume image into a volume image with 1 mm^3 isovoxels, from which relevant brain structures can be delineated [21–26]. This automated method has been shown to be statistically indistinguishable from manual raters and reduces random errors, rater error, and intersubject variability typical of manual techniques [24]. Fractional Anisotropy (FA) maps were acquired from the DTI images from the software DTI Studio [27] and were then coregistered automatically to the MP-RAGE images using a mutual information cost function and a 12 parameter affine transformation. Eddy current correction was performed prior to registration. As the DTI images are co-registered to the subjects' structural images, FA images were also automatically delineated for the separate brain structures using the same delineation parameters in the structural images and FA parameters of relevant brain structures were obtained.

The test-retest (intrarater) reliability of the measurement technique of the cortical FAs were assessed by repeated measurement of eight randomly selected subjects (4 from controls and 4 from patients) over a minimum interval of 2 weeks. On the basis of a two-factor random effects model for intraclass correlation coefficient calculation, alpha values were all greater than 0.90 for the all the cortical FA indices. Inter-rater reliability evaluation performed on a separate subset of eight subjects (4 from controls and 4 from patients) revealed alpha values of greater than 0.90 for the cortical FA indices.

2.5. Statistical Analyses. Demographic variables between BD and HC were compared using two sample student t-test and chi-square test for continuous and categorical variables, respectively. For quality control, the samples were in Hardy-Weinberg equilibrium (HWE $P \geq 0.05$). The HWE P-value was obtained using the Haploview v4.2 [28], and the rests of the statistical analyses were performed using PASW 18. The genotype effect, diagnosis effect, and genotype-diagnosis interactions were further analyzed using the two-way analysis of covariance (ANCOVA) to control for covariates such as age, gender, education, handedness, and intracranial volume. Post hoc tests were performed for white matter regions with significant genotype-diagnosis interactions within HC and BD patient groups. The significance level for statistical tests was set at at two tailed $P < 0.005$.

3. Results

3.1. Sociodemographic and Clinical Characteristics. In the whole sample, there was no significant difference between BD and HC groups in age and gender. Significant difference between the groups was only found in years of education, whereby the BD group had less years of education compared to the HC group. In the BD group, the mean age of onset of the illness was 32.3 (SD 13.5) years. Overall, the mean duration of illness in BD patients was 4.07 years (SD 5.62) and the duration of untreated illness was 0.25 years (SD 0.34) (Table 1).

3.2. The Effect of GRIN2B Gene on White Matter Integrity in Bipolar Disorder. Overall, the T allele frequency for the GRIN2B risk variant amongst patients in the present study was 85.7%. The genotype frequencies of the GRIN2B risk variant are shown in Table 2. There were significant effects of diagnosis by genotype effect interactions observed in the bilateral frontal region (left: $F_{1,32} = 25.5$, $P < 0.001$; right: $F_{1,32} = 18.7$, $P < 0.001$), left parietal region ($F_{1,32} = 15.8$, $P < 0.001$), bilateral occipital region (left: $F_{1,32} = 10.8$, $P = 0.002$; right: $F_{1,32} = 28.1$, $P < 0.001$), and left cingulate gyrus (left: $F_{1,32} = 18.6$, $P < 0.001$). These interactions remained significant after controlling for covariates (left frontal region: adjusted $F_{1,30} = 22.4$, $P < 0.001$; right frontal region: adjusted $F_{1,30} = 17.4$, $P < 0.001$; left parietal lobe: adjusted $F_{1,30} = 13.0$, $P = 0.001$; left occipital region: adjusted $F_{1,30} = 8.93$, $P = 0.006$; right occipital region: adjusted $F_{1,30} = 24.8$, $P < 0.001$; left cingulate gyrus: adjusted $F_{1,30} = 20.9$, $P < 0.001$). (Table 3).

Table 2: Genotype frequencies of GRIN2B risk variant rs890G/T in our sample.

Locus	SNP	Chromosome position	Genotype frequency (%)						HWE P
			BD (n = 14)			HC (n = 22)			
			GG	GT	TT	GG	GT	TT	
GRIN2B	rs890	13715308	1 (7.1)	2 (14.3)	11 (78.6)	3 (13.6)	5 (22.7)	14 (63.6)	0.05

BD: patients with bipolar disorder; HC: healthy controls; HWE P: Hardy-Weinberg equilibrium P value.

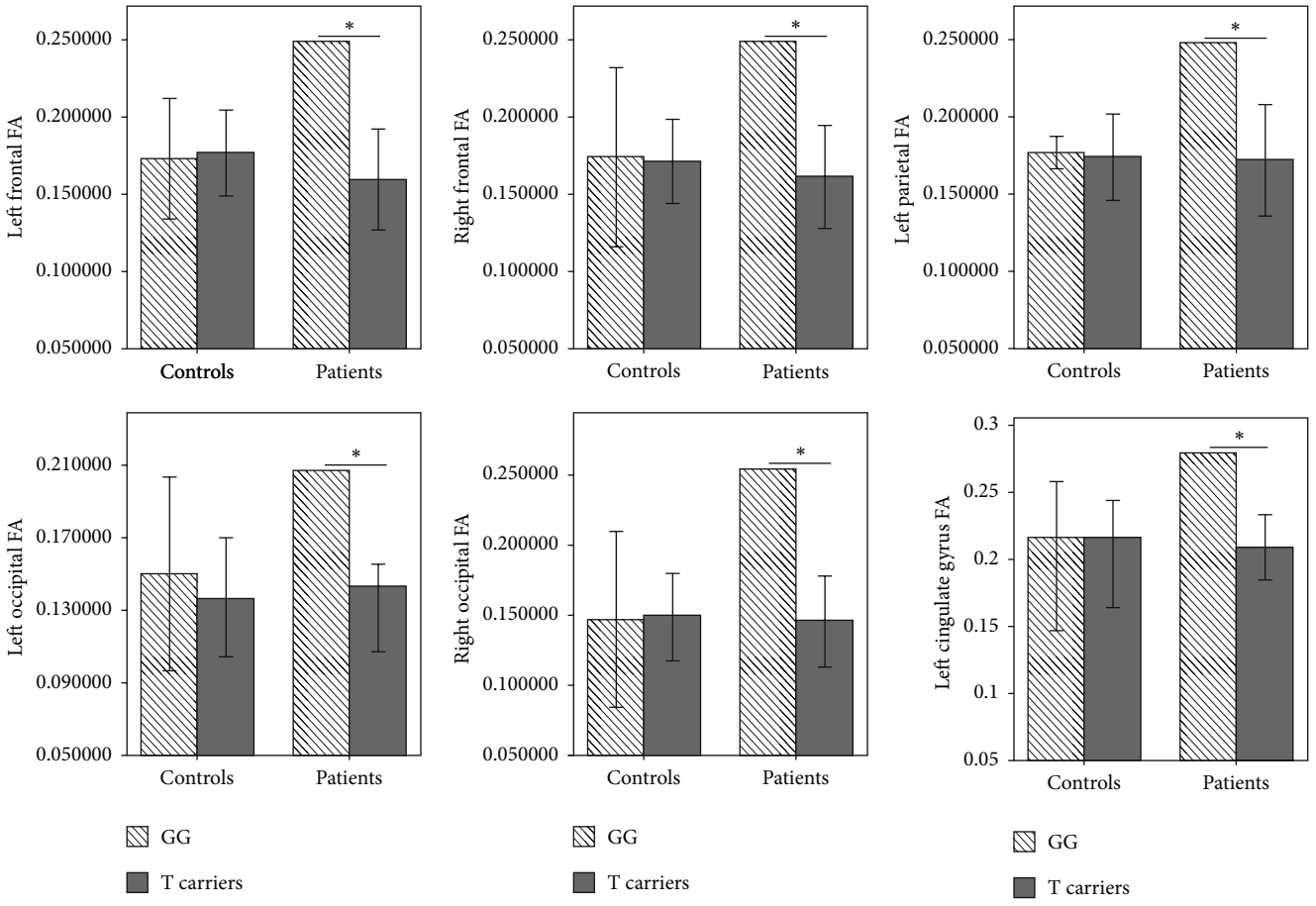

Figure 1: The association between GRIN2B rs890G/T genotypes and the brain white matter regions (T-bar: SD; $^{*}P < 0.005$).

As the diagnosis-genotype interactions were found to be significant for bilateral frontal, bilateral occipital, left parietal regions and left cingulate gyrus, we analyzed the genotype effects on these brain regions within patient and control groups (Figure 1). There was no significant difference within the HC group; however, brain FA values were significantly lower in BD patients with risk T genotypes compared to those with G/G genotype (left frontal region: $F_{1,10} = 24.05$, $P = 0.001$; right frontal region: $F_{1,10} = 17.85$, $P = 0.002$; left parietal region: $F_{1,10} = 9.29$, $P = 0.001$; left occipital region: $F_{1,10} = 22.19$, $P = 0.001$; right occipital region: $F_{1,10} = 33.05$; $P < 0.001$; left cingulate gyrus: $F_{1,10} = 21.50$, $P = 0.001$).

4. Discussion

To the best of our knowledge, this is the first DTI study investigating the interrelationship between the GRIN2B risk gene variant and brain white matter abnormalities in patients with BD. We found specific significant associations between GRIN2B rs890 risk allele and brain FA reductions involving bilateral frontal regions, left parietal region, bilateral occipital regions, and left cingulate gyrus within BD patients but not in healthy controls suggesting disorder specific genetic effect on brain white matter.

Our findings are consistent with those from previous neuroimaging studies which found widespread brain white matter abnormalities in BD involving the cortical regions such as frontal, parietal, and occipital regions, as well as altered association and projection fibers although not in the context of imaging-genetic examination [17, 29–36]. A neurobiological model of affective disorders includes cortical and subcortical neural systems and can be divided into two neural networks [37]. The first is the ventral limbic network which comprises the amygdala, insula, orbitofrontal

Table 3: The effects of GRIN2B of rs890G/T on brain white matter regions (mean fractional anisotropy).

	HC (n = 22)				BD (n = 14)				ANOVA (unadjusted)						ANCOVA[a] (adjusted)					
	GG (n = 3)		T carriers (n = 19)		GG (n = 1)		T carriers (n = 13)		Diagnosis effect		Genotype effect		Interactions effect		Diagnosis effect		Genotype effect		Interactions effect	
	Mean	SD	Mean	SD	Mean	SD	Mean	SD	F	P	F	P	F	P	F	P	F	P	F	P
Left occipital lobe	0.150	0.027	0.137	0.016	0.207	—	0.131	0.012	6.99	.013	21.4	<.001	10.8	.002	7.06	.012	16.2	<.001	8.93	.006
Right occipital lobe	0.147	0.031	0.149	0.016	0.254	—	0.145	0.016	24.9	<.001	26.4	<.001	28.1	<.001	25.4	<.001	20.7	<.001	24.8	<.001
Left parietal lobe	0.177	0.005	0.174	0.014	0.248	—	0.172	0.018	13.7	.001	18.2	<.001	15.8	<.001	13.7	.001	14.2	.001	13.0	.001
Right parietal lobe	0.177	0.020	0.174	0.153	0.218	—	0.175	0.021	3.78	.061	4.34	.045	3.41	.074	3.58	.068	2.53	.122	2.68	.112
Left temporal lobe	0.164	0.004	0.163	0.009	0.163	—	0.161	0.008	0.09	.764	0.11	.743	0.01	.934	0.08	.783	0.13	.719	0.00	.956
Right temporal lobe	0.157	0.005	0.160	0.012	0.156	—	0.155	0.009	0.17	.685	0.05	.832	0.09	.771	0.17	.686	0.02	.898	0.17	.682
Left frontal lobe	0.173	0.020	0.177	0.014	0.249	—	0.159	0.016	9.96	.003	21.4	<.001	25.5	<.001	9.62	.004	19.0	<.001	22.4	<.001
Right frontal lobe	0.174	0.029	0.171	0.014	0.249	—	0.161	0.017	10.9	.002	21.6	<.001	18.7	<.001	10.8	.003	20.9	<.001	17.4	<.001
Left cingulate gyrus	0.217	0.021	0.217	0.014	0.280	—	0.208	0.012	10.9	.002	18.6	<.001	18.6	<.001	12.6	.001	24.2	<.001	20.9	<.001
Right cingulate gyrus	0.200	0.017	0.196	0.017	0.250	—	0.193	0.017	5.06	.032	8.82	.006	6.47	.016	6.86	.014	13.6	.001	7.16	.012

[a] Adjusted for age, gender, education, handedness, and intracranial volume.
BD: patients with bipolar disorder; HC: healthy controls.

cortex, and the striatum and is responsible for identifying emotional valence of a stimulus and production of automatic affective states. The second is the dorsal cognitive network which includes the frontal cortices, anterior and posterior cingulate cortices, precuneus, and cuneus, which is involved in attention, executive and cognitive functioning [37–41]. Earlier data suggest that BD is associated with decreased activity in the dorsal network and hyperactivity in the ventral limbic network [37, 41], which can manifest as impaired performance on cognitive tasks, attention, and working memory deficits, dysregulation of mood, and abnormal emotional processing [39, 40]. Our current findings indicate GRIN2B risk allele associated reductions of white mater integrity in brain cortical regions within the dorsal network. Furthermore, the cingulate region has been hypothesized to facilitate the communication between the dorsal and the ventral systems and contribute to the regulation and integration of mood, cognitive, somatic, and autonomic responses [37]. The cingulate cortex has connections with the ventral network anatomy such as the limbic structures and facilitates top-down process of voluntary suppression/inhibition of an immediate response towards external stimuli [35, 42–45]. Disruption of white mater integrity in the cingulate gyrus may underlie increased biases towards negative and emotional stimuli or faces and diminished prefrontal modulation of affect exhibited in BD patients [37, 39].

Our study found an association between GRIN2B risk allele and lower FA in the parietal and occipital regions in BD. This is consistent with earlier DTI findings, although limited, of white matter abnormalities in the parietal and occipital regions in BD [34, 36, 46] as well as functional neuroimaging studies which have suggested abnormalities in similar parietal and occipital regions in BD [42, 43, 47]. Malhi et al. [42] performed a functional MRI (fMRI) study involving 10 euthymic BD patients and 10 matched healthy controls with the subjects engaged in a modified word-based memory task designed to implicitly invoke negative, positive or neutral affect. Compared to healthy subjects, BD patients exhibited reduced activations in the left inferior parietal lobule, right posterior cingulate gyrus, bilateral anterior cingulate gyrus, thalamus, and other cortical regions when presented with words with negative affect. Likewise, when presented with words with positive affect, BD patients showed decreased activations in the bilateral frontal gyri, right anterior cingulate gyrus, left posterior cingulate gyrus, and bilateral occipital regions compared to healthy subjects. The same research group found that poor performance during a Theory of Mind (ToM) task by euthymic BD patients was associated with less cortical activations and higher activations in the anterior cingulate gyrus and bilateral occipital regions [43]. Furthermore, a structural MRI study noted reduced gray matter density in the right parietal lobule which was associated with higher interference during the Stroop color word task in remitted patients with bipolar disorder I [47].

It was slightly surprising that no significant genotype-diagnosis interaction was noted in the temporal region despite the abundance of NR2B receptors in these regions. It is unclear how treatment with mood stabilisers such as valproate and lithium may have stabilized extant dysregulated glutamatergic neurotransmission in this region. For instance, chronic exposure to lithium was found to indirectly inhibit NMDA-receptor-mediated Ca^{2+} influx and decrease NR2B phosphorylation in temporal brain region [4–6]. Valproate induces neuroprotective proteins such as heat-shock protein (HSP70) by directly targeting histone deacetylase (HDAC) inhibition in the cortical including temporal and striatal brain regions [48].

There are several limitations to the study. First, due to the small sample of subjects our findings need to be replicated with bigger sample size. Second, analyses of other brain structural measures including cortical thickness, subcortical structures, and specific white matter tracts will complement our understanding of the impact of GRIN2B on brain white matter integrity in BD. Third, we did not correlate the structural findings with neurocognitive data which would provide better insight into the cognitive impact of GRIN2B gene in BD.

In conclusion, we found that GRIN2B was associated with reductions of brain white matter integrity within the fronto-parietal-occipital cortical regions in patients with BD. Further elucidation of the interactions between different glutamate genes and their relationships with these structural, functional, and chemical brain substrates will enhance our understanding of dysregulated glutamatergic neurotransmission and its relation to neuroimaging endophenotypes in BD. This has the potential to shed light on neurobiological mechanisms that underlie BD and provide targets for future intervention.

Acknowledgments

This study was supported by the National Healthcare Group, Singapore (SIG/05004, SIG/05028), and the Singapore Bioimaging Consortium (RP C-009/2006) research grants awarded to Dr. Kang Sim. The authors would like to thank all participants, their families, and our hospital staff for their support of this study.

References

[1] S. Y. T. Cherlyn, P. S. Woon, J. J. Liu, W. Y. Ong, G. C. Tsai, and K. Sim, "Genetic association studies of glutamate, GABA and related genes in schizophrenia and bipolar disorder: a decade of advance," *Neuroscience and Biobehavioral Reviews*, vol. 34, no. 6, pp. 958–977, 2010.

[2] D. C. Goff and J. T. Coyle, "The emerging role of glutamate in the pathophysiology and treatment of schizophrenia," *The American Journal of Psychiatry*, vol. 158, no. 9, pp. 1367–1377, 2001.

[3] S. M. Clinton and J. H. Meadow-Woodruff, "Abnormalities of the NMDA receptor and associated intracellular molecules in the thalamus in schizophrenia and bipolar disorder," *Neuropsychopharmacology*, vol. 29, no. 7, pp. 1353–1362, 2004.

[4] R. Hashimoto, C. Hough, T. Nakazawa, T. Yamamoto, and D. Chuang, "Lithium protection against glutamate excitotoxicity in rat cerebral cortical neurons: involvement of NMDA receptor inhibition possibly by decreasing NR2B tyrosine phosphorylation," *Journal of Neurochemistry*, vol. 80, no. 4, pp. 589–597, 2002.

[5] L. E. Hokin, J. F. Dixon, and G. V. Los, "A novel action of lithium: stimulation of glutamate release and inositol 1,4,5 trisphosphate accumulation via activation of the N-methyl D-aspartate receptor in monkey and mouse cerebral cortex slices," *Advances in Enzyme Regulation*, vol. 36, pp. 229–244, 1996.

[6] S. Nonaka, C. J. Hough, and D. Chuang, "Chronic lithium treatment robustly protects neurons in the central nervous system against excitotoxicity by inhibiting N-methyl-D-aspartate receptor-mediated calcium influx," *Proceedings of the National Academy of Sciences of the United States of America*, vol. 95, no. 5, pp. 2642–2647, 1998.

[7] D. J. Laurie, I. Bartke, R. Schoepfer, K. Naujoks, and P. H. Seeburg, "Regional, developmental and interspecies expression of the four NMDAR2 subunits, examined using monoclonal antibodies," *Molecular Brain Research*, vol. 51, no. 1-2, pp. 23–32, 1997.

[8] A. M. Schito, A. Pizzuti, E. Di Maria et al., "mRNA distribution in adult human brain of GRIN2B, a N-methyl-D-aspartate (NMDA) receptor subunit," *Neuroscience Letters*, vol. 239, no. 1, pp. 49–53, 1997.

[9] C. Lorenzi, D. Delmonte, A. Pirovano et al., "Searching susceptibility loci for bipolar disorder: a sib pair study on chromosome 12," *Neuropsychobiology*, vol. 61, no. 1, pp. 10–18, 2009.

[10] M. D. Fallin, V. K. Lasseter, D. Avramopoulos et al., "Bipolar I disorder and schizophrenia: a 440-single-nucleotide polymorphism screen of 64 candidate genes among Ashkenazi Jewish case-parent trios," *The American Journal of Human Genetics*, vol. 77, no. 6, pp. 918–936, 2005.

[11] D. Avramopoulos, V. K. Lasseter, M. D. Fallin et al., "Stage II follow-up on a linkage scan for bipolar disorder in the Ashkenazim provides suggestive evidence for chromosome 12p and the GRIN2B gene," *Genetics in Medicine*, vol. 9, no. 11, pp. 745–751, 2007.

[12] Q. Zhao, R. Che, Z. Zhang et al., "Positive association between GRIN2B gene and bipolar disorder in the Chinese Han Population," *Psychiatry Research*, vol. 185, no. 1-2, pp. 290–292, 2011.

[13] L. Martucci, A. H. C. Wong, V. de Luca et al., "N-methyl-d-aspartate receptor NR2B subunit gene GRIN2B in schizophrenia and bipolar disorder: polymorphisms and mRNA levels," *Schizophrenia Research*, vol. 84, no. 2-3, pp. 214–221, 2006.

[14] S. Dalvie, N. Horn, C. Nossek, L. van der Merwe, D. Stein, and R. Ramesar, "Psychosis and relapse in bipolar disorder are related to GRM3, DAOA, and GRIN2B genotype," *African Journal of Psychiatry*, vol. 13, no. 4, pp. 297–301, 2010.

[15] Y. A. Kurnianingsih, C. N. Kuswanto, R. S. McIntyre, A. Qiu, B. C. Ho, and K. Sim, "Neurocognitive-genetic and neuroimaging-genetic research paradigms in schizophrenia and bipolar disorder," *Journal of Neural Transmission*, vol. 118, no. 11, pp. 1621–1639, 2011.

[16] C. J. Carter, "eIF2B and oligodendrocyte survival: where nature and nurture meet in bipolar disorder and schizophrenia?" *Schizophrenia Bulletin*, vol. 33, no. 6, pp. 1343–1353, 2007.

[17] S. Heng, A. W. Song, and K. Sim, "White matter abnormalities in bipolar disorder: insights from diffusion tensor imaging studies," *Journal of Neural Transmission*, vol. 117, no. 5, pp. 639–654, 2010.

[18] M. B. First, R. L. Spitzer, M. Gibbon, and J. B. W. Williams, *Structured Clinical Interview for DSM-IV Axis I Disorders-Patient Version (SCID-P)*, American Psychiatric Press, Washington, DC, USA, 1994.

[19] M. B. First, R. L. Spitzer, M. Gibbon, and J. B. W. Williams, *Structured Clinical Interview for DSM-IV Axis I Disorders-Non-Patient Version (SCID-NP)*, American Psychiatric Press, Washington, DC, USA, 2002.

[20] T. Ohtsuki, K. Sakurai, H. Dou, M. Toru, K. Yamakawa-Kobayashi, and T. Arinami, "Mutation analysis of the NMDAR2B (GRIN2B) gene in schizophrenia," *Molecular Psychiatry*, vol. 6, no. 2, pp. 211–216, 2001.

[21] A. M. Dale, B. Fischl, and M. I. Sereno, "Cortical surface-based analysis: I. Segmentation and surface reconstruction," *NeuroImage*, vol. 9, no. 2, pp. 179–194, 1999.

[22] B. Fischl, M. I. Sereno, and A. M. Dale, "Cortical surface-based analysis: II. Inflation, flattening, and a surface-based coordinate system," *NeuroImage*, vol. 9, no. 2, pp. 195–207, 1999.

[23] B. Fischl, M. I. Sereno, R. B. Tootell, and A. M. Dale, "High-resolution intersubject averaging and a coordinate system for the cortical surface," *Human Brain Mapping*, vol. 8, no. 4, pp. 272–284, 1999.

[24] B. Fischl, D. H. Salat, E. Busa et al., "Whole brain segmentation: automated labeling of neuroanatomical structures in the human brain," *Neuron*, vol. 33, no. 3, pp. 341–355, 2002.

[25] B. Fischl, D. H. Salat, A. J. W. van der Kouwe et al., "Sequence-independent segmentation of magnetic resonance images," *NeuroImage*, vol. 23, supplement 1, pp. S69–S84, 2004.

[26] B. Fischl, A. van der Kouwe, C. Destrieux et al., "Automatically parcellating the human cerebral cortex," *Cerebral Cortex*, vol. 14, no. 1, pp. 11–22, 2004.

[27] H. Jiang, P. C. M. van Zijl, J. Kim, G. D. Pearlson, and S. Mori, "DtiStudio: resource program for diffusion tensor computation and fiber bundle tracking," *Computer Methods and Programs in Biomedicine*, vol. 81, no. 2, pp. 106–116, 2006.

[28] J. C. Barrett, B. Fry, J. Maller, and M. J. Daly, "Haploview: analysis and visualization of LD and haplotype maps," *Bioinformatics*, vol. 21, no. 2, pp. 263–265, 2005.

[29] C. M. Adler, J. Adams, M. P. DelBello et al., "Evidence of white matter pathology in bipolar disorder adolescents experiencing their first episode of mania: a diffusion tensor imaging study," *The American Journal of Psychiatry*, vol. 163, no. 2, pp. 322–324, 2006.

[30] C. M. Adler, S. K. Holland, V. Schmithorst et al., "Abnormal frontal white matter tracts in bipolar disorder: a diffusion tensor imaging study," *Bipolar Disorders*, vol. 6, no. 3, pp. 197–203, 2004.

[31] S. Bruno, M. Cercignani, and M. A. Ron, "White matter abnormalities in bipolar disorder: a voxel-based diffusion tensor imaging study," *Bipolar Disorders*, vol. 10, no. 4, pp. 460–468, 2008.

[32] W. Y. Chan, G. L. Yang, M. Y. Chia et al., "Cortical and subcortical white matter abnormalities in adults with remitted first-episode mania revealed by tract-based spatial statistics," *Bipolar Disorders*, vol. 12, no. 4, pp. 383–389, 2010.

[33] F. Lin, S. Weng, B. Xie, G. Wu, and H. Lei, "Abnormal frontal cortex white matter connections in bipolar disorder: a DTI tractography study," *Journal of Affective Disorders*, vol. 131, no. 1–3, pp. 299–306, 2011.

[34] W. T. Regenold, C. A. D'Agostino, N. Ramesh, M. Hasnain, S. Roys, and R. P. Gullapalli, "Diffusion-weighted magnetic resonance imaging of white matter in bipolar disorder: a pilot study," *Bipolar Disorders*, vol. 8, no. 2, pp. 188–195, 2006.

[35] F. Vederine, M. Wessa, M. Leboyer, and J. Houenou, "A meta-analysis of whole-brain diffusion tensor imaging studies in

bipolar disorder," *Progress in Neuro-Psychopharmacology and Biological Psychiatry*, vol. 35, no. 8, pp. 1820–1826, 2011.

[36] A. Versace, J. R. C. Almeida, S. Hassel et al., "Elevated left and reduced right orbitomedial prefrontal fractional anisotropy in adults with bipolar disorder revealed by tract-based spatial statistics," *Archives of General Psychiatry*, vol. 65, no. 9, pp. 1041–1052, 2008.

[37] H. S. Mayberg, "Limbic-cortical dysregulation: a proposed model of depression," *Journal of Neuropsychiatry and Clinical Neurosciences*, vol. 9, no. 3, pp. 471–481, 1997.

[38] M. L. Phillips, W. C. Drevets, S. L. Rauch, and R. Lane, "Neurobiology of emotion perception I: the neural basis of normal emotion perception," *Biological Psychiatry*, vol. 54, no. 5, pp. 504–514, 2003.

[39] M. L. Phillips, W. C. Drevets, S. L. Rauch, and R. Lane, "Neurobiology of emotion perception II: implications for major psychiatric disorders," *Biological Psychiatry*, vol. 54, no. 5, pp. 515–528, 2003.

[40] S. M. Strakowski, M. P. DelBello, and C. M. Adler, "The functional neuroanatomy of bipolar disorder: a review of neuroimaging findings," *Molecular Psychiatry*, vol. 10, no. 1, pp. 105–116, 2005.

[41] M. Wessa, J. Houenou, M. Leboyer et al., "Microstructural white matter changes in euthymic bipolar patients: a whole-brain diffusion tensor imaging study," *Bipolar Disorders*, vol. 11, no. 5, pp. 504–514, 2009.

[42] G. S. Malhi, J. Lagopoulos, A. M. Owen, B. Ivanovski, R. Shnier, and P. Sachdev, "Reduced activation to implicit affect induction in euthymic bipolar patients: an fMRI study," *Journal of Affective Disorders*, vol. 97, no. 1–3, pp. 109–122, 2007.

[43] G. S. Malhi, J. Lagopoulos, P. Das, K. Moss, M. Berk, and C. M. Coulston, "A functional MRI study of theory of mind in euthymic bipolar disorder patients," *Bipolar Disorders*, vol. 10, no. 8, pp. 943–956, 2008.

[44] M. N. Pavuluri, A. M. Passarotti, E. M. Harral, and J. A. Sweeney, "An fMRI study of the neural correlates of incidental versus directed emotion processing in pediatric bipolar disorder," *Journal of the American Academy of Child and Adolescent Psychiatry*, vol. 48, no. 3, pp. 308–319, 2009.

[45] F. Wang, J. H. Kalmar, Y. He et al., "Functional and structural connectivity between the perigenual anterior cingulate and amygdala in bipolar disorder," *Biological Psychiatry*, vol. 66, no. 5, pp. 516–521, 2009.

[46] N. Barnea-Goraly, K. D. Chang, A. Karchemskiy, M. E. Howe, and A. L. Reiss, "Limbic and corpus callosum aberrations in adolescents with bipolar disorder: a tract-based spatial statistics analysis," *Biological Psychiatry*, vol. 66, no. 3, pp. 238–244, 2009.

[47] M. Haldane, G. Cunningham, C. Androutsos, and S. Frangou, "Structural brain correlates of response inhibition in bipolar disorder I," *Journal of Psychopharmacology*, vol. 22, no. 2, pp. 138–143, 2008.

[48] D. Chuang, "The antiapoptotic actions of mood stabilizers: molecular mechanisms and therapeutic potentials," *Annals of the New York Academy of Sciences*, vol. 1053, pp. 195–204, 2005.